Nanoscale Polymeric Amphiphiles by Combination of Controlled Polymerizations and "Click" Reactions: Implications for Drug Delivery

Javakhishvili, Irakli

Publication date:
2010

Document Version
Publisher's PDF, also known as Version of record

Nanoscale Polymeric Amphiphiles by Combination of Controlled Polymerizations and "Click" Reactions: Implications for Drug Delivery

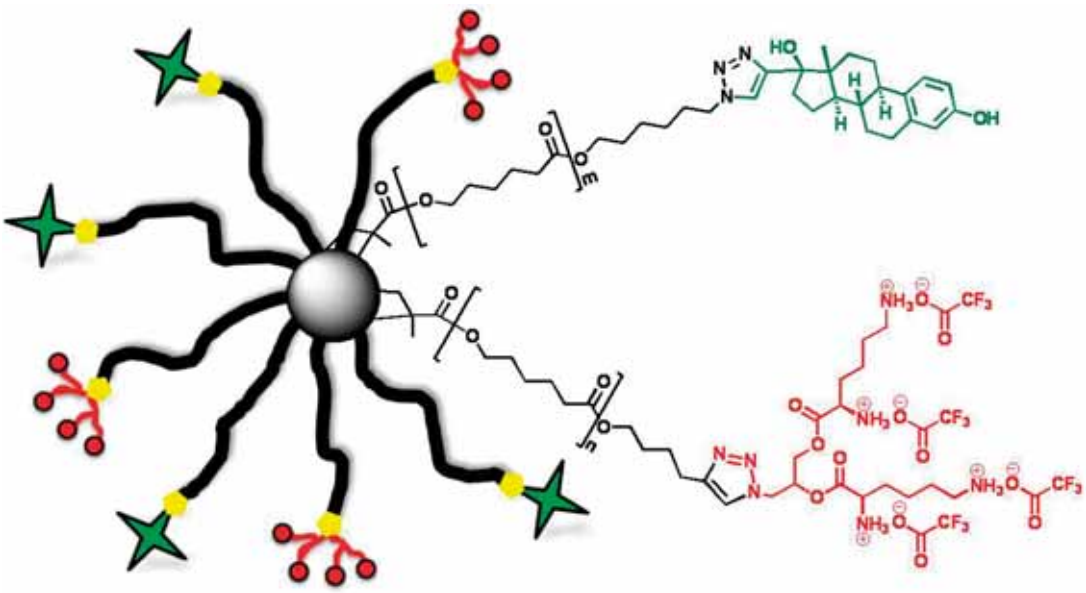

Irakli Javakhishvili

Ph.D. Thesis

August 2010

DTU Chemical Engineering
Department of Chemical and Biochemical Engineering

Nanoscale Polymeric Amphiphiles by Combination of Controlled Polymerizations and "Click" Reactions: Implications for Drug Delivery

Irakli Javakhishvili

Ph.D. Thesis

August 2010

DTU Chemical Engineering
Department of Chemical and Biochemical Engineering

Address: Danish Polymer Centre
Department of Chemical and
Biochemical Engineering
Technical University of Denmark
Søltofts Plads, Building 229
DK-2800 Kgs. Lyngby
Denmark
Phone: +45 4525 2800
Fax: +45 4525 4588
Web: www.kt.dtu.dk

Print: J&R Frydenberg A/S
København
January 2011

ISBN: 978-87-92481-34-4

Preface

The Ph. D. project has been conducted at the Danish Polymer Centre, Department of Chemical and Biochemical Engineering, Technical University of Denmark, from 2007 to 2010. The financial support by the Technical University of Denmark is greatly appreciated.

I would like to express my gratitude to Professor Søren Hvilsted who has been my supervisor throughout the project. I am thankful for permitting me being part of your team. You have been exceedingly helpful with supplying new ideas, discussing attained results, devising synthetic strategies, and suggesting ways to execute them. I appreciate your flexibility allowing me to implement some of my own approaches. I would like to thank you for your trust, priceless scientific input in this project, and encouragement and support in daily life.

I would like to thank Associate Professor Katja Jankova for the extensive discussions about the controlled radical polymerizations and experimental setups; also for being invaluably supportive throughout my stay in Denmark.

I would like to thank our laboratory coordinator Kim Chi Szabo for her assistance with the thermal analysis techniques, size exclusion chromatography, and other everyday issues at the lab.

Dr. Jakob B. Wagner and the Center for Electron Nanoscopy at the Technical University of Denmark are acknowledged for their assistance in TEM investigations.

I would like to express my gratitude to Professor Wolfgang Binder from the Martin-Luther University Halle-Wittenberg for the collaboration including MALDI-TOF spectrometry of our samples, interpretation of the data, and instructive correspondence.

I would like to thank my colleagues whom I share the office with – Dr. Anders Daugaard, Charlotte Fristrup, and Mads Nielsen for numerous valuable discussions and help at the laboratory, as well as my colleagues and staff at the Danish Polymer Centre for creating a splendid working environment. I would like to thank Associate Professor Ivaylo Dimitrov for the fertile discussions about the polymerizations and his assistance at the lab.

Finally, I would like to thank my friends in Denmark and at home, and my family for being encouraging and motivating.

Irakli Javakhishvili

August 2010

Kgs. Lyngby, Denmark

Abstract

The Ph. D. project consists of three distinct themes that are interwoven by the immeasurable versatility and valuable properties of α,ω-hetero-bifunctional poly(ε-caprolactone). The library of α,ω-hetero-bifunctional poly(ε-caprolactone)s incorporating alkynyl, alkenyl, bromoalkyl, and bromoisobutyryl moieties at the α-terminus, and protected thiyl, alkenyl, and methacryloyl moieties at the ω-terminus have been obtained. These multifaceted building blocks have been synthesized by "coordination-insertion" ring-opening polymerization initiated by an ω-functional alcohol and catalyzed by tin (II) ethylhexanoate. The polymerizations are well-controlled, and produce polyesters with narrow molecular weight distribution. Incorporation of the terminal functional groups has been proven to be near to quantitative.

These precisely-controlled macromolecular architectures have then been employed in preparation of amphiphilic block copolymers with preprogrammed structure and composition. Thus, the amphiphilic block copolymer HS-poly(ε-caprolactone)-*b*-poly(acrylic acid) has been synthesized by chain-extending the appropriate polyester macroinitiator by Ni (II)-mediated atom transfer radical polymerization of *tert*-butyl acrylate followed by a deblocking reaction. The chain extension is marked with excellent control, and results in the block copolymers with low polydispersity indices. The amphiphilic macrothiol has been utilized in passivation of gold clusters to afford stable, aggregation-free monolayer protected gold nanoparticles. The mean diameter of the gold cores has been estimated to be 9.0 ± 3.1 nm.

The polyester precursor with terminal alkyne and alkene functional groups has been ligated with a cholesteryl moiety and a second generation L-lysine dendron by making use of the Cu^{I}-catalyzed azide-alkyne 1,3-cycloaddition and radical thiol-ene "click" reactions. First, the Boc-protected L-lysine dendron with an azide functionality at the focal point has been prepared. Then it has been conjugated to the polyester chain end by Cu^{I}-mediated "click" reaction. The UV-initiated radical thiol-ene reaction between this linear-dendritic block copolymer and thiocholesterol, and subsequent removal of Boc protecting groups furnish amphiphilic rodcoil dendron bearing rod-like cholesteryl, coil-like poly(ε-caprolactone), and dendritic L-lysine segments. Both "click" reactions afford near to quantitative derivatization while preserving the polyester backbone intact.

The α-azido-ω-methacryloyl-poly(ε-caprolactone) chains have been linked to 17α-ethynylestradiol and ethynylferrocene by Cu^{I}-catalyzed "click" reaction to obtain macromonomers with terminal estradiol and ferrocene moieties. In a similar fashion, ω-methacryloyl-poly(ε-caprolactone)-*b*-(di-Boc-L-lysine)$_{G2}$ – a linear-dendritic macromonomer with protected amine groups – has been synthesized. These macromonomers have been employed in preparation of miktoarm core-crosslinked star copolymers by Cu-mediated atom transfer radical polymerization of the mixture of the macromonomers of choice and a difunctional cross-linker. The miktoarm core-crosslinked stars with free amine functionalities and estradiol residues as well as with Boc-protected amine groups and ferrocene moieties on the peripheries have been prepared. The stars exhibit fairly low polydispersity indices, and their sizes fall in the range of 10-20 nm.

Thus, the controlled polymerization techniques together with the "click" reactions comprise a reliable and resourceful battery of synthetic methods interplay of which facilitates construction of diverse multivalent amphiphiles with core-shell type structure and the potential as drug delivery devices in cancer treatment.

Resumé

Denne ph.d.-afhandling er baseret på tre forskellige temaer, der er sammenflettet af den uvurdelige alsidighed og de værdifulde egenskaber af α,ω-heterobifunktionel poly(ε-caprolacton). Et bibliotek af α,ω-heterobifunktionelle poly(ε-caprolacton)er med alkyn, alken, bromoalkyl og α-bromoiosbutyryl grupper i α-terminalen, og thiol, alken, og methacryl grupper i ω-terminalen er tilvejebragt. Disse multifaceterede byggeblokke er fremstillet ved "koordinations-indsætnings" ringåbnings polymerisation initieret af en ω-funktionel alkohol og katalyseret af tin(II) ethylhexanoate. Polymerisationerne er velkontrollerede og resulterer i polyestere med snævre molekylvægts fordelinger. Inkorporering af de terminale, funktionelle grupper er påvist at være tæt på kvantitativ.

De velkontrollerede makromolekylære arkitekturer er anvendt til fremstilling af amfifile blok copolymerer med forud bestemt struktur og sammensætning. Således er den amfifile blok copolymer HS-poly(ε-caprolacton)-*b*-polyacrylsyre syntetiseret ved kædeforlængelse af den relevante polyester makroinitiator ved Ni(II)-medieret atom transfer radikal polymerisation (ATRP) af *tert*-butylacrylat efterfulgt af en debeskyttelses reaktion. Kædeforlængelsen er karakteriseret ved udstrakt kontrol, der resulterer i blok copolymerer med lave polydipersitets indeks. Den amfifile makrothiol er anvendt til pacificering af guld klustre, der danner aggregerings fri monolags beskyttede guld nanopartikler. Middeldiameteren af guldkernen er estimeret til 9.0 ± 3.1 nm.

Polyester forstadiet med terminale alkyn og alken funktionelle grupper er reageret med henholdsvis en kolesteryl gruppe og en anden generations L-lysine dendron ved anvendelse af Cu^{I}-katalyseret azid-alkyn 1,3-cycloaddition og thiol-en "klik" koblingsreaktioner. Indledningsvis er en Boc-beskyttet L-lysine dendron med azid-funktionalitet i den fokale position fremstillet. Dendronen er derefter konjugeret til polyester terminalen ved en Cu^{I}-katalyseret "klik" sammenkobling. En UV-initieret radikal thiol-en reaktion mellem denne lineært-dendritiske blok copolymer og thiokolesterol resulterer efter Boc-debeskyttelse i en amfifil stav-spiral dendron med en stav-lignende kolesterol, en spiralformet poly(ε-caprolacton), samt et dendritisk L-lysine segment. Begge "klik"-koblinger udføres i tilnærmelsesvis kvantitative reaktioner, som bevarer polyester hovedkæden intakt.

α-Azid-ω-methacryloyl-poly(ε-caprolacton) kæder er koblet til henholdsvis 17α-ethynylestradiol og ethynylferrocene ved Cu^{I}-katalyseret "klik" reaktioner med henblik på fremstilling af makro-monomere med estradiol og ferrocene endegrupper. På lignende vis er ω-methacryloyl-poly(ε-caprolacton)-*b*-(di-Boc-L-lysine)$_{G2}$, en lineært-dendritisk makromonomer med beskyttede amin-grupper, syntetiseret. Makromonomererne er anvendt til fremstilling af miktoarm kerne-tværbundne stjerne copolymere ved Cu-medieret ATRP i blanding med en difunktionel tværbinder. Miktoarm kernetværbundne stjerner med såvel frie amin funktionaliteter og estradiol grupper som Boc-beskyttede amingrupper og ferrocene funktionaliteter på overfladerne er fremstillet. De stjernelignende copolymere har relativt lave polydispersitets indeks med størrelser i området 10-20 nm.

De anvendte kontrollerede polymerisationsteknikker i effektivt samspil med "klik"-reaktioner udgør et pålideligt og særdeles anvendeligt arsenal af syntetiske strategier der muliggør konstruktion af diverse multivalente amfifile materialer med kerne-skal struktur og potentialet til medicin levering ved cancer behandling.

Table of Contents

List of Abbreviations

ATR FT IR	attenuated total reflectance Fourier transform infrared spectroscopy
ATRP	atom transfer radical polymerization
AuNPs	gold nanoparticles
b	block
BA	*n*-butyl acrylate
BDMA	1,4-butandiol dimethacrylate
bis-MPA	2,2-bis(hydroxymethyl)propionic acid
BMPB	2-bromo 2-methylpropionyl bromide
Boc	*tert*-butyloxycarbonyl
cat	catalyst
CCS	core-crosslinked star
ε-CL	ε-caprolactone
cmc	critical micelle concentration
COSY	correlation spectroscopy
CRP	controlled radical polymerization
CuAAC	Cu^{I}-mediated azide-alkyne 1,3-cycloaddition
Da	Dalton
DCC	*N*,*N*'-dicyclohexylcarbodiimide
DEAD	diethyl azodicarboxylate
DLS	dynamic light scattering
DMAEMA	*N*,*N*-dimethylamino-2-ethyl methacrylate
DMF	*N*,*N*-dimethylformamide
4-DMAP	4-(dimethylamino)pyridine
DMPA	2,2-dimethoxy-2-phenylacetophenone
DMSO	dimethyl sulfoxide
DNA	deoxyribonucleic acid
dNPTAA	α-(2,4-dinitrophenylthio)acetic acid
DP	degree of polymerization
DVB	divinyl benzene
E_2	estradiol
EB*i*B	ethyl α-bromoisobutyrate
EPR	enhanced permeability and retention
ER	estrogen receptor
eROP	enzymatic ring-opening polymerization
FDA	US Food and Drug Agency
g	graft
G_2	second generation dendron
G_6PLL	sixth generation poly(L-lysine) dendrimer
HEBI	2-hydroxyethyl 2-bromoisobutyrate
HEMA	2-hydroxyethyl methacrylate
HMTETA	1,1,4,7,10,10-hexamethyltriethylenetetramine
HPC	hydroxypropylcellulose
HSQC	heteronuclear single quantum coherence
MA	methacrylic acid
MALDI-TOF	matrix-assisted laser desorption and ionization time-of-flight
MI	macroinitiator

MM	macromonomer
MMA	methyl methacrylate
Mmt	monomethoxytrityl
MmtTAA	α-(4-monomethoxytritylthio)acetic acid
M_n	number average molecular weight
mPEGMA	poly(ethylene glycol) methyl ether methacrylate
MRI	magnetic resonance imaging
M_w	weight average molecular weight
MWD	molecular weight distribution
NIR	near-infrared
NMR	nuclear magnetic resonance
PAA	poly(acrylic acid)
PCL	poly(ε-caprolactone)
PDI	polydispersity index
PEG	poly(ethylene glycol)
PLA	poly(lactic acid)
PLL	poly(L-lysine)
PMDETA	*N,N,N´,N´,N´´*-pentamethyldiethylenetriamine
PRE	persistent radical effect
PS	polystyrene
RAFT	reversible addition-fragmentation chain transfer
RES	reticuloendothelial system
RF	radiofrequency
RI	refractive index
ROP	ring-opening polymerization
RT	room temperature
SEC	size exclusion chromatography
$SnOct_2$	tin octoate
SPR	surface plasmon resonance
*t*BA	*tert*-butyl acrylate
TEM	transmission electron microscopy
TES	triethylsilane
TFA	trifluoroacetic acid
TGA	thermogravimetric analysis
THF	tetrahydrofuran
TPP	triphenylphosphine
UV	ultraviolet
δ-VL	δ-valerolactone

Objectives and Outline

The objectives of the study include synthesis and structural characterization of the amphiphilic block copolymers that afford core-shell type nanoscale entities that have potential as drug delivery vehicles in cancer therapy. Consequently, the materials that are known to exert none or minimal adverse effects on a human body have been chosen. Since building predetermined macromolecular architectures with a large number of functional groups is desired, controlled polymerization techniques in combination with highly efficient, selective, and flexible "click" reactions have been employed.

Gold nanoparticles protected with polymeric shell may combine ablative therapy and site-specific drug delivery in cancer treatment. This may be accomplished by tailoring the surface properties and the size of the gold clusters. The former may be addressed by devising polymeric ligands with desirable features and functional groups. The synthesis of the effective macroligand that allows preparation of the stable gold clusters, and provides nanoenvironment for hydrophobic anticancer drugs and mucoadhesive surface for anchoring on mucous membranes is one of the objectives of this study.

The second aim of the study is the ligation of biologically active moieties to the termini of a hydrophobic polymeric chain to afford the amphiphilic linear-dendritic macromolecule that comprises rod-like, coil-like, and dendritic fragments, and may self-assemble in solid state as well as in aqueous solutions. Contriving robust, facile, and effective synthetic strategy is of the utmost importance.

The third objective involves the preparation of core-crosslinked amphiphilic star copolymers with hydrophobic interior, charged hydrophilic surface, and targeting motifs. Such nanoscopic core-shell type architectures are envisioned to be excellent candidates as drug delivery devices owing to the enhanced stability in biological fluids. Moreover, they permit site-specific delivery of their cargo due to the presence of the pilot molecules on their surfaces.

The dissertation is based on three publications listed below:

1) Javakhishvili, I.; Hvilsted, S. Gold Nanoparticles Protected with Thiol-Derivatized Amphiphilic Poly(ε-caprolactone)-*b*-poly(acrylic acid). *Biomacromolecules* **2009**, *10*, 74-81.
2) Javakhishvili, I.; Binder, W. H.; Tanner, S.; Hvilsted, S. Facile Synthesis of Linear-dendritic Cholesteryl-poly(ε-caprolactone)-*b*-(L-lysine)$_{G2}$ by Thiol-ene and Azide-alkyne ''Click'' Reactions. *Polym. Chem.* **2010**, *1*, 506-513.
3) Javakhishvili, I.; Hvilsted, S. Miktoarm Core-crosslinked Star Copolymers with Biologically Active Moieties on Peripheries. *Polym. Chem.* **2010**, *1*, 1650-1661.

The material is split in six chapters which introduce the polymeric drug delivery devices, the pool of chemical reactions that have been utilized in this project, the library of α,ω-hetero-telechelic poly(ε-caprolactone)s and three distinct amphiphilic structures built upon it. The dissertation is closed with a conclusion and future outlook.

The characterization methods are summarized in Appendix I, while the original publications are attached as Appendix II, III, and IV.

Chapter 1 Nanoparticles in Drug Delivery

Poorly water-soluble anticancer drugs suffer from inadequate adsorption and low bioavailability. They may aggregate and lead to different complications including local toxic effects. Therefore, half of the promising drug candidates never reach further development stage. Drug delivery and drug targeting vehicles such as synthetic polymers, micelles, liposomes, and capsules, are the subject of meticulous and prolific investigations due to their immense role in: a) reducing the drug decomposition upon administration, b) eliminating negative side effects exerted on normal cells by cytotoxic drugs, and c) enhancing drug bioavailability and concentration at the site of action. The potential of such delivery systems is further increased by tailoring their biodegradation rate, rendering them stimuli-responsive, and decorating them with various targeting moieties.[1]

There are a number of parameters that may be altered to fine-tune the properties of the above mentioned nanoparticles if intended as drug delivery devices. Conventional chemotherapy involves random delivery of toxic therapeutic agents jeopardizing normal cells and tissues. This necessitates devising delivery vehicles for more site-specific intervention. The carries for cancer treatment should be in the range of 10-100 nm to take advantage of the peculiarities of tumor vasculature.[2] Leaky, dilated, and irregularly shaped blood vessels are characteristic for cancer. Moreover, tumor tissues exhibit compromised lymphatic drainage. This implies that macromolecules are leaked into and retained in tumor tissue. This phenomenon designated the enhanced permeability and retention (EPR) effect is one of the approaches in selective targeting of the macromolecular drugs, polymer conjugates, micellar and liposomal delivery systems.[3,4] Yet another requirement for a successful carrier is a long blood circulation time.[1] This is greatly influenced by the surface properties of the nanoparticles: A high curvature and hydrophilic surface are necessary to decrease the opsonization and clearance by macrophages. “Stealthy” nanoparticles remain invisible to macrophages, and thus exhibit longer half-life in the blood compartment allowing discriminative extravasation at the diseased sites.[5] Longer circulation times alone can augment uptake in tumors.

Block copolymer micelles – spherical, nanosized supramolecular assemblies of amphiphilic copolymers with core-shell type architecture – afford enhanced bioavailability, diminished toxic effects, and increased permeability through the physiological barriers.[1] The core of the pharmaceutical polymeric micelle should display a high loading capacity and a controlled drug-release profile. Furthermore, good compatibility between the compartmentalized drug and the polymer chains that form the micellar core is necessary. The micelle corona should afford effective steric stabilization, and reactive functional groups for the modification of the micellar surface. The corona dictates micelle hydrophilicity, charge, and valency. These properties define: pharmacokinetics, biocompatibility, circulation time, biodistribution, surface adsorption, interaction with biosurfaces and targetability.[6] Poly(ethylene glycol) (PEG) has been vastly employed as the hydrophilic block for its low cost, low toxicity, effectual steric stabilization and protection, and for being approved by regulatory agencies. The hydrophobic block is often comprised of units of propylene oxide, aspartic acid, β-benzoyl-L-aspartate, γ-benzyl-L-glutamate, D,L-lactic acid, and ε-caprolactone (ε-CL).[1] Poly(ε-caprolactone) (PCL) is degraded in physiological conditions, exhibits good permeability to small pharmaceutical agents, does not alter the pH of the environment after degradation, and can be employed in prolonged delivery due to slow erosion rate, and therefore has been frequently used in bioimplants, controlled release and targeted delivery devices, and scaffolds for tissue engineering.[7] Importantly, it is approved by US Food and Drug Agency (FDA).[7] PEG-*b*-PCL micelles have been detected in various organelles of a cell as a result of non-specific uptake which considerably enhanced internalization of the

compartmentalized model agent compared to the free agent.[8] PEG-polyester vesicles provide handle for controlling the content release time by tailoring the degradation rates, and have been exploited for incorporation of hydrophilic drugs, proteins, and nucleic acids. Poly(ethylene glycol)-*b*-poly(lactic acid) (PEG-*b*-PLA) polymersomes possess a membrane core that can be loaded with hydrophobic paclitaxel and, within the interior, soluble doxorubicin as a second anticancer drug. Combination of long circulation time, EPR-effect, and controlled drug release, with the rate increasing at low pH inside the cellular endolysosomes, forge an interesting candidate for a drug delivery vehicle. Observations suggest that these polymersomes induce sustained cancer cell suicide.[9]

Sterically stabilized nanoparticles with small negative or positive surface charge exhibit minimal interactions amongst each other and the environement.[2] Although cationic systems are frequently chosen as a delivery device since they facilitate cellular uptake by a "proton sponge" effect[9], increase in the surface charge leads to enhanced macrophage scavenging and clearance by reticuloendothelial system (RES).[2,9] Hence, adjusting the surface charge density prudently may be of assistance in smuggling the payload through biological barriers.

Nanocarriers with targeting ligands exhibit superior cellular uptake via receptor-mediated endocytosis. Due to their large surface area, nanoparticulate delivery systems may contain numerous targeting motifs that permit multivalent attachment to cell-surface receptors. Since cancer cells exhibit a plethora of receptors on the surface, the targeted nanocontainers can engage numerous receptors simultaneously, and thus amplify interactions.[1,2] These pilot molecules may be sugar moieties, antibodies, transferrin, and folate residues. The last two are particularly useful since many cancer cells feature overabundance of transferrin and folate receptors.[1] For instance, it has been demonstrated that galactose- and lactose-modified micelles prepared from PEG-*b*-PLA block copolymer specifically engage lectins,[10,11] while folate moieties on PEG-*b*-poly(L-histidine) and PEG-*b*-PLLA block copolymer mixed micelles assist efficient delivery of the cargo to cancer cells *in vitro*.[12]

Another way of attaining site-specific drug delivery is by incorporating mucoadhesive hydrophilic polymers in pharmaceutical formulations. Mucoadhesion is defined as adhesion involving mucus or mucous membrane.[13,14] Mucoadhesion facilitates intimate contact with the adsorption site, and prolonged residence time of the formulation at the site of action, and thus improves bioavailability. Mucus, composed of primarily water, mucin glycoproteins, lipids, proteins, and inorganic salts, is a viscous sticky compound which serves as a lubricant. It is an obstruction for pathogens and harmful substances but is permeable to gases and nutrients. Glycoproteins create a highly entangled network of macromolecules which are held together by non-covalent bonds. Presence of pendant sialic acid (pK_a=2.6) and sulphate groups of the glycoproteins makes mucin act as an anionic polyelectrolyte at neutral pH.[14] Mucoadhesion involves interdiffusion-entanglement, and secondary interactions between the polymer material and the substrate.[13] Poly(acrylic acid) (PAA), chitosan, and sodium alginate represent the first generation mucoadhesives.[13] PAA derivatives – polycarbophil and carbomer – have been investigated for applications in drug delivery in the gastrointestinal tract. Excellent swelling and hydrogen-bonding capabilities at neutral pH ensure high affinity and binding to mucosal surfaces. Furthermore, PAA is not toxic, does not induce irritation, and is regarded as safe for oral administration by FDA.[14] Amongst numerous factors affecting mucoadhesion are: a) the density of hydrogen-bond-forming functional groups such as carboxyl, hydroxyl, amine, and sulphate; b) the degree of hydration of the polymer; c) the molecular weight facilitating

interpenetration and entanglement; d) the pH and charge defining the mechanism of mucoadhesion.[14] Drug delivery platforms featuring PAA as biocompatible and mucoadhesive component have been designed and elucidated.[15,16]

Chapter 2 Chemical Toolbox

Construction of a multifaceted, robust, and effectual nanoreservoir that amalgamates site-specific drug delivery and ablative cancer therapy demands a pool of synthetic techniques that allow preparation of well-defined macromolecules with precisely controlled type and number of functional groups. These synthetic tools should be highly efficient and reliable, and easy to implement. This chapter gives an overview of the synthetic means that have been put in practice in the project.

2.1 Ring-Opening Polymerization

Polymeric drug delivery devices often consist of aliphatic polyesters, polyethers, polyamides, polyanhydrides, and polyurethanes. These synthetic polymers exhibit biodegradability and biocompatibility.[17] Polyesters intended for the drug and gene delivery or tissue engineering applications must display controlled biodegradation rate, bioadherence, and suitable glass transition temperature and crystallinity.[17,18] Ring-opening polymerization (ROP) allows synthesis of the polymers with predetermined molecular weight characteristics under mild reaction conditions from lactones of various ring-size and with or without different pendant functional groups. Furthermore, plethora of functional initiators permits incorporation of specific end functionalities.[17,18] Thus, ROP facilitates construction of the polyesters with tailor-made properties. Cyclic monomers that have been polymerized via ROP include ε-CL, δ-valerolactone (δ-VL), β-butyrolactone, lactide, and glycolide.[18]

ROP encompasses mechanisms involving anionic, cationic, and coordinative initiating species.[17] While ionic species engage in adverse inter- and intramolecular transesterification reactions responsible for decreasing the molecular weight and broadening the molecular weight distribution (MWD), the organometallic compounds that incorporate metals possessing *d*-orbitals of favorable energy establish good control over the polymerization reaction. Provided the reaction conditions are appropriately adjusted, ROP of lactones and lactides is a living/controlled process resulting in the polymer of predetermined molecular weight and narrow MWD. ROP involves two major mechanistic routes defined by the organometallics used: a) monomer activation by catalyst complexation with the carbonyl group of the monomer followed by nucleophilic attack by any nucleophile present in the polymerization mixture, and b) coordination-insertion – metal alkoxide's coordination with the carbonyl group of the monomer followed by the rupture of the acyl-oxygen bond of the monomer and insertion into the metal-alkoxide bond.[17]

The following paragraphs elucidate advantages and limitations of the metal-based catalytic systems in the ROP of ε-CL, and thus justify the catalyst of choice for this project.

Alkali metal-based catalysts support the polymerization through the anionic mechanism. Therefore, the transesterification reactions intrinsic to the anionic route deteriorate control. Employing alkaline earth metals such as magnesium and calcium is rather appealing since they exhibit high activity and low toxicity. In case of magnesium complexes the polymerization is initiated via insertion of alkyl or alkoxy groups into the monomer depending whether an alcohol is used as the initiator. Calcium-based catalysts trigger the polymerization via coordination-insertion mechanism: cleavage of the acyl-oxygen bond of the monomer is followed by the insertion into the calcium-oxygen bond of the calcium alkoxide. Termination is accomplished by addition of an acid. Both catalytic systems provide polymers with medium to high molecular weights and a broad range of MWD.[19]

Aluminum- and tin-based systems are the ones most frequently used in ROP of ε-CL.[19] Aluminum is not as active a catalyst as many other metals employed in the ROP of lactones, but it offers good control over the polymerization reaction.[19] Aluminum (III) triflate has been shown to be active in the ROP of ε-CL initiated by glycerol. The polymerization displays living character, but is accompanied by a small share of transesterification reactions, and results in a fairly high polydispersity index (PDI) (1.94).[20] ROP of ε-CL catalyzed by triethylaluminum-amine and diethylaluminum ω-amino alkoxide complexes has been carried out resulting in mono- and difunctional polymers with moderate PDI. Coordination-insertion mechanism – insertion of the monomer into the O-Al bond present at the growing chain end – is reported to be responsible for the ROP.[21] One of the most scrutinized catalytic system for the ROP of ε-CL is aluminum (III) isopropoxide, which affords excellent control while suppressing intramolecular transesterification and backbiting reactions.[19] The major shortcoming of using $Al(O^iPr)_3$ is the forced presence of the isopropoxide chain end. However, it can be remedied by employing triethyl aluminum as a catalyst and a functional alcohol as an initiator.[18] In general, aluminum alkoxides (Et_2AlOR, $EtAl(OR)_2$, and $Al(OR)_3$) provide high selectivity, good control over the molecular weight and chain end functionalities of polyesters. α-Terminus of the polyester chain is capped by RO – the alkoxy group of the initiator, while the hydrolysis of the propagating chains affords ω-hydroxyl end-group. However, different nucleophiles can be employed to terminate the chains with desirable functionality. High degree of control over the polymerization reaction allows preparation of various macromolecular architectures including comb, star, graft, and hyperbranched (co)polyesters.[17] Numerous aluminum Schiff base complexes have also been utilized in the ROP of ε-CL.[19]

Stannous (II) ethylhexanoate (tin octoate, $Sn(Oct)_2$) is the most frequent catalyst of choice for the ROP of ε-CL. The advantages which tin octoate offers are commercial availability, ease of handling, efficiency, and solubility in numerous organic solvents. In combination with an alcohol, tin octoate allows synthesis of the polymer in a controlled manner.[19] The polymerization mechanism consists of transformation of $Sn(Oct)_2$ into tin alkoxide upon reaction with an alcohol, and a subsequent coordination-insertion step. Hence, the molecular weight of the polymer can be tuned by adjusting the monomer-to-alcohol molar ratio.[17] Thus, together with the alcohol initiators with embedded functionalities, this simple catalytic system affords excellent control over the molecular weight, and ensures near to quantitative integration of end-groups.[18] Furthermore, it has been approved by FDA as a food additive.[17] The disadvantage of tin octoate is the necessity of applying elevated temperatures to the reaction mixture provoking inter- and intramolecular esterification reactions which broaden the MWD.[19] Penczek *et al*.[22] and Duda *et al*.[23] have elucidated the mechanism of the tin octoate catalyzed ROP of ε-CL, and concluded the following: a) the polymerization is living; b) the added alcohol serves as the initiator when it is introduced in a level up to twice the amount of the catalyst and assumes the role of the chain transfer agent too when introduced in a greater excess; c) the liberated octanoic acid retards the polymerization rate by reversibly decreasing the number of instantaneously growing centers; d) the polymerization proceeds via the monomer insertion in Sn-O bond of the tin alkoxide. Other tin-based catalytic complexes such as tin triflate and dibutyltin dimethoxide, have also been employed.[19]

An extensive survey of the metal catalysts for the polymerization of ε-CL is presented in a couple of recent reviews.[19,24]

Besides polymerizations mediated by the metal-based catalytic complexes, enzymatic ROP (eROP) has also been exercised for preparation PCL. Since it is crucial for biomedical applications to avoid toxic metallic

contaminants, the eROP seems to be an attractive alternative. Lipase-catalyzed eROP of ε-CL has been investigated thoroughly. The degree of control in eROP is inferior to that attained in chemical ROP, with PDI being higher than 2.[17] However, the chemoselective enzymatic catalyst affords incorporation of various terminal functional groups without protection and deprotection chemistries.[19]

"All-organic" initiating systems include *n*-BuOH/HCl·Et_2O combination – cationic catalyst for the controlled ROP of ε-CL and δ-VL.[17,25] The nucleophilic catalysts such as phosphines, tertiary amines, *N*-imidazolium carbenes, and thiazaolium carbenes have been used in the ROP of lactide initiated by alcohols. The mechanism involves nucleophilic attack of the catalyst on the carbonyl group of the monomer resulting in the formation of an active intermediate that can react with an alcohol.[17] Aza-compounds, phosphazene bases, and various organic acids can also serve as catalysts in ROP of ε-CL.[19]

Derivatization of aliphatic polyesters is more demanding and painstaking than that of non degradable polymers. The reaction conditions that result in rupture of the ester bonds may lead to premature polymer decomposition. Therefore, substantial investigations have been conducted for developing the ways for preparation of functional polyesters. Incorporation of the functional groups along the polyester backbone may be achieved through polymerization of the monomers containing functional groups in α- or γ-position, or by attaching functionalities in the α-position of the carbonyl of the preformed chain.[17]

ε-CL substituted by acrylate,[26] protected hydroxyl group,[27] bromide,[28] and PEG[29] have been prepared, and then homo- and copolymerized by ROP. ε-CL with a pendant acrylate group is a difunctional monomer that can be polymerized by both ROP and controlled radical polymerization (CRP) in a living/controlled way.[26] PCL with protected hydroxyl groups along the chain is an excellent macromolecular scaffold for initiation of ROP of various monomers. Making use of orthogonal protecting groups allows selective deprotection and grafting from the PCL macroinitiator.[27] Introducing these functional groups along the polymer chain allows myriads of chemical transformations resulting in the polyesters with desirable properties. For instance, brominated homo- and copolymers of ε-CL have been quaternized by pyridine yielding in degradable polycations that form nanoparticles with a strong interaction with plasmid DNA.[30] Incorporation of pendant hydroxyl groups leads to the polyesters with amphiphilic nature. The amphiphilic PCL-*g*-PEG with a comb-like structure comprising biodegradable hydrophobic backbone has been prepared by the ROP of ε-CL bearing PEG substituent.[31] The major downside of using substituted lactones is the necessity of protecting those functional groups that may interfere with metal alkoxides during the ROP. Also, the deprotection protocol must be mild enough in order to retain the polyester backbone intact.[17]

Coupling of ROP of ε-CL with other polymerization techniques as well as modification of preformed PCL chains shall be discussed later in this chapter.

2.2 Atom Transfer Radical Polymerization

CRP techniques involve suppressing the chain breaking reactions, and synchronized chain growth attained by almost instantaneous initiation. CRP is built on the idea of sporadic formation of active propagating radicals that are reversibly deactivated to thwart the termination reactions. It is this dynamic equilibrium between the propagating species and dormant entities that permits conducting the polymerization in a controlled fashion. This reversible deactivation is a consequence of the persistent radical effect (PRE) in atom transfer radical polymerization (ATRP).[32]

ATRP is centered on the distinct combination of the transition metal (Mt^n) with an aptitude for expanding its coordination sphere and increasing its oxidation number, a complexing ligand (L), and a counterion which is capable of covalently or ionicly bonding with the metal center. Such catalytic complex is a subject of virtually innumerable permutations, and thus allows fine-tuning of the polymerization parameters.[32]

Abundance of commercially available initiators makes ATRP more appealing than other CRP techniques. Species, which contain halogen atoms activated by α-carbonyl, cyano, vinyl or phenyl groups, serve as effective ATRP initiators. The bond dissociation energy of the alkyl halide determines the initiator's reactivity. Also, the degree of substitution, the leaving group, and the nature of the radical stabilizing group dramatically influence the activation rate constants. The homolytic cleavage of the initiator's alkyl halogen bond (R-X) by the transition metal complex (Mt^n-L) produces an organic radical R· and the new metal halide complex (Mt^{n+1}X-L) where the metal center has a higher oxidation state. This step is characterized by the activation rate constant k_{act}. The organic radical R· is capable of: a) propagation by reacting with a vinyl monomer – defined by the propagation rate constant k_p, b) termination by bimolecular coupling or disproportionation – characterized by the termination rate constant k_t, and c) reversible deactivation providing a dormant polymer chain capped with the halogen atom and regenerating the catalytic complex (Mt^n-L) – marked by the deactivation rate constant k_{deact}. The bimolecular termination reactions in the early phase of ATRP are responsible for the buildup of the persistent radical, which shifts the ATRP equilibrium, defined as $K_{ATRP}=k_{act}/k_{deact}$, towards the dormant species, and thus suppresses the chain-breaking reactions.[32]

Numerous transition metals, including Ru, Ni, and Cu, have proved to be efficient in catalyzing ATRP. The copper-based catalytic systems have been vastly employed in ATRP of variety of monomers in a wide range of reaction media. The ATRP equilibrium can be tailored by manipulating with the complexing ligands, which frequently comprise of the derivatives of bidentate bipyridine, tridentate diethylenetriamine, and tetradentate tris(2-aminoethyl)amine for the copper-based systems. Besides the structure of the initiating species, the k_{act} is influenced by the complexing ligand activity, which is determined by the linking unit between the nitrogen atoms and the coordination angle, the topology (cyclic, linear, or branched), the class (aromatic amine/imine, aliphatic amine/imine), and the steric bulk around the metal center.[32] Nickel-based catalytic complex frequently consists of phosphorus-containing ligands.[33] Besides fine-tuning the ATRP equilibrium, a ligand renders the transition metal salt soluble in organic milieu.[34]

The polymerization rate is proportional to the initial initiator concentration and the molar ratio of the activator to deactivator. Narrow MWD can be obtained at adequate deactivator concentration, high rate of deactivation, and high monomer conversion. Fast activation and deactivation are the necessary requirements to establish good control over the polymerization reaction.[32]

ATRP facilitates the synthesis of (co)polymers of various architecture – linear, comb, star, and dendritic – in a controlled manner with predetermined molecular weight and narrow MWD.[35] Furthermore, ATRP allows incorporation of numerous functional groups along the polymer chain by polymerization of functional monomers, and at the terminal of the polymeric backbone by employing functional initiators or by modification of the alkyl halide chain end. Applications of ATRP for preparation of polymer-biomolecule hybrids, biodegradable polymers and networks, star-like and hyperbranched polymers, and for surface modification are addressed in a recent review by Matyjaszewski and Tsarevsky.[35]

2.3 Cu^{I}-Catalyzed Azide-Alkyne Cycloaddition

The Cu (I)-mediated azide-alkyne 1,3-cycloaddition (CuAAC), also referred as Cu^{I}-catalyzed "click" reaction, is a quantitative and regioselective reaction[36,37] that has been firmly established as a flexible, orthogonal, and efficient tool in polymer synthesis. There are a number of extensive reviews that detail the application of CuAAC in the field of polymer chemistry ranging from the assembly of polymeric fragments into more sophisticated architectures to derivatization of functionalities along or at the termini of macromolecules.[38,39,40] ATRP and CuAAC have been successfully combined by making use of alkyne- and azide-functionalized initiators, by introducing the azide functional group at the alkyl halide chain end, and by employing monomers bearing pendant azido- and acetylenic moieties.[39] A library of complex macromolecular structures including graft, star, dendritic, and dendronized (co)polymers have also been prepared.[40]

This section will cover a few examples of the implementation of the Cu^{I}-catalyzed "click" reaction in the modification of aliphatic polyesters prepared by ROP. Aliphatic polyesters with pendant or terminal functionalities have been synthesized, and grafted with diverse functional groups and macromolecular segments (Fig. 2.1).[41]

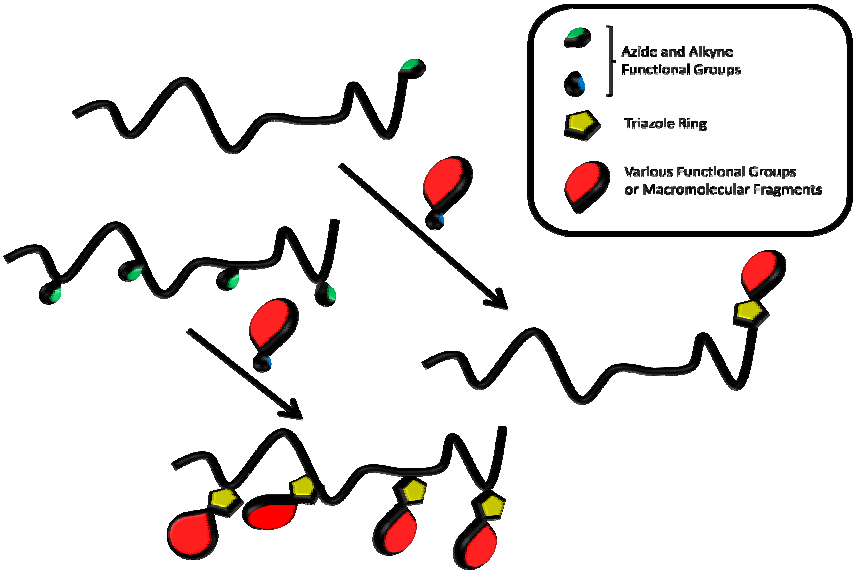

Figure 2.1 Schematic representation of the derivatization of aliphatic polyesters by CuAAC.

Thus, PCL with alkyne end-group has been conjugated with azide containing sugar moieties. These amphiphiles appear to form vesicle-type aggregates in water.[42] PCL chains with the azide functionalities along the backbone have been grafted with hydroxyl, acrylate, and ATRP initiating groups. Moreover, PCL-*g*-PEG has been synthesized by cycloaddition of the alkyne terminated PEG onto the preformed PCL chain.[43] A potent anticancer drug camptothecin, incorporating azido moiety, and PEG-N_3 have been ligated to the copolymer of ε-CL and δ-VL, which possessed pendant acetylenic fragments linked to the δ-VL repeating units, to afford water soluble and biodegradable drug delivery device.[44] In a similar approach, the PEG-N_3

and azide-terminated peptide sequence GRGDS were conjugated to the aliphatic polyesters with the acetylenic moieties along the backbone.[45] Amphiphilic PEG-*b*-PS-*b*-PCL has been prepared by Cu^{I}-catalyzed "click" coupling of the PEG-*b*-PS-N_3 block copolymer, obtained by ATRP of styrene from the PEG macroinitiator and end-group modification by a nucleophilic substitution with sodium azide, to the α-propargyl-PCL synthesized by ROP.[46]

2.4 Thiol-Ene Reaction

Thiol-ene reaction, which has been regarded as a "click" reaction, has emerged in polymer synthesis as a simple, facile, resourceful and orthogonal means due to its tolerance to various reaction conditions, and a range of easily accessible starting materials.[47] Furthermore, thiol-ene reactions are rapid, can be conducted in the presence of oxygen and moisture, and lead to the corresponding thioether in a near quantitative yield.[48] Thiol-ene reactions comprise of the radical addition of thiols to the electron rich enes, and the Michael-type addition of thiols to the electron deficient enes. The reaction mechanisms and the application of these reactions in the synthesis of myriads of functional materials have been scrupulously discussed in a number of recent reviews.[47-50] Since this study involves the radical thiol-ene "click" reaction, this section will introduce a handful from numerous examples of preparation and derivatization of macromolecules with thiol-ene coupling.

Schlaad and co-workers have reported modification of 1,2-polybutadiene homo- and block copolymers with ω-functional mercaptans incorporating various functionalities via free-radical addition.[51] Availability of a vast number of thiols allows facile preparation of polymers with desirable functional groups along the chain. However, the degree of functionalization lower than quantitative is reported. In another example, Schlaad and co-workers derivatized poly(2-(3-butenyl)-2-oxazoline) by employing 1.2-1.5 equivalents of the thiol with respect to the unsaturation, and triggering the reaction by exposure to UV light without additional initiator.[52] Hawker *et al*. demonstrated the specificity and reliability of the thiol-ene "click" reaction by constructing dendrimers and functionalizing the chain ends.[53] The thiol-ene photochemical coupling was utilized in conjunction with epoxy-amine reaction for building internally functionalized dendrimers.[54] Hawker and co-workers investigated efficiency of photochemically and thermally induced thiol-ene "click" couplings in modification of the terminal and pendant unsaturations of different polymeric backbones including PCL. The compatibility of the thiol-ene reaction with various functional groups was validated by linking a wide range of mercaptans to the unsaturations with photochemically initiated addition displaying higher efficiency and shorter reaction times. The orthogonality was verified by stepwise derivatization of a hetero-bifunctional polymer by thiol-ene and CuAAC reactions.[55] Allyl functionalized polyester nanoparticles have been ligated with dendritic transporter moieties bearing a thiol group at the focal point and linear and cyclic peptides by thiol-ene reaction in the absence of an initiator. These bioconjugates have potential to target tumor vasculature.[56] Waldmann and Niemeyer and co-workers have adopted the thiol-ene coupling to afford covalent patterning of surfaces with proteins and small molecules.[57]

The Ph. D. project integrates all four synthetic tools amongst others to generate multifunctional amphiphilic macromolecules in a controlled fashion. Some combinations of these techniques for preparation of topologically distinct amphiphiles with the PCL hydrophobic segment are summarized in Table 2.1.

Table 2.1 Amphiphilic Block, Star, and Graft Copolymers Featuring PCL as the Hydrophobic Component.

Hydrophilic Component and Topology			Comments
Block	*Star*	*Graft*	
Dextran			The block copolymer Dextran-S-S-PCL is prepared by coupling PCL-SH with orthopyridyl disulfide end-capped dextran. Doxorubicin-loaded micelles exhibit rapid internalization and drug release inside cells, which is ascribed to the disulfide bridge rupture induced by glutathione present in the intracellular compartments.[58]
	PEG		Per-6-(*tert*-butyldimethylsilyl)-β-cyclodextrin is employed as the multifunctional initiator in the ROP of ε-CL catalyzed by $Sn(Oct)_2$ to generate 14-arm PCL star polymer. The terminal hydroxyl groups of PCL arms are conjugated with a model drug ibuprofen. CuAAC is utilized to link 7 PEG chains to the cyclodextrin core. These miktoarm star copolymers assemble into spherical as well as wormlike aggregates in water.[59]
Poly(L-lysine)			ROP of ε-CL catalyzed by $Sn(Oct)_2$ is performed using amino-terminated poly(Z-L-lysine) as the macroinitiator. After deblocking of the amine functional groups, poly(L-lysine)-*b*-PCL forms core-shell type and vesicular morphologies depending on the ratio of hydrophilic and hydrophobic blocks.[60]
	Poly(mPEGMA)		$Sn(Oct)_2$ catalyzed ROP of ε-CL using pentaerythritol and dipentaerythritol as the initiators results in 4- and 6-arm star-shaped structures, respectively. The derivatization of hydroxyl end-groups of PCL arms by 2-bromo 2-methylpropionyl bromide (BMPB) is followed by CuBr/ *N,N,N´,N´,N´´*-pentamethyldiethylenetriamine (PMDETA) mediated ATRP of PEG methyl ether methacrylate (mPEGMA). The star block copolymers exist as unimers in water. Compartmentalization of dyes and commercially available drugs is demonstrated.[61]
	PAA		$Sn(Oct)_2$ catalyzed ROP ε-CL is conducted employing hydroxypropylcellulose (HPC) as a multifunctional initiating scaffold to obtain biocompatible comb copolymer. Modification of the hydroxyl termini of the PCL grafts with BMPB, and subsequent CuBr/PMDETA mediated ATRP of *tert*-butyl acrylate (*t*BA) afford HPC-*g*-PCL-*b*-P*t*BA. Deprotection of P*t*BA block, and cross-linking using a diamine cross-linker provide amphiphilic HPC-*g*-PCL-*b*-PAA, which displays capacity of encapsulating pyrene in water.[62]
	PAA		Boltron HBP H40 hyperbranched polyester serves as the multifunctional initiator in $Sn(Oct)_2$ catalyzed ROP of ε-CL. The hydroxyl end-groups of the obtained star-shaped polymer are converted to the activated halides by reacting with BMPB. ATRP of *t*BA is catalyzed by CuBr/2,2′-bipyridyl complex. Removal of *tert*-butyl protecting groups leads to amphiphilic star block copolymer capable of encapsulating small hydrophobic and volatile molecules such as fragrances.[63]
PDMAEMA			Poly(*N*,*N*-dimethylamino-2-ethyl methacrylate) (PDMAEMA) is a pH- and temperature-responsive polymer; it can be absorbed by endocytosis, and can be utilized as a nonviral DNA vector. The following synthetic protocol is exercised: ROP of ε-CL initiated by $Al(O^iPr)_3$, end-functionalization with BMPB to obtain the ATRP initiating sites, and subsequent CuBr/1,1,4,7,10,10-hexamethyltriethylenetetramine (HMTETA) catalyzed ATRP of DMAEMA. Size of the micelles depends on the copolymer concentration, pH, and the relative amount of PCL.[64]
		PDMAEMA	ROP of α-propargyl-ε-CL together with ε-CL is followed by conjugation of the α-azido-PDMAEMA chains to the polyester backbone by CuAAC. Water soluble copolymers are prepared by quaternization of the amino groups with methyl iodide. The graft copolymers assemble in core-shell type structures. These micelles can be loaded with a hydrophobic drug clofazimine.[65]
PEG			The average block proportions in PEG-*b*-PCL determine the dominant morphology of the block copolymer aggregates in aqueous solutions. Giant and flexible worm micelles are prepared. "Chain-end cleavage" of the PCL block triggers worm-to-sphere transition.[66]
		PEG	Michael-type addition has been exercised to graft PEG chains onto a PCL backbone. Initially, PCL possessing pendant acrylate functional groups has been prepared by the copolymerization of γ-acryloyloxy-ε-CL with ε-CL. Then PEG-SH has been linked to the PCL backbone in a base-catalyzed Michael-type addition. The reaction conditions are particularly suitable for delicate polyester chains.[56]

Chapter 3 Library of α,ω-Hetero-bifunctional Poly(ε-caprolactone)s: Cornerstone for Building Multivalent Amphiphiles

Introduction

As evident from the previous chapter, ROP of cyclic esters allows preparation of hetero-telechelic macromolecules incorporating desirable end-functionalities. This can easily be accomplished by employing functional initiators. PCL bearing primary bromide, *n*-alkene, or methacrylic function at the α-terminus has been obtained by ROP of ε-CL making use of functional aluminum alkoxides. Hydrolysis of the growing site results in ω-hydroxyl terminated polymers.[68] α-Methacryloyl-PCL, ω-methacryloyl-PCL, and α,ω-dimethacryloyl-PCL have been prepared by Jérôme *et al*.[69] The latter has been synthesized by initiating the ROP with diethylaluminum 2-hydroxyethyl methacrylate, and terminating it by reacting with methacryloyl chloride. Graft copolymer PHEMA-*g*-PCL has then been prepared through copolymerization of the PCL macromonomer with HEMA under free radical polymerization conditions. Jérôme *et al*. have reported the synthesis of α-amino-PCL through the ROP of ε-CL initiated by diethylaluminum 12-bromo-1-dodecyl oxide followed by conversion of the primary bromide into azide by nucleophilic substitution with sodium azide, and by reduction of the latter into a primary amine in the presence of triphenylphosphine (TPP).[70] Yagci *et al*. have obtained PCL macroinitiators for photochemically initiated polymerization of methyl methacrylate (MMA).[71] This is achieved by conducting ROP of ε-CL using benzoin or other photolabile species as initiators and $Sn(Oct)_2$ as catalyst. The PCL chain containing the residue of any of these photoinitiators is capable of triggering polymerization of MMA upon UV irradiation. Hilborn and Hedrick and co-workers have accomplished synthesis of PCL bearing thiol functional group at the α-terminus.[72,73] ROP is initiated by α-(2,4-dinitrophenylthio)ethanol/Al complex. Removal of the protecting group affords macrothiols of controlled molecular architecture. Incorporation of thiol functional group at PCL chain end has been attained by eROP of ε-CL employing 2-mercaptoethanol as the initiator as well.[74] Such an approach, built around the catalyst's chemoselectivity between thiols and alcohols, negates necessity of protection and deprotection steps. However, initiation from the thiol function cannot be altogether eliminated. Schubert and co-workers have carried out ROP of ε-CL using 5-hexyn-1-ol and $Sn(Oct)_2$ as the initiator and catalyst, respectively.[75] PCL with high end-group fidelity has been obtained and engaged in building star-shaped polymer via CuAAC. In a similar fashion, Hizal and Tunca and co-workers have synthesized α-alkyne-functional PCL by making use of the propargyl alcohol/$Sn(Oct)_2$ system. Subsequent CuAAC in combination with Diels-Alder reaction results in ABC triblock copolymer.[76] ROP of ε-CL has been conducted under enzymatic conditions employing *trans*,*trans*-2,4-hexadien-1-ol as the initiator resulting in a polymer with a PDI of 1.37. PS-*b*-PCL has then been prepared by hetero Diels-Alder cycloaddition of the dithioester-terminated PS obtained by RAFT polymerization to the PCL incorporating diene at the chain end.[77] Scherman and Celiz have reported about the synthesis of PCL possessing terminal hydrogen-bonding moiety inherited from the initiator.[78] ROP has been catalyzed by $Sn(Oct)_2$. Polymers with fairly broad MWD have been obtained due to reversible interactions of the initiating species under the polymerization conditions. Besides alkyne-functional PCL, PCL with azide end-group has also been prepared through the $Sn(Oct)_2$ catalyzed ROP with 3-azidopropanol assuming the role of the initiator.[79] Polymers with low PDI have been obtained, and further derivatized by reacting with 4-pentynoic anhydride resulting in α-azido-ω-ethynyl-PCL, which has been cyclized via CuAAC.

Result and Discussions

α,ω-Hetero-bifunctional PCLs, which have been prepared and exploited in this work, are summarized in Scheme 3.1. Coupling of ROP with ATRP for preparation of well-defined block copolymers can be attained by making use of double-headed initiators.[80] The sequence of the polymerization reactions where ROP is followed by ATRP has been chosen to avoid rigorous purification of the macroinitiator intended for the ROP of ε-CL. Thus, the dual initiator 2-hydroxyethyl 2-bromoisobutyrate (HEBI) furnished hetero-bifunctional PCL incorporating α-bromoester and ω-hydroxyl end groups (Scheme 3.1, **1-0**). The polymerization was catalyzed by $Sn(Oct)_2$, thus eluding an additional step associated with the preparation of functional aluminum alkoxides. Furthermore, $Sn(Oct)_2$ is easier to handle, making it a suitable candidate for a less scrupulous reaction setup. Undesirable side reactions that could be induced by the high initial catalyst concentration (~0.05 M) and low initial initiator to catalyst molar ratio (~2.2) were thwarted by carrying out the polymerization at low temperature (62 °C) and thus evading or diminishing the contribution of the collateral esterification and transesterification reactions involving HEBI and the displaced octanoic acid.[19,22,81] The monomer conversion estimated gravimetrically was about 59.6%, which implies that the degree of polymerization (DP) of 32 has been achieved. The DP approximated by ^{1}H NMR spectroscopy was 30. This, in concert with unimodal and symmetrical size exclusion chromatography (SEC) trace and low PDI (1.09), signifies near to quantitative integration of the dual initiator and negligible share of side reactions. Thus, superior control over the reaction is attained under these conditions rather than when lower catalyst concentration, higher temperature, and extended reaction time are utilized.[82] These reaction conditions have been applied throughout the project while employing various functional initiators (Scheme 3.1).

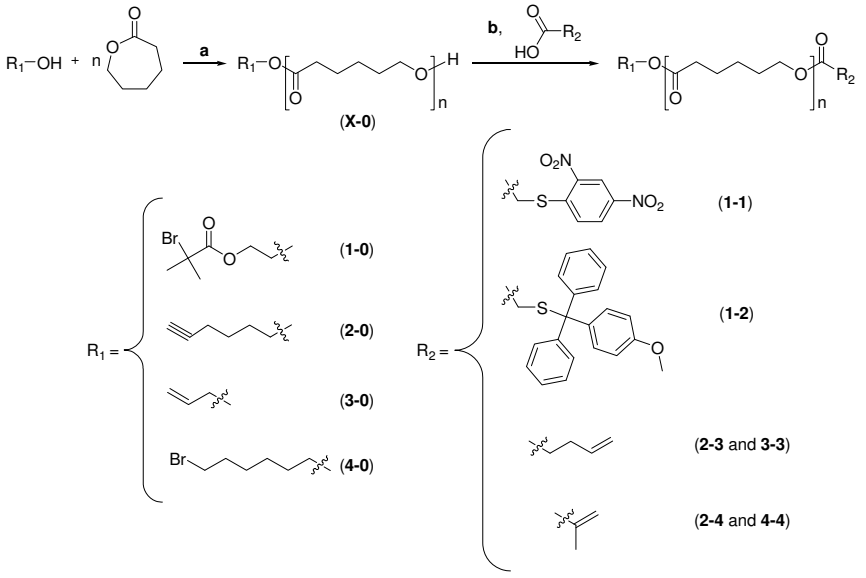

Scheme 3.1 Synthetic pathway leading to α,ω-hetero-bifunctional PCLs. Reagents and conditions: (a) $Sn(Oct)_2$, THF, 62 °C; (b) DEAD, TPP, THF, RT. PCL with ω-hydroxyl group is designated as X-0 where X (X=1,…4) denotes the functional initiators. The functional groups incorporated at the ω-chain end by Mitsunobu esterification are designated with numbers from 1 to 4 as well.

ω-Hydroxyl functionality facilitates further transformations, and allows preparation of macromolecules with precisely controlled structure. Such α,ω-hetero-bifunctional PCLs are versatile building blocks, and manipulation with end-groups permits not only marriage of mechanistically distinct polymerization techniques, but also expands the scope of applications of PCL as a resourceful biodegradable and biocompatible component. As discussed in the introduction, PCL – a splendid habitat for hydrophobic drugs – is frequently used when constructing drug delivery devices. Therefore, it is a step forward to build a library of functional PCLs with enhanced potential as constituents of complex amphiphilic architectures.

In order to introduce a latent thiol function at the ω terminus of **1-0**, the ω-hydroxyl group was reacted with α-(2,4-dinitrophenylthio)acetic acid (dNPTAA) using diethyl azodicarboxylate (DEAD) and TPP following the modification of the synthetic pathway previously applied by Hedrick and Hilborn and co-workers.[83] The modification includes substituting diisopropyl azodicarboxylate with DEAD, and more importantly, increasing the equivalents of dNPTAA, DEAD, and TPP relative to the ω-hydroxyl functionality in order to achieve near to quantitative conversion (estimated from ^{1}H NMR data). Slight excess of dNPTAA in comparison to DEAD was taken to ensure the protonation of DEAD to certain extent, and thus preventing it from attacking the polyester backbone. Monomodal SEC trace and narrow polydispersity (1.08) point to the absence of any side reactions. However, removal of 2,4-dinitrophenyl protecting group is carried out under basic conditions; it is reversible, and requires large excess of low molecular weight mercaptan to shift the equilibrium to the macrothiol.[72,73] Mercaptans are disposed to auto-oxidation and disulfide formation in basic conditions.[84] Therefore, it would be beneficial to employ the thiol protecting group which could be irreversibly eliminated under acidic conditions that are mild enough to retain the polyester chain intact. 4-Monomethoxytrityl (Mmt) group has been successfully utilized in peptide chemistry as a sulfhydryl protection for mercapto acids: it can be irreversibly removed in tandem with *tert*-butyl ester groups when treated with trifluoroacetic acid (TFA) in CH_2Cl_2/triethylsilane (TES).[85] Esterification of **1-0** with α-(4-monomethoxytritylthio)acetic acid (MmtTAA) was performed in a similar manner as for dNPTAA. The obtained Br-PCL-MmtTA (**1-2**, Scheme 3.1) displayed near to quantitative degree of functionalization and low PDI (<1.1). The molecular weight characteristics of these macroinitiators are summarized in Table 3.1.

Table 3.1 Molecular weight characteristics of α,ω-hetero-bifunctional PCLs estimated by SEC and ^{1}H NMR.

compound	M_n [a] (Da)	M_n [b] (Da)	M_w/M_n [b]
1-1	3880	6200	1.08
1-2	3990	6300	1.09
2-3	2460	4100	1.11
2-4	2560	4300	1.09
3-3	1620	2500	1.13
4-4	3560	4600	1.09

[a] By ^{1}H NMR. [b] By SEC (PS calibration).

Hence, synthesis of the PCL macroinitiators featuring masked thiol functionality has been accomplished. Utilization of both base-labile and acid-labile thiol-protecting groups increases the degree of freedom when choosing monomers for ATRP, and provides a means for broadening the library of macrothiols.

α-Alkynyl-PCL (**2-0**) with the low PDI (1.11) and high end-group fidelity has been prepared through the ROP initiated by 5-hexyn-1-ol. The DP estimated by ^{1}H NMR spectroscopy was 20. Esterification of the ω-hydroxyl terminus with 4-pentenoic acid, according to the above-mentioned Mitsunobu protocol, furnished

hetero-bifunctional PCL incorporating terminal alkyne and alkene functional groups (**2-3**). The α-alkynyl-ω-alkenyl-PCL exhibited narrow MWD (PDI=1.11). Near to quantitative functionalization was validated by the ^{1}H NMR and MALDI-TOF analysis data (Fig. 3.1). The MALDI-TOF spectrum displays signal spacing of approximately 114 Da, which corresponds to the molecular weight of one repeating unit in the PCL chain.

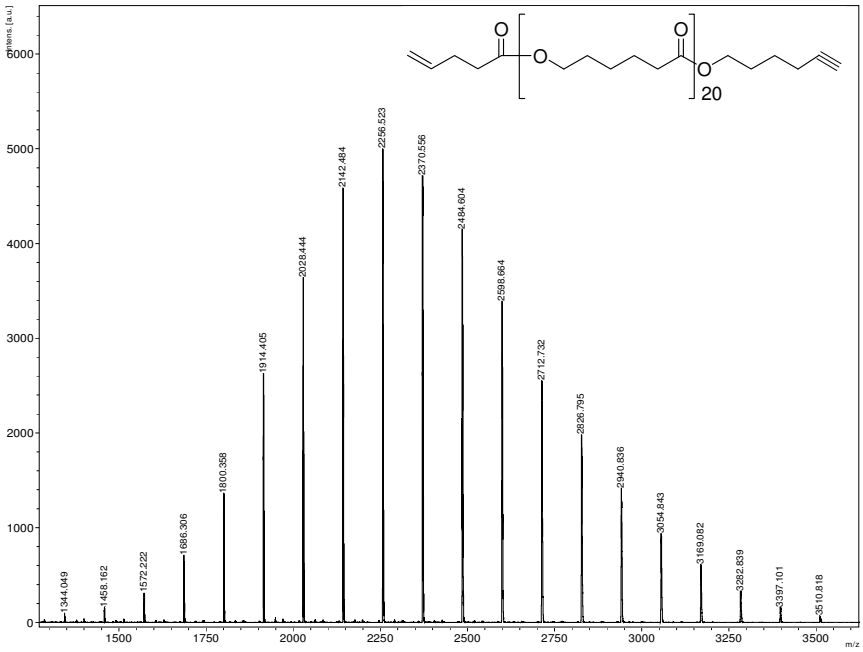

Figure 3.1 MALDI-TOF spectrum of α-alkynyl-ω-alkenyl-PCL (2-3).

PCL **2-3** possessing terminal alkyne and alkene groups, represents a multifaceted element in the toolbox for building sophisticated macromolecular designs. It can engage in orthogonal CuAAC and thiol-ene "click" reaction. Thus, PCL **2-3** may be employed for preparation of block-, graft- and star polymers, and for conjugation of biologically active molecules.

Esterification of **2-0** with methacrylic acid (MA) resulted in α-alkynyl-ω-methacryloyl-PCL (**2-4**). While Jérôme *et al*. conducted the esterification assisted by *N*,*N*'-dicyclohexylcarbodiimide (DCC)/4-(dimethylamino)pyridine combination (4-DMAP),[69] traditional Mitsunobu conditions were chosen in case of **2-0**. **2-4**, with low PDI (Table 3.1) and high end-group content, is a novel macromonomer (MM) for ATRP with a potential to be derivatized by CuAAC. However, it is imperative that ATRP follows CuAAC to avoid undesirable participation of the α-alkynyl group in radical reactions. It would be advantageous to synthesize PCL MM which can engage in ATRP and Cu^{I}-catalyzed "click" reaction irrespective of the reaction sequence. α-Azido-ω-methacryloyl-PCL is envisioned as such a MM since ATRP conditions can be tolerated by azide functions.

Synthetic pathways leading to azide functional PCL involve either nucleophilic substitution of α-bromo terminus of α-bromo-ω-hydroxyl-PCL by sodium azide[70] or ROP of ε-CL initiated by an azide containing initiator.[79] The latter bears the risk of reducing the azide functional groups by TPP in the ensuing step of

Mitsunobu coupling of α-azido-ω-hydroxyl-PCL and MA.[70] Therefore, the route considering the conversion of bromo termini to corresponding azides after the esterification reaction has been chosen. This implies that α-bromo-ω-methacryloyl-PCL (**4-4**) is prepared first. ROP of ε-CL initiated by diethylaluminum 2-bromoethoxide and diethylaluminum 12-bromo-1-dodecyloxide in toluene at 25 °C has resulted in well-defined macromolecules.[70] Therefore, initially the polymerization was carried out in THF at 62 °C utilizing 2-bromoethanol and $Sn(Oct)_2$ as initiator and catalyst, respectively. However, poor control over the reaction was observed: the SEC trace was unsymmetrical, and the PDI was relatively high (1.24). The reaction rate was higher compared to the reactions when HEBI and 5-hexyn-1-ol were used as the initiators. This may be attributed to the inductive effects originating from the close proximity of Br and O atoms in 2-bromoethanol. Indeed, when 6-bromo-1-hexanol was employed as the initiator, the polymerization proceeded smoothly, and the SEC experiment produced a monomodal, symmetrical trace and a low PDI of 1.09. α-Bromo-ω-hydroxyl-PCL with the DP of 22, 29, and 41 has been prepared. Afterwards, the hydroxy chain end of **4-0** was reacted with MA. Near to quantitative functionalization was confirmed by ^{1}H NMR experiment. Two-fold precipitation in MeOH was sufficient to eliminate the excess of TPP. This is important since TPP may reduce the azide end groups in the reaction concurrent to the nucleophilic substitution of the bromo termini by NaN_3. After the reaction, the PDI was unchanged, which implies that the polyester backbone did not suffer degradation. Thus, α-bromo-ω-methacryloyl-PCLs (Scheme 3.1, **4-4**) of various molecular weights have been obtained and elaborated. Conversion of the primary bromide to azide is discussed in Chapter **6**.

Since UV-triggered thiol-ene "click" reaction is emerging as a powerful tool for metal-free conjugation of biologically active moieties, α,ω-dialkenyl-PCL might be exploited as symmetrically functionalized hydrophobic linker with the capacity to undergo biodegradation. ROP of ε-CL initiated by allyl alcohol has been carried out under similar conditions to those applied for other initiators. α-Alkenyl-PCL (**3-0**) has been obtained with the DP of 13 (estimated from ^{1}H NMR data). SEC revealed a monomodal and symmetrical trace and narrow MWD (PDI=1.19). α-Alkenyl-PCL (**3-0**) was then derivatized by reacting with 4-pentenoic acid to afford α,ω-dialkenyl-PCL (Scheme 3.1, **3-3**). The SEC trace was again symmetrical, and the PDI had remained low (Fig. 3.2, Table 3.1).

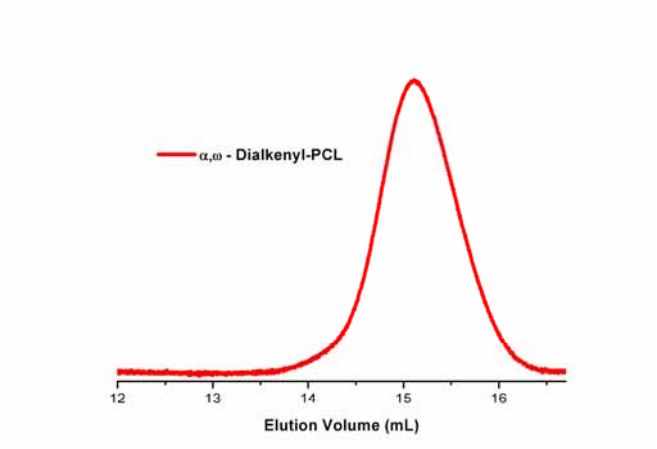

Figure 3.2 SEC trace of α,ω-dialkenyl-PCL (3-3) acquired by the RI detector.

The structure of **3-3** has been elucidated by ^{1}H NMR. Resonance signals originating from the initiating species have been designated as **a**, **b**, and **c** (Fig. 3.3). Peak **i** is attributed to the methylene group next to the hydroxy chain end of **3-0**. After esterification **i** disappears completely, which implies that the extent of the reaction is near to quantitative. Furthermore, resonances **m** and **l** appear, and are ascribed to the unsaturation at the ω-terminus. All other peaks related to the polyester backbone have also been identified (Fig. 3.3).

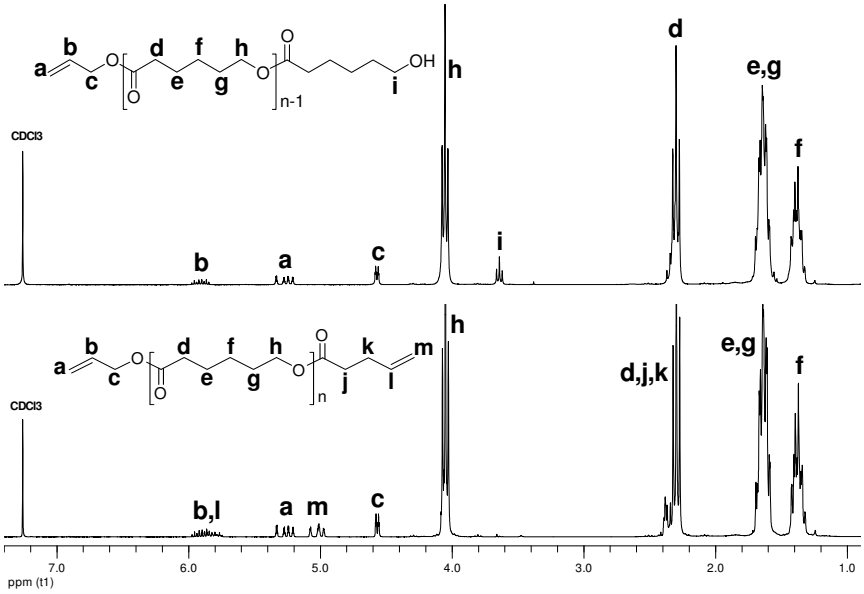

Figure 3.3 ^{1}H NMR spectra of α-alkenyl-ω-hydroxyl-PCL (3-0) and α,ω-dialkenyl-PCL (3-3).

As it will be obvious from the following chapters, these α,ω-hetero-telechelic PCLs (Scheme 3.1) represent exceedingly flexible and useful units which in combination with ATRP and "click" reactions open new avenues to intricate macromolecular amphiphiles.

Chapter 4 Gold Nanoparticles with Amphiphilic Corona: Implications for Mucoadhesive Drug Delivery

Introduction

Tumor diagnosis and treatment may be facilitated and improved by exploiting gold nanoparticles (AuNP). AuNP feature surface plasmon resonance (SPR) which boosts light absorption and scattering. They have been proved to be biocompatible and non-cytotoxic. Multivalency of the nanoparticle surface allows ligation of multiple functionalities. By taking advantage of gold-thiol chemistry, numerous biological and synthetic molecules can be fastened to the nanoparticle surface. Modification of the surface of AuNPs with pilot molecules facilitates ligand-specific cancer detection. For instance, the nanoparticles decorated with antibodies, folate residues, aptamers, cell-penetrating peptides and viruses, are capable of selective recognition of cancer cells. PEGylated AuNPs exhibit long circulation times in the blood compartment.[86,87]

Optical properties of AuNPs can be manipulated by varying their size and shape. For biomedical applications, nanoparticles with strong absorbing and scattering potentials are required. Based on Mie theory, gold nanospheres with a diameter of 20 nm exhibit primarily surface plasmon enhanced absorption and minor scattering, while increase of the diameter to 80 nm results in a significant increase in surface plasmon scattering.[86] Ashkenazi *et al*. reported that antibody-conjugated gold nanorods provided high contrast for non-invasive photoacoustic imaging of targeted tumor tissues.[88] Furthermore, a change in the SPR wavelength can be exploited in the analysis of biological molecules since it is sensitive to the change in the refractive index or dielectric constant of the surroundings of the nanoparticle surface.[86]

The arsenal for fighting cancer is comprised of surgical intervention and chemo- and radiotherapy. However it suffers from numerous limitations and drawbacks such as inaccessibility of the tumors, lateral effects induced by the chemotherapy, and detrimental impact of the radiotherapy on healthy tissues located in the radiation pathway. Overall these approaches are rather invasive, noxious, painful, and linked to myriads of undesirable acute and chronic consequences.[1,2]

One merit of AuNPs is effectual conversion of light into localized heat. Laser hyperthermia – tumor ablation by employing optical heating – may be the way to circumvent undesirable negative effects. Selective thermal ablation may be carried out by saturating the tumor tissue with strong photoabsorbers. Since AuNPs rapidly transform absorbed light into heat, site-specific accumulation of the AuNPs in malignant cells allows annihilation of diseased cells without exerting harmful effects on healthy ones. Moreover, adjustment of SPR absorption and scattering facilitates simultaneous imaging and therapy.[86] El-Sayed *et al*. have demonstrated that 40 nm AuNPs with the absorption maximum at 530 nm are rather effacious in photothermal destruction of cancer cells when the AuNP-bound cells are exposed to the laser light at 514 nm. The antibody conjugated AuNPs have been found to selectively attach to the malignant cells and thus spare normal ones.[89] West and co-workers have employed silica-gold nanoshells with a strong absorption in the near-infrared (NIR) region.[90] The NIR region represents the window where tissue penetration is optimal, and optical absorption is minimal. The nanoshells of 110 nm diameter core coated with 10 nm-thick gold layer exhibit the absorption peak at 820 nm. They have been covered by a PEG layer to reduce aggregation in physiological milieu. As a consequence of the exposure to NIR light, localized, irrevocable photothermal ablation of the tumor tissue, incubated with nanoshells, have been attained.[90]

Radiofrequency (RF) ablation is used to eliminate a number of malignant tumors, but features several downsides ranging from incomplete elimination of tumor, non-specific character of the therapy, and complications following the procedure. Since external RF energy fields are capable of penetrating human tissue, non-invasive cancer therapy involving RF fields would be possible at various sites of the body provided the site of action contains intracellular or intratumoral agents that generate heat when exposed to the RF field. If such agents are specifically targeted to malignant cells collateral damage of normal cells could be avoided. Curley *et al*. have demonstrated that 5 nm diameter AuNPs are internalized by the human cancer cells, and placed in vesicles.[91] These AuNP-containing vesicles exhibit no cytotoxicity, and do not hamper the cell proliferation. However, when addressed by an external non-invasive RF field, the AuNPs evolve heat causing lethal injury to the cells.[91]

Besides beneficial optical properties, AuNPs' capacity as drug carries can be exploited as well. Monolayer protected AuNPs provide enhanced stability compared to polymeric micelles. With the abundance of surficial functional groups, low toxicity, and elusiveness from the RES ensured by their small size, AuNPs emerge as excellent platforms for the delivery of therapeutic agents.[92,93] Methods for the preparation of AuNPs include a) reduction of $HAuCl_4$ in a boiling solution of sodium citrate, and b) passivation of the gold clusters, formed after reduction of $HAuCl_4$, with thiol capping ligands. Employing polymeric ligands for the stabilization the gold clusters has drawn considerable attention due to the robustness and versatility of the AuNPs thus obtained. The polymeric monolayer facilitates fine-tuning of the surface properties, tailoring solubility and compatibility of AuNPs.[94] Provided the surface of AuNP is capped with the suitable polymeric ligand, successful coupling of chemo- and thermal therapies can be realized. PCL-*b*-PAA – an amphiphilic diblock copolymer – combines precious features intrinsic to the constituting blocks. These exceedingly valuable properties have been detailed in Chapter **1**. It would be sufficient to mention that the micelles composed of PCL-*b*-PAA may find application in mucoadhesive drug delivery. However, if intended for bladder cancer treatment, the drug delivery vehicle should exhibit robust structure which can sustain severe dilution. Polymeric micelles tend to disintegrate upon dilution as the polymer concentration falls below the critical micelle concentration (cmc). Therefore, it would be advantageous to stabilize the micelle core by trapping and arresting the chains, and thus creating a unimolecular container with rigid structure.[95] Covalent cross-linking of the core shall be discussed in Chapter **6**, instead we shall concentrate on the stabilization of the nanostructure by anchoring the polymer chains on the surface of AuNP through the gold-thiol interactions. Attachment of this diblock copolymer to the AuNP surface should result in a core-shell-type architecture where the shell consists of outer and inner layers of hydrophilic PAA and hydrophobic PCL, respectively, and the AuNP represents the core. Wooley *et al*. have obtained shell cross-linked nanoparticles composed of diblock copolymer PCL-*b*-PAA.[96] The PCL core was selectively removed from these water miscible nanostructures to afford cage-like membranes. On the other hand, PCL-*b*-PEG incorporating a disulfide moiety at the PCL chain end has been synthesized, and employed as the ligand for stabilization of AuNPs. The authors pointed out that these nanoparticles may be used as drug delivery vehicles, and as markers for the investigation of subcellular processes.[97] Leaning on these approaches, we have developed the synthetic cascade encompassing preparation of HS-PCL-*b*-PAA, and we have proved the effectiveness of this macroligand in passivation of AuNPs.

Results and Discussions

The synthetic layout for preparation of HS-PCL-*b*-PAA is depicted in Scheme 4.1. In Chapter **3** the library of α,ω-hetero-bifunctional PCLs has been introduced. PCLs **1-1** and **1-2** – carrying a masked thiol functional

group and an ATRP initiating site – represent the fundamental building blocks. The ATRP of *t*BA from the PCL macroinitiator **1-1** was mediated by the CuBr/PMDETA catalytic complex in bulk at 100 °C. The diblock copolymer with a relatively high PDI (1.5) was obtained. The SEC experiment produced an unsymmetrical trace with a shoulder on the high molecular weight side symptomatic of poor control over the reaction. The loss of control may be attributed to the catalyst deactivation due to the hypothetical ligation of copper with 2,4-dinitrophenyl group or with the polyester chain. The liberated PMDETA may participate in destructive lateral reactions by attacking electrophilic carbonyl carbon atoms, and provoking cleavage of the PCL chains.

To ameliorate this condition $NiBr_2(PPh_3)_2$ was chosen as the catalyst, thus eliminating the need for nitrogen based ligands. The ATRP was conducted in bulk at 90 °C. 0.8 equivalent of the catalyst in comparison to the initiating group was employed. Taking less amount of the catalyst than suggested by the stoichiometry has been proposed by Hedrick and co-workers[98] to circumvent the evolution of the unsymmetrical SEC chromatograms. However, further decrease of the catalyst to macroinitiator initial molar ratio led to sluggish polymerization and ineffectual, incomplete initiation.[99] Decreasing the ratio of the initial molar concentrations of the monomer and initiator $[M]_0/[I]_0$ from 210 for **4.1a** to 170 for **4.1b**, and consequently increasing the catalyst and initiator initial molar concentrations, considerably shortened the polymerization time necessary to achieve similar monomer conversion (Table 4.1).

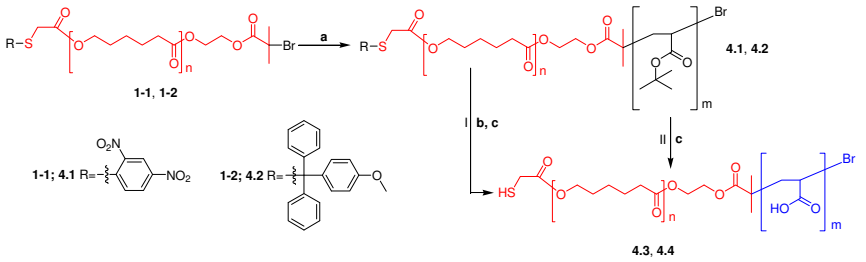

Scheme 4.1 Synthetic cascade for preparation of HS-PCL-*b*-PAA. Reagents and conditions: (a) *t*BA, $NiBr_2(PPh_3)_2$, 90 °C; (b) CH_3CH_2SH, NEt_3, $CHCl_3$; (c) TFA, TES, CH_2Cl_2.

That excellent control over the reaction had been established was evident from the narrow MWD. Absence of the unreacted macroinitiator in the SEC chromatograms points towards the high initiation efficiency. Formation of the P*t*BA block as well as maintenance of the protected thiol functional group was verified by ^{1}H NMR experiment (Fig. 4.1). DP of the P*t*BA block is estimated by comparing the integral of the resonance signal attributed to the methylene group in the PCL repeating unit (**c**) to the integral of the overlapping resonance signals assigned to the methylene protons in the PCL and the methine proton in the P*t*BA repeating units (**b** and **i**).

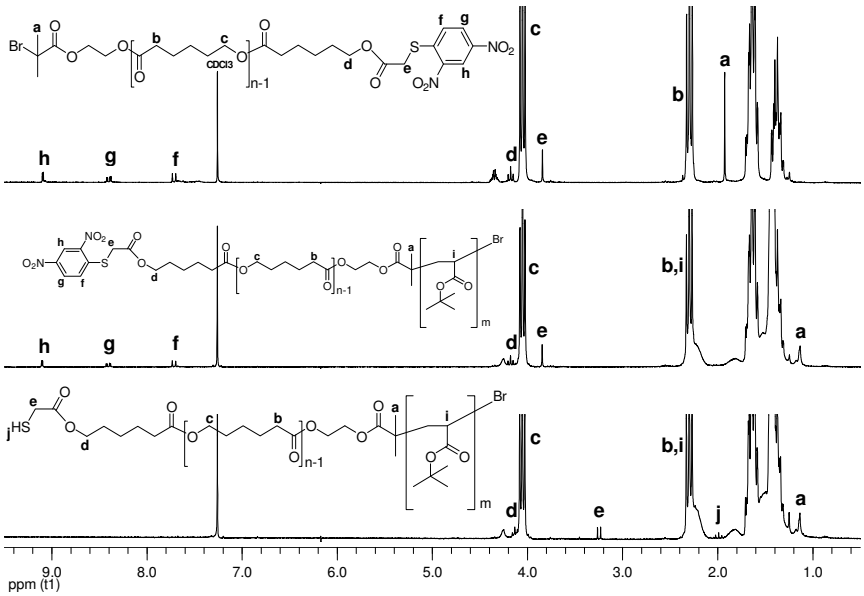

Figure 4.1 ^{1}H NMR spectra of the macroinitiator 1-1, the diblock copolymer 4.1, and the diblock copolymer HS-PCL-*b*-P*t*BA.

The reaction conditions and the results for the diblock copolymers obtained from the macroinitiator **1-1** are given in Table 4.1 (**4.1a**, **4.1b**).

Table 4.1 ATRP conditions and molecular weight characteristics of PCL_n-*b*-P*t*BA_m.[a]

compound	$[M]_0/[I]_0/[cat]_0$[b]	reaction time (h)	m	M_n[c]	M_n[d]	M_w/M_n[d]
4.1a	210:1:0.8	48	31	7900	10800	1.27
4.1b	170:1:0.8	20	24	7000	10200	1.17
4.2a	220:1:0.8	42	70	13000	15300	1.39
4.2b	170:1:0.8	20	50	10400	14000	1.29

[a] n=30; [b] Ratio of initial molar concentrations of the monomer to initiator and catalyst; [c] By ^{1}H NMR; [d] By SEC (PS calibration).

The 2,4-dinitrophenyl protecting group of **4.1** was removed by treating the diblock copolymer with a large excess of ethanethiol in chloroform following the procedure exercised by Carrot *et al*.[73] The resulting HS-PCL-*b*-P*t*BA (Scheme 4.1, Ib) was analyzed by attenuated total reflectance (ATR) FT IR and ^{1}H NMR spectroscopy (Fig. 4.1). Both techniques suggest neat deprotection: the resonances assigned to the 2,4-dinitropenyl group (**f**, **g**, **h**) are no longer detected, whereas the resonance signal ascribed to the methylene protons next to the thiol function (**e**) shifts upfield from 3.85 ppm to 3.25 ppm, and is split into doublet as a result of coupling with the thiol proton (**j**). ^{1}H NMR and ATR FT IR spectroscopy proved to be handy techniques for monitoring incorporation and elimination of 2,4-dinitropenyl protecting group. The SEC experiment produced the trace which was shifted to the smaller retention volume and somewhat broader MWD,[72] which may be the result of intra- and intermolecular interactions that take place after deblocking of the thiol functionality and/or of the interaction with the SEC column. *tert*-Butyl ester groups of **4.1** were selectively removed in CH_2Cl_2 utilizing TFA[100] and TES as the cation scavenger[101] (Scheme 4.1, Ic). Mild

reaction conditions are required to preserve the polyester backbone. Almost full deprotection of P*t*BA was attained leading to the amphiphilic thiol-functionalized block copolymer **4.3**.

The macrothiols may form disulfides when in contact with air debilitating them as efficient macroligands for the passivation of AuNPs.[102] Also, large excess of the small molecular weight thiol is required to overpower the reversible deprotection of 2,4-dinitropenyl group. As an alternative, the Mmt protecting group was introduced in Chapter **3**. The Mmt group can be irreversibly removed together with the *tert*-butyl ester groups under acidic conditions, and thus the exposure time of the macrothiols to air can be minimized. Thus, **1-2** was employed in the ATRP of *t*BA to incorporate the Mmt-protected sulfhydryl function at the terminal position of the diblock copolymer **4.2** (Scheme 4.1). While employing similar ATRP conditions, the macroinitiator **1-2** furnished the diblock copolymer with higher DP of *t*BA than the macroinitiator **1-1** (Table 4.1). Inexplicable interaction of the thiol protecting groups with the catalytic complex in the ATRP may be responsible for the difference in the reaction rates. The unimodal SEC trace and fairly low PDI suggest minimal share of undesirable collateral reactions, and high initiation efficiency. ^{1}H NMR experiment corroborated the structure of the diblock copolymer **4.2**. DP of the P*t*BA block is approximated in a similar fashion as for **4.1**. Concurrent removal of the Mmt and *tert*-butyl ester groups was accomplished by working up the PCL-*b*-P*t*BA **4.2** with 2 M TFA in CH_2Cl_2/TES (Scheme 4.1, IIc). The structure of **4.4** was elucidated by ^{1}H NMR spectroscopy. The maintenance of the PCL backbone is proved: the ratio of integrals of the resonance peaks corresponding to the PCL and P*t*BA repeating units appear almost unchanged after deprotection.[96] This is crucial for the particle formation step since loss of the thiol functionality as a result of chain cleavage would incapacitate the block copolymer in stabilization of AuNPs. A broad resonance signal originating from free carboxylic groups is identified at 12.26 ppm. However, the signal from the residual *tert*-butyl ester moieties is also detected. The amount of the remaining *t*BA units has been approximated to be 5%. Incomplete deprotection may be attributed to the amphiphilic nature of the diblock copolymer: partially deprotected PAA blocks which are no longer soluble in dichloromethane may aggregate to form a core-shell type structure with the PCL outer layer, and thus conceal the remaining *tert*-butyl ester groups.

The AuNPs were prepared following a literature procedure[97] with slight modification: a freshly prepared solution of lithium borohydride (5-fold excess compared to the gold salt) was quickly added to the solution of **4.4a** and gold(III) chloride trihydrate in THF. Reduction of the gold salt manifested with instantaneous change of color from yellow to purple and vicious gas evolution. No flocculation and precipitation took place. Hence, the formation of stable AuNPs was accomplished despite the scarcity of the macrothiols. This fact highlights the effectiveness of the polymeric shell in preventing the gold clusters from agglomeration. The UV-visible spectrum of a water solution of the AuNPs features an absorption at 522 nm, which indicates that the AuNPs do not aggregate in aqueous medium.[103] Transmission electron microscopy (TEM) image (Fig. 4.2) reveals the nanoparticles with a mean diameter of 9.0 ± 3.1 nm.

Thus, α,ω-hetero-bifunctional PCL possessing protected thiol and activated bromide functionalities facilitates preparation of well-defined amphiphilic diblock copolymer HS-PCL-*b*-PAA by combination of ROP and ATRP. HS-PCL-*b*-PAA permits steadfast stabilization of the gold nanoparticles. The ATRP of *t*BA mediated by $NiBr_2(PPh_3)_2$ is well controlled, and polymers with low PDI are obtained. Employing the Mmt protecting group is particularly beneficial because it allows simultaneous deblocking of thiol functional

group and P*t*BA block. Stable, aggregation-free nanoparticles can be obtained even if a relatively mild reducing agent is used pointing towards the effectiveness of HS-PCL-*b*-PAA in protecting the gold cores.

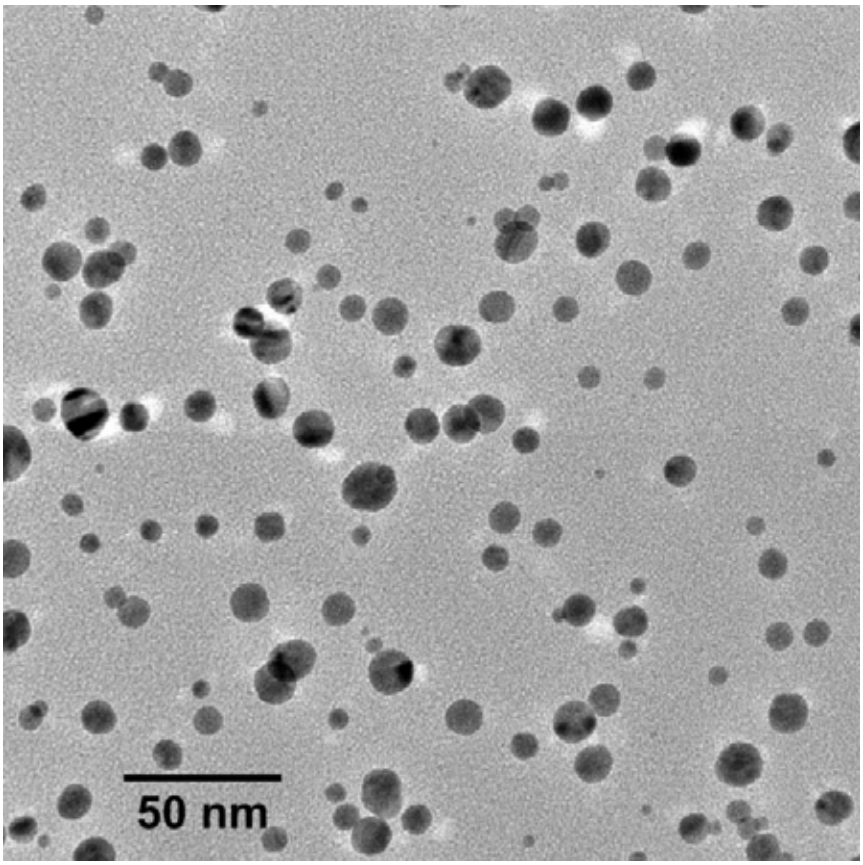

Figure 4.2 TEM image of AuNPs.[§]

The gold nanoparticle with the amphiphilic corona is schematically represented in Fig. 4.3. TEM affords visualization of the gold core solely. The polymeric shell cannot be pictured due to the minute difference in contrast between the shell and the relatively thick carbon film which serves as the support of the TEM sample. However, we may hypothesize that in aqueous solution the corona consists of an extended, hydrated layer of PAA, and a collapsed, dehydrated layer of PCL. In fact, the diameter of the nanoparticles obtained from TEM does not correlate with that extrapolated from UV-visible spectrum.[104] One can only surmise that the absorption peak has experienced the hypsochromic shift observed by Tenhu and co-workers.[103,105]

The nanoparticles contain approximately 16 % of gold as estimated by thermogravimetric analysis (TGA).

[§] Adopted from Javakhishvili, I.; Hvilsted, S. *Biomacromolecules* **2009**, *10*, 74-81.

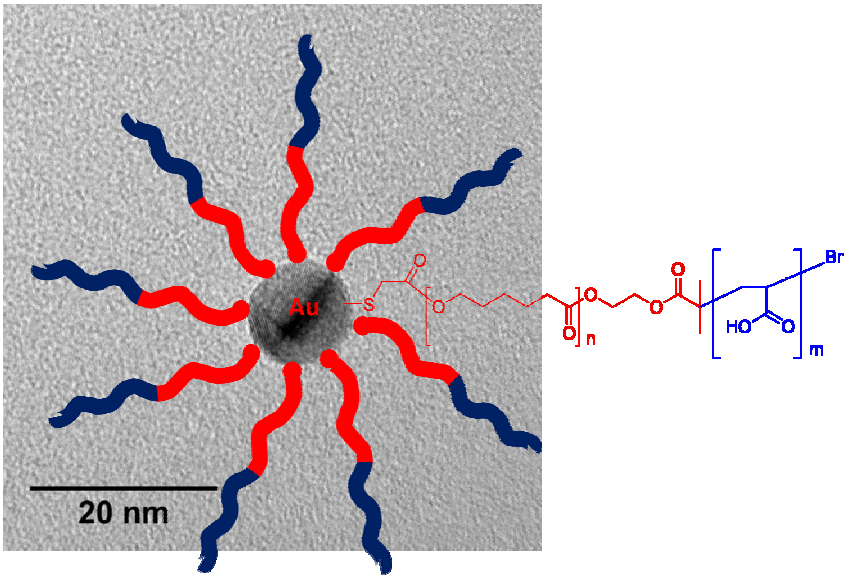

Figure 4.3 TEM image of the AuNP and schematic depiction of the polymeric shell.

The aggregate depicted in Fig. 4.3 may have the potential to combine mucoadhesive drug delivery, and RF field induced ablative therapy. Thus, the PCL layer may be loaded with hydrophobic anticancer therapeutic agents, while PAA layer may facilitate anchoring of the nanoparticle to mucous membranes resulting in site-specific delivery. Carboxylic groups of PAA may be employed for the ligation of biologically active molecules to boost the cellular uptake. The gold core insures structural stability, and may serve as a marker in localization studies.

Chapter 5 Linear-dendritic Rod-coil Amphiphiles: Implications for Self-assembly

Introduction

Amphiphilic linear-dendritic block copolymers are one of the beacons in modern polymer chemistry due to their intrinsic features that induce self-assembly into different shapes. The facility of forming complex supramolecular structures stipulates for the availability of a battery of diverse constituting blocks.[106]

Hedrick *et al*. have devised linear-dendritic amphiphiles that possess traits of naturally occurring phospholipids.[107] The hydrophilic dendritic wedges composed of 2,2-bis(hydroxymethyl)propionic acid (bis-MPA) (A) were fastened with the linear fragment of the hydrophobic PCL (B) by initiating the ROP of ε-CL from the multifunctional dendrons. The symmetric linear-dendritic triblock copolymer (ABA) was also obtained via the Mitsunobu esterification of the hydroxyl chain end of the linear-dendritic block copolymer (AB) with the acid-functionalized dendrons.[107] Fréchet *et al*. prepared linear-dendritic block copolymers by employing divergent growth of the bis-MPA based dendrons from a PEG terminus.[108] Step-by-step preparative technique that provides a well-defined architecture with a predetermined number of peripheral functional groups for subsequent transformations is an ingenious tool for building stimuli responsive self-assembled aggregates which may serve as drug delivery vehicles.[109] Fréchet and co-workers reported the synthesis of PEG-dendritic poly(L-lysine) (PLL) and PEG-dendritic polyester featuring peripheral acid-labile hydrophobic moieties.[109] These polymers assembled into pH responsive micelles that would rupture at mildly acidic pH. Core-shell type nanostructures based on precise monodisperse, linear-dendritic polymers have also been suggested.[110] Synthesis involves ligation of a thiol functionalized di-dendron with a single strand DNA. Conjugation of this linear-dendritic copolymer with the suitable counterpart comprising appropriate complementary DNA as the linear fragment affords a core-shell nanostructure featuring base-paired DNA core entrenched by two di-dendrons. Cao *et al*. designed the route for preparation of PLLA-*b*-dendritic PLL employing the metal free ROP of the L-lactide initiated by the hydroxyl-functional Boc-protected PLL dendrons.[111] The authors have emphasized the role of PLL as a functional vector for DNA transfection. Zubarev and Stupp developed the synthetic cascade for building hybrid structures: dendron rodcoils. These macromolecular bodies incorporate dendritic, rod-like, and coil-like molecular fragments, and have been constructed by convergent or divergent approach.[112] Amphiphilic "tree-shaped" comb-dendritic block copolymer has been obtained with hydrophobic, rigid comb block – poly(γ-*n*-dodecyl-L-glutamate) – that facilitates self-assembly into very stable micelles, and multivalent dendritic exterior – the polyester dendritic wedge modified with PEG – that can be utilized to conjugate biocompatible targeting motifs.[113] Stupp *et al*. have also prepared amphiphilic rodcoil dendrons where a hydrophilic dendron was linked with a rigid segment via a hydrophobic polyester spacer.[114] Synthesis of these sophisticated macromolecular constructs combines ROP of L-lactide initiated by cholesterol, and esterification of the hydroxyl chain end of this cholesteryl-oligo(L-lactic acid) with the L-lysine dendritic wedge. Liquid crystalline nature of the cholesteryl moiety could induce self-assembly of the rodcoil dendron, and the L-lysine dendritic wedge could influence the development of the nanostructure. Both cholesterol and L-lysine could interact with the cell membrane, and thus enhance cell adhesion.[114]

But this synthetic layout is quite delicate, intricate and challenging. This chapter postulates a synthetic pathway for the generation of similar macromolecules in a more facile but comprehensive way. In Chapter **2** successful implementation of CuAAC and UV initiated thiol-ene "click" reactions in the field of the

macromolecular chemistry has been highlighted. Chapter **3** emphasized enormous potential of the α,ω-hetero-bifunctional PCLs as convenient and supple building entities. Thus, by making use of the PCL **2-3** – the linear component that possesses terminal alkyne and alkene functional groups – the synthetic strategy for preparation of the rodcoil dendrons can be accelerated. Moreover, the "click" chemistry approach offers greater degree of freedom since all three structural units can be linked to evade the default presence of either a cholesterol or L-lysine dendron as is the case in the approaches exercised earlier.[111,114] CuAAC "click" reaction has been successfully utilized for the synthesis of unsymmetrical dendrimers,[115] dendronized linear polymers[116] as well as linear-dendritic block copolymers,[117,118] and thus has been established as a flexible and handy technique. Haddleton *et al*. have combined CuAAC with thio-Michael addition,[119] while Anseth *et al*. have married copper-free "click" chemistry and thiol-ene photocoupling.[120] The proposed synthetic cascade for the preparation of the rodcoil dendron based on cholesterol, PCL, and dendritic L-lysine is amongst these pioneering endeavors in building such multifunctional macromolecular architectures by coupling CuAAC and thiol-ene "click" reaction.

Results and Discussions

PCL **2-3** has been introduced in Chapter **3**. The second generation dendron of L-lysine, $(L\text{-lysine})_{G2}$ (**5.3**), which bears an azide function at the focal point, was prepared according to Scheme 5.1.

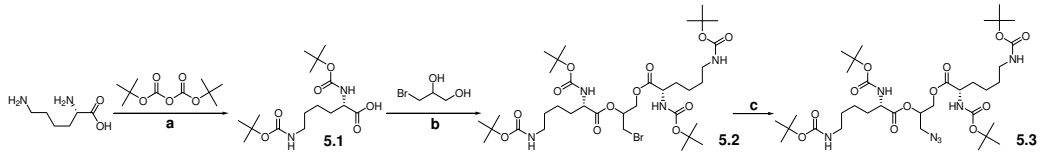

Scheme 5.1 Synthetic pathway leading to the azide-functional dendron 5.3. Reagents and conditions: (a) NaOH, H_2O, 1,4-dioxane; (b) DCC, 4-DMAP, CH_2Cl_2; (c) NaN_3, DMF.

This strategy permits immediate integration of the primary bromide functionality at the focal point (compound **5.2** on Scheme 5.1), and thus eliminates the necessity of additional esterification reaction which would be unavoidable if following the standard procedure of building dendrons[115]: taking L-lysine as the core-forming molecule.[114] Facile and neat nucleophilic substitution of the bromide group provides second generation azide-functional dendron with high yield and purity. **5.2** was obtained by applying the straightforward esterification protocol involving 3-bromo-1,2-propandiol and N_α,N_ε-di-Boc-L-lysine (1.1 equivalents) in the presence of DCC and 4-DMAP. There was no need for column chromatography since simple extractions gave a pure product. **5.2** was treated with NaN_3 (2 equivalents) at 40°C overnight resulting in the quantitative conversion into the corresponding azide. The structure of **5.3** and the extent of the substitution reaction were investigated by the heteronuclear single quantum coherence (HSQC) NMR spectroscopy (Fig. 5.1). The resonance signal corresponding to the Br-CH_2CH methylene group in the compound **5.2** has not been detected. The appearance of $\mathbf{e_1}$,$\mathbf{e_2}$ at 50.7 ppm signifies the presence of N_3-CH_2CH fragment-containing species only. Inasmuch as ^{1}H NMR experiment does not provide sufficient information about the extent of the reaction since the proton chemical shifts of the methylene groups adjacent to bromide and azide functionalities coincide in the 1D spectrum, HSQC experiment appears to be a precious tool to decipher the structure, and to assess the degree of substitution.

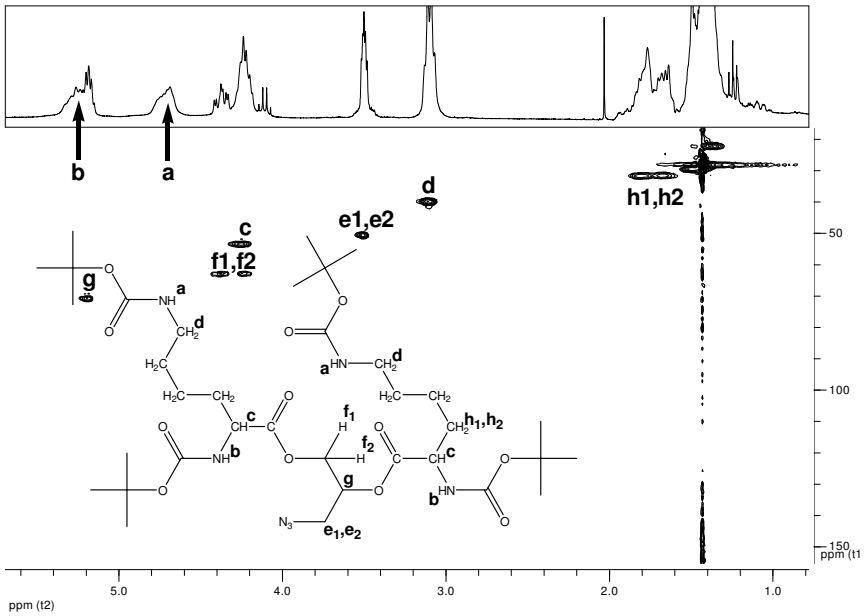

Figure 5.1 HSQC NMR spectrum of the compound 5.3.

The sequence of CuAAC and UV-initiated thiol-ene "click" reactions was carried out according to Scheme 5.2. It must be accentuated that it is imperative to conduct the CuAAC before the thiol-ene reaction since the latter lacks the selectivity between alkyne and alkene functional groups. The "click" reaction between the PCL **2-3** and bis-(di-Boc-L-lysine)-3-azido-1,2-propandiol **5.3** (2 equivalents) was conducted in THF in the presence of CuI (1 equivalent in comparison to the alkyne) and NEt_3 at 35°C for 24 h.[121] The L-lysine dendron **5.3** was used in excess due to the following considerations: a) to drive the reaction to completion at relatively low local concentration of the functional groups, and b) the dendron can be smoothly removed by precipitation in MeOH-H_2O mixture. The structure of the product was elucidated by SEC, NMR, and MALDI-TOF experiments, the latter being conducted by Professor W. H. Binder at the Martin-Luther University Halle-Wittenberg in Germany.

Unimodal and symmetrical chromatogram that has shifted to the smaller elution volume and the PDI of 1.10 have been obtained. This implies that: a) the PCL chains remain intact during the reaction: the nucleophilic NEt_3 does not induce the chain cleavage, and b) the overwhelming majority of the PCL chains have reacted. Indeed, near to quantitative functionalization was confirmed by NMR experiments (Fig. 5.2): the resonance signal attributed to the acetylenic proton (**d**) disappears, whereas the resonance peak assigned to the methylene group next to the alkyne function (**c**) exhibits downfield shift. In addition, the peaks attributable to the dendritic wedge have been identified. The signals originating from the alkene moiety are detected at 5.00 ppm and 5.80 ppm proving the preservation of this functional group. Furthermore, the integrals of the peaks assigned to the terminal alkene (**b**, 5.80 ppm) and C*H*$_2$NHBoc (**e**, 2.93-3.22 ppm) fragment of the dendron are in good agreement with the theoretical values.

The MALDI-TOF experiment resulted in a spectrum with two series and the signal spacing of approximately 114 Da – a number matching the molecular weight of one repeating unit in the PCL chain.

The thiol-ene "click" reaction between **5.4** and thiocholesterol, which is commercially available, results in the rapid conjugation of the cholesteryl moiety to the terminal of the linear-dendritic block copolymer (Scheme 5.2). **5.4**, thiocholesterol, and 2,2-dimethoxy-2-phenylacetophenone (DMPA) (1:10:3.5 molar ratio) were dissolved in a minimal amount of toluene, and irradiated at 365 nm while stirring in the presence of oxygen. When less equivalents of the thiol and the photoinitiator were employed, incomplete functionalization was observed. This may be attributed to the rigidity and hindered mobility of thiocholesterol.[122] Near to quantitative functionalization was attained according to the NMR and MALDI-TOF experiments. The ^{1}H NMR spectrum (Fig. 5.2) unequivocally points to the total exhaustion of the terminal alkene groups: resonances **a** and **b** have shifted upfield. The presence of the cholesteryl moiety is also evident (**h**). The MALDI-TOF analysis resulted in the spectrum characteristic for the species corresponding to the compound **5.5**. The SEC trace exhibits a small shoulder on the high molecular weight side, but the PDI remains rather low (1.15). The shoulder might have originated as a result of the intra- or intermolecular side reactions (coupling) of radical nature that might have occurred in the course of the reaction.

Selective removal of the Boc protecting groups of the cholesteryl-PCL-*b*-(di-Boc-L-lysine)$_{G2}$ (**5.5**) was carried out in TFA-CH_2Cl_2 (1:5) mixture. The analysis of the product by ^{1}H NMR spectroscopy and MALDI-TOF spectrometry confirmed the formation of the structure **5.6**.

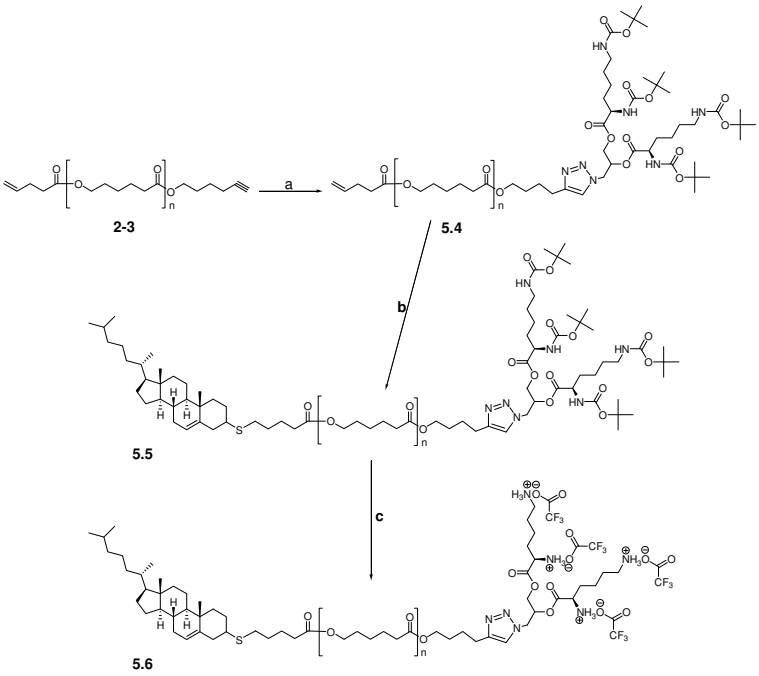

Scheme 5.2 Synthetic pathway involving CuAAC, thiol-ene "click" reaction, and removal of Boc protecting groups. Reagents and conditions: (a) 5.3, CuI, NEt_3, THF, 35 °C; (b) thiocholesterol, DMPA, UV, toluene, RT; (c) TFA, CH_2Cl_2.

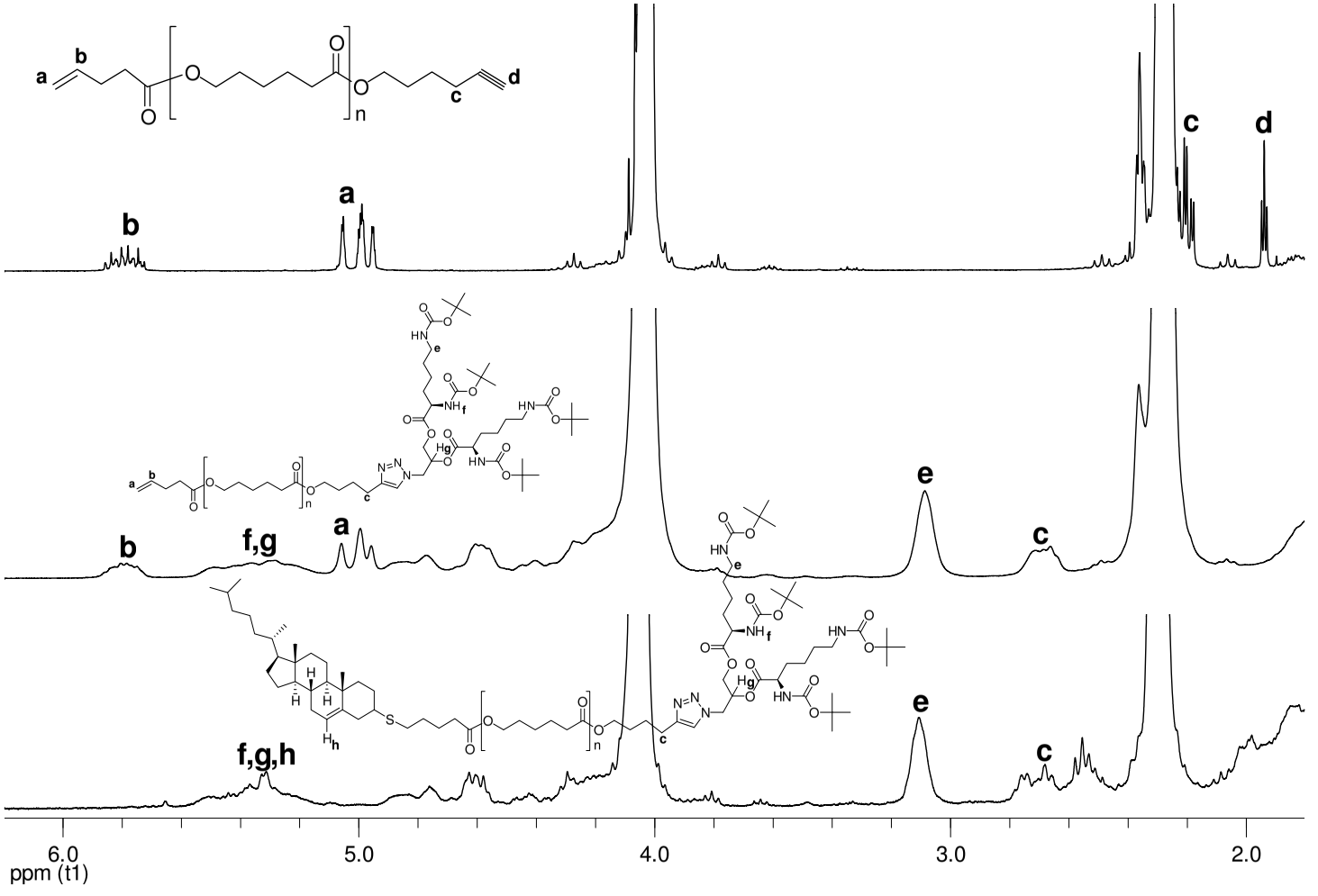

Figure 5.2 ^{1}H NMR spectra of the compounds 2-3, 5.4, and 5.5 in $CDCl_3$.

Thus, this synthetic strategy has once again demonstrated the flexibility of α,ω-hetero-bifunctional PCL – α-alkynyl-ω-alkenyl-PCL in this particular case – in coupling the orthogonal azide-alkyne and thiol-ene "click" reactions for building the linear-dendritic amphiphilic macromolecule. The "click" reactions significantly reduce the number of synthetic steps required for constructing such macromolecular architectures compared to the conventional esterification reactions. The α,ω-hetero-bifunctional PCL allows conjugation of different structural entities at the opposite chain-ends, and thus expends the pool of complex amphiphilic structures. However, one can only surmise that **5.6** may self-assemble in aqueous solutions or in solid state, and this aspect demands detailed investigations.

Chapter **2** introduced thiol-ene "click" reaction as a benign method for the ligation of biological molecules. After successfully linking thiocholesterol to the polymer terminus, α,ω-dialkenyl-PCL has been derivatized with the reduced glutathione via UV-triggered thiol-ene reaction. Thus, α,ω-dialkenyl-PCL **3-3** has been reacted with the reduced glutathione in the presence of DMPA (1:3.5:2.5 molar ratio) in THF-H_2O (1:2) mixture bringing both components into solution. The structure of the product has been investigated by ^{1}H NMR spectroscopy using DMSO-d_6 as the solvent. The juxtaposition of the spectra before and after the ligation (Fig. 5.3) explicitly indicates the conjugation of the glutathione on the expense of the terminal unsaturations. The resonance signals **a**, **b**, **l**, and **m** – corresponding to the α- and ω-alkenyl moieties – have disappeared after the reaction, and the signals **n**, **o**, and **p** – associated with the glutathione – have emerged.

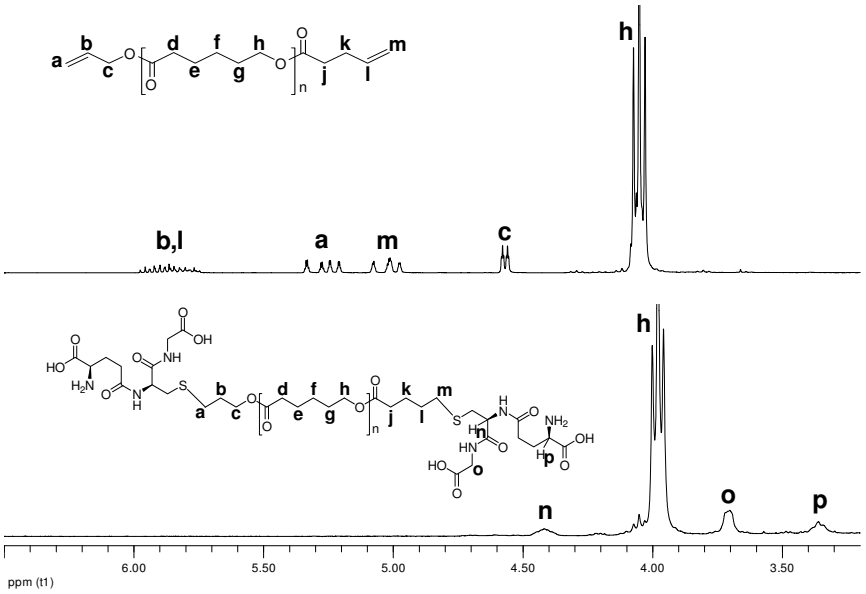

Figure 5.3 ^{1}H NMR spectra of the α-ω-dialkenyl-PCL 3-3 (in $CDCl_3$) and the thiol-ene "click" reaction product (in DMSO-d_6).

However, the product requires rigorous purification by multiple precipitations to remove the excess of the reagents and the reaction byproducts.

Chapter 6 Core-crosslinked Star Copolymers with Biologically Active Moieties on Peripheries: Implications for Targeted Drug Delivery

Introduction

α,ω-Hetero-bifunctional PCLs – **2-4** and **4-4** – capped with the methacrylic moiety have been introduced in Chapter **3**. Obviously, these macromolecules are attractive building blocks for construction of graft- and core-crosslinked star (CCS) polymers. CCS polymers have enormous potential in a multitude of fields featuring polymer therapeutics, catalysis, membrane technology and lithography amongst others due to their distinctive spherical shape, intricate macromolecular architecture with a core-shell type nanoenvironment, and an abundance of external and internal reactive functionalities.[123,124] Synthetic layout for preparation of CCS polymers by ATRP is comprised of the polymerization of difunctional cross-linkers together with MMs and/or macroinitiators (MI): the difunctional cross-linker thus forms the core while the trapped and confined MMs and/or MIs – radiating arms.[123] Matyjaszewski and co-workers have synthesized CCS polymer via the ATRP of the divinyl benzene (DVB) cross-linker from the polystyrene (PS) MI bearing an activated halide moiety.[125] However, this approach features a downside inasmuch as the preparation of the PS MI by ATRP involves the unavoidable radical termination reactions which incapacitate a fraction of thus formed polymer chains for being used as MIs. By making use of the MI strategy, the CCS polymers with functional exterior incorporating P*t*BA arms with terminal epoxy, cyano, hydroxyl, and amino groups have been obtained.[126] Homoarm star polymers incorporate arms which do not differ in molecular weight and chemical composition, whereas miktoarm stars are built from arms with diverse chemistry and/or molecular weights.[123] The preparation of a miktoarm CCS copolymer via "in-out" method involves grafting of the arms of different chemical composition from the preformed CCS polymer. Thus, the cross-linker incorporating a degradable disulfide moiety has been polymerized from the PMMA MI resulting in the core-degradable CCS polymer. The latter has been exploited as the MI in ATRP of *n*-butyl acrylate (BA) to afford the miktoarm CCS copolymer.[127] ATRP of the second monomer initiated by the alkyl halide moieties in the core of the preformed CCS polymer is not free from drawbacks which include star-star and intrastar couplings responsible for the broadening of the MWD, and low initiation efficiency of the star MI.[127] Group transfer polymerization of MMA has also been employed for preparation of the star polymer possessing a degradable core.[128]

The MI approach is characterized by star-star coupling reaction occurring during the entire star formation process and thus broadening the MWD.[129] When the MI method is employed, the number of initiating sites in the core is equivalent to the number of arms. The overabundance of the initiating moieties facilitates the coupling reactions between the cores. Provided the ratio of initiating sites to arms per star can be decreased, the star-star coupling can be limited, and better control leading to improved consistency can be established.[129] Matyjaszewski and co-workers have devised a way to overcome this shortcoming: it lies on the initiation of the copolymerization of linear MMs and difunctional cross-linkers by low molecular weight ATRP initiators.[129] In this scenario, the number of initiating sites and arms are controlled separately, and thus the share of the star-star coupling reactions can be diminished to afford narrow MWDs. This approach was taken for the preparation of the miktoarm CCS copolymers incorporating PBA and PEG MMs.[130] Star congestion and shielding of the initiating sites can be remedied by step-wise addition of the cross-linker and initiator resulting in high yields and low polydispersities.[130]

Since PCL is a valuable synthetic polymer that is often employed as a hydrophobic component of a drug delivery vehicle, we shall cover a few examples of the CCS polymers that feature PCL arms. Miktoarm CCS copolymer incorporating PCL and PS arms have been prepared by "in-out" method: DVB was polymerized from the PCL MI possessing bromoisobutyryl terminus. Then PS arms were grafted from the star PCL MI by ATRP of styrene.[131] Alongside controlled radical polymerization technique such as ATRP, ROP has also been utilized for the synthesis of CCS PCL.[132] In Chapter **2** the versatility of ROP as a means for preparation of functional materials has been discussed. ROP of ε-CL provides MI for the subsequent cross-linking by ROP of a bislactone. These reactions can be conducted step-wise in one pot making the approach rather convenient. However, due to the presence of adventitious water there is a risk of producing α,ω-difunctional PCL that may bridge the stars and cause macrogelation.[132] Various degradable CCS polymers including core-degradable, arm-degradable, partially arm-degradable, and fully degradable stars have been prepared by making use of a dual initiator for coupling ATRP and ROP.[133] By adjusting coronal composition, the physical properties of the stars can be tailored.[134] CCS polymers with hydrolysable outer coronal layer, with initiating sites attached to the coronal surface, and with initiating moieties in the core as well as on the exterior have been obtained by employing the PCL building blocks amongst others.[134] Hawker *et al*. have synthesized CCS polymers with surficial amine and hydroxyl functional groups by making use of the functional initiators for nitroxide-mediated free radical polymerization.[135] Cross-linking of the linear-dendritic MIs, incorporating Fréchet type or polyester dendrons, resulted in the CCS with dendron-decorated exterior.[136,137] Transformation of the dendron functionalities considerably changes the morphologies produced by the star polymers.[137]

Investigation of the potential of star polymers in drug delivery has gained significant attention since the polymeric stars may alleviate the problems posed by the innate thermodynamic instability of classical amphiphilic copolymer micelles. Amphiphilic copolymers assemble into micelles only above the cmc. The micelles tend to disintegrate below the cmc. Since the drug delivery device undergoes severe dilution upon administration, the micelles may rupture. This process undermines their application *in vivo*.[138] Making use of dendrimers, star and CCS polymers, which possess robust structure, may be the alternative.[138] Roovers *et al*. have obtained amphiphilic star polymer based on polyamidoamine dendritic core which was employed as the macroinitiator to prepare the hydrophobic PCL inner block and then fasten the hydrophilic PEG outer block on it. Hence, the arms of the star are comprised of biocompatible and biodegradable polymers. Core-crosslinked micelles – unimolecular reservoirs – display all the valuable properties of classical micelles. Furthermore, they offer improved stability in biological fluids.[139] Core-crosslinked micelles have been synthesized by crosslinking di- and triblock copolymers PEG-*b*-PCL and PEG-*b*-PCL-*b*-PEG which carried maleic acid residue at the terminus of PCL block. These core-crosslinked micelles exhibit higher loading capacity than the classical ones.[139] Attaining the augmented stability of the nanostructure was one of the reasons for fastening an amphiphilic diblock copolymer PCL-*b*-PAA on the surface of a gold core as it has been scrutinized in Chapter **4**.

Chapter **1** shed light over the targeting mechanisms involved in drug delivery. Besides passive targeting, which is based on the EPR effect, delivery of drugs involving specific molecular recognition is of prime interest.[140] Gadolinium based MRI contrast agent conjugated to the selective estrogen receptor modulator, which is capable of binding to the estrogen receptor (ER) with high affinity, has been developed.[140] 17β-Estradiol (E_2) is the most potent estrogen which easily penetrates the cell, and binds to nuclear estrogen receptors. Derivatization of E_2 by linking bulky substituents at the 17α position has no detrimental effect on

its affinity to ER. Thus, conjugation of 17α-ethynylestradiol with appropriate chelate for gadolinium provided ER targeting contrast agent.[140] ER are overexpressed in 75-80 % of all breast tumors. Since an antiestrogen compound tamoxifen competitively binds ER, AuNPs with tamoxifen-PEG-SH shell have been prepared to augment potency and selective particle uptake.[141]

Kostarelos *et al*. have observed obstruction in tumor growth induced by the sixth generation cationic PLL dendrimer (G_6PLL).[142] Such an effect has been attributed to the antiangiogenic activity of G_6PLL. It has been shown that G_6PLL, which has 64 amino groups on its exterior, accumulates and retains at the tumor site owing to the strong electrostatic interactions between the dendrimer and the tumor neovasculature. Thus, coupling of this dendrimer with anticancer drugs and diagnostic agents may result in a versatile device for cancer treatment.

This chapter will focus on the preparation and structural characterization of PCL miktoarm CCS copolymers featuring multitude of amine functional groups and targeting moieties on the periphery. The preparation of the miktoarm CCS copolymers involves cross-linking of the MMs such as linear-dendritic (di-Boc-L-lysine)$_{G2}$-*b*-PCL-methacrylate and linear E_2-PCL-methacrylate or ferrocene-PCL-methacrylate. The MMs are obtained by exploiting α,ω-hetero-bifunctional PCLs **2-4** and **4-4** in conjunction with Cu (I)-mediated "click" reaction. The miktoarm CCS copolymers are then synthesized via cross-linking of the mixtures of MMs with 1,4-butandiol dimethacrylate (BDMA) by ATRP. Deblocking of the surficial amino groups of L-lysine dendrons affords amphiphilic nanoparticles that may find application in targeted drug delivery. On the contrary to classical amphiphilic copolymer micelles, this potential nanocarrier represents a sturdy, resourceful architecture that amalgamates numerous exceedingly important properties including: cationic hydrophilic surface, ER targeting motifs, covalently stabilized core, and hydrophobic and biodegradable interior. This elegant synthetic strategy facilitates tailoring the composition and properties of the CCS copolymers.

Results and Discussions

The synthesis of the linear-dendritic macromonomer (di-Boc-L-lysine)$_{G2}$-*b*-PCL-methacrylate (MM **6.1**) follows the pathway presented in Scheme 6.1. This algorithm has been elucidated in Chapter **5**. The synthetic cascade allows exhaustive characterization of each structural element (**2-4** and **5.3**), and thus facilitates the construction of a precisely controlled architecture. The DP of the linear segment as well as the generation number of the dendritic wedge can be tuned easily. However, the MM of a relatively small molecular weight is desired to ensure reasonable monomer conversion in the subsequent ATRP step. The CuAAC furnished MM **6.1** with narrow MWD suggestive of the absence of undesirable collateral reactions. The extent of the reaction was near to quantitative as judged from the ^{1}H NMR experiment data. The spectroscopic changes included total disappearance of the acetylenic hydrogen resonance signal. The presence of the resonance peaks related to the MA residue confirmed the preservation of the vinyl double bond which is the prerequisite for efficient participation of the MM in the cross-linking reactions. HSQC NMR experiment revealed that the "click" reaction had produced two regioisomers. Formation of two regioisomers when employing THF as the reaction medium has been reported.[143] The molecular weight characteristics of the MMs are summarized in Table 6.1.

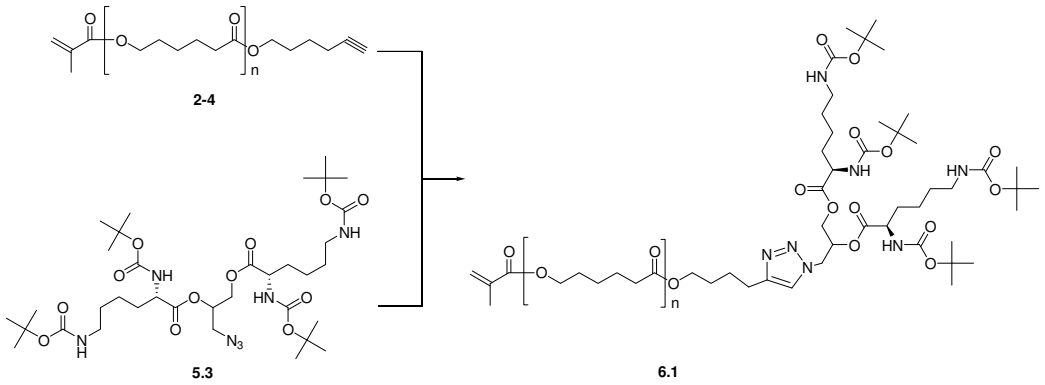

Scheme 6.1 Synthetic pathway for preparation of the linear-dendritic MM 6.1. Reagents and conditions: CuI, NEt_3, THF, 35 °C.

Table 6.1 Molecular weight characteristics of the MMs and CCS copolymers.

compound	M_n[a] (Da)	M_n[b] (Da)	M_w[b] (Da)	M_w/M_n[b]	M_w[c] (Da)	M_w/M_n[c]	*F*/*f*(**6.1**)[d]
6.1	3340	4900	5300	1.08			
6.2k	2720	3900	4300	1.11			
6.2m	3520	4800	5200	1.10			
6.2p	4890	6500	7300	1.12			
6.3	3820	5100	5600	1.10			
6.4	3730	5200	5700	1.10			
6.5					1.61×10^6	1.43	
6.6					2.00×10^6	1.55	
6.8					2.65×10^5	1.29	51/24
6.9					1.16×10^5	1.37	27/15

[a] By ^{1}H NMR. [b] By SEC with PS calibration. [c] By SEC with light scattering detector. [d] *F* is the total number of arms.

The linear MMs N_3-PCL-Methacrylate (the designation "MM **6.2**" is preserved for the α-azido-ω-methacryloyl-PCL with unspecified DP, whereas the designations "MM **6.2k**", "MM **6.2m**" and "MM **6.2p**" imply that the degrees of polymerization differ, and equal to 22, 29, and 41, respectively), E_2-PCL-Methacrylate (MM **6.3**), and ferrocene-PCL-Methacrylate (MM **6.4**) have been obtained according to the synthetic route depicted in Scheme 6.2. Again, the key compound is the hetero-bifunctional α-bromo-ω-methacryloyl-PCL **4-4**. α-Azido-ω-methacryloyl-PCL **6.2** was first prepared as proposed by Teyssié and co-workers:[70] **4-4** was treated with 5 equivalents of NaN_3 in DMF at 30 °C. The analysis by SEC produced a chromatogram featuring a small shoulder on the high molecular weight side. The appearance of the shoulder was attributed to the nucleophilic attack of the azide anion on the electrophilic carbonyl carbon atoms of the PCL chain. In an attempt to suppress this collateral reaction, 3 equivalents of NaN_3 were taken, and the reaction was carried out at room temperature (RT) in DMF. The shoulder was less-pronounced, and the PDI was fairly low (1.1). According to the NMR experiments the reaction reached completion, and no discernible side products were perceived. These results raised the speculation that the intermolecular addition of the terminal azide functionalities to the methacrylic residues took place even at RT. However, the contribution of this side reaction was minute inasmuch as NMR spectroscopy failed to detected considerable amount of the products. This conjecture was put on test by treating the α-bromo-ω-hydroxyl-PCL **4-0** with sodium azide under identical conditions. The SEC analysis produced a unimodal

chromatogram, and thus pointed towards the plausibility of the azide-methacrylate reaction in the previous experiments. This innuendo was further corroborated by the fact that MM **6.2** exhibited a limited shelf-life at RT. After several days the SEC experiment revealed a trace with bimodal distribution. Triazolines, formed from 1,3-cycloaddition, were identified after meticulous investigations by ^{1}H, COSY, and HSQC NMR experiments (Fig. 6.1).

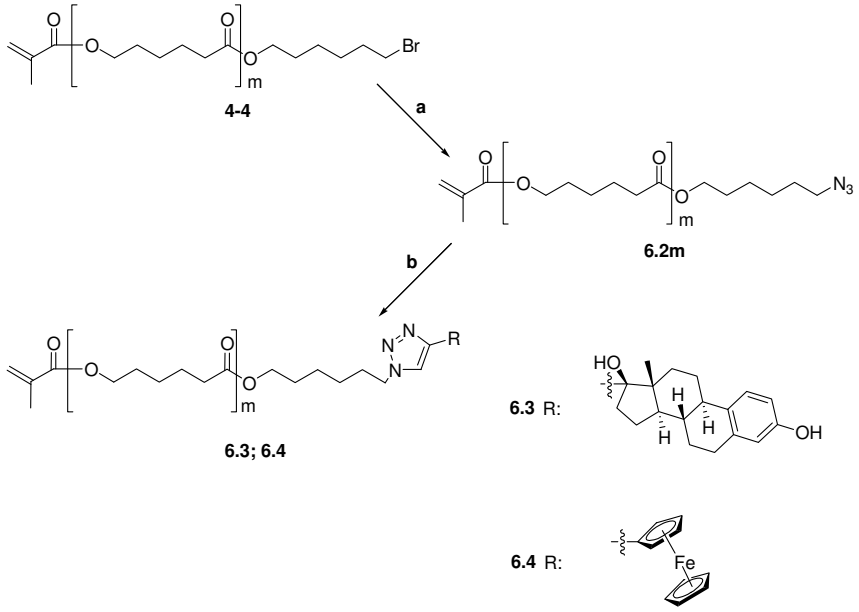

Scheme 6.2 Synthetic sequence leading to the MMs 6.2, 6.3 and 6.4. m denotes the DP of the MM 6.2. Reagents and conditions: (a) NaN_3, DMF; (b) 17α-ethynylestradiol or ethynylferrocene, CuI, NEt_3, THF, 35 °C.

Even though methacrylic monomers possessing pendant azide functional groups proved to be relatively stable at RT due to the steric hindrance,[144-146] these findings unequivocally demonstrate that uncatalyzed cycloaddition occurred during the substitution reaction, and continued throughout the matrix of the isolated MM manifesting itself in bimodal SEC chromatogram and additional resonances in NMR spectra. This result is rather astonishing if taken into consideration quite low local concentration of the terminal functional groups in case of the MM with the molecular weight of almost 5 000 Da. It must be highlighted, that the latent azide-methacrylate reaction was unveiled at the later stage of our experiments, and before that the preparation of the CCS polymers from the MM **6.2** had been attempted as will be discussed below.

The MMs, which carry terminal E_2 or ferrocene moieties, were synthesized by the CuAAC between the MM **6.2m** and 17α-ethynylestradiol or ethynylferrocene affording MM **6.3** and MM **6.4**, respectively (Scheme 6.2). The CuAAC involving ethynylferrocene has already been reported.[147] 17α-Ethynylestradiol too has been employed in the synthesis of E_2-peptoid[148] and E_2-cyclodextrin[149] conjugates by the Cu (I)-mediated "click" reaction. However, the participation of the azide end-capped PCL in the CuAAC has been limited to the preparation of a cyclic PCL.[41,79] Therefore, MM **6.3** is a unique hormone-synthetic polymer conjugate which has been constructed via this "click" reaction and utilized in ATRP. Once again, α,ω-hetero-bifunctional PCL **4-4** has proved itself as an exceedingly resourceful building block. In the "click" reaction, 3

equivalents of the alkyne were used to achieve full conversion, and to avert involvement of the methacrylic moieties in undesirable collateral reaction such as the azide-methacrylate addition. The SEC experiment produced a chromatogram with narrow MWD (PDI=1.1). Moreover, the intensity of the shoulder was unaltered. Evidently, no chain scission or triazoline formation took place. The structure of the MM **6.3** was investigated by ^{1}H NMR spectroscopy: the coupling was near to quantitative. The resonance signals attributed to the methacrylic acid residue (**h**, **i**, and **j**) confirmed the preservation of the vinyl double bond. The triazole proton (**k**) appeared at 7.41 ppm, and the signals originating from the E_2 moiety were detected as well (Fig. 6.2). Examination of the MM **6.4** by SEC and NMR experiments (Fig. 6.2) produced splendid results: SEC trace ruled out considerable chain scrambling and azide-methacrylate cycloaddition, and the NMR experiment verified almost quantitative functionalization.

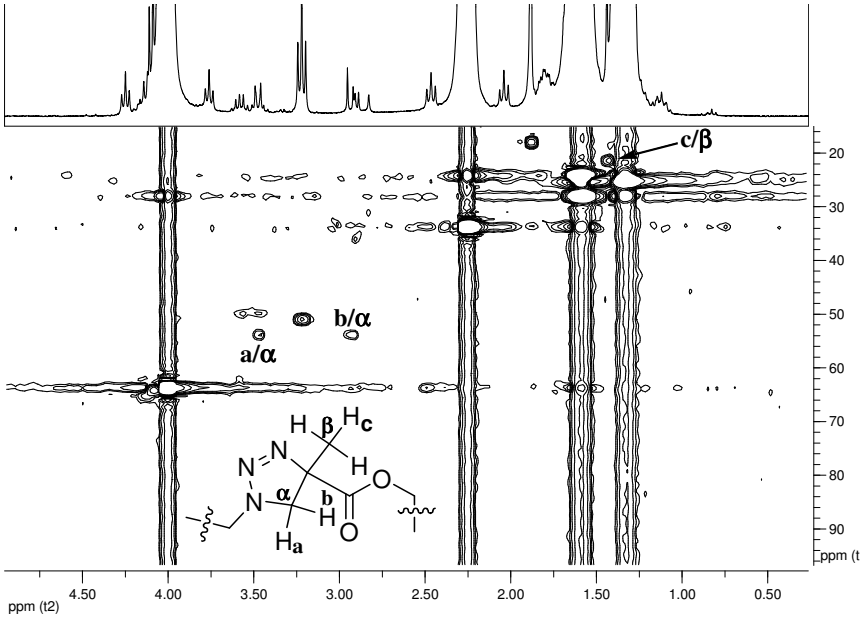

Figure 6.1 HSQC NMR spectrum of 6.2p: Evidence of the azide-methacrylate 1,3-cycloaddition.

With the azide-methacrylate reaction still lurking, the first type of the CCS polymer based solely on the MM **6.2k** was prepared. The CCS polymers with peripheral alkyne groups have been synthesized before.[150,151] Employing α-azido-ω-methacryloyl-PCL in the cross-linking reaction would produce stars with azide functionalities on the surface. The ATRP of the mixture of the MM **6.2k** and BDMA was initiated by ethyl α-bromoisobutyrate (EB*i*B) (Scheme 6.3).

There is a dearth of reports covering the PCL MMs in the CRP techniques.[152,153] Therefore, considerable adjustment of the reaction conditions was required to increase the MM conversion and maintain narrow MWD. The MM conversion was roughly approximated from the RI detector signal intensities on the SEC trace. This was a qualitative estimate, and no attempts have been made to quantify the MM conversion.

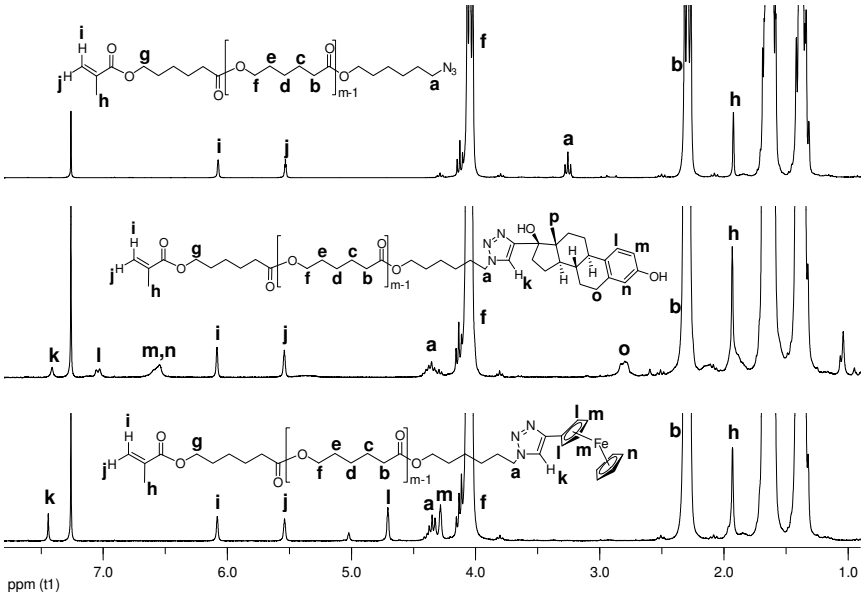

Figure 6.2 ^{1}H NMR spectra of the MMs 6.2m, 6.3, and 6.4 in $CDCl_3$.

Initially, the ATRP was carried out in anisole, taking into account better solubility of copper (II) complex in polar media,[126] at 50 °C using the CuBr/PMDETA catalytic complex and low initiator to MM molar ratio [MM **6.2k**]$_0$:[BDMA]$_0$:[CuBr]$_0$:[PMDETA]$_0$:[EB*i*B]$_0$=1:3:0.15:0.15:0.1. Only 3 equivalents of the cross-linker (BDMA) were taken since higher amounts could cause gelation of the reaction mixture. After a few hours relatively low MM conversion was attained. Extending the reaction time was of no use. This was blamed on the early blockage of the initiating sites due to the core congestion, loss of the active alkyl bromide moieties which has significant adverse effect at such a low concentration of the initiating groups, and catalyst deactivation.

Since long reaction times favor star-star couplings and thus broaden the MWD, increasing the MM incorporation at the early stage of the reaction seemed to be one way of alleviating the problem. The reaction conditions were improved by replacing anisole with toluene in order to increase the solubility of the PCL MM, substituting PMDETA with HMTETA to enhance the stability of the catalytic complex, and using the following initial molar ratios: [MM **6.2k**]$_0$:[BDMA]$_0$:[CuBr]$_0$:[HMTETA]$_0$:[EB*i*B]$_0$=1:15:2.25:4.5:1.5. The concentrations of the reagents were reduced by diluting the reaction mixture in order to avoid possible gelation at such a high cross-linker to MM ratio. Making use of 1.5 equivalents of the initiator contradicts the scheme proposed by Matyjaszewski – reducing the number of initiating sites to diminish the extent of star-star coupling.[129,130] Achieving a reasonable MM conversion on the expense of the MWD was expected. This sacrifice was necessary to avoid wasting of the MMs **6.1**, **6.2**, **6.3**, and **6.4** because of the delicate multistep synthetic protocols involved in their preparation. The molecular weight characteristics of the CCS polymer **6.5** were estimated using light scattering detector. The PDI was relatively low (1.43), but the weight average molecular weight M_w was rather high (1.61×10^6 Da) (Table 6.1). Such a large M_w has not been described before.[125-127,129-134]

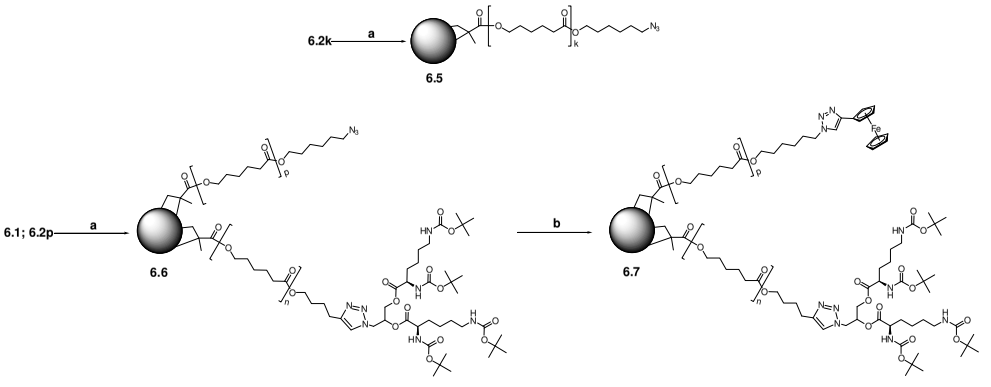

Scheme 6.3 Preparation and derivatization of CCS (co)polymers 6.5 and 6.6. Reagents and conditions: (a) BDMA, CuBr/HMTETA, EB*i*B, toluene, 50 °C; (b) ethynylferrocene, CuI, NEt_3, THF, 64 °C.

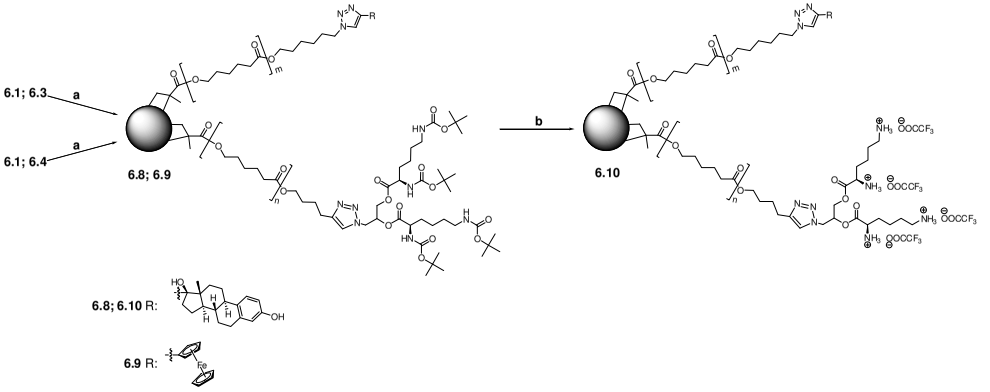

Scheme 6.4 Preparation of CCS copolymers 6.8, 6.9, and 6.10 bearing peripheral E_2 or ferrocene moieties. Reagents and conditions: (a) BDMA, CuBr/HMTETA, EB*i*B, toluene, 50 °C; (b) TFA, CH_2Cl_2.

The formation of such a large CCS polymer was ascribed to the star-star coupling reactions provoked by relatively high concentration of the initiating sites and the cross-linker with soft aliphatic spacer.[154] The azide-methacrylate cycloaddition reaction, which was not suspected at this point, could significantly contribute to the star-star coupling as well. The ^{1}H NMR spectroscopy data proved the formation of a core-shell structure: broad resonances from the nanogel core overlapped with those from the PCL arms, and resulted in a slight broadening at the baseline. The signals corresponding to the unreacted double bonds were barely detected. The star periphery contained a certain amount of azide functional groups. The miktoarm CCS **6.6** was then prepared under similar reaction conditions: the mixture of the linear-dendritic MM **6.1** and the linear MM **6.2p** was cross-linked with BDMA. The structure of the CCS copolymer was scrutinized by NMR spectroscopy, and the incorporation of both arms into the CCS **6.6** was confirmed. SEC trace was not symmetrical pointing towards the presence of a number of the star populations as a result of the coupling reactions. However no unreacted MMs were observed. The molecular characteristics were obtained using the light scattering detector, and are given in Table 6.1. But after a few days, the CCS **6.6** displayed limited solubility in THF and other common organic solvents hinting that a certain type of cross-linking reaction was taking place in the bulk of the isolated product. It is obvious that the ATRP initiating sites embedded in the core are not responsible for this cross-linking reaction. The only reactive functionalities are the peripheral azide groups and remaining internal methacrylic moieties. However, the NMR analysis of the CCS **6.6** was obstructed by the partial solubility of the compound in $CDCl_3$, and therefore it was impossible to identify the side reaction products. The investigation of the MM **6.2**, which had been isolated for a while, by NMR spectroscopy uncovered the copper-free azide-methacrylate cycloaddition. Indeed, this reaction links the stars to each other during the ATRP as well as after isolation of the product, and is responsible for the large M_w and broad MWD. Thus, conjugating the MM **6.2** to the desirable moiety by the CuAAC before the cross-linking reaction appears to be crucial. Even though the CCS **6.6** was only partially soluble in THF, it was derivatized with ethynylferrocene by conducting the Cu^I-catalyzed "click" reaction in a heterogeneous mixture (Scheme 6.3). Three-fold excess of ethynylferrocene and CuI were employed. The ^{1}H NMR experiment proved, though unsubstantially due to the limited solubility, that the accessible surficial azide groups had reacted since the resonance signal ascribed to the methylene group neighboring the azide function disappeared, and the peaks attributable to the ferrocene moiety were detected.

After shutting down the azide functions, the MMs **6.1**, **6.3** and **6.4** were employed in preparation of the miktoarm CCS copolymers as depicted in Scheme 6.4. The ATRP of the MM **6.1**, MM **6.3**, and BDMA lead to gelation when the conditions used for the synthesis of the CCS **6.6** were applied. The gel formation was avoided by diluting the reaction mixture. The molecular characteristics were estimated using the light scattering detector, and are given in Table 6.1. Fairly low PDI (1.29) implies that the ATRP was under control, and that a considerable reduction of the star-star coupling was achieved. Fig. 6.3 is the ^{1}H NMR spectrum of the CCS **6.8**. The resonance signals arising from the PCL backbone and the nanogel core overlap. The peaks related to the methyl group of the Boc protection (**a**), the methylene group adjacent to the Boc protected amino group (**b**), and the triazole protons (**c**) of the MM **6.1** can be identified. The signals, originating from the E_2 moiety and the triazole proton of the MM **6.3**, have been assigned as well. The resonances **o** and **p** are attributed to the methacrylic acid residues of the core: the segmental mobility of the core has not been frozen completely.

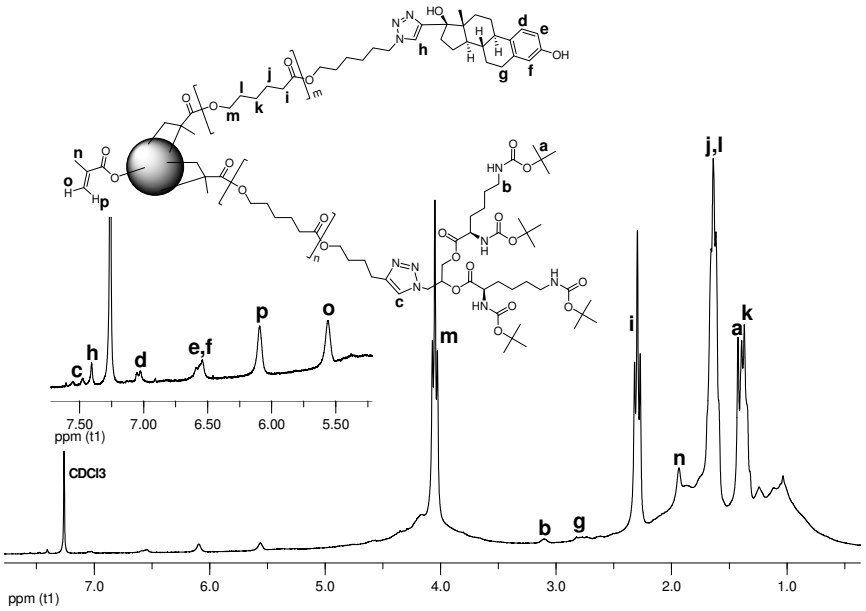

Figure 6.3 ^{1}**H NMR spectrum of the CCS 6.8.**[‡‡]

It is obvious from Fig. 6.3 that the intensities of the resonance signals of the L-lysine and E_2 moieties are too weak to be used in determination of the composition of the CCS copolymer **6.8**. Consequently, TGA has been utilized to estimate the ratio and the number of arms of the MMs. The overlay of the TGA thermograms (Fig. 6.4) permits assessment of the weight fraction of the MM **6.1** as follows: the weight loss of 3.7 % between 222 °C and 273 °C is ascribed to the decomposition of the Boc protecting groups, and correlates to about 31 % of the MM **6.1**. Approximately 26 % weight loss in the temperature range 423-511 °C is attributed to the decomposition of the core. Thus, the weight fraction of the MM **6.3** is around 43 %. Obviously these weight fractions are rough estimates; nevertheless, they are indispensable in gaining some insight about the star composition. Exploiting the following equation: $f = \frac{WF_{arms} \times M_{w,CCS}}{M_{w,arms}}$, where f is the average number of arms, WF_{arms} is the weight fraction of the arms determined by TGA, and $M_{w,CCS}$ and $M_{w,arms}$ are the weight average molecular weights of the CCS copolymer and the arms, respectively, it can be calculated that the CCS **6.8** is comprised of on average 24 (di-Boc-L-lysine)$_{G2}$-*b*-PCL and 27 E_2-PCL arms. The molar ratio of the incorporated arms is [E_2-PCL]/[(di-Boc-L-lysine)$_{G2}$-*b*-PCL]=1.2, whereas in the initial mixture the molar ratio of the MMs was [MM **6.3**]$_0$/[MM **6.1**]$_0$=1.8. The discrepancy between the initial and final compositions may be attributed to the higher reactivity of the MM **6.1** as a result of its lower molecular weight.[133] The total number of arms (*F*) is given in Table 6.1; *f*(**6.1**) denotes the number of linear-dendritic arms.

The CCS copolymer **6.8** was treated with TFA in order to deprotect the amine functional groups of the L-lysine dendrons (Scheme 6.4). The CCS copolymer **6.10**, which possesses about 96 amine functions on the surface, was analyzed with ^{1}H NMR spectroscopy using DMSO-d_6 as solvent. The resonance signals assigned

[‡‡] Adopted from Javakhishvili, I.; Hvilsted, S. *Polym. Chem.* **2010**, *1*, 1650-1661.

to the *tert*-butyl groups were no longer detected, while the broad peaks corresponding to the free amine functions emerged. All the other characteristic peaks were also observed. The signals from the core were somewhat diminished in intensity, probably due to the limited solubility of the interior of the CCS **6.10** in as polar a solvent as DMSO-d_6.

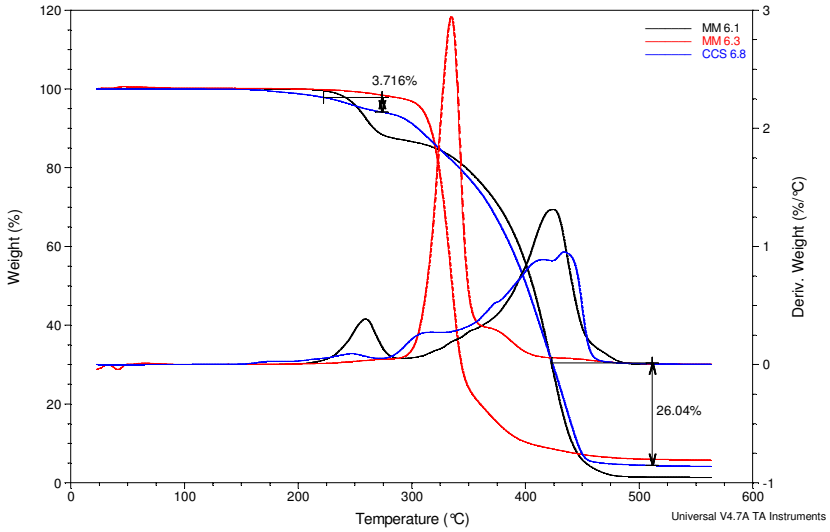

Figure 6.4 TGA thermograms of the MM 6.1, MM 6.3, and CCS copolymer 6.8.

After determining the optimal reaction parameters for the synthesis of the CCS copolymer **6.8**, the mixture of the MM **6.1** and MM **6.4** was cross-linked with BDMA under similar conditions resulting in the CCS **6.9.** The CCS **6.9** was examined by ^{1}H NMR spectroscopy: both arms had been integrated in the star copolymer. The following molecular characteristics were obtained using the SEC with light scattering detector: M_w=1.16x10^5 Da and PDI=1.37 (Table 6.1). The composition of the CCS **6.9** was estimated by TGA: 45 % of the MM **6.1**, 41 % of the MM **6.4**, and 14 % of the core. Hence, the CCS **6.9** consists of 15 (di-Boc-L-lysine)$_{G2}$-*b*-PCL and 12 ferrocene-PCL arms (Table 6.1). Clusters of the CCS **6.9** were observed by TEM without additional staining (Fig. 6.5). Spherical nanoparticles in the range of 10-20 nm can be identified. The clustering of the nanoparticles may be the result of poor repulsive interactions among the coronas of the CCS copolymers. Low contrast and aggregation do not allow accurate evaluation of the size and distribution of these nanoparticles.

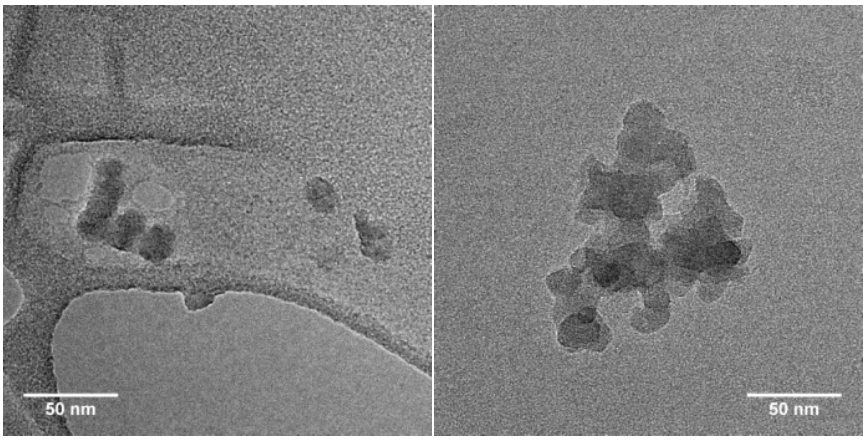

Figure 6.5 TEM images of the CCS copolymer 6.9.[§§]

Thus, the synthesis of miktoarm CCS copolymers consisting of linear-dendritic and linear PCL arms has been accomplished. The cornerstone for preparation of these CCS polymers is the library of well-defined MMs, which in turn is based on α,ω-hetero-bifunctional PCLs. These hetero-telechelic building blocks are characterized with low PDI and high degree of functionality. Elaboration of the structure and composition of the intermediate and final products proves the robustness, flexibility, efficiency and high degree of control offered by the proposed synthetic sequences. CCS copolymer **6.10** is schematically represented in Fig. 6.6. This nanoscale aggregate possesses hydrophilic, cationically charged exterior decorated with targeting ligands, and hydrophobic, bioerodible core, and may have potential in targeted drug delivery.

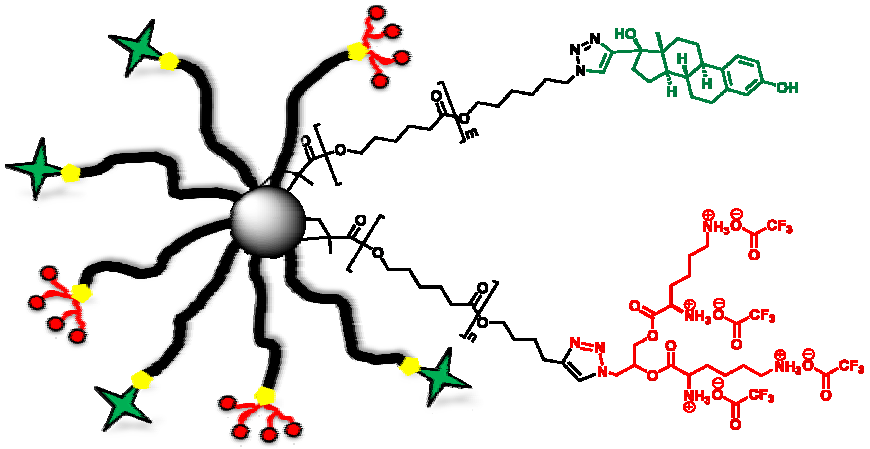

Figure 6.6 Schematic representation of the CCS copolymer 6.10.

[§§] Adopted from Javakhishvili, I.; Hvilsted, S. *Polym. Chem.* **2010**, *1*, 1650-1661.

Conclusions

The Ph. D. project encompasses preparation and characterization of functional nanostructures with the potential in cancer treatment. Features such as biocompatibility, biodegradability and ease of excretion from the body after accomplishment of the therapeutic mission are of utmost importance. Therefore, these nanostructures integrate natural and synthetic building blocks that are known to be harmless upon administration in human body and do not trigger adverse reactions. Furthermore, these nanoscopic entities have the capacity to combine various approaches to fight cancer: laser hyperthermia, RF ablative therapy, and non-specific or ligand-targeted, selective drug delivery.

The battery of synthetic tools includes ROP, ATRP, CuAAC, and thiol-ene "click" reaction. Combination of these accurate, robust, and effectual techniques allows preparation and conjugation of various macromolecular fragments into more sophisticated architectures. The main element in the anthology of these molecular fragments is the α,ω-hetero-bifunctional PCL with well-defined, precisely controlled structure, and high end group fidelity, that facilitates construction of the amphiphilic copolymers.

AuNPs with the amphiphilic shell consisting of PCL-*b*-PAA diblock copolymer have been obtained by employing "coordination-insertion" ROP of ε-CL and Ni (II)-mediated ATRP of *t*BA. These controlled polymerization techniques and subtle protection-deprotection chemistry have been coupled using the dual initiator strategy to afford the amphiphilic block copolymer HS-PCL-*b*-PAA with the thiol functional group at the PCL chain end. Both polymerization steps are well controlled, and provide polymeric blocks with narrow MWDs. Introduction of the acid-labile sulfhydryl protecting group allows unmasking of thiol and acrylic acid functionalities in one pot. The gold clusters are then prepared by reducing the gold salt in the presence of these macrothiols to afford aggregation-free AuNPs with the diameter of 9.0 ± 3.1 nm highlighting the reliability of the macroligand. Owing to their size and the monolayer composition, these AuNPs may combine RF ablation, and site-specific drug delivery. While the size of the gold cores is within the range where it can be manipulated with the RF energy fields, the polymeric corona features hydrophobic layer for drug compartmentalization and mucoadhesive layer for anchoring on mucous membranes. The gold core bestows this nanostructure stability in biological fluids, and therefore may be employed for bladder cancer treatment.

Amphiphilic rodcoil dendron cholesteryl-PCL-*b*-(L-lysine)$_{G2}$ has been constructed by employing the cascade of orthogonal "click" reactions. The hetero-telechelic α-alkynyl-ω-alkenyl-PCL is the fundamental and versatile building unit that allows coupling of CuAAC and UV induced radical thiol-ene "click" reaction. The second generation dendron of L-lysine is obtained by divergent growth, and bears built-in primary bromide function. The ensuing nucleophilic substitution with NaN_3 promptly furnishes the wedge with the azide functional group at the focal point, and thus the number of synthetic steps is considerably reduced. The efficiency of these sequential "click" reactions permits near to quantitative conjugation of the dendron as well as cholesteryl moiety. This synthetic strategy is marked with a high degree of freedom, and allows linking of virtually innumerable building blocks because of a wide range of commercially available mercaptans, ease of preparation of organic azides, and reliability of α-alkynyl-ω-alkenyl-PCL. The radical thiol-ene reaction has been utilized for the ligation of reduced glutathione with α,ω-dialkenyl-PCL as well. These amphiphilic macromolecules incorporate biocompatible PCL segment, and naturally occurring moieties of the biological importance. Therefore, they may find application in drug delivery or tissue engineering.

The final accord of the Ph. D. project is preparation of the miktoarm CCS copolymers. The miktoarm CCS copolymers are comprised of linear PCL and linear-dendritic PCL-*b*-(L-lysine)$_{G2}$ arms. They have been synthesized following the MM approach where the MMs with terminal methacrylic moiety are polymerized together with a difunctional monomer BDMA by ATRP. The miktoarm stars exhibit fairly low PDI, and are within the range of approximately 10-20 nm in diameter. The CCS copolymers feature cross-linked core, PCL inner compartment, and functional exterior bearing amine functional groups, E_2 or ferrocene moieties. The MMs have been obtained from the α,ω-hetero-telechelic PCLs by making use of the CuAAC, once again accentuating the ingenuity of these macromolecular fragments. Two types of the miktoarm CCS copolymers have been prepared, and their compositions have been investigated by TGA. One of them contains 27 E_2-PCL and 24 PCL-*b*-(L-lysine)$_{G2}$ arms, while the other integrates 12 ferrocene-PCL and 15 PCL-*b*-(L-lysine)$_{G2}$ arms. The former exhibits some of the essential traits of a drug delivery vehicle: it possesses a hydrophobic interior to accommodate lipophilic drugs, and a positively charged hydrophilic surface decorated with pilot molecules. The constituent elements should not induce undesirable side effects but facilitate selective delivery of anticancer therapeutic agents.

Future Work

Development of the reaction sequences and scrupulous characterization of the structure and composition of the intermediate and goal products is the leitmotiv of this project. However, the synthetic layouts can be optimized further, and the compounds can be elaborated even more.

The influence of the following variables on the size and distribution of the AuNPs can be elucidated: a) composition of the HS-PCL-*b*-PAA macroligand, b) reducing agent, c) rate of reduction, and d) gold salt to macroligand initial molar ratio. Solution properties of the AuNPs, including the effect of the pH and temperature, ought to be investigated by the dynamic light scattering (DLS) technique. DLS allows estimation of the thickness of the polymeric shell as well. Mucoadhesive properties of the AuNPs, and the stability of the substrate-nanoparticles complex must be assessed. It would be very interesting to probe the heat evolution by the AuNPs when addressed by the RF energy fields.

The linear-dendritic block copolymer cholesteryl-PCL-*b*-(L-lysine)$_{G2}$ does have all the necessary components to self-assemble in solution as well as in solid state, but this self-assembly needs rather meticulous investigation. Moreover, the length of the PCL linear segment and the generation number of the L-lysine dendron must be varied, and the influence of these parameters on self-assembly must be explored. Investigation of the thermal properties by differential scanning calorimetry seems rather alluring since it can uncover the existence of the organized phases and the corresponding transition temperatures. This again requires a collection of the block copolymers with different DP and generation number. The solution properties can be studied by DLS. If the block copolymer assembles into micelles, then the cmc should be estimated.

In case of the miktoarm CCS copolymers the reaction conditions require further optimization. It would be beneficial to attain incorporation of a predetermined number of arms. A wide range of parameters such as initial molar ratios of the MMs, cross-linker and the initiator as well as concentration and the catalytic complex should be adjusted in the quest of lower PDI and higher MM conversion. It is obvious that the MMs with such a large number of functional groups may interfere with the ATRP equilibrium. Therefore, various nitrogen ligands, or even a different transition metal should be tested. TGA has been indispensible in gaining insight about the composition of the CCS copolymers. However, an alternative route to verify the results or make them more accurate ought to be developed. The size and distribution of these nanoparticles can be measured either in solution by DLS, or on a solid support by TEM, scanning electron microscopy, and atomic force microscopy. Methodology for sample preparation for the electron microscopy should be optimized to achieve an enhanced resolution.

Drug loading and release capacity of these materials should be investigated by employing model pharmaceuticals. The content of the residual metal catalysts should be quantified, and the biocompatibility of the final products should be evaluated by conducting cell viability experiments. The biodegradability studies in physiological milieu may be performed. For the CCS copolymers evaluation of the specific cellular uptake is essential to assess the contribution of the E_2 moieties as cancer cell targeting motifs.

References:

1. Torchilin, V. P. *Pharmaceut. Res.* **2007**, *24*, 1-16.
2. Davis, M. E.; Chen, Z.; Shin, D. M. *Nat. Rev. Drug Discov.* **2008**, *7*, 771-782.
3. Lyer, A. K.; Khaled, G.; Fang, J.; Maeda, H. *Drug Discov. Today* **2006**, *11*, 812-818.
4. Maeda, H.; Bharate, G. Y.; Daruwalla, J. *Eur. J. Pharm. Biopharm.* **2009**, *71*, 409-419.
5. Brigger, I.; Dubernet, C.; Couvreur, P. *Adv. Drug Deliv. Rev.* **2002**, *54*, 631-651.
6. Torchilin, V. P. *Cell. Mol. Life Sci.* **2004**, *61*, 2549-2559.
7. Ghoroghchian, P. P.; Li, G.; Levine, D. H.; Davis, K. P.; Bates, F. S.; Hammer, D. A.; Therien, M. J. *Macromolecules* **2006**, *39*, 1673-1675.
8. Savic, R.; Luo, L.; Eisenberg, A.; Maysinger, D. *Science* **2003**, *300*, 615-618.
9. Discher, D. E.; Ortiz, V.; Srinivas, G.; Klein, M. L.; Kim, Y.; Christian, D.; Cai, S.; Photos, P.; Ahmed, F. *Prog. Polym. Sci.* **2007**, *32*, 838-857.
10. Nagasaki, Y.; Yasugi, K.; Yamamoto, Y.; Harada, A.; Kataoka, K. *Biomacromolecules* **2001**, *2*, 1067-1070.
11. Jule, E.; Nagasaki, Y.; Kataoka, K. *Bioconjugate Chem.* **2003**, *14*, 177-186.
12. Lee, E. S.; Na, K.; Bae, Y. H. *J. Control. Release* **2003**, *91*, 103-113.
13. Smart, J. D. *Adv. Drug Deliv. Rev.* **2005**, *57*, 1556-1568.
14. Andrews, G. P.; Laverty, T. P.; Jones, D. S. *Eur. J. Pharm. Biopharm.* **2009**, *71*, 505-518.
15. Inoue, T.; Chen, G.; Nakamae, K.; Hoffman, A. S. *J. Control. Release* **1998**, *51*, 221-229.
16. Lele, B. S.; Hoffman, A. S. *J. Control. Release* **2000**, *69*, 237-248.
17. Jérôme, C.; Lecomte, Ph. *Adv. Drug Deliv. Rev.* **2008**, *60*, 1056-1076.
18. Dove, A. P. *Chem. Commun.* **2008**, 6446-6470.
19. Labet, M.; Thielemans, W. *Chem. Soc. Rev.* **2009**, *38*, 3484-3504.
20. Wang, Y.; Kunioka, M. *Macromol. Symp.* **2005**, *224*, 193-205.
21. Dubois, Ph.; Degée, Ph.; Jérôme, R.; Teyssié, Ph. *Macromolecules* **1992**, *25*, 2614-2618.
22. Kowalski, A.; Duda, A.; Penczek, S. *Macromol. Rapid Commun.* **1998**, *19*, 567-572.
23. Kowalski, A.; Duda, A.; Penczek, S. *Macromolecules* **2000**, *33*, 689-695.
24. Arbaoui, A.; Redshaw, C. *Polym. Chem.* **2010**, *1*, 801-826.
25. Shibasaki, Y.; Sanada, H.; Yokoi, M.; Sanda, F.; Endo, T. *Macromolecules* **2000**, *33*, 4316-4320.
26. Mecerreyes, D.; Humes, J.; Miller, R. D.; Hedrick, J. L.; Detrembleur, C.; Lecomte, Ph:; Jérôme, R.; San Roman, J. *Macromol. Rapid Commun.* **2000**, *21*, 779-784.
27. Stassin, F.; Halleux, O.; Dubois, Ph.; Detrembleur, C.; Lecomte, Ph.; Jérôme, R. *Macromol. Symp.* **2000**, *153*, 27-39.
28. Detrembleur, C.; Mazza, M.; Halleux, O.; Lecomte, Ph.; Mecerreyes, D.; Hedrick, J. L.; Jérôme, R. *Macromolecules* **2000**, *33*, 14-18.
29. Rieger, J.; Bernaerts, K. V.; Du Prez, F. E.; Jérôme, R.; Jérôme, C. *Macromolecules* **2004**, *37*, 9738-9745.
30. Vroman, B.; Mazza, M.; Fernandez, M. R.; Jérôme, R.; Préat, V. *J. Control. Release* **2007**, *118*, 136-144.
31. Rieger, J.; Van Butsele, K.; Lecomte, P.; Detrembleur, C.; Jérôme, R.; Jérôme, C. *Chem. Commun.* **2005**, 274-276.
32. Braunecker, W. A.; Matyjaszewski, K. *Prog. Polym. Sci.* **2007**, *32*, 93-146.
33. Kamigaito, M.; Ando, T.; Sawamoto, M. *Chem. Rev.* **2001**, *101*, 3689-3745.

34. Matyjaszewski, K.; Xia, J. *Chem. Rev.* **2001**, *101*, 2921-2990.
35. Matyjaszewski, K.; Tsarevsky, N. V. *Nat. Chem.* **2009**, *1*, 276-288.
36. Rostovtsev, V. V.; Green, L. G.; Fokin, V. V.; Sharpless, K. B. *Angew. Chem., Int. Ed.* **2002**, 41, 2596-2599.
37. Tornøe, C. W.; Christensen, C.; Meldal, M. *J. Org. Chem.* **2002**, *67*, 3057-3064.
38. Meldal, M. *Macromol. Rapid Commun.* **2008**, *29*, 1016-1051.
39. Binder, W. H.; Sachsenhofer, R. *Macromol. Rapid Commun.* **2008**, *29*, 952-981.
40. Iha, R. K.; Wooley, K. L.; Nyström, A. M.; Burke, D. J.; Kade, M. J.; Hawker, C. J. *Chem. Rev.* **2009**, *109*, 5620-5686.
41. Lecomte, Ph.; Riva, R.; Jérôme, C.; Jérôme, R. *Macromol. Rapid Commun.* **2008**, *29*, 982-997.
42. Xu, N.; Lu, F.-Z.; Du, F.-S.; Li, Z.-C. *Macromol. Chem. Phys.* **2007**, *208*, 730–738.
43. Riva, R.; Schmeits, S.; Jérôme, C.; Jérôme, R.; Lecomte, Ph. *Macromolecules* **2007**, *40,* 796-803.
44. Parrish, B.; Emrick, T. *Bioconjugate Chem.* **2007**, *18*, 263-267.
45. Parrish, B.; Breitenkamp, R. B.; Emrick, T. *J. Am. Chem. Soc.* **2005**, *127*, 7404-7410.
46. He, X.; Liang, L.; Xie, M.; Zhang, Y.; Lin, S.; Yan, D. *Macromol. Chem. Phys.* **2007**, *208*, 1797-1802.
47. Kade, M. J.; Burke, D. J.; Hawker, C. J. *J. Polym. Sci. Polym. Chem.* **2010**, *48*, 743-750.
48. Lowe, A. B. *Polym. Chem.* **2010**, *1*, 17-36.
49. Lowe, A. B.; Harvison, M. A. *Aust. J. Chem.* **2010**, *63*, 1251-1266.
50. Hoyle, C. E.; Lowe, A. B.; Bowman, C. N. *Chem. Soc. Rev.* **2010**, *39*, 1355-1387.
51. Justynska, J.; Hordyjewicz, Z.; Schlaad, H. *Polymer* **2005**, *46*, 12057-12064.
52. Gress, A.; Völkel, A.; Schlaad, H. *Macromolecules* **2007**, *40*, 7928-7933.
53. Killops, K. L.; Campos, L. M.; Hawker, C. J. *J. Am. Chem. Soc.* **2008**, *130*, 5062-5064.
54. Kang, T.; Amir, R. J.; Khan, A.; Ohshimizu, K.; Hunt, J. N.; Sivanandan, K.; Montanez, M. I.; Malkoch, M.; Ueda, M.; Hawker, C. J. *Chem. Commun.* **2010**, *46*, 1556-1558.
55. Campos, L. M.; Killops, K. L.; Sakai, R.; Paulusse, J. M. J.; Damiron, D.; Drockenmuller, E.; Messmore, B. W.; Hawker, C. J. *Macromolecules* **2008**, *41*, 7063-7070.
56. van der Ende, A.; Croce, T.; Hamilton, S.; Sathiyakumar, V.; Harth, E. *Soft Matter* **2009**, *5*, 1417-1425.
57. Jonkheijm, P.; Weinrich, D.; Köhn, M.; Engelkamp, H.; Christianen, P. C. M.; Kuhlmann, J.; Maan, J. C.; Nüsse, D.; Schroeder, H.; Wacker, R.; Breinbauer, R.; Niemeyer, C. M.; Waldmann, H. *Angew. Chem. Int. Ed.* **2008**, *47*, 4421-4424.
58. Sun, H.; Guo, B.; Li, X.; Cheng, R.; Meng, F.; Liu, H.; Zhong, Z. *Biomacromolecules* **2010**, *11*, 848–854.
59. Gou, P.-F.; Zhu, W.-P.; Shen, Z.-Q. *Biomacromolecules* **2010,** *11,* 934–943.
60. Motola-Timol, S.; Jhurry, D.; Zhou, J.; Bhaw-Luximon, A.; Mohun, G.; Ritter, H. *Macromolecules* **2008**, *41*, 5571-5576.
61. Schramm, O. G.; Meier, M. A. R.; Hoogenboom, R.; van Erp, H. P.; Gohy, J.-F.; Schubert, U. S. *Soft Matter* **2009**, *5*, 1662-1667.
62. Östmark, E.; Nyström, D.; Malmström, E. *Macromolecules* **2008**, *41*, 4405-4415.
63. Ternat, C.; Kreutzer, G.; Plummer, C. J. G.; Nguyen, T. Q.; Herrmann, A.; Ouali, L.; Sommer, H.; Fieber, W.; Velazco, M. I.; Klok, H.-A.; Månson, J.-A. E. *Macromol. Chem. Phys.* **2007**, *208*, 131-145.
64. Bougard, F.; Jeusette, M.; Mespouille, L.; Dubois, Ph.; Lazzaroni, R. *Langmuir* **2007**, *23*, 2339-2345.
65. Darcos, V.; Habnouni, A. E.; Nottelet, B.; Ghzaoui, A. E.; Coudane, J. *Polym. Chem.* **2010**, *1*, 280-282.

66. Geng, Y.; Discher, D. *J. Am. Chem. Soc.* **2005**, *127*, 12780-12781.
67. Rieger, J.; Van Butsele, K.; Lecomte, Ph.; Detrembleur, C., Jérôme, R.; Jérôme, C. *Chem. Commun.* **2005**, 274-276.
68. Dubois, Ph.; Jérôme, R.; Teyssié, Ph. *Polym. Bull.* **1989**, *22*, 475-482.
69. Dubois, Ph.; Jérôme, R.; Teyssié, Ph. *Macromolecules* **1991**, *24*, 977-981.
70. Degée, Ph.; Dubois, Ph.; Jérôme, R.; Teyssié, Ph. *Macromolecules* **1992**, *25*, 4242-4248.
71. Degirmenci, M.; Hizal, G.; Yagci, Y. *Macromolecules* **2002**, *35*, 8265-8270.
72. Carrot, G.; Hilborn, J.; Hedrick, J. L.; Trollsås, M. *Macromolecules* **1999**, *32*, 5171-5173.
73. Carrot, G.; Hilborn, J. G.; Trollsås, M.; Hedrick, J. L. *Macromolecules* **1999**, *32*, 5264-5269.
74. Hedfors, C.; Östmark, E.; Malmström, E.; Hult, K.; Martinelle, M. *Macromolecules* **2005**, *38*, 647-649.
75. Hoogenboom, R.; Moore, B. C.; Schubert, U. S. *Chem. Commun.* **2006**, 4010-4012.
76. Durmaz, H.; Dag, A.; Altintas, O.; Erdogan, T.; Hizal, G.; Tunca, U. *Macromolecules* **2007**, *40*, 191-198.
77. Sinnwell, S.; Inglis, A. J.; Davis, T. P.; Stenzel, M. H.; Barner-Kowollik, C. *Chem. Commun.* **2008**, 2052-2054.
78. Celiz, A. D.; Scherman, O. A. *Macromolecules* **2008**, *41*, 4115-4119.
79. Hoskins, J. N.; Grayson, S. M. *Macromolecules* **2009**, *42*, 6406-6413.
80. Hawker, C. J.; Hedrick, J. L.; Malmström, E. E.; Trollsås, M.; Mecerreyes, D.; Moineau, G.; Dubois, Ph.; Jérôme, R. *Macromolecules* **1998**, *31*, 213–219.
81. Kricheldorf, H. R. *Macromol. Symp.* **2000**, *153*, 55–65.
82. Jakubowski, W.; Lutz, J.-F.; Slomkowski, S.; Matyjaszewski, K. *J. Polym. Sci. Polym. Chem.* **2005**, *43*, 1498–1510.
83. Trollsås, M.; Hawker, C. J.; Hedrick, J. L.; Carrot, G.; Hilborn, J. *Macromolecules* **1998**, *31*, 5960–5963.
84. Hu, J.; Fox, M. A. *J. Org. Chem.* **1999**, *64*, 4959–4961.
85. Mourtas, S.; Gatos, D.; Kalaitzi, V.; Katakalou, C.; Barlos, K. *Tetrahedron Lett.* **2001**, *42*, 6965–6967.
86. Jain, P. K.; El-Sayed, I. H.; El-Sayed, M. A. *Nano Today* **2007**, *2*, 18-29.
87. Cherukuri, P.; Glazer, E. S.; Curley, S. A. *Adv. Drug Deliv. Rev.* **2010**, *62*, 339-345.
88. Agarwal, A.; Huang, S. W.; O'Donnell, M.; Day, K. C.; Day, M.; Kotov, N.; Ashkenazi, S. *J. Appl. Phys.* **2007**, *102*, 064701.
89. El-Sayed, I. H.; Huang, X.; El-Sayed, M. A. *Cancer Lett.* **2006**, *239*, 129-135.
90. Hirsch, L. R.; Stafford, R. J.; Bankson, J. A.; Sershen, S. R.; Rivera, B.; Price, R. E.; Hazle, J. D.; Halas, N. J.; West, J. L. *Proc. Natl. Acad. Sci. U.S.A.* **2003**, *100*, 13549–13554.
91. Gannon, C. J.; Patra, C. R.; Bhattacharya, R.; Mukherjee, P.; Curley, S. A. *Journal of Nanobiotechnology* **2008**, *6*, DOI: 10.1186/1477-3155-6-2.
92. Gibson, J. D.; Khanal, B. P.; Zubarev, E. R. *J. Am. Chem. Soc.* **2007**, *129*, 11653–11661.
93. Hong, R.; Han, G.; Fernández, J. M.; Kim, B.-j.; Forbes, N. S.; Rotello, V. M. *J. Am. Chem. Soc.* **2006**, *128*, 1078–1079.
94. Shan, J.; Tenhu, H. *Chem. Commun.* **2007**, 4580–4598.
95. Wang, F.; Bronich, T. K.; Kabanov, A. V.; Rauh, R. D.; Roovers, J. *Bioconjugate Chem.* **2005**, *16*, 397-405.
96. Zhang, Q.; Remsen, E. E.; Wooley, K. L. *J. Am. Chem. Soc.* **2000**, *122*, 3642–3651.

97. Azzam, T.; Eisenberg, A. *Langmuir* **2007**, *23*, 2126–2132.
98. Hedrick, J. L.; Trollsås, M.; Hawker, C. J.; Atthoff, B.; Claesson, H.; Heise, A.; Miller, R. D.; Mecerreyes, D.; Jérôme, R.; Dubois, Ph. *Macromolecules* **1998**, *31*, 8691–8705.
99. Moineau, G.; Minet, M.; Dubois, Ph.; Teyssié, P.; Senninger, T.; Jérôme, R. *Macromolecules* **1999**, *32*, 27–35.
100. Ma, Q.; Wooley, K. L. *J. Polym. Sci. Polym. Chem.* **2000**, 38, 4805–4820.
101. Mehta, A.; Jaouhari, R.; Benson, T. J.; Douglas, K. T. *Tetrahedron Lett.* **1992**, *33*, 5441–5444.
102. Shan, J.; Nuopponen, M.; Jiang, H.; Kauppinen, E.; Tenhu, H. *Macromolecules* **2003**, *36*, 4526–4533.
103. Raula, J.; Shan, J.; Nuopponen, M.; Niskanen, A.; Jiang, H.; Kauppinen, E.; Tenhu, H. *Langmuir* **2003**, *19*, 3499–3504.
104. Hussain, I.; Graham, S.; Wang, Z.; Tan, B.; Sherrington, D. C.; Rannard, S. P.; Cooper, A. I.; Brust, M. *J. Am. Chem. Soc.* **2005**, *127*, 16398-16399.
105. Shan, J.; Chen, J.; Nuopponen, M.; Viitala, T.; Jiang, H.; Peltonen, J.; Kauppinen, E.; Tenhu, H. *Langmuir* **2006**, *22*, 794-801.
106. Gitsov, I. *J. Polym. Sci. Polym. Chem.* **2008**, *46*, 5295-5314.
107. Würsch, A.; Möller, M.; Glauser, T.; Lim, L. S.; Voytek, S. B.; Hedrick, J. L.; Frank C. W.; Hilborn, J. G. *Macromolecules* **2001**, *34*, 6601-6615.
108. Ihre, H.; Padilla De Jesús, O. L.; Fréchet, J. M. J. *J. Am. Chem. Soc.* **2001**, *123*, 5908-5917.
109. Gillies, E. R.; Jonsson, T. B.; Fréchet, J. M. J. *J. Am. Chem. Soc.* **2004**, *126*, 11936-11943.
110. DeMattei, C. R.; Huang, B.; Tomalia, D. A. *Nano Lett.* **2004**, *4*, 771-777.
111. Li, Y.; Li, Q.; Li, F.; Zhang, H.; Jia, L.; Yu, J.; Fang, Q.; Cao, A. *Biomacromolecules* **2006**, *7*, 224-231.
112. Zubarev, E.R; Stupp, S. I. *J. Am. Chem. Soc.* **2002**, *124*, 5762-5773.
113. Tian, L.; Hammond, P. T. *Chem. Mater.* **2006**, *18*, 3976-3984.
114. Klok, H.-A.; Hwang, J. J.; Hartgerink, J. D.; Stupp, S. I. *Macromolecules* **2002**, *35*, 6101-6111.
115. Wu, P.; Malkoch, M.; Hunt, J. N.; Vestberg, R.; Kaltgrad, E.; Finn, M. G.; Fokin, V. V.; Sharpless, K. B.; Hawker, C. J. *Chem. Commun.* **2005**, 5775-5777.
116. Helms, B.; Mynar, J. L.; Hawker, C. J.; Fréchet, J. M. J. *J. Am. Chem. Soc.* **2004**, *126*, 15020-15021.
117. Hua, C.; Peng, S.-M.; Dong, C.-M. *Macromolecules* **2008**, *41*, 6686-6695.
118. del Barrio, J.; Oriol, L.; Alcalá, R.; Sánchez, C. *Macromolecules* **2009**, *42*, 5752-5760.
119. Nurmi, L.; Lindqvist, J.; Randev, R.; Syrett, J.; Haddleton, D. M. *Chem. Commun*. **2009**, 2727-2729.
120. DeForest, C. A.; Polizzotti, B. D.; Anseth, K. S. *Nat. Mater.* **2009**, *8*, 659-664.
121. Riva, R.; Schmeits, S.; Stoffelbach, F.; Jérôme, C.; Jérôme, R.; Lecomte, Ph. *Chem. Commun.* **2005**, 5334-5336.
122. ten Brummelhuis, N.; Diehl, C.; Schlaad, H. *Macromolecules* **2008**, *41*, 9946-9947.
123. Gao, H.; Matyjaszewski, K. *Prog. Polym. Sci.* **2009**, *34*, 317-350.
124. Blencowe, A.; Tan, J. F.; Goh, T. K.; Qiao, G. *Polymer* **2009**, *50*, 5-32.
125. Xia, J.; Zhang, X.; Matyjaszewski, K. *Macromolecules* **1999**, *32*, 4482-4484.
126. Zhang, X.; Xia, J.; Matyjaszewski, K. *Macromolecules* **2000**, *33*, 2340-2345.
127. Gao, H.; Tsarevsky, N. V.; Matyjaszewski, K. *Macromolecules* **2005**, *38*, 5995-6004.
128. Kafouris, D.; Themistou, E.; Patrickios, C. S. *Chem. Mater.* **2006**, *18*, 85-93.
129. Gao, H.; Ohno, S.; Matyjaszewski, K. *J. Am. Chem. Soc.* **2006**, *128*, 15111-15113.
130. Gao, H.; Matyjaszewski, K. *Macromolecules* **2008**, *41*, 4250-4257.

131. Du, J.; Chen, Y. *Macromolecules* **2004**, *37*, 3588-3594.
132. Wiltshire, J. T.; Qiao, G. G. *Macromolecules* **2006**, *39*, 4282-4285.
133. Wiltshire, J. T.; Qiao, G. G. *Macromolecules* **2006**, *39*, 9018-9027.
134. Wiltshire, J. T.; Qiao, G. G. *Macromolecules* **2008**, 41, 623-631.
135. Bosman, A. W.; Vestberg, R.; Heumann, A.; Fréchet, J. M. J.; Hawker, C. J. *J. Am. Chem. Soc.* **2003**, *125*, 715-728.
136. Connal, L. A.; Vestberg, R.; Hawker, C. J.; Qiao, G. G. *Macromolecules* **2007**, *40*, 7855-7863.
137. Connal, L. A.; Vestberg, R.; Hawker, C. J.; Qiao, G. G. *Adv. Funct. Mater.* **2008**, *18*, 3706-3714.
138. Wang, F.; Bronich, T. K.; Kabanov, A. V.; Rauh, R. D.; Roovers, J. *Bioconjugate Chem.* **2005**, *16*, 397-405.
139. Shuai, X.; Merdan, T.; Schaper, A. K.; Xi, F.; Kissel, T. *Bioconjugate Chem.* **2004**, *15*, 441-448.
140. Gunanathan, C.; Pais, A.; Furman-Haran, E.; Seger, D.; Eyal, E.; Mukhopadhyay, S.; Ben-David, Y.; Leitus, G.; Cohen, H.; Vilan, A.; Degani, H.; Milstein, D. *Bioconjugate Chem.* **2007**, *18*, 1361-1365.
141. Dreaden, E. C.; Mwakwari, S. C.; Sodji, Q. H.; Oyelere, A. K.; El-Sayed, M. A. *Bioconjugate Chem.* **2009**, *20*, 2247-2253.
142. Al-Jamal, K. T.; Al-Jamal, W. T.; Akerman, S.; Podesta, J. E.; Yilmazer, A.; Turton, J. A.; Bianco, A.; Vargesson, N.; Kanthou, C.; Florence, A. T.; Tozer, G. M.; Kostarelos, K. *Proc. Natl. Acad. Sci. U.S.A.* **2010**, *107*, 3966-3971.
143. Englert, B. C.; Bakbak, S.; Bunz, U. H. F. *Macromolecules* **2005**, *38*, 5868-5877.
144. Li, Y.; Yang, J.; Benicewicz, B. C. *J. Polym. Sci. Polym. Chem.* **2007**, *45*, 4300-4308.
145. Ladmiral, V.; Legge, T. M; Zhao, Y.; Perrier, S. *Macromolecules* **2008**, *41*, 6728-6732.
146. Li, G.; Zheng, H.; Bai, R. *Macromol. Rapid Commun.* **2009**, *30*, 442-447.
147. Collman, J. P.; Devaraj, N. K.; Chidsey, C. E. D. *Langmuir* **2004**, *20*, 1051-1053.
148. Holub, J. M.; Garabedian, M. J.; Kirshenbaum, K. *QSAR Comb. Sci.* **2007**, *26*, 1175-1180.
149. Kim, H.-Y.; Sohn, J.; Wijewickrama, G. T.; Edirisinghe, P.; Gherezghiher, T.; Hemachandra, M.; Lu, P.-Y.; Chandrasena, R. E.; Molloy, M. E.; Tonetti, D. A.; Thatcher, G. R. J. *Bioorg. Med. Chem.* **2010**, *18*, 809-821.
150. Wiltshire, J. T.; Qiao, G. G. *J. Polym. Sci. Polym. Chem.* **2009**, *47*, 1485-1498.
151. Durmaz, H.; Dag, A.; Erdogan, E.; Demirel, A. L.; Hizal, G.; Tunca, U. *J. Polym. Sci. Polym. Chem.* **2010**, *48*, 99-108.
152. Hawker, C. J.; Mecerreyes, D.; Elce, E.; Dao, J.; Hedrick, J. L.; Barakat, I.; Dubois, Ph.; Jérôme, R.; Volksen, W. *Macromol. Chem. Phys.* **1997**, *198*, 155-166.
153. Mespouille, L.; Degée, Ph.; Dubois, Ph. *Eur. Polym. J.* **2005**, *41*, 1187-1195.
154. Baek, K.-Y.; Kamigaito, M.; Sawamoto, M. *Macromolecules* **2001**, *34*, 215-221.

Appendix I

Characterization Methods

Characterization

NMR spectroscopy experiments were conducted on the Bruker 250 MHz and Bruker 300 MHz spectrometers using $CDCl_3$ or DMSO-d_6 as solvents.

Molecular weights and polydispersity indices were estimated by SEC using the following instruments: a) Viscotek 200 instrument using two PLgel mixed-D columns (Polymer Laboratories (PL)), assembled in series, and a RI detector. SEC samples were run in THF at room temperature (1 mL/min). b) Viscotek GPCmax VE-2001 equipped with Viscotek TriSEC Model 302 triple detector array (RI detector, viscometer detector, and laser light scattering detector with the light wavelength of 670 nm, and measuring angles of 90° and 7°) and a Knauer K-2501 UV detector using two PLgel mixed-D columns (from PL). The samples were run in THF at 30 °C (1 mL/min). Molecular weights were calculated using PS standards from PL.

Mass spectra were acquired by the MALDI-TOF mass spectrometry using a Bruker autoflex III smartbeam mass spectrometer, equipped with the laser that produces pulses at 337 nm. Samples using 2,5-dihydroxyacetophenon as matrix and NaTFA as additive were prepared by dissolving the polymer in THF at a concentration of 20 mg/mL. A 10 µL aliquot of this solution was added to 100 µL of a 20 mg/mL matrix solution, and 1 µL NaTFA as a THF solution (20 mg/mL) was added as the cationzation agent.

ATR FT IR analysis was carried out on Perkin-Elmer Spectrum One apparatus. The spectra were recorded in the range of 4000-600 cm^{-1} with 4 cm^{-1} resolution.

UV-visible spectrum has been recorded on Perkin-Elmer Lambda 5 spectrometer. The sample for UV-visible spectroscopy was prepared by shaking the solution of the AuNPs in distilled water (1 mg/mL) for 3 h.

The TEM images of the AuNPs were acquired on FEI Titan microscope operated at 300 kV. Sample for TEM was prepared by evaporating droplets of the solution of the AuNPs in distilled water (8 mg/mL) on copper grids.

The TEM images of the miktoarm CCS copolymers were obtained using Tecnai T20 instrument operated at 200 kV. The samples for TEM were prepared by evaporating droplets of the dilute solutions of the CCS polymers in THF, filtered through 0.45 µm Teflon filters, on lacey carbon coated nickel grids.

TGA was performed on a TGA Q500 instrument from 20-600 °C or 20-800 °C with a heating rate of 20 °C/min under nitrogen flow.

Appendix II

Reprinted with permission from Javakhishvili, I.; Hvilsted, S. Gold Nanoparticles Protected with Thiol-Derivatized Amphiphilic Poly(ε-caprolactone)-*b*-poly(acrylic acid). *Biomacromolecules* 2009, *10*, 74-81.

Gold Nanoparticles Protected with Thiol-Derivatized Amphiphilic Poly(ϵ-caprolactone)-*b*-poly(acrylic acid)

Irakli Javakhishvili and Søren Hvilsted*

Technical University of Denmark, Department of Chemical and Biochemical Engineering, Danish Polymer Centre, Building 423, DK-2800 Kgs. Lyngby, Denmark

Received August 1, 2008; Revised Manuscript Received October 27, 2008

Amphiphilic poly(ϵ-caprolactone)-*b*-poly(acrylic acid) (HS-PCL-*b*-PAA) with a thiol functionality in the PCL terminal has been prepared in a novel synthetic cascade. Initially, living anionic ring-opening polymerization (ROP) of ϵ-caprolactone (ϵ-CL) employing the difunctional initiator, 2-hydroxyethyl 2-bromoisobutyrate, followed by esterification with 2,4-dinitrophenyl- or 4-monomethoxytrityl-protected mercaptoacetic acids (Prot-), provided well-defined PCL macroinitiators capped with protected thiols. The macroinitiators allowed atom transfer radical polymerization (ATRP) of *tert*-butyl acrylate (*t*BA) in a controlled fashion by use of $NiBr_2(PPh_3)_2$ catalyst to produce Prot-PCL-*b*-P*t*BA with narrow polydispersities (1.17−1.39). Subsequent mild deprotection protocols provided HS-PCL-*b*-PAA. Reduction of a gold salt in the presence of this macroligand under thiol-deficient conditions afforded stable, aggregation-free nanoparticles, as evidenced from UV−vis spectroscopy and transmission electron microscopy (TEM), the latter revealed nanoparticles with a mean diameter of 9.0 ± 3.1 nm.

Introduction

Gold nanoparticles (AuNPs) are envisioned to be superior to polymeric micelles as candidates for constructing drug delivery devices. Encapsulation and controlled release of drugs, as well as adequate masking from reticuloendothelial system (RES) remain as a challenge in the case of the polymeric micelles.[1] On the contrary, monolayer protected AuNPs offer improved stability, low toxicity, versatility of surface functionalities, and small size, rendering them unrecognizable by RES, and thus may serve as excellent reservoirs for hydrophobic drugs. Tailoring the surface properties of the AuNPs bestows the system site-specificity and prolonged circulation time.[1,2] Antibody conjugated AuNPs provide high contrast for noninvasive imaging of targeted cancer tissues.[3] AuNPs with tunable optical properties find application in thermal ablative therapy for cancer.[4]

AuNPs are generally prepared by reduction of $HAuCl_4$ in a boiling sodium citrate solution or in the presence of thiol capping ligands. Using polymeric ligands as stabilizers has attracted much attention due to the enhanced stability they impart to AuNPs. Moreover, they provide better means to alter the surface properties, solubility, and compatibility of AuNPs.[5]

Numerous studies were reported where amphiphilic block copolymer micelles were utilized for stabilization of AuNPs.[5,6] Biocompatible and biodegradable poly(ϵ-caprolactone)-*b*-poly(ethylene oxide) has been end-functionalized with disulfide moiety and employed as the ligand for protection of AuNPs, which may be exploited as drug delivery device as well as for subcellular localization studies.[7]

Zhang et al. have prepared water miscible shell cross-linked nanoparticles based on diblock copolymers of poly(ϵ-caprolactone) (PCL) and poly(acrylic acid) (PAA) and obtained nanoscale cage-like membranes after hydrolysis of PCL core.[8]

Herein, we report about synthesis of thiol-functionalized amphiphilic diblock copolymer HS-PCL-*b*-PAA and demonstrate its capacity in passivation of AuNPs. PCL, comprising the core of the nanoparticle, is biocompatible and exhibits high permeability to small drug molecules,[9] whereas PAA, constituting the shell, is biocompatible and mucoadhesive.[10] Therefore, the AuNPs may have potential as drug carriers in bladder cancer therapy.

Experimental Section

Materials and Methods. *tert*-Butyl acrylate (*t*BA; Aldrich, 98%) and ϵ-caprolactone (ϵ-CL; Fluka, ≥99%) were dried over CaH_2 and distilled under reduced pressure. Tetrahydrofuran (THF; Sigma-Aldrich, 99.9%), dichloromethane (DCM; Sigma-Aldrich, 99.8%), chloroform (Sigma-Aldrich, 99.8%), *N*,*N*-dimethylformamide (DMF; Fluka, 99.8%), and triethylamine (TEA; Sigma-Aldrich, 99%) were dried over CaH_2, and distilled under nitrogen flow. Tin octoate ($Sn(Oct)_2$; Sigma, ∼95%) was distilled under reduced pressure. Diethyl ether (Sigma-Aldrich, 99.5%) was kept over molecular sieves. Methanol (Sigma-Aldrich, 99.9%), heptane (Sigma-Aldrich, 99%), anhydrous ethylene glycol (Aldrich, 99.8%), 2-bromoisobutyryl bromide (Aldrich, 98%), mercaptoacetic acid (Aldrich, 99+ %), 4-methoxytriphenylchloromethane (Mmt-Cl; Fluka, ≥97%), *N*,*N*-diisopropylethylamine (DIPEA; Sigma-Aldrich, 99.5%), 1-fluoro-2,4-dinitrobenzene (Sigma, 99%), diethyl azodicarboxylate (DEAD; Aldrich), triphenylphosphine (TPP) (Fluka, ∼97%), $NiBr_2(PPh_3)_2$ (Aldrich, 99%), CuBr (Aldrich, 98%), *N*,*N*,*N*′,*N*′,*N*″-pentamethyldiethylenetriamine (Aldrich, 99%), ethanethiol (Aldrich, 97%), trifluoroacetic acid (TFA; Sigma-Aldrich, ≥98%), triethylsilane (TES; Aldrich, 99%), lithium borohydride (2.0 M solution in THF; Aldrich), and gold(III) chloride trihydrate (Sigma-Aldrich, 99.9+%) were used as received. 2-Hydroxyethyl 2-bromoisobutyrate (HEBI) was synthesized according to the literature procedure.[11] α-(2,4-Dinitrophenylthio)acetic acid (dNPTAA) was prepared as described elsewhere.[12] The synthesis of α-(4-monomethoxytritylthio)acetic acid (MmtTAA) was carried out according to the literature procedure.[13] Dialysis tubing (regenerated cellulose, MWCO 12000−14000) was obtained from Membrane Filtration Products, Inc. Carbon-coated copper grids (200 mesh) were purchased from Electron Microscopy Sciences.

Characterization by ^{1}H NMR was conducted on Bruker 250 MHz spectrometer using $CDCl_3$ or DMSO-d_6 as solvents (both from Aldrich). All spectra were recorded with 32 scans. Molecular weights and polydispersity indices were estimated by size exclusion chromatography

* To whom correspondence should be addressed. E-mail: sh@kt.dtu.dk.

10.1021/bm800860t CCC: $40.75
Published on Web 11/24/2008

(SEC) on Viscotek 200 instrument using two PLgel mixed-D columns (Polymer Laboratories (PL)), assembled in series, and a refractive index detector. SEC samples were run in THF at room temperature (1 mL/min). Molecular weights were calculated using polystyrene (PS) standard from PL using TriSEC software. FT IR analysis was conducted on Perkin-Elmer Spectrum One apparatus. The spectra were recorded in the range of 4000−600 cm^{-1} with 4 cm^{-1} resolution and 32 scans. UV−visible spectrum has been recorded on Perkin-Elmer Lambda 5 spectrometer. The sample for UV−visible spectroscopy was prepared by shaking the solution of the gold nanoparticles in distilled water (1 mg/ml) for 3 h. Transmission electron microscopy (TEM) image of the gold nanoparticles was acquired on FEI Titan microscope operated at 300 kV. Sample for TEM was prepared by evaporating droplets of the solution of the gold nanoparticles in distilled water (8 mg/ml) on copper grids.

Synthesis. All reactions were carried out under a nitrogen atmosphere.

Ring-Opening Polymerization of ϵ-CL. The glass equipment was dried in the oven at 150 °C. A two-neck flask and a Schlenk tube were equipped with stirring bars and rubber septa, and dried with heat-gun: twice while evacuating and once under a nitrogen flow.

The two-neck flask was charged with $Sn(Oct)_2$ (0.2454 g, 0.61 mmol) and THF (4 mL), and the solution was stirred for 30 min. HEBI (0.2840 g, 1.35 mmol) was weighed in a glass vial and dissolved in THF (0.95 mL). ϵ-CL (7.7 mL, 72.6 mmol), a solution of HEBI, and a solution of $Sn(Oct)_2$ were introduced into the Schlenk tube under a nitrogen flow. Reaction mixture was stirred and purged with nitrogen at room temperature for 30 min: it turned from opaque to transparent. Then the tube was immersed into preheated oil bath at 62 °C, and the reaction was carried out for 13 h. Reaction mixture was allowed to cool down to ambient temperature. It was exposed to air, diluted with THF, and precipitated into 10-fold excess of cold MeOH. The polymer was recovered via filtration, and dried in the vacuum oven at room temperature until constant weight. Degree of polymerization (DP), designated as n, has been estimated from ^{1}H NMR spectrum (Figure S1) by comparing the integral of the resonance peak arising from the methylene group located next to the hydroxy chain end to the integral of the resonance peak corresponding to the methylene group in the repeating unit. n = 30, M_n = 3640 (by ^{1}H NMR), M_n = 6100 (by SEC), and M_w/M_n = 1.09 (by SEC).

ν_{max}/cm^{-1} 2945, 2866, 1722, 1471, 1419, 1397, 1366, 1293, 1239, 1175, 1108, 1046, 961, 841, 732. δ_H (250 MHz; $CDCl_3$) 4.28−4.39 (4H, m, $BrC(CH_3)_2C(O)OCH_2CH_2OC(O)(CH_2)_5$), 4.04 (2H, t, $J_{1,3}$ = 6.7, -$(CH_2)_4CH_2OC(O)$-), 3.63 (2H, t, $J_{1,3}$ = 6.4, -$(CH_2)_4CH_2OH$,), 2.29 (2H, t, $J_{1,3}$ = 7.5, -$OC(O)CH_2(CH_2)_4$-), 1.92 (6H, s, $BrC(CH_3)_2C(O)$-O-), 1.63 (4H, m, -$OC(O)CH_2CH_2CH_2CH_2CH_2$-), 1.36 (2H, m, -$OC(O)CH_2CH_2CH_2CH_2CH_2$-).

End-Functionalization of PCL with dNPTAA. (**1**) A previously dried 50 mL two-neck flask was charged with Br-PCL-OH (3 g, 0.82 mmol), dNPTAA (0.761 g, 2.95 mmol), and TPP (0.764 g, 2.91 mmol). THF (10 mL) was added, and the solution was stirred for 30 min at room temperature and for 30 min in an ice/water bath. DEAD (0.45 mL, 2.86 mmol) was introduced dropwise, and the mixture was stirred in an ice/water bath for another 30 min. Then it was allowed to warm up to ambient temperature, and the reaction was carried out for 24 h. The reaction mixture was diluted with THF (5 mL) and precipitated into a large excess of cold MeOH. The product was isolated on filter paper and dried in the vacuum oven at room temperature for 48 h. M_n = 3880 (by ^{1}H NMR), M_n = 6200 (by SEC), and M_w/M_n = 1.08 (by SEC).

ν_{max}/cm^{-1} 2945, 2866, 1721, 1595, 1524, 1471, 1419, 1397, 1366, 1293, 1239, 1168, 1108, 1045, 961, 733. δ_H (250 MHz; $CDCl_3$) 9.10 (1H, d, J_m = 2.5, -Ar), 8.40 (1H, dd, J_m = 2.5, J_o = 9.0, -Ar), 7.72 (1H, d, J_o = 9.0, -Ar), 4.29−4.40 (4H, m, $BrC(CH_3)_2C(O)OCH_2CH_2OC(O)(CH_2)_5$), 4.18 (2H, t, $J_{1,3}$ = 6.5, -$(CH_2)_4CH_2OC(O)CH_2S$−Ar), 4.05 (2H, t, $J_{1,3}$ = 6.7, -$(CH_2)_4CH_2OC(O)$-), 3.84 (2H, s, $OC(O)CH_2S$−Ar), 2.30 (2H, t, $J_{1,3}$ = 7.5, -$OC(O)CH_2$-$(CH_2)_4$-), 1.93 (6H, s, $BrC(CH_3)_2C(O)$-O-), 1.65 (4H, m, -$OC(O)CH_2CH_2$-$CH_2CH_2CH_2$-), 1.37 (2H, m, -$OC(O)CH_2CH_2CH_2CH_2CH_2$-).

End-Functionalization of PCL with MmtTAA. The protocol described for end-functionalization of PCL with dNPTAA was employed.

(**2a**) Br-PCL-OH (0.9900 g, 0.27 mmol), MmtTAA (0.3784 g, 1.04 mmol), and TPP (0.2547 g, 0.97 mmol) were dissolved in THF (5 mL). DEAD (0.15 mL, 0.95 mmol) was added dropwise to the resulting solution. M_n = 3990 (by ^{1}H NMR), M_n = 6300 (by SEC), and M_w/M_n = 1.09 (by SEC).

ν_{max}/cm^{-1} 2945, 2866, 1721, 1608, 1509, 1471, 1419, 1397, 1365, 1293, 1239, 1165, 1107, 1044, 961, 807, 732.

δ_H (250 MHz; $CDCl_3$) 6.81−7.44 (14H, m, -Ar), 4.30−4.40 (4H, m, $BrC(CH_3)_2C(O)OCH_2CH_2OC(O)(CH_2)_5$), 4.05 (2H, t, $J_{1,3}$ = 6.7, -$(CH_2)_4CH_2OC(O)$-), 3.97 (2H, t, $J_{1,3}$ = 6.6, -$(CH_2)_4CH_2OC(O)CH_2S$−C-$(Ar)_3$), 3.79 (3H, s, CH_3O−Ar), 2.95 (2H, s, $OC(O)CH_2S$−C-$(Ar)_3$), 2.30 (2H, t, $J_{1,3}$ = 7.5, -$OC(O)CH_2(CH_2)_4$-), 1.93 (6H, s, $BrC(CH_3)_2C(O)$-O-), 1.64 (4H, m, -$OC(O)CH_2CH_2CH_2CH_2CH_2$-), 1.38 (2H, m, -$OC(O)CH_2CH_2CH_2CH_2CH_2$-).

(**2b**) Br-PCL-OH (0.8500 g, 0.23 mmol), MmtTAA (0.3060 g, 0.84 mmol), and TPP (0.2190 g, 0.83 mmol) were dissolved in THF (4.30 mL). DEAD (0.13 mL, 0.83 mmol) was added dropwise to the resulting mixture. M_n = 3990 (by ^{1}H NMR), M_n = 7100 (by SEC), and M_w/M_n = 1.08 (by SEC).

ν_{max}/cm^{-1} 2945, 2867, 1721, 1606, 1509, 1471, 1419, 1397, 1365, 1293, 1239, 1171, 1108, 1046, 961, 820, 732.

δ_H (250 MHz; $CDCl_3$) 6.80−7.44 (14H, m, -Ar), 4.29−4.40 (4H, m, $BrC(CH_3)_2C(O)OCH_2CH_2OC(O)(CH_2)_5$), 4.05 (2H, t, $J_{1,3}$ = 6.7, -$(CH_2)_4CH_2OC(O)$-); 3.96 (2H, t, $J_{1,3}$ = 6.7, -$(CH_2)_4CH_2OC(O)CH_2S$-C-$(Ar)_3$), 3.78 (3H, s, CH_3O-Ar), 2.95 (2H, s, $OC(O)CH_2S$-C-$(Ar)_3$), 2.30 (2H, t, $J_{1,3}$ = 7.5, -$OC(O)CH_2(CH_2)_4$-), 1.93 (6H, s, $BrC(CH_3)_2C(O)$-O-), 1.65 (4H, m, -$OC(O)CH_2CH_2CH_2CH_2CH_2$-), 1.37 (2H, m, -$OC(O)CH_2CH_2CH_2CH_2CH_2$-).

ATRP of *t*BA from PCL Macroinitiator (1, 2). *General Procedure.* A previously dried Schlenk tube was charged with $NiBr_2(PPh_3)_2$ and PCL macroinitiator (**1** or **2**). It was evacuated and backfilled with nitrogen three times. *t*BA was injected, and three freeze−pump−thaw cycles were performed. Reaction mixture was allowed to warm up to ambient temperature while stirring, and then the tube was immersed into preheated oil bath at 90 °C. Reaction was carried out under nitrogen flow. After certain time the reaction was quenched by immersing the tube in dry ice/propanol-2 bath. Afterward, the reaction mixture was exposed to air and diluted with THF. The catalyst was removed with basic Al_2O_3. The solution was filtered, concentrated under reduced pressure, and precipitated into 10-fold excess of cold MeOH:H_2O (10:1) mixture. The block copolymer was isolated via filtration, and dried in the vacuum oven at room temperature until constant weight. DP of P*t*BA block, designated as m, has been estimated by ^{1}H NMR.

(**3a**) $NiBr_2(PPh_3)_2$ (0.1570 g, 0.21 mmol) and **1** (1 g, 0.26 mmol) were employed in ATRP of *t*BA (8.0 mL, 54.6 mmol). The reaction was carried out for 48 h. n = 30, m = 31, M_n = 7900 (by ^{1}H NMR), M_n = 10800 (by SEC), and M_w/M_n = 1.27 (by SEC).

ν_{max}/cm^{-1} 2972, 2939, 2867, 1722, 1596, 1524, 1458, 1393, 1366, 1294, 1243, 1188, 1145, 1109, 1047, 962, 845, 734.

δ_H (250 MHz; $CDCl_3$) 9.10 (1H, d, J_m = 2.5, -Ar), 8.41 (1H, dd, J_m = 2.5, J_o = 9.0, -Ar), 7.72 (1H, d, J_o = 9.0, -Ar), 4.22−4.29 (4H, m, $C(CH_3)_2C(O)OCH_2CH_2OC(O)(CH_2)_5$), 4.18 (2H, t, $J_{1,3}$ = 6.6, -$(CH_2)_4CH_2OC(O)CH_2S$−Ar), 4.05 (2H, t, $J_{1,3}$ = 6.7, -$(CH_2)_4CH_2OC(O)$-), 3.85 (2H, s, $OC(O)CH_2S$−Ar), 2.1−2.35 (3H, m, -$OC(O)CH_2(CH_2)_4$- and $CH_2CH(COOC(CH_3)_3)$), 1.57−1.9 (6H, m, -$OC(O)CH_2CH_2CH_2CH_2CH_2$- and $CH_2CH(COOC(CH_3)_3)$), 1.43 (9H, s, $CH_2CH(COOC(CH_3)_3)$), 1.2−1.57 (4H, m, -$OC(O)CH_2CH_2$-$CH_2CH_2CH_2$- and $CH_2CH(COOC(CH_3)_3)$), 1.13 (6H, s, -$C(CH_3)_2C(O)$-O-).

(**3b**) $NiBr_2(PPh_3)_2$ (0.0625 g, 0.084 mmol) and **1** (0.4 g, 0.103 mmol) were employed in ATRP of *t*BA (2.6 mL, 17.7 mmol). The reaction was carried out for 20 h. n = 30, m = 24, M_n = 7000 (by ^{1}H NMR), M_n = 10200 (by SEC), and M_w/M_n = 1.17 (by SEC).

Scheme 1. Synthetic Pathway for Preparation of PCL Macroinitiators (**1**, **2**)[a]

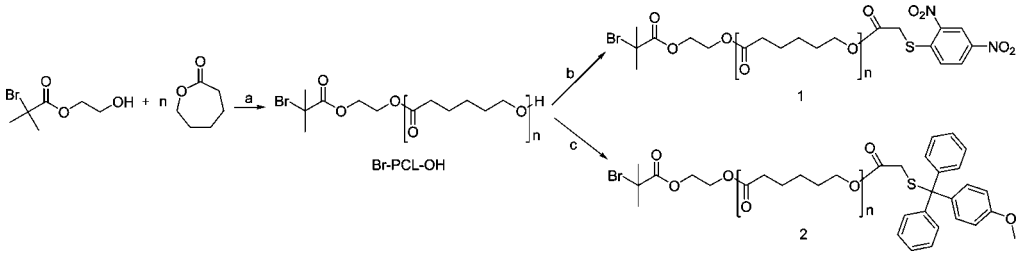

[a] Reagents and conditions: (a) $Sn(Oct)_2$, 62 °C, THF; (b) dNPTAA, DEAD, TPP, THF; (c) MmtTAA, DEAD, TPP, THF.

Scheme 2. Synthetic Pathway for Preparation of HS-PCL-*b*-PAA (**5**, **6**)[a]

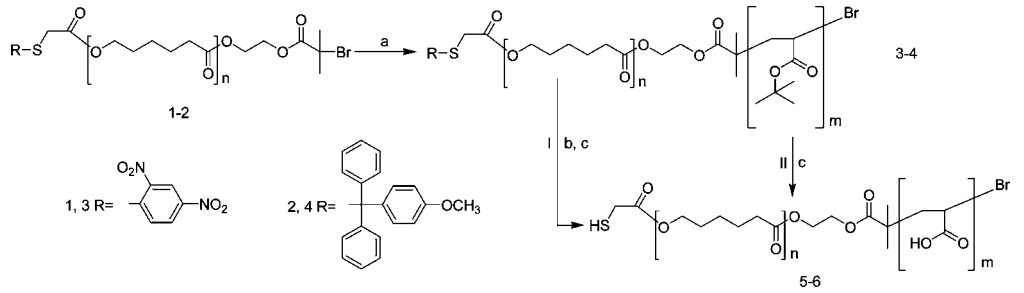

[a] Reagents and conditions: (a) *t*BA, $NiBr_2(PPh_3)_2$, 90 °C; (b) CH_3CH_2SH, TEA, $CHCl_3$; (c) TFA, TES, CH_2Cl_2.

Table 1. Characteristics of Br-PCL-OH and PCL Macroinitiators (**1**, **2**) Estimated by SEC and ^{1}H NMR

compound	M_n[b]	M_n[c]	M_w/M_n[c]
Br-PCL-OH[a]	3640	6100	1.09
1	3880	6200	1.08
2a	3990	6300	1.09
2b	3990	7100	1.08

[a] DP of PCL estimated by ^{1}H NMR is 30. [b] By ^{1}H NMR. [c] By SEC.

(**4a**) $NiBr_2(PPh_3)_2$ (0.1125 g, 0.15 mmol) and **2a** (0.73 g, 0.18 mmol) were employed in ATRP of *t*BA (5.8 mL, 39.6 mmol). The reaction was carried out for 42 h. $n = 30$, $m = 70$, $M_n = 13000$ (by ^{1}H NMR), $M_n = 15300$ (by SEC), and $M_w/M_n = 1.39$ (by SEC).

ν_{max}/cm^{-1} 2976, 2935, 2866, 1722, 1608, 1509, 1449, 1393, 1366, 1245, 1144, 1046, 963, 845, 732.

δ_H (250 MHz; $CDCl_3$) 6.80−7.44 (14H, m, -Ar); 4.21−4.29 (4H, m, $C(CH_3)_2C(O)OCH_2CH_2OC(O)(CH_2)_5$), 4.05 (2H, t, $J_{1,3} = 6.7$, $-(CH_2)_4CH_2OC(O)-$), 3.97 (2H, t, $J_{1,3} = 7$, $-(CH_2)_4CH_2OC(O)CH_2S-C-(Ar)_3$), 3.78 (3H, s, CH_3O-Ar), 2.95 (2H, s, $OC(O)CH_2S-C-(Ar)_3$), 2.1−2.35 (3H, m, $-OC(O)CH_2(CH_2)_4-$ and $CH_2CH(COOC(CH_3)_3)$), 1.57−1.9 (6H, m, $-OC(O)CH_2CH_2CH_2CH_2CH_2-$ and $CH_2CH(COOC(CH_3)_3)$), 1.43 (9H, s, $CH_2CH(COOC(CH_3)_3)$), 1.2−1.57 (4H, m, $-OC(O)CH_2CH_2CH_2CH_2CH_2-$ and $CH_2CH(COOC(CH_3)_3)$), 1.13 (6H, s, $-C(CH_3)_2C(O)O-$).

(**4b**) $NiBr_2(PPh_3)_2$ (0.0598 g, 0.08 mmol) and **2b** (0.4 g, 0.1 mmol) were employed in ATRP of tBA (2.5 mL, 17.1 mmol). The reaction was carried out for 20 h. $n = 30$, $m = 50$, $M_n = 10400$ (by ^{1}H NMR), $M_n = 14000$ (by SEC), and $M_w/M_n = 1.29$ (by SEC).

Sequential Removal of 2,4-Dinitrophenyl and *tert*-Butyl Ester Groups (Scheme 2, Route I). (3-(SH)-a) 3a (1.15 g, 0.15 mmol) was placed in a previously dried two-neck flask. Chloroform (20 mL) was added, and the mixture was stirred until the polymer dissolved completely. Ethanethiol (1.5 mL, 20.3 mmol) was injected, followed by addition of TEA (1.3 mL, 9.3 mmol). Reaction was carried out overnight at room temperature. The copolymer was precipitated into large excess of cold MeOH/H_2O (10:1) mixture. The product was isolated on filter paper, and dried in the vacuum oven at room temperature. $M_n = 7730$ (by ^{1}H NMR), $M_n = 13000$ (by SEC), and $M_w/M_n = 1.32$ (by SEC).

ν_{max}/cm^{-1} 2942, 2867, 1722, 1458, 1393, 1366, 1295, 1244, 1191, 1144, 1109, 1047, 962, 845, 732.

δ_H (250 MHz; $CDCl_3$) 4.20−4.30 (4H, m, $C(CH_3)_2C(O)-OCH_2CH_2OC(O)(CH_2)_5$), 4.13 (2H, t, $J_{1,3} = 6.6$, $-(CH_2)_4CH_2-OC(O)CH_2SH$), 4.06 (2H, t, $J_{1,3} = 6.7$, $-(CH_2)_4CH_2OC(O)-$), 3.25 (2H, d, $J_{1,3} = 8.2$, $OC(O)CH_2SH$), 2.1−2.38 (3H, m, $-OC(O)CH_2(CH_2)_4-$ and $CH_2CH(COOC(CH_3)_3)$), 1.99 (1H, t, $J_{1,3} = 8.2$, $OC(O)CH_2SH$), 1.57−1.9 (6H, m, $-OC(O)CH_2CH_2CH_2CH_2CH_2-$ and $CH_2CH-(COOC(CH_3)_3)$), 1.43 (9H, s, $CH_2CH(COOC(CH_3)_3)$), 1.2−1.57 (4H, m, $-OC(O)CH_2CH_2CH_2CH_2CH_2-$ and $CH_2CH(COOC(CH_3)_3)$), 1.14 (6H, s, $-C(CH_3)_2C(O)O-$).

(**3-(SH)-b**) **3b** (0.35 g, 0.05 mmol) was dissolved in chloroform (7 mL), and ethanethiol (0.46 mL, 6.2 mmol) and TEA (0.41 mL, 2.9 mmol) were added afterward. $M_n = 6830$ (by ^{1}H NMR), $M_n = 11300$ (by SEC), and $M_w/M_n = 1.27$ (by SEC).

(**5b**) A previously dried two-neck flask was charged with **3-(SH)-b** (0.2 g, 0.70 mmol of *tert*-butyl ester) and DCM (1.3 mL). The solution was stirred for 20 min at room temperature and for 15 min in an ice/water bath. TES (0.3 mL, 1.9 mmol) and TFA (0.29 mL, 3.8 mmol) were added, and the reaction mixture was stirred for 5 min in an ice/water bath. Then it was allowed to warm up to room temperature. Reaction was carried out for 24 h. The mixture was diluted with DCM (3 mL) and precipitated into a large excess of cold diethyl ether/heptane (1:1). The block copolymer was isolated on filter paper and washed with diethyl ether/heptane (1:1). It was dried in the vacuum oven at room temperature. $M_n = 5490$ (by ^{1}H NMR, assuming complete removal of *tert*-butyl). ν_{max}/cm^{-1} 3400−2500, 2945, 2866, 1762, 1721, 1454, 1419, 1396, 1367, 1294, 1240, 1186, 1163, 1108, 1045, 961, 841, 732.

δ_H (250 MHz; DMSO-d_6) 12.26 (1H, br s, $CH_2CH(COOH)$), 4.10−4.25 (4H, m, $C(CH_3)_2C(O)OCH_2CH_2OC(O)(CH_2)_5$), 3.90−4.08 (4H, m, $-(CH_2)_4CH_2OC(O)CH_2SH$ and $-(CH_2)_4CH_2OC(O)-$), 3.31 (2H, d, $J_{1,3} = 8.1$, $OC(O)CH_2SH$), 2.1−2.36 (3H, m, $-OC(O)CH_2(CH_2)_4-$ and $CH_2CH(COOH)$), 1.47−1.88 (6H, m, $-OC(O)CH_2CH_2-CH_2CH_2CH_2-$ and $CH_2CH(COOH)$), 1.23−1.43 (11H, m, CH_2CH-

Table 2. Conditions of ATRP and Characteristics of PCL_n-*b*-$PtBA_m$ (**3**, **4**) Estimated by SEC and ^{1}H NMR

compound	$[M]_0/[I]_0/[cat]_0$[a]	reaction time, h	*n*	*m*	M_n (^{1}H NMR)	M_n (SEC)	M_w/M_n (SEC)
3a	210:1:0.8	48	30	31	7900	10800	1.27
3b	170:1:0.8	20	30	24	7000	10200	1.17
4a	220:1:0.8	42	30	70	13000	15300	1.39
4b	170:1:0.8	20	30	50	10400	14000	1.29

[a] Ratio of initial molar concentrations of the monomer to initiator and catalyst.

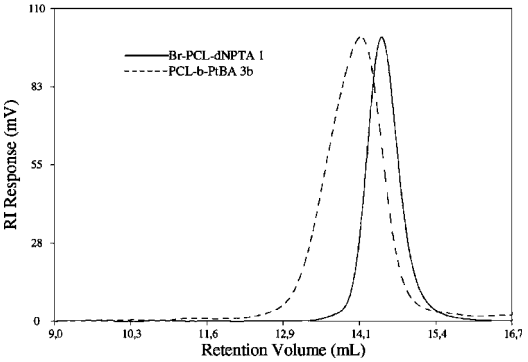

Figure 1. SEC trace of PCL-*b*-P*t*BA **3b**.

(COOC(CH_3)$_3$) and -OC(O)$CH_2CH_2CH_2CH_2CH_2$-), 1.07 (6H, s, -C(CH_3)$_2$C(O)O-).

Simultaneous Deblocking of 4-Monomethoxytrityl and *tert*-Butyl Ester Groups (Scheme 2, Route II). The reaction protocol was similar to the one employed for preparation of **5a**.

(**6a**) The solution of **4a** (1 g, 5.38 mmol of *tert*-butyl ester) in DCM (10 mL) was treated with TES (2.2 mL, 13.8 mmol) and TFA (2.1 mL, 27.3 mmol). M_n = 8810 (by ^{1}H NMR, assuming complete removal of *tert*-butyl).

ν_{max}/cm^{-1} 3400−2500, 2942, 2866, 1762, 1719, 1702, 1453, 1416, 1367, 1239, 1157, 1106, 1045, 800.

δ_H (250 MHz; DMSO-d_6) 12.26 (1H, br s, CH_2CH(COO*H*)), 4.10−4.25 (4H, m, C(CH_3)$_2$C(O)OCH_2CH_2OC(O)(CH_2)$_5$), 3.90−4.08 (4H, m, -(CH_2)$_4CH_2$OC(O)CH_2SH and -(CH_2)$_4CH_2$OC(O)-), 3.31 (2H, d, $J_{1,3}$ = 8.1, OC(O)CH_2SH), 2.1−2.36 (3H, m, -OC(O)CH_2(CH_2)$_4$- and CH_2CH(COOH)), 1.47−1.88 (6H, m, -OC(O)CH_2CH_2-$CH_2CH_2CH_2$- and CH_2CH(COOH)), 1.23−1.43 (11H, m, CH_2-CH(COOC(CH_3)$_3$) and -OC(O)$CH_2CH_2CH_2CH_2CH_2$-), 1.07 (6H, s, -C(CH_3)$_2$C(O)O-).

(**6b**) **4b** (0.4 g, 1.92 mmol of *tert*-butyl ester) was dissolved in DCM (3.5 mL) and treated with TES (0.81 mL, 5.1 mmol) and TFA (0.78 mL, 10.1 mmol). M_n = 7330 (by ^{1}H NMR, assuming complete removal of *tert*-butyl).

ν_{max}/cm^{-1} 3400−2500, 2943, 2867, 1764, 1722, 1704, 1454, 1417, 1396, 1366, 1239, 1158, 1106, 1045, 960, 805, 732.

δ_H (250 MHz; DMSO-d_6) 12.31 (1H, br s, CH_2CH(COO*H*)), 4.10−4.25 (4H, m, C(CH_3)$_2$C(O)OCH_2CH_2OC(O)(CH_2)$_5$), 3.90−4.08 (4H, m, -(CH_2)$_4CH_2$OC(O)CH_2SH and -(CH_2)$_4CH_2$OC(O)-), 3.31 (2H, d, $J_{1,3}$ = 8.1, OC(O)CH_2SH), 2.1−2.36 (3H, m, -OC(O)CH_2(CH_2)$_4$- and CH_2CH(COOH)), 1.42−1.90 (6H, m, -OC(O)CH_2CH_2-$CH_2CH_2CH_2$- and CH_2CH(COOH)), 1.20−1.42 (11H, m, CH_2CH-(COOC(CH_3)$_3$) and -OC(O)$CH_2CH_2CH_2CH_2CH_2$-), 1.06 (6H, s, -C(CH_3)$_2$C(O)O-).

Preparation of Gold Nanoparticles. A 50 mL two-neck flask had been washed with distilled water and dried in the oven at 150 °C. $HAuCl_4 \cdot 3H_2O$ (0.065 g, 0.165 mmol) and **6a** (0.48 g, 0.054 mmol) were placed in the flask and dissolved in THF (16.2 mL). Resulting transparent yellow solution was stirred in the dark under a nitrogen atmosphere and at room temperature for 24 h. Afterward, freshly prepared 0.25 M $LiBH_4$ (3.3 mL, 0.825 mmol) was added quickly in small aliquots under vigorous stirring. The reaction mixture immediately turned from yellow to dark purple; violent gas evolution was observed. Stirring continued for 4 h at room temperature. The reaction mixture was then transferred into dialysis tubing. It was dialyzed against THF for 48 h. The solution was then added dropwise to 20-fold excess of diethyl ether. Dark purple precipitate fell out instantaneously. It was isolated on filter paper and dried in the vacuum oven at room temperature.

Results and Discussions

For preparation of HS-PCL-*b*-PAA dual initiator strategy combining different living polymerization techniques has been utilized.[14] ROP of ϵ-CL from double-headed initiator, 2-hydroxyethyl 2-bromoisobutyrate (HEBI),[11] afforded heterotelechelic PCL bearing hydroxy and bromoester end groups (Scheme 1, a). The polymerization was catalyzed with tin octoate ($Sn(Oct)_2$). Undesirable side effects that could originate from high initial catalyst concentration (∼0.05 M) and low initial initiator to catalyst ratio (∼2.2) was counteracted by conducting the polymerization at low temperature (62 °C) and thus suppressing collateral esterification and transesterification reactions involving HEBI and liberated octanoic acid.[15,16] The monomer conversion determined gravimetrically is about 59.6%, which corresponds to the DP of 32. The DP estimated from ^{1}H NMR experiment is approximately 30 (Figure S1). This, together with symmetrical size exclusion chromatography (SEC) trace and narrow polydispersity index (PDI, Table 1), indicates almost quantitative incorporation of the dual initiator and minimal share of side reactions. Hence, better control over the reaction is achieved under these conditions rather than when lower catalyst concentration, elevated temperature, and prolonged reaction time are used.[11]

Incorporation of a protected thiol functionality was attained by esterification of hydroxy chain end of PCL with α-(2,4-dinitrophenylthio)acetic acid (dNPTAA) using diethyl azodicarboxylate (DEAD) and triphenylphosphine (TPP) in modification of the synthetic protocol which had previously been exercised by Trollsås et al.[17] (Scheme 1, b). Br-PCL-dNPTA **1** with near to quantitative functionalization (estimated from ^{1}H NMR data, Figure S2) and narrow polydispersity was obtained (Figure S3, Table 1, **1**).

Br-PCL-dNPTA **1** was employed as macroinitiator in subsequent ATRP of *t*BA (Scheme 2, a). ATRP of *t*BA mediated by $NiBr_2(PPh_3)_2$ was carried out in bulk at 90 °C. Less than stoichiometric amount of the catalyst (0.8 equiv in comparison to the initiating site) was taken as advocated by Hedrick et al.[18] to avoid unsymmetrical SEC traces.

High monomer concentration overpowered otherwise sluggish polymerization.[19] Ratio of the initial molar concentrations of the monomer and initiator $[M]_0/[I]_0$ was decreased from 210 for **3a** to 170 for **3b**. This significantly decreased polymerization time necessary to attain similar monomer conversion (Table 2). SEC revealed narrow molecular weight distribution and no unreacted macroinitiator indicating good control over the reaction (Figure 1).

^{1}H NMR spectrum of **3b** (Figure 2) confirmed successful formation of the P*t*BA block and preservation of protected thiol

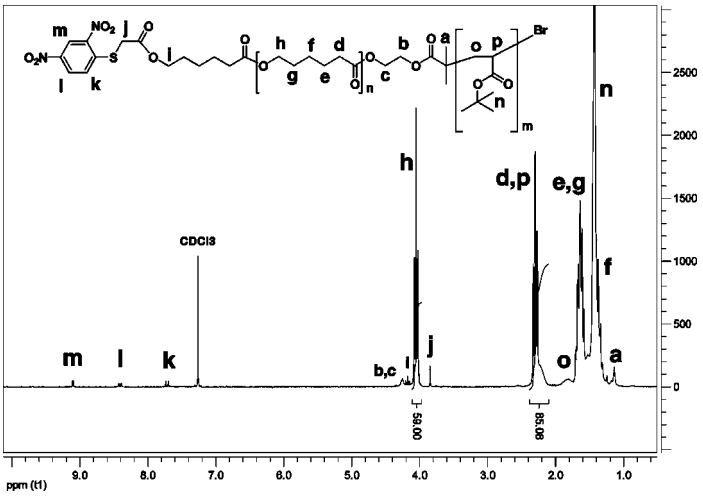

Figure 2. [1]H NMR spectrum of PCL-*b*-P*t*BA **3b**.

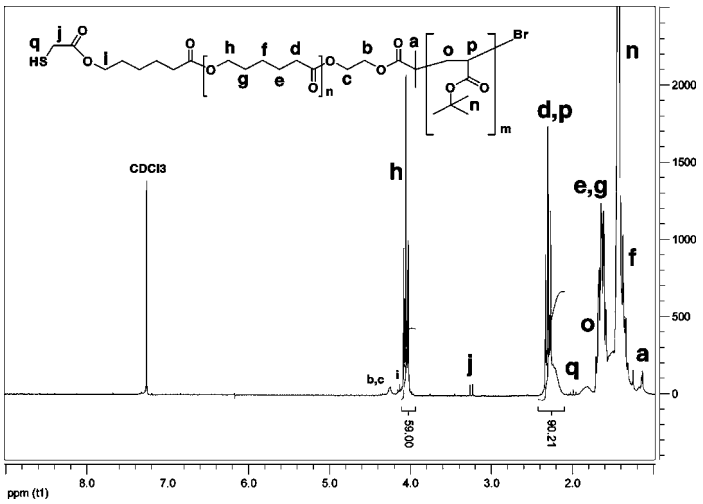

Figure 3. [1]H NMR spectrum of HS-PCL-*b*-P*t*BA **3-(SH)-a**.

functionality. DP of P*t*BA block has been determined by comparison of the integral of the resonance **h**, which is ascribed to the methylene group from PCL repeating unit, to the resonance **d**,**p**, which corresponds to **d** methylene protons in PCL and **p** methine proton in P*t*BA repeating units, respectively.

The results for diblock copolymers prepared from the macroinitiator Br-PCL-dNPTA **1** are summarized in Table 2 (**3a**, **3b**).

Viability of the CuBr/*N*,*N*,*N*′,*N*′,*N*″-pentamethyldiethylenetriamine (PMDETA) catalyzed ATRP of *t*BA from Br-PCL-dNPTA **1** macroinitiator was assessed by conducting the reaction in bulk at 100 °C. This resulted in the block copolymer with broad molecular weight distribution (1.5). The SEC trace was asymmetrical with shoulder appearing on the high molecular weight side. The poor control over the reaction may be ascribed to the loss of the catalyst activity due to possible ligation of copper with 2,4-dinitrophenyl group or with the polyester backbone. Liberated PMDETA may engage in undesirable side reactions by attacking electrophilic carbonyl carbon atoms, and thus induce scission of PCL chain. Investigation of the possible adverse effect that nucleophilic nitrogen exerts on PCL is underway.

Removal of 2,4-dinitrophenyl protecting group from **3** was conducted in $CHCl_3$ using large excess of ethanethiol in the presence of triethylamine (TEA) according to the procedure reported by Carrot et al.[12] This provided HS-PCL-*b*-P*t*BA (Scheme 2, Ib). Full deprotection was confirmed by [1]H NMR (Figure 3) and FT IR spectroscopy: the three resonance peaks arising from 2,4-dinitropenyl group disappear completely, while the resonance peak attributed to the methylene protons next to the thiol functionality (designated as **j**) shifts upfield from 3.85 ppm to 3.25 ppm, and is split into doublet due to coupling with the thiol proton. The latter appears as a triplet **q** at 1.99 ppm. Furthermore, in FT IR spectrum bands at 1596 cm^{-1} and 1524 cm^{-1}, corresponding to asymmetrical and symmetrical stretching of the NO bonds, are no longer detectable.

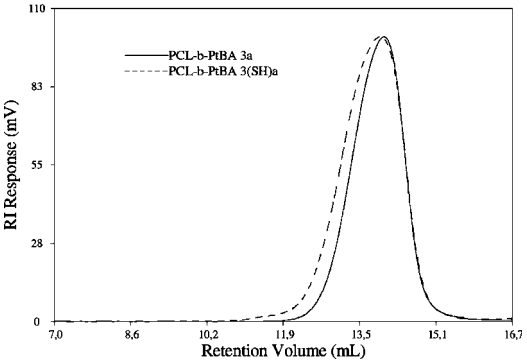

Figure 4. SEC traces of PCL-*b*-P*t*BA **3a** and HS-PCL-*b*-P*t*BA **3-(SH)-a**.

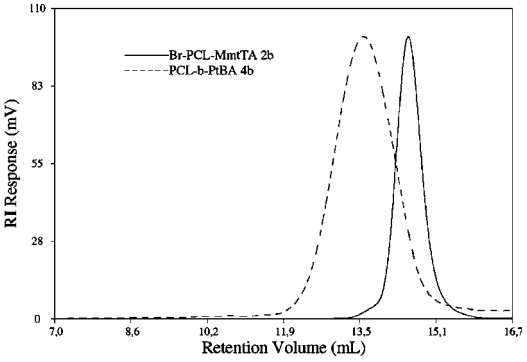

Figure 5. SEC trace of PCL-*b*-P*t*BA **4b**.

Slight broadening of the molecular weight distribution, and peculiar shift of the hydrodynamic volume, similar to the one reported by Carrot et al.,[20] were observed (Figure 4). This phenomenon may be attributed to intra- and intermolecular interactions that arise after unmasking of sulfhydryl functionality as well as to the interaction with SEC column.

Selective cleavage of *tert*-butyl ester groups of **3** was carried out in CH_2Cl_2 employing trifluoroacetic acid (TFA)[21] and triethylsilane (TES) as the cation scavenger[22] (Scheme 2, Ic). Under these relatively mild conditions (2 M TFA) almost complete deprotection of P*t*BA was achieved.

However, thiols are inclined to auto-oxidation and disulfide formation under basic conditions[23] as well as when in contact with air, which may decrease the effectiveness of the macroligand in stabilization of AuNPs.[24] Moreover, removal of 2,4-dinitrophenyl protecting group is reversible and demands large excess of low molecular weight thiol to shift the equilibrium to the macrothiol.[12,20] Therefore, it would be an advantage to make use of thiol protecting group deblocking of which could be irreversibly carried out concurrently with the cleavage of *tert*-butyl ester groups. Such a reaction would be run under acidic conditions, and would limit the time of contact of the macrothiol with air as well.

4-Monomethoxytrityl (Mmt) group has been successfully employed in peptide synthesis as sulfhydryl protection for mercapto acids: It is very acid-labile, succumbs to irreversible deprotection, and can be removed simultaneously with *tert*-butyl ester groups when treated with TFA in CH_2Cl_2/TES.[13] Indeed, it proved to be an efficient and convenient protecting group in the synthesis of thiol-derivatized HS-PCL-*b*-PAA.

Protection of mercaptoacetic acid with Mmt was accomplished by reacting the acid with 4-monomethoxytrityl chloride.[13] Esterification of PCL with α-(4-monomethoxytritylthio)acetic acid (MmtTAA) was conducted as described for Br-PCL-dNPTA **1** (Scheme 1, c). This yielded Br-PCL-MmtTA **2** with near quantitative functionalization (Figure S4) and low PDI (Figure S5, Table 1, **2a**, **2b**).

Br-PCL-MmtTA **2** was successfully chain-extended by ATRP of *t*BA resulting in block copolymer **4** (Scheme 2, a). Interestingly, under similar conditions, macroinitiator **2** afforded higher DP of *t*BA than macroinitiator **1** (Table 2). This may be attributed to hypothetical interaction of the thiol protecting groups with catalytic center in ATRP. However, SEC analysis produced monomodal trace with fairly narrow molecular weight distribution, which proved absence of any undesirable side reactions, and high efficacy of the macroinitiator (Figure 5).

^{1}H NMR spectrum of the block copolymer **4a** (Figure 6) reveals all characteristic resonances: **k** and **l** (overlap with the residual solvent peak) as well as **m** correspond to the thiol-protecting Mmt moiety. The methylene group next to the sulfur atom gives rise to singlet **j**, indicating that no deblocking reaction took place. Had the partial deblocking reaction occurred during the ATRP of *t*BA, the methylene group would have produced at least two resonances corresponding to the -CH_2- group next to the protected thiol, and to that next to the free thiol. Hence, besides singlet **j**, one would observe a doublet or a singlet with different chemical shift value originating from HS-C$\boldsymbol{H}_2$- fragment. As long as the methylene group resonates as a singlet at 2.95 ppm only, we may conclude that there are none (or negligible amount) of the other types of methylene groups.

DP of the P*t*BA blocks is estimated in a similar manner as for **3**.

Simultaneous deblocking of Mmt and *tert*-butyl ester groups by treating PCL-*b*-P*t*BA **4** with TFA (2 M) in CH_2Cl_2/TES provided **6** (Scheme 1, IIc). ^{1}H NMR data confirmed the preservation of PCL backbone: ratio of integrals of the resonances originating from PCL and P*t*BA repeating units (**h** and **d**,**p**, respectively) remained almost unaltered after deprotection (Figures 6 and 7).[8] Singlet **m** attributed to the methoxy group of the protecting species disappears completely, while singlet **j**, originating from the methylene group next to the sulfur atom, shifts downfield and is split into doublet. Broad resonance **r** at 12.26 ppm originates from liberated carboxylic groups (Figure 7). Peak at 1.42 ppm must be attributed to the residual *tert*-butyl ester units, amount of which has been estimated to be approximately 5%. Amphiphilic nature, which the block copolymer acquires during the course of the deprotection reaction, must be the reason of incomplete deprotection: PAA blocks may be shielded by PCL blocks from unfavorable interactions with CH_2Cl_2, which in turn debars TFA from effective interactions with *tert*-butyl ester groups within the coil.

That PCL block remains essentially intact is vital for the following step of the particle formation. Loss of the thiol functionality due to the chain scission would render the block copolymer impotent in passivation of the gold nanoparticles.

AuNPs were synthesized according to a modified literature procedure:[7] To the solution of **6a** (0.054 mmol) and gold(III) chloride trihydrate (0.165 mmol) in THF (16.2 mL) was quickly added freshly prepared solution of lithium borohydride (0.825 mmol). Reduction was marked with immediate change of color from yellow to purple and vigorous gas evolution. Thus, gold nanoparticles were formed employing 3-fold excess of the gold salt compared to the macrothiol. No insoluble matter was

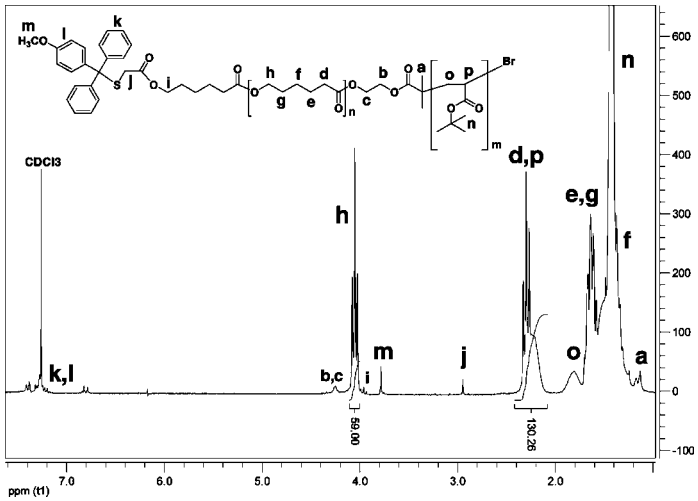

Figure 6. ^{1}H NMR spectrum of PCL-*b*-P*t*BA **4a**.

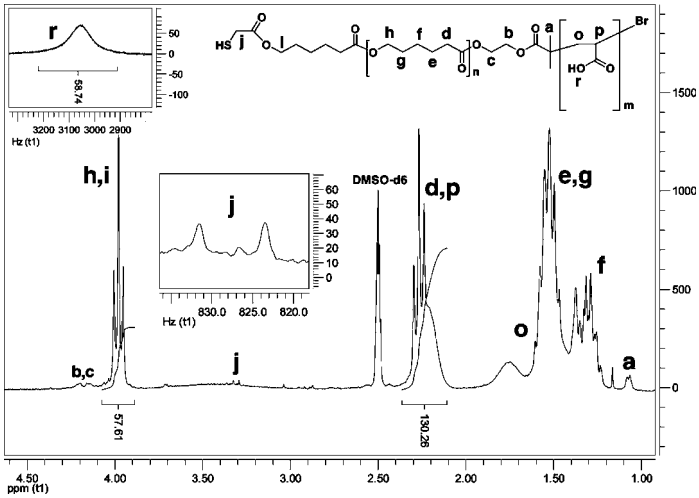

Figure 7. ^{1}H NMR spectrum of HS-PCL-*b*-PAA **6a**.

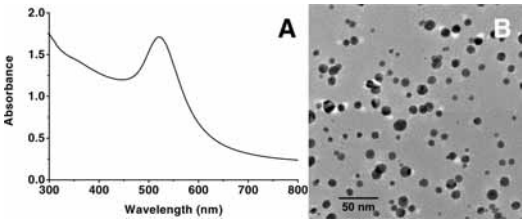

Figure 8. UV−visible spectrum (A) and TEM image (B) of the gold nanoparticles.

observed under these thiol-deficient conditions. UV−visible spectrum of water solution of the nanoparticles (Figure 8A) exhibits absorption at 522 nm^{-1}, a characteristic for aggregation-free AuNPs.[25] Transmission electron microscopy (TEM) image shows well-separated AuNPs with moderate dispersity. The particles shown in Figure 8B have a mean diameter of 9.0 ± 3.1 nm.

Conclusions

In summary, we have demonstrated the ease of preparation of well-defined amphiphilic diblock copolymer bearing thiol end group, HS-PCL-*b*-PAA, which affords reliable stabilization of the gold nanoparticles. Synthetic protocol of ROP of ϵ-CL initiated by HEBI has been optimized to yield the macroinitiator with narrow molecular weight distribution, and high degree of functionality. Quantitative functionalization of Br-PCL-OH is achieved employing protected mercaptoacetic acid/DEAD/TPP combination. ATRP of *t*BA is well controlled when $NiBr_2(PPh_3)_2$ is used and results in low PDI. While both deprotection schemes afford almost complete removal of thiol-protecting groups, 4-monomethoxytrityl group is advantageous for this particular system because it allows deprotection of thiol and P*t*BA block in one pot. Reduction of the gold salt with relatively mild reducing agent provides stable, well-separated nanoparticles, which signifies fairly high efficiency of HS-PCL-*b*-PAA in the passivation of the gold nanoparticles. Coupling

of two controlled polymerization techniques, ROP and ATRP, allows good control over the molecular architecture, and thus provides means for broadening the library of macrothiols.

Supporting Information Available. ^{1}H NMR spectra and SEC chromatograms of the following compounds **Br-PCL-OH**, Br-PCL-dNPTA **1**, and Br-PCL-MmtTA **2a**. This material is available free of charge via the Internet at http://pubs.acs.org.

References and Notes

(1) Gibson, J. D.; Khanal, B. P.; Zubarev, E. R. *J. Am. Chem. Soc.* **2007**, *129*, 11653–11661.
(2) Hong, R.; Han, G.; Fernández, J. M.; Kim, B.-j.; Forbes, N. S.; Rotello, V. M. *J. Am. Chem. Soc.* **2006**, *128*, 1078–1079.
(3) Agarwal, A.; Huang, S. W.; O'Donnell, M.; Day, K. C.; Day, M.; Kotov, N.; Ashkenazi, S. *J. Appl. Phys.* **2007**, *102*, 064701.
(4) Hirsch, L. R.; Stafford, R. J.; Bankson, J. A.; Sershen, S. R.; Rivera, B.; Price, R. E.; Hazle, J. D.; Halas, N. J.; West, J. L. *Proc. Natl. Acad. Sci. U.S.A.* **2003**, *100*, 13549–13554.
(5) Shan, J.; Tenhu, H. *Chem. Commun.* **2007**, 4580–4598.
(6) Abraham, S.; Kim, I.; Batt, C. A. *Angew. Chem., Int. Ed.* **2007**, *46*, 5720–5723.
(7) Azzam, T.; Eisenberg, A. *Langmuir* **2007**, *23*, 2126–2132.
(8) Zhang, Q.; Remsen, E. E.; Wooley, K. L. *J. Am. Chem. Soc.* **2000**, *122*, 3642–3651.
(9) Ghoroghchian, P. P.; Li, G.; Levine, D. H.; Davis, K. P.; Bates, F. S.; Hammer, D. A.; Therien, M. J. *Macromolecules* **2006**, *39*, 1673–1675.
(10) Lele, B. S.; Hoffman, A. S. *J. Controlled Release* **2000**, *69*, 237–248.
(11) Jakubowski, W.; Lutz, J.-F.; Slomkowski, S.; Matyjaszewski, K. *J. Polym. Sci., Part A: Polym. Chem.* **2005**, *43*, 1498–1510.
(12) Carrot, G.; Hilborn, J. G.; Trollsås, M.; Hedrick, J. L. *Macromolecules* **1999**, *32*, 5264–5269.
(13) Mourtas, S.; Gatos, D.; Kalaitzi, V.; Katakalou, C.; Barlos, K. *Tetrahedron Lett.* **2001**, *42*, 6965–6967.
(14) Hawker, C. J.; Hedrick, J. L.; Malmström, E. E.; Trollsås, M.; Mecerreyes, D.; Moineau, G.; Dubois, P.; Jérôme, R. *Macromolecules* **1998**, *31*, 213–219.
(15) Kowalski, A.; Duda, A.; Penczek, S. *Macromol. Rapid Commun.* **1998**, *19*, 567–572.
(16) Kricheldorf, H. R. *Macromol. Symp.* **2000**, *153*, 55–65.
(17) Trollsås, M.; Hawker, C. J.; Hedrick, J. L.; Carrot, G.; Hilborn, J. *Macromolecules* **1998**, *31*, 5960–5963.
(18) Hedrick, J. L.; Trollsås, M.; Hawker, C. J.; Atthoff, B.; Claesson, H.; Heise, A.; Miller, R. D.; Mecerreyes, D.; Jérôme, R.; Dubois, P. *Macromolecules* **1998**, *31*, 8691–8705.
(19) Moineau, G.; Minet, M.; Dubois, P.; Teyssié, P.; Senninger, T.; Jérôme, R. *Macromolecules* **1999**, *32*, 27–35.
(20) Carrot, G.; Hilborn, J.; Hedrick, J. L.; Trollsås, M. *Macromolecules* **1999**, *32*, 5171–5173.
(21) Ma, Q.; Wooley, K. L. *J. Polym. Sci., Part A: Polym. Chem.* **2000**, *38*, 4805–4820.
(22) Mehta, A.; Jaouhari, R.; Benson, T. J.; Douglas, K. T. *Tetrahedron Lett.* **1992**, *33*, 5441–5444.
(23) Hu, J.; Fox, M. A. *J. Org. Chem.* **1999**, *64*, 4959–4961.
(24) Shan, J.; Nuopponen, M.; Jiang, H.; Kauppinen, E.; Tenhu, H. *Macromolecules* **2003**, *36*, 4526–4533.
(25) Raula, J.; Shan, J.; Nuopponen, M.; Niskanen, A.; Jiang, H.; Kauppinen, E.; Tenhu, H. *Langmuir* **2003**, *19*, 3499–3504.

BM800860T

Supporting Information

Gold Nanoparticles Protected with Thiol-Derivatized Amphiphilic Poly(ε-caprolactone)-*b*-poly(acrylic acid)

Irakli Javakhishvili, Søren Hvilsted*

Technical University of Denmark, Department of Chemical and Biochemical Engineering, Danish Polymer Centre, Building 423, DK-2800 Kgs. Lyngby, Denmark

Email: sh@kt.dtu.dk

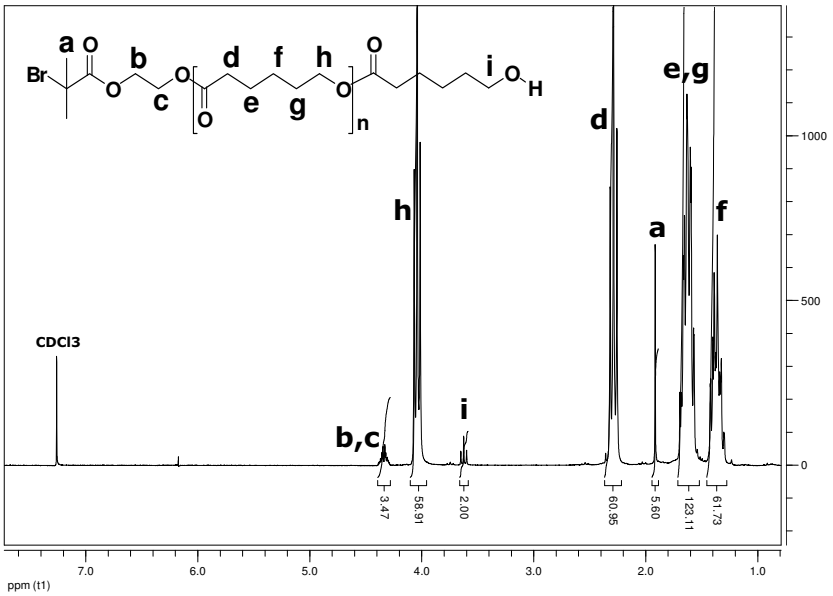

Figure S1. [1]H NMR spectrum of **Br-PCL-OH**

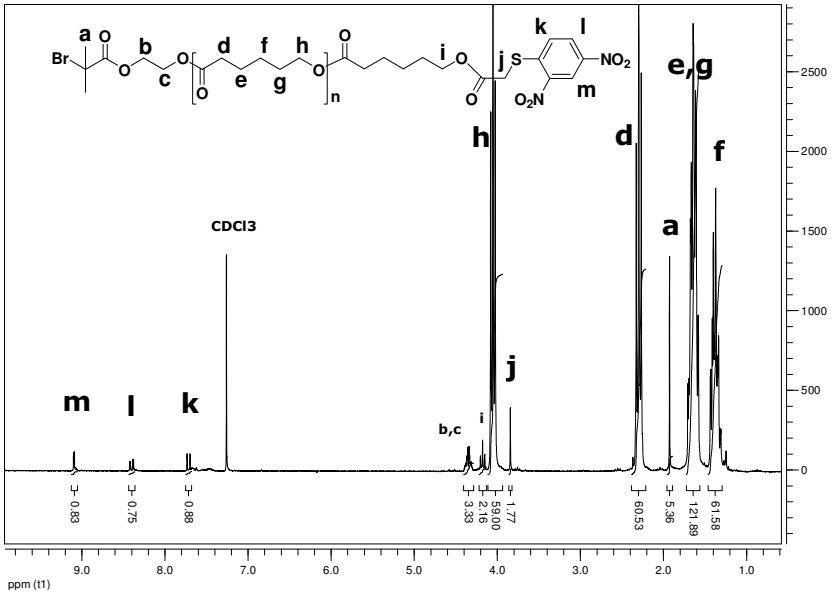

Figure S2. [1]H NMR spectrum of Br-PCL-dNPTA **1**. Downfield shift of triplet **i** from 3.63 ppm to 4.18 ppm indicates that the extent of functionalization is close to quantitative.

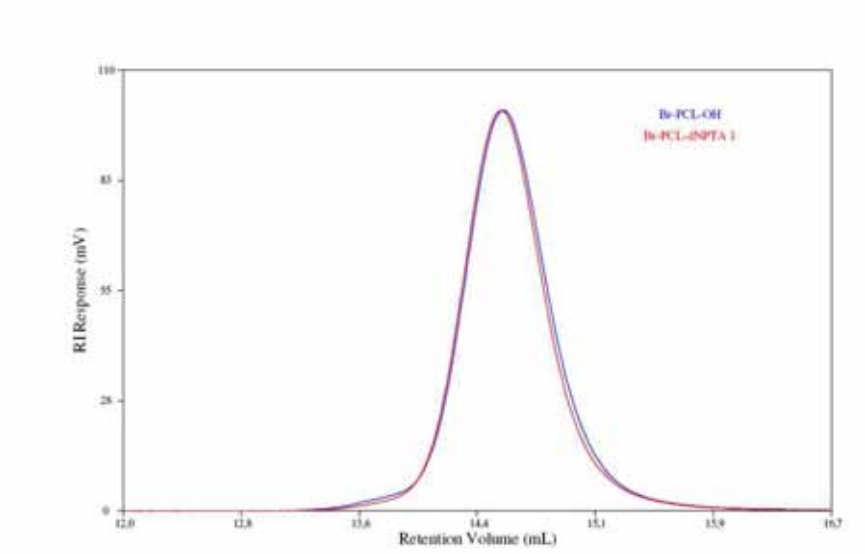

Figure S3. SEC chromatograms of **Br-PCL-OH** and Br-PCL-dNPTA **1**

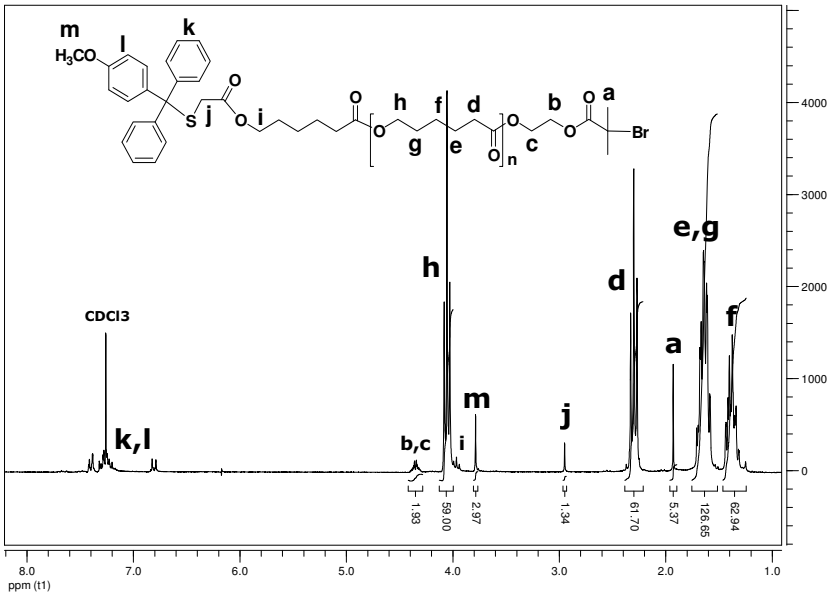

Figure S4. [1]H NMR spectrum of Br-PCL-MmtTA **2a**. Extent of esterification is near to quantitative.

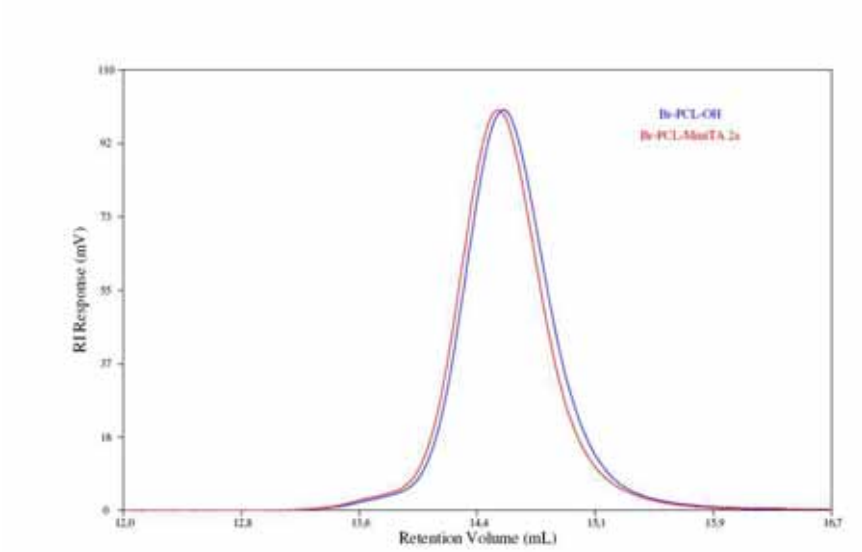

Figure S5. SEC chromatogram of Br-PCL-MmtTA **2a**

Appendix III

Javakhishvili, I.; Binder, W. H.; Tanner, S.; Hvilsted, S. Facile Synthesis of Linear-dendritic Cholesteryl-poly(ε-caprolactone)-*b*-(L-lysine)$_{G2}$ by Thiol-ene and Azide-alkyne ''Click'' Reactions. *Polym. Chem.* 2010, *1*, 506-513 – Reproduced by permission of the Royal Society of Chemistry.

Facile synthesis of linear-dendritic cholesteryl-poly(ε-caprolactone)-*b*-(L-lysine)$_{G2}$ by thiol-ene and azide-alkyne "click" reactions†

Irakli Javakhishvili,[a] Wolfgang H. Binder,[b] Susanne Tanner[b] and Søren Hvilsted*[a]

Received 16th October 2009, Accepted 21st December 2009
First published as an Advance Article on the web 14th January 2010
DOI: 10.1039/b9py00303g

The construction of a linear-dendritic block copolymer consisting of terminal cholesteryl moiety, poly(ε-caprolactone), and a second generation L-lysine dendron has been accomplished by the combination of copper(I) catalyzed azide-alkyne and UV-triggered thiol-ene "click" reactions. Ring-opening polymerization of ε-caprolactone initiated by 5-hexyn-1-ol and Mitsunobu coupling with 4-pentenoic acid provide hetero-telechelic poly(ε-caprolactone) bearing terminal alkyne and alkene groups. It is then employed in the sequential "click" reactions with the azide-functionalized dendritic wedge and thiocholesterol. Near to quantitative functionalization of the intermediate and final products has been attained as confirmed by NMR spectroscopy and MALDI-TOF spectrometry.

Introduction

Amphiphilic linear-dendritic block copolymers have gained significant importance due to their peculiar properties that drive self-assembly into various shapes. Different combinations of the constituting blocks have been prepared, and their capacity of forming complex supramolecular architectures has been investigated.[1]

Hedrick and co-workers have designed linear-dendritic amphiphiles that resemble naturally occuring phospholipids.[2] The hydrophilic dendrons based on 2,2-bis(hydroxymethyl)propionic acid (bis-MPA) (A) were combined with the linear segment of the hydrophobic poly(ε-caprolactone) (PCL) (B) *via* ring-opening polymerization (ROP) of ε-caprolactone (ε-CL) initiated by the dendrons possessing multiple functionalities. The symmetric linear-dendritic triblock copolymer (ABA) was also prepared *via* the Mitsunobu coupling of the linear-dendritic block copolymer (AB) with the acid-functionalized dendrons.[2] Fréchet and co-workers[3] obtained linear-dendritic block copolymers by divergently growing bis-MPA based dendrons from poly(ethylene glycol) (PEG) chain-end.

A step-wise synthetic protocol that affords well-defined structures with a controlled number of peripheral functional groups available for subsequent functionalization can render self-assembled aggregates stimuli responsive, and prompts the application of such nanocarriers as drug delivery devices.[4] Thus, poly(ethylene oxide) (PEO)-dendritic polylysine and PEO-dendritic polyester have been prepared, and then peripheral functional groups have been modified by acid-labile hydrophobic moieties to obtain pH responsive micelles.[4]

Tomalia and co-workers[5] have prepared core-shell nanostructures from precise monodisperse, linear-dendritic polymers. First a thiol functionalized di-dendron is conjugated with single strand DNA. Together with the other linear-dendritic copolymer incorporating appropriate complementary DNA as the linear segment, these structures may be used as supramacromolecular components to build core-shell nanostructures possessing base-paired DNA cores surrounded by four dendrons.[5]

Cao and co-workers developed the route towards poly(L-lactide)-*b*-dendritic poly(L-lysine) based on the metal free ROP of the L-lactide initiated by the hydroxyl end-capped Boc-protected poly(L-lysine) dendrons.[6] The authors have pointed out the role of poly(L-lysine) as a functional vector for DNA transfection.[6]

Zubarev and Stupp[7] demonstrated a synthetic pathway leading to hybrid structures: dendron rodcoils. These macromolecules comprise dendritic, rod-like, and coil-like molecular segments, and have been obtained *via* convergent or divergent strategies.[7] Amphiphilic "tree-shaped" comb-dendritic block copolymer has been prepared with hydrophobic, rigid comb block, poly(γ-n-dodecyl-L-glutamate), that results in the formation of extremely stable micelles, and highly functional dendritic exterior – the polyester dendron modified with PEG – that can be used to attach biocompatible ligands for efficient targeting.[8] Self-assembly of this linear-dendritic hybrid block copolymer in solution provides a potential route to core-shell micellar nanostructures with various surface functionalities. The semirigid rod nature of the comb block determines the unique shape of the macromolecular structure and assists self-assembly.[8] Stupp and co-workers have also reported about the synthesis of the amphiphilic rodcoil dendrons where the dendritic wedge was connected with the rigid moiety *via* the polyester spacer.[9] Preparation of these intricate structures involved ROP of L-lactide initiated by cholesterol, and substitution of the hydroxyl terminus of this cholesteryl-oligo(L-lactic acid) with the L-lysine dendron. While liquid chrystalline character of the cholesteryl moiety could drive self-assembly of the rodcoil

[a]*Technical University of Denmark, Department of Chemical and Biochemical Engineering, Danish Polymer Centre, Building 423, DK-2800 Kgs. Lyngby, Denmark. E-mail: sh@kt.dtu.dk; Tel: +45 4525 2965*
[b]*Martin-Luther University Halle-Wittenberg, Faculty of Natural Sciences II/Institute of Chemistry, Lehrstuhl Makromolekulare Chemie, von Danckelmannplatz 4, D-06120 Halle (Saale), Germany; Tel: +49 (0)345 55 25930*

† Electronic supplementary information (ESI) available: NMR and MALDI-TOF spectra. See DOI: 10.1039/b9py00303g

dendron, the L-lysine wedge could provide sterics to direct the nanostructure formation. Furthermore, both cholesterol and L-lysine could interact with the cell membrane, and thus promote and facilitate cell adhesion.[9]

However, this synthetic procedure, though subtle, is quite tedious and demanding. With the advance of the copper(I) catalyzed azide-alkyne cycloaddition[10] (CuAAC) and UV initiated thiol-ene[11] "click" reactions, and their successful implementation in the field of the macromolecular chemistry,[12] we believe that the synthetic approach towards the rodcoil dendrons can be accelerated, and made more robust and versatile: all three constituent blocks can be coupled to avoid the default presence of either a cholesterol or L-lysine wedge as is the case in the strategies discussed above.[6,9] CuAAC "click" reaction has previously been employed in the preparation of unsymmetrical dendrimers,[13] dendronized linear polymers[14] as well as linear-dendritic block copolymers,[15] and thus has proved to be a highly efficient and convenient approach.

Herein, we present the synthetic layout for the preparation of the rodcoil dendron based on cholesterol, PCL, and dendritic L-lysine. Since Hawker and co-workers pointed out the efficiency and compatibility of these orthogonal "click" reactions,[16] we believe this is one of the first successful attempts to employ this strategy in building such multifunctional macromolecular architecture alongside Haddleton and co-workers, where CuAAC reaction has been coupled with thio-Michael addition,[17] and Anseth and co-workers, where copper-free "click" chemistry has been conjugated with thiol-ene photocoupling.[18]

Experimental

Materials and methods

ε-CL (Fluka, ≥99%) was dried over CaH_2, and distilled under reduced pressure. Tetrahydrofuran (THF) (Sigma-Aldrich, 99.9%), *N*,*N*-dimethylformamide (DMF) (Fluka, 99.8%), toluene (Sigma-Aldrich, 99.9%), and triethylamine (TEA) (Sigma-Aldrich, 99%) were dried over CaH_2, and distilled under nitrogen flow. Tin octoate ($Sn(Oct)_2$) (Sigma, ~95%) was distilled under reduced pressure. Methanol (Sigma-Aldrich, 99.9%), heptane (Sigma-Aldrich, 99%), dichloromethane (DCM) (Sigma-Aldrich, 99.8%), dioxane (Riedel-de Haën, 99%), ethyl acetate (Sigma-Aldrich, 99.7%), 5-hexyn-1-ol (Aldrich, 96%), 4-pentenoic acid (Aldrich, 97%), L-lysine (Fluka, purum; crystallized; ≥98%), di-*tert*-butyl dicarbonate (Aldrich, 97%), *N*,*N*′-dicyclohexylcarbodiimide (DCC) (Aldrich, 99%), 3-bromo-1,2-propanediol (Fluka, ≥96%), diethyl azodicarboxylate (DEAD) (Aldrich), triphenylphosphine (TPP) (Fluka, ~97%), sodium azide (Aldrich, 99%), CuI (Aldrich, 98%), thiocholesterol (Aldrich), trifluoroacetic acid (TFA) (Sigma-Aldrich, ≥98%), 2,2-dimethoxy-2-phenylacetophenone (DMPA) (Aldrich, 99%), 4-di(methylamino)pyridine (4-DMAP) (Fluka, >98%) were used as received.

Characterization by NMR spectroscopy was conducted on Bruker 300 MHz spectrometer using $CDCl_3$ or DMSO-d_6 as solvents (both from Aldrich). The coupling constants are given in Hz. Molecular weights and polydispersity indices were estimated by size exclusion chromatography (SEC) on Viscotek 200 instrument using two PLgel mixed-D columns (Polymer Laboratories (PL)), assembled in series, and a refractive index detector. SEC samples were run in THF at room temperature (1 mL min^{-1}). Molecular weights were calculated using polystyrene (PS) standards from PL. Mass spectra were acquired by matrix-assisted laser desorption and ionization time-of-flight (MALDI-TOF) mass spectrometry using a Bruker autoflex III smartbeam mass spectrometer, equipped with the laser that produces pulses at 337 nm. Samples using 2,5-dihydroxyacetophenon as matrix and NaTFA as additive were prepared by dissolving the polymer in THF at a concentration of 20 mg mL^{-1}. A 10 μL aliquot of this solution was added to 100 μL of a 20 mg mL^{-1} matrix solution, and 1 μL NaTFA as a THF solution (20 mg mL^{-1}) was added as cationzation agent.

All reactions were carried out under the nitrogen atmosphere unless otherwise stated.

Synthesis

1: Boc protection of L-lysine was carried out according to the procedure reported elsewhere.[19]

2: **1** (5.00 g, 14.45 mmol), 3-bromo-1,2-propanediol (1.02 g, 6.58 mmol), and 4-DMAP (0.17 g, 1.39 mmol) were placed in a 250 mL two-neck flask, and dissolved in DCM (60 mL). The reaction mixture was stirred and cooled in an ice/water bath, and the solution of DCC (3.00 g, 14.54 mmol) in DCM was injected. Afterward, the ice/water bath was removed, and the reaction was carried out at room temperature for 24 h. After completion of the reaction, the mixture was filtered to remove dicyclohexylurea, and extracted with dilute $NaHCO_3$ (2 × 50 mL), dilute $NaHSO_4$ (1 × 50 mL), distilled water (1 × 50 mL), and brine (1 × 50 mL). The solution was dried over anhydrous $MgSO_4$, and concentrated under reduced pressure. Yield: 4.64 g (87%).

δ_H (300 MHz; $CDCl_3$) 5.10–5.45 (3H, br, CHN*H*Boc and OCH_2CHO), 4.55–4.85 (2H, br, CH_2NHBoc), 4.37–4.53 (m, OCH_2CHO), 4.14–4.37 (m, OCH_2CHO and $CHNHBoc$) (4.14–4.53 corresponds to 4H), 3.38–3.60 (2H, m, CH_2Br), 2.95–3.25 (4H, m, CH_2NHBoc), 1.58–2.00 (m, $CH_2CH_2CHNHBoc$), 1.25–1.58 (m, $BocNHCH_2CH_2CH_2CH_2CHNHBoc$ and $C(CH_3)_3$) (1.25–2.00 corresponds to 48H).

3: **2** (4.58 g, 5.64 mmol) and sodium azide (0.73 g, 11.23 mmol) were placed in a round-bottom flask, and dissolved in DMF (50 mL). The reaction mixture was stirred at 40 °C overnight. Afterward, it was diluted with distilled water (70 mL), and extracted with ethyl acetate (7 × 50 mL). The organic layers were combined, and washed with distilled water (6 × 100 mL), brine (1 × 75 mL), and distilled water (1 × 100 mL). The solution was then dried over anhydrous $MgSO_4$, and concentrated on rotary-evaporator. Yield: 3.96 g (91%).

δ_H (300 MHz; $CDCl_3$) 5.10–5.40 (3H, br, CHN*H*Boc and OCH_2CHO), 4.60–4.83 (2H, br, CH_2NHBoc), 4.31–4.45 (1H, m, OCH_2CHO), 4.15–4.31 (3H, m, OCH_2CHO and $CHNHBoc$), 3.40–3.60 (2H, m, CH_2N_3), 2.95–3.20 (4H, m, CH_2NHBoc), 1.60–1.97 (m, $CH_2CH_2CHNHBoc$), 1.28–1.60 (m, $BocNHCH_2CH_2CH_2CH_2CHNHBoc$ and $C(CH_3)_3$) (1.28–1.97 corresponds to 48H). The resonances at 4.11 (q), 2.03 (s), 1.25 (t) correspond to the residual ethyl acetate.

4: Ring opening polymerization of ε-CL was conducted as reported earlier.[20] Degree of polymerization estimated by ^1H NMR is 20, $M_n = 2380$ Da. SEC: $M_n = 4200$ Da, $M_w = 4700$ Da, $M_w/M_n = 1.11$.

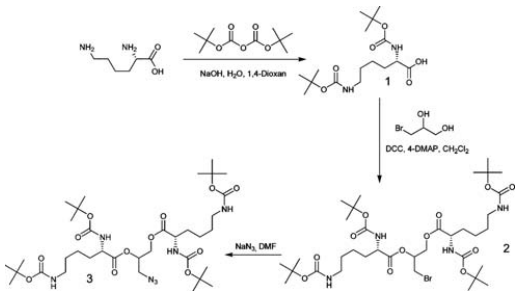

Scheme 1 Preparation of bis-(di-Boc-L-lysine)-3-azido-1,2-propandiol

δ_H (300 MHz; $CDCl_3$) 4.05 (40H, t, $J_{1,3}$ 6.7, $(CH_2)_4CH_2OC(O)$ and $C(O)OCH_2(CH_2)_3C{\equiv}CH$), 3.64 (2H, t, $J_{1,3}$ 6.5, $(CH_2)_4CH_2OH$), 2.30 (t, $J_{1,3}$ 7.5, $OC(O)CH_2(CH_2)_4$), 2.23 (td, $J_{1,4}$ 2.6, $J_{1,3}$ 7.1, $CH_2C{\equiv}CH$) (2.18–2.40 corresponds to 42 H), 1.96 (1H, t, $J_{1,4}$ 2.6, $CH_2C{\equiv}CH$), 1.50–1.81 (84H, m, $OC(O)CH_2CH_2CH_2CH_2CH_2$ and $C(O)OCH_2CH_2CH_2CH_2CH_2$-$C{\equiv}CH$), 1.25–1.50 (40H, m, $OC(O)CH_2CH_2CH_2CH_2CH_2$).

5: The Mitsunobu coupling was performed under the same conditions as in ref. 20. SEC: M_n = 4100 Da, M_w = 4500 Da, M_w/M_n = 1.11. δ_H (300 MHz; $CDCl_3$) 5.80 (1H, m, $CH_2CH=CH_2$), 5.00 (2H, m, $CH_2CH{=}CH_2$), 4.05 (40H, t, $J_{1,3}$ 6.7, $(CH_2)_4CH_2OC(O)$ and $C(O)OCH_2(CH_2)_3C{\equiv}CH$), 2.36 (m, $OC(O)CH_2CH_2CH{=}CH_2$), 2.28 (t, $J_{1,3}$ 7.5, $OC(O)CH_2(CH_2)_4$), 2.21 (td, $J_{1,4}$ 2.6, $J_{1,3}$ 7.1, $CH_2C{\equiv}CH$) (2.16–2.42 corresponds to 46H), 1.94 (1H, t, $J_{1,4}$ 2.6, $CH_2C{\equiv}CH$), 1.48–1.80 (84H, m, $OC(O)CH_2CH_2CH_2CH_2CH_2$ and $C(O)OCH_2CH_2CH_2CH_2CH_2$-$C{\equiv}CH$), 1.20–1.48 (40H, m, $OC(O)CH_2CH_2CH_2CH_2CH_2$).

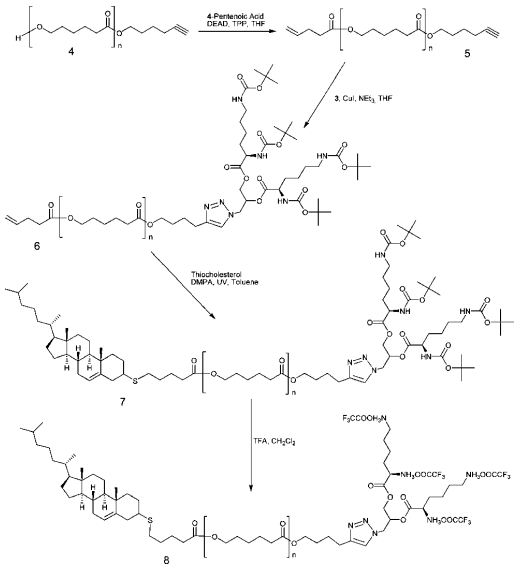

Scheme 2 CuAAC and thiol-ene "click" reactions followed by the removal of Boc protecting groups

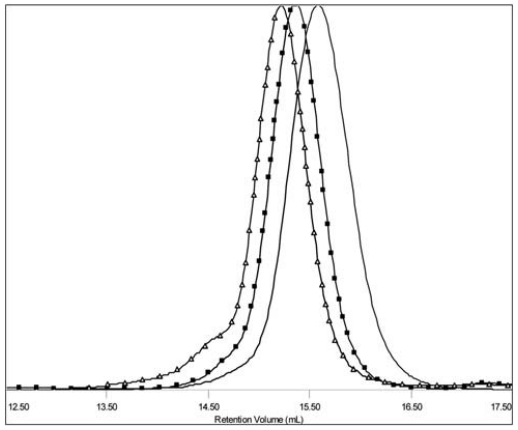

Fig. 1 Normalized SEC traces of α-alkenyl-ω-alkynyl-PCL (**5**) (M_n = 4100 Da, M_w/M_n = 1.11), alkenyl-PCL-*b*-(di-Boc-L-lysine)$_{G2}$ (**6**) (M_n = 5100 Da, M_w/M_n = 1.10) ■, cholesteryl-PCL-*b*-(di-Boc-L-lysine)$_{G2}$ (**7**) (M_n = 5900 Da, M_w/M_n = 1.15) △.

6: A 50 mL two-neck flask was charged with **5** (1.4 g, 0.57 mmol), **3** (0.93 g, 1.2 mmol), CuI (0.11 g, 0.58 mmol), and THF (19 mL). The reaction mixture was stirred at room temperate until the polymer dissolved completely. Then TEA (0.32 mL, 2.3 mmol) was introduced. The reaction was conducted at 35 °C for 24 h. Afterward, the mixture was diluted with THF, and treated with basic Al_2O_3. The solution was then filtered, concentrated under reduced pressure, and precipitated into the large excess of cold MeOH–H_2O (5 : 1) mixture. The block copolymer was isolated *via* filtration, and dried in the vacuum oven at room temperature until constant weight. SEC: M_n = 5100 Da, M_w = 5600 Da, M_w/M_n = 1.10. δ_H (300 MHz; $CDCl_3$) 7.5 (1H, br, Ar), 5.80 (1H, m, $CH_2CH=CH_2$), 5.10–5.60 (br, CHN*H*Boc and OCH_2CHO), 5.00 (m, $CH_2CH{=}CH_2$), 3.85–4.93 (br m, CH_2NHBoc, OCH_2CHO, CHNHBoc, CH_2Ar, $(CH_2)_4CH_2OC(O)$ and $C(O)OCH_2(CH_2)_3Ar$) (3.85–5.60 corresponds to 53H), 2.93–3.22 (4H, br, CH_2NHBoc), 2.58–2.85

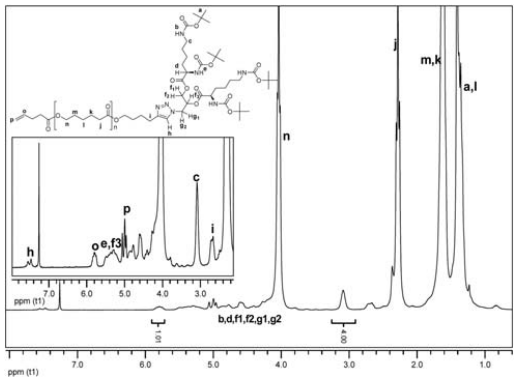

Fig. 2 ^{1}H NMR spectrum of alkenyl-PCL-*b*-(di-Boc-L-lysine)$_{G2}$ (**6**). The spectrum was recorded in $CDCl_3$.

(2H, br, C(O)O(CH$_2$)$_3$CH_2Ar), 2.03–2.55 (44H, br m, OC(O)CH_2CH_2CH=CH$_2$ and OC(O)CH_2(CH$_2$)$_4$), 1.50–1.97 (m, CH$_2$CH_2CHNHBoc, OC(O)CH$_2$CH_2CH$_2$CH_2CH$_2$ and C(O)OCH$_2$CH_2CH_2CH$_2$Ar), 1.05–1.60 (m, BocNHCH$_2$CH_2-CH_2CH$_2$CHNHBoc, C(CH_3)$_3$ and OC(O)CH$_2$CH$_2$CH_2CH$_2$-CH$_2$) (1.05–1.97 corresponds to 172H).

7: **6** (150 mg, 0.046 mmol), thiocholesterol (187 mg, 0.46 mmol), DMPA (42 mg, 0.16 mmol), and toluene (1.2 mL) were placed in a 15 mL round-bottom open vial equipped with a magnetic stirring bar. Having dissolved all the solid components, the vial was placed under the UV lamp (365 nm), and irradiated for 1.5 h while stirring under air. The reaction was

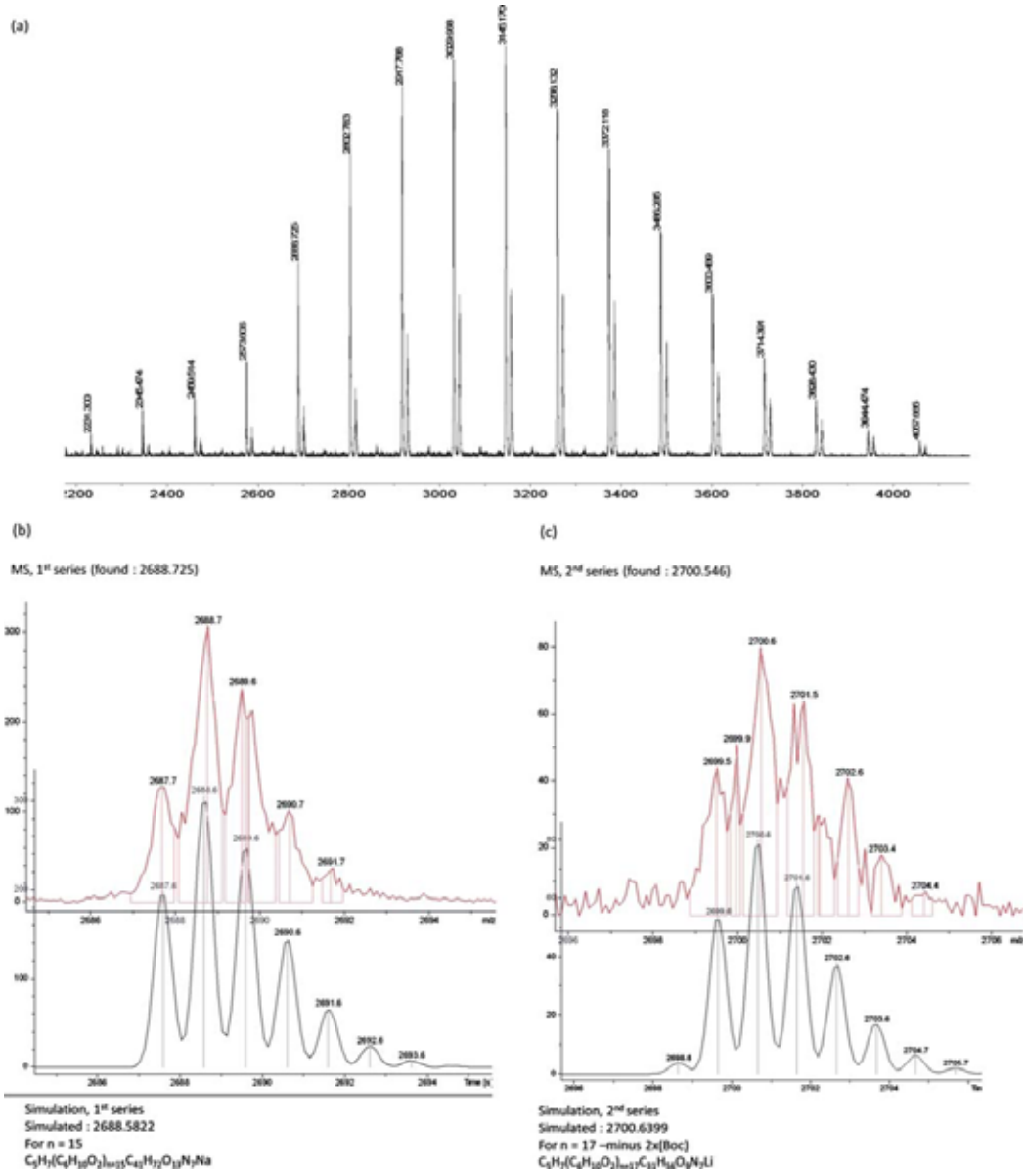

Fig. 3 MALDI-TOF spectrum of alkenyl-PCL-*b*-(di-Boc-L-lysine)$_{G2}$ (**6**): (a) full spectrum, (b) expansion (top) and simulation (bottom) of 1st-series, (c) expansion (top) and simulation (bottom) of 2nd series.

monitored by SEC and ^{1}H NMR. After completion of the reaction, the mixture was diluted with DCM, and precipitated into the large excess of cold heptane. The polymer was isolated on the filter paper, washed with heptane, and dried in the vacuum oven at room temperature. SEC: $M_n = 5900$ Da, $M_w = 6800$ Da, $M_w/M_n = 1.15$.

δ_H (300 MHz; $CDCl_3$) 7.5 (1H, br, Ar), 5.05–5.70 (4H, br, thiocholesterol C*H* = C, CHN*H*Boc and OCH_2CHO), 3.86–4.96 (48H, br m, CH_2NHBoc, OCH_2CHO, $CHNHBoc$, CH_2Ar, $(CH_2)_4CH_2OC(O)$ and $C(O)OCH_2(CH_2)_3Ar$), 2.97–3.22 (4H, br, CH_2NHBoc), 2.44–2.83 (5H, m, $OC(O)(CH_2)_3CH_2SCH$, $SCHCH_2C{=}CH$, $C(O)O(CH_2)_3CH_2Ar$), 2.30 (44H, t, $J_{1,3}$ 7.5, $OC(O)CH_2(CH_2)_3SCH$, $OC(O)CH_2(CH_2)_4$, and $SCHCH_2C{=}CH$ (this multiplet is dominated by the large triplet from the PCL backbone)), 1.55–1.97 (m, $CH_2CH_2CHNHBoc$, $OC(O)CH_2CH_2CH_2CH_2CH_2$ and $C(O)OCH_2CH_2CH_2CH_2Ar$), 1.25–1.60 (m, $BocNHCH_2CH_2CH_2CH_2CHNHBoc$, $C(CH_3)_3$ and $OC(O)CH_2CH_2CH_2CH_2CH_2$), 0.99 (s, $CH_3CC{=}CH$), 0.91 (s, 3H, $CH_3CH(CH)CH_2$), 0.87 (s, $CH_3CH(CH_3)CH_2$), 0.85 (s, $CH_3CH(CH_3)CH_2$), 0.67 (s, $CH_3C(CH)CH$). Other signals originating from the cholesteryl moiety overlap with the peaks corresponding to the block copolymer, and, therefore, cannot be unambiguously assigned.

8: A 25 mL two-neck flask was charged with **7** (123 mg, 0.034 mmol) and DCM (3.6 mL). The flask was immersed in an ice/water bath, and TFA (0.75 mL) was injected. The reaction mixture was stirred for 30 min in the ice/water bath, and for 90 min at room temperature. Then it was concentrated under reduced pressure, and the product was dried in the vacuum oven at room temperature.

δ_H (300 MHz; DMSO-d_6) 8.30–8.80 (6H, br, $CHNH_3OOCCF_3$), 7.65–8.05 (br, $CH_2NH_3OOCCF_3$), 7.94 (s, Ar) (7.65–8.05 corresponds to 7H), 5.20–5.70 (2H, br m, thiocholesterol C*H* = C and OCH_2CHO), 4.55–4.90 (2H, br, CH_2Ar), 3.80–4.55 (44H, m, OCH_2CHO and $CHNH_3OOCCF_3$, $(CH_2)_4CH_2OC(O)$ and $C(O)OCH_2(CH_2)_3Ar$), 2.42–2.94 (br, $CH_2NH_3OOCCF_3$, $OC(O)(CH_2)_3CH_2SCH$, $SCHCH_2C{=}CH$, $C(O)O(CH_2)_3CH_2Ar$, overlaps with DMSO-d_6), 2.27 (44H, t, $J_{1,3}$ 7.1, $OC(O)CH_2(CH_2)_3SCH$, $OC(O)CH_2(CH_2)_4$, and $SCHCH_2C{=}CH$), 1.42–2.00 (m, $CH_2CH_2CHNH_3OOCCF_3$, $F_3CCOONH_3CH_2CH_2CH_2CH_2$, $OC(O)CH_2CH_2CH_2CH_2CH_2$ and $C(O)OCH_2CH_2CH_2CH_2Ar$), 1.18–1.42 (m, $OC(O)CH_2CH_2CH_2CH_2CH_2CH_2$), 0.86–0.94 (m, $CH_3CC{=}CH$ and $CH_3CH(CH)CH_2$), 0.85 (s, $CH_3CH(CH_3)CH_2$), 0.83 (s, $CH_3CH(CH_3)CH_2$), 0.64 (s, $CH_3C(CH)CH$).

Results and discussions

ROP of ε-CL initiated by 5-hexyn-1-ol and catalyzed by tin(II) octoate at elevated temperature in bulk has been reported by Schubert and co-workers.[21] The polydispersity index (PDI) of 1.19 was achieved. We have shown that better control over the reaction can be gained by conducting it at moderate temperature with high catalyst concentration.[20] Thus, PCL with the PDI = 1.11 and high end-group fidelity has been obtained. The degree of polymerization estimated by ^{1}H NMR was 20. Esterification of the hydroxyl chain end with 4-pentenoic acid according to Mitsunobu protocol[20] afforded hetero-telechelic PCL bearing alkyne and alkene functional groups. The α-alkenyl-ω-alkynyl-PCL had narrow molecular weight distribution (PDI = 1.11), and near to quantitative functionality as confirmed by ^{1}H NMR (Fig. S2†) and MALDI-TOF analysis (Fig. S6†).

The synthesis of the second generation dendron of L-lysine, (L-lysine)$_{G2}$ (**3**), with the azide functional group in the focal point was carried out according to Scheme 1.

This approach allows immediate incorporation of the primary bromo function in the core. Therefore, it is not necessary to introduce bromoalkyl moiety by additional esterification reaction as would be the case in the standard procedure of building dendrons.[13] Subsequent nucleophilic substitution furnishes azide functional dendritic wedge of the second generation with high yield and purity.

Thus, 3-bromo-1,2-propandiol was reacted with N_α,N_ε-di-Boc-L-lysine (1.1 eq) in the presence of DCC and 4-DMAP. The purification step did not require column chromatography, and sufficed with extractions. Afterward, **2** was converted to the corresponding azide by treating it with sodium azide (2 eq) at 40 °C overnight. The heteronuclear single quantum coherence (HSQC) NMR experiment (Fig. S1†) confirmed full conversion under these reaction conditions. The structure was further verified by MALDI-TOF spectrometry (Fig. S4 and S5†).

Azide-alkyne and UV initiated thiol-ene "click" reactions were conducted as depicted in Scheme 2.

CuAAC reaction between α-alkenyl-ω-alkynyl-PCL **5** and bis-(di-Boc-L-lysine)-3-azido-1,2-propandiol **3** (2 eq) was catalyzed by CuI (1 eq in comparison to the alkyne). The "click" components were reacted in THF in the presence of NEt_3 at 35 °C for 24 h.[22] The excess of **3** was removed by precipitation in MeOH–H_2O mixture. The product was analyzed by SEC, NMR, and MALDI-TOF.

SEC revealed monomodal, symmetrical trace, which was shifted to the higher molecular weight (Fig. 1), and low PDI of 1.10. This implies that no chain scission took place nor did the polymer chains remain unreacted. Near to quantitative functionalization was attained as judged from NMR experiments. Both ^{1}H and HSQC NMR data indicated almost full conversion as the resonances corresponding to the alkyne functional group could no longer be detected. Furthermore, the peaks ascribed to the

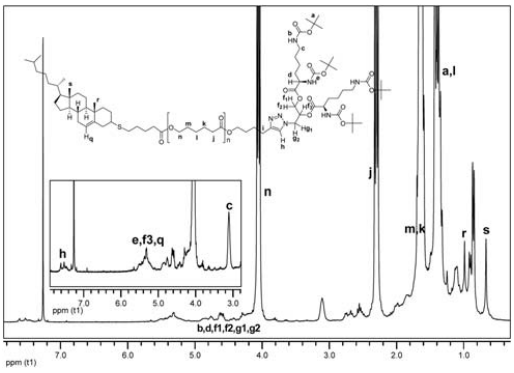

Fig. 4 ^{1}H NMR spectrum of Cholesteryl-PCL-*b*-(di-Boc-L-lysine)$_{G2}$ (**7**). The spectrum was recorded in $CDCl_3$.

dendritic wedge and triazol ring (**h**) emerged (Fig. 2). The signals assigned to the alkene moiety were observed at 5.00 ppm and 5.80 ppm (**p** and **o**). The integrals of the resonances from the alkene end-group (5.80 ppm, **o**) and CH_2NHBoc (2.93–3.22 ppm, **c**) were in good agreement with the theoretical values.

The MALDI-TOF analysis produced a spectrum with the signal spacing of approximately 114 Da (Fig. 3), corresponding to the molecular weight of one repeating unit in the PCL chain. Two series were observed: one fitting the experimental molecular weight of the alkenyl-PCL-*b*-(di-Boc-L-lysine)$_{G2}$ (**6**) as the M-Na^+-series, while the other minor series being assignable to the M-Li^+-series with the loss of two of the Boc groups during the ionization process.

The cholesteryl moiety was introduced *via* the thiol-ene "click" reaction between the alkenyl-PCL-*b*-(di-Boc-L-lysine)$_{G2}$ and thiocholesterol (Scheme 2). The solution of **6**, thiocholesterol, and DMPA (1 : 10 : 3.5 molar ratio) in toluene was stirred and irridiated at 365 nm in the presence of oxygen. Large excess of the thiol and the photoinitiator were taken to overcome the obstacles posed by rigid structure and hindered mobility of thiocholesterol,[23] and to achieve near to quantitative functionalization as concluded after investigations by NMR and MALDI-TOF. In the ^{1}H NMR spectrum (Fig. 4) the signals from the alkene chain end disappeared completely, and the resonances originating from the cholesteryl moiety (**q**, **r**, and **s**) could be observed. The MALDI-TOF analysis revealed the

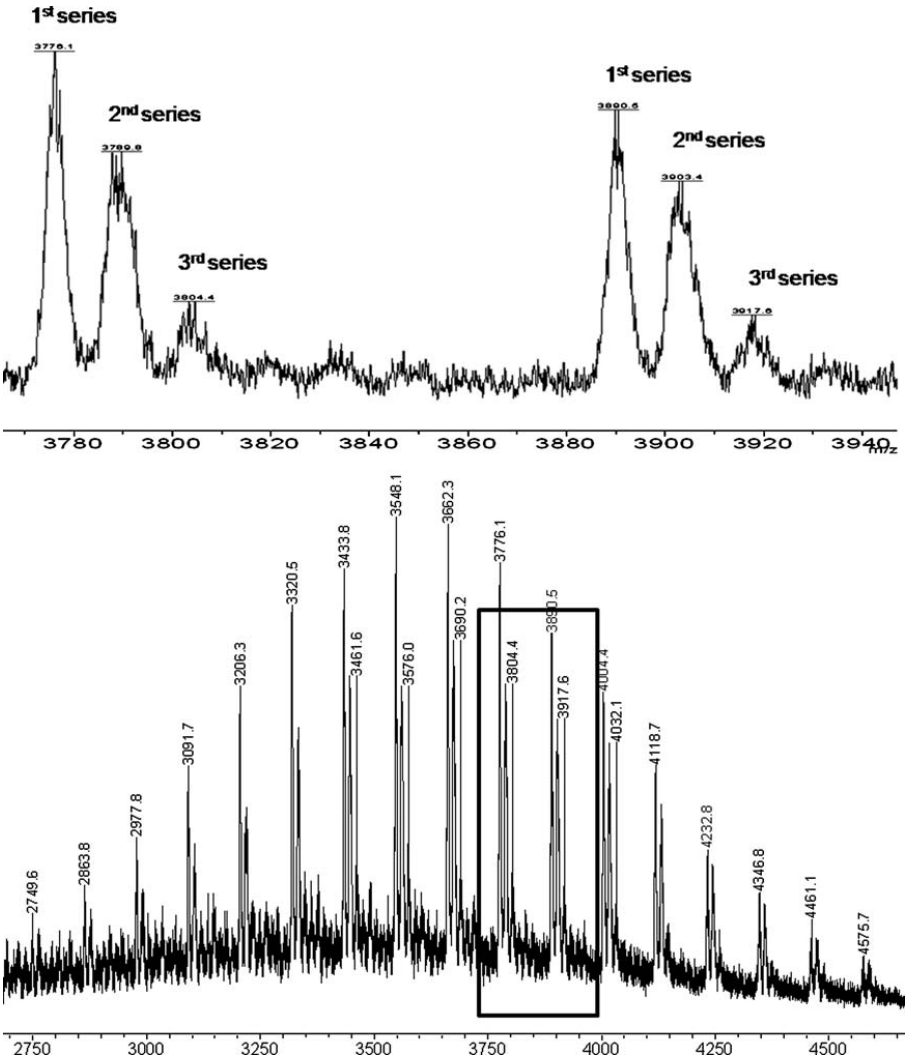

Fig. 5 MALDI-TOF spectrum of Cholesteryl-PCL-*b*-(di-Boc-L-lysine)$_{G2}$ (**7**), bottom: full spectrum; top: expansion of the indicated region.

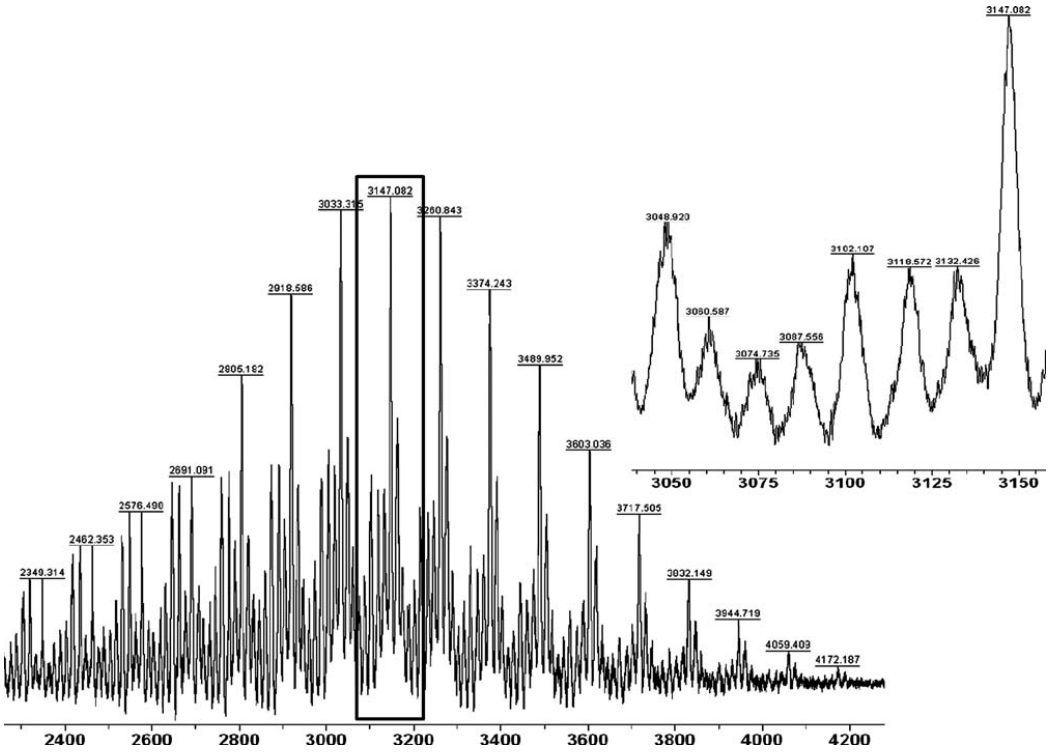

Fig. 6 MALDI-TOF spectrum of Cholesteryl-PCL-*b*-(L-lysine)$_{G2}$ (**8**).

species of the molecular weight that correspond to **7** (Fig. 5). The signal spacing of 114 Da indicative of the repeating unit of the PCL was again observed. In total, three series were observed as M–Na+-adducts with the main series being the M–Na+-series of **7**, while the other two series indicated again the loss of either one or two Boc moieties (Fig. S7†).

However, the SEC trace had a small shoulder (Fig. 1), though PDI was still fairly low (1.15). The appearance of the shoulder could tentatively be ascribed to the intramolecular side reactions of radical nature that could take place during the thiol-ene "click" reaction.

The final step involved deblocking of the amine functionalities. **7** was treated with TFA in CH_2Cl_2. The solvent and the excess of the acid were removed *in vacuo*, and the product was analyzed by NMR and MALDI-TOF. In ^{1}H NMR spectrum (Fig. S3†) the signal corresponding to *tert*-butyl group was not observed, while the broad peaks related to the free amine groups were detected at 8.30–8.80 ppm and 7.65–8.05 ppm. The triazole proton resonated at 7.94 ppm. Such a dramatic shift could be explained by the cardinal changes in solubility of the macromolecule (the spectrum was recorded in DMSO-d_6). MALDI-TOF mass spectrometry showed several series, proving the final structure with sequential loss of the trifluoroacetate moieties during the ionization process (Fig. 6, S8–S12†).

Thus, a series of peaks with loss of trifluoroacetate moieties was detected by simulation of the isotope pattern of the respective peaks and subsequent comparison with the measured (relatively broad) mass peaks. In addition, fragments with truncated structures stemming from the relatively hard ionization conditions and the reflectron-modus were also detected. However, in accordance with the NMR data, the formation of the structure of **8** was unambiguously proved by MALDI-TOF mass spectrometry as well.

Conclusions

In conclusion, we have demonstrated the effectiveness and flexibility of the orthogonal azide-alkyne and thiol-ene "click" reactions in preparation of the linear-dendritic cholesteryl-PCL-*b*-(L-lysine)$_{G2}$. The "click" reactions considerably shorten the synthetic cascade for building such macromolecules compared to the conventional esterification reactions. Moreover, the versatility of the heterofunctional PCL in combination with these orthogonal "click" reactions provides greater degree of freedom for incorporation of different structural elements, and thus opens new avenues to much larger library of complex amphiphilic architectures.

Notes and references

1 I. Gitsov, *J. Polym. Sci., Part A: Polym. Chem.*, 2008, **46**, 5295.
2 A. Würsch, M. Möller, T. Glauser, L. S. Lim, S. B. Voytek, J. L. Hedrick, C. W. Frank and J. G. Hilborn, *Macromolecules*, 2001, **34**, 6601.

3 H. Ihre, O. L. Padilla De Jesús and J. M. J. Fréchet, *J. Am. Chem. Soc.*, 2001, **123**, 5908.
4 E. R. Gillies, T. B. Jonsson and J. M. J. Fréchet, *J. Am. Chem. Soc.*, 2004, **126**, 11936.
5 C. R. DeMattei, B. Huang and D. A. Tomalia, *Nano Lett.*, 2004, **4**, 771.
6 Y. Li, Q. Li, F. Li, H. Zhang, L. Jia, J. Yu, Q. Fang and A. Cao, *Biomacromolecules*, 2006, **7**, 224.
7 E. R. Zubarev and S. I. Stupp, *J. Am. Chem. Soc.*, 2002, **124**, 5762.
8 L. Tian and P. T. Hammond, *Chem. Mater.*, 2006, **18**, 3976.
9 H.-A. Klok, J. J. Hwang, J. D. Hartgerink and S. I. Stupp, *Macromolecules*, 2002, **35**, 6101.
10 (*a*) V. V. Rostovtsev, L. G. Green, V. V. Fokin and K. B. Sharpless, *Angew. Chem., Int. Ed.*, 2002, **41**, 2596; (*b*) C. W. Tornøe, C. Christensen and M. Meldal, *J. Org. Chem.*, 2002, **67**, 3057.
11 K. L. Killops, L. M. Campos and C. J. Hawker, *J. Am. Chem. Soc.*, 2008, **130**, 5062.
12 (*a*) W. H. Binder and R. Sachsenhofer, *Macromol. Rapid Commun.*, 2008, **29**, 952; (*b*) R. K. Iha, K. L. Wooley, A. M. Nyström, D. J. Burke, M. J. Kade and C. J. Hawker, *Chem. Rev.*, 2009, **109**, 5620.
13 P. Wu, M. Malkoch, J. N. Hunt, R. Vestberg, E. Kaltgrad, M. G. Finn, V. V. Fokin, K. B. Sharpless and C. J. Hawker, *Chem. Commun.*, 2005, 5775.
14 B. Helms, J. L. Mynar, C. J. Hawker and J. M. J. Fréchet, *J. Am. Chem. Soc.*, 2004, **126**, 15020.
15 (*a*) C. Hua, S.-M. Peng and C.-M. Dong, *Macromolecules*, 2008, **41**, 6686; (*b*) J. del Barrio, L. Oriol, R. Alcalá and C. Sánchez, *Macromolecules*, 2009, **42**, 5752.
16 L. M. Campos, K. L. Killops, R. Sakai, J. M. J. Paulusse, D. Damiron, E. Drockenmuller, B. W. Messmore and C. J. Hawker, *Macromolecules*, 2008, **41**, 7063.
17 L. Nurmi, J. Lindqvist, R. Randev, J. Syrett and D. M. Haddleton, *Chem. Commun.*, 2009, 2727.
18 C. A. DeForest, B. D. Polizzotti and K. S. Anseth, *Nat. Mater.*, 2009, **8**, 659.
19 P. Agrawal, U. Gupta and N. K. Jain, *Biomaterials*, 2007, **28**, 3349.
20 I. Javakhishvili and S. Hvilsted, *Biomacromolecules*, 2009, **10**, 74.
21 R. Hoogenboom, B. C. Moore and U. S. Schubert, *Chem. Commun.*, 2006, 4010.
22 R. Riva, S. Schmeits, F. Stoffelbach, C. Jérôme, R. Jérôme and Ph. Lecomte, *Chem. Commun.*, 2005, 5334.
23 N. ten Brummelhuis, C. Diehl and H. Schlaad, *Macromolecules*, 2008, **41**, 9946.

Supporting Information

Facile synthesis of linear-dendritic cholesteryl-poly(ε-caprolactone)-*b*-(L-lysine)$_{G2}$ by thiol-ene and azide-alkyne "click" reactions

Irakli Javakhishvili,[a] Wolfgang H. Binder,[b] Susanne Tanner[b] and Søren Hvilsted*[a]

[a] *Technical University of Denmark, Department of Chemical and Biochemical Engineering, Danish Polymer Centre, Building 423, DK-2800 Kgs. Lyngby, Denmark. Tel: +45 4525 2965. E-mail: sh@kt.dtu.dk*

[b] *Martin-Luther University Halle-Wittenberg, Faculty of Natural Sciences II / Institute of Chemistry, Lehrstuhl Makromolekulare Chemie, von Danckelmannplatz 4, D-06120 Halle (Saale), Germany; Tel: +49 (0) 345 55 25930.*

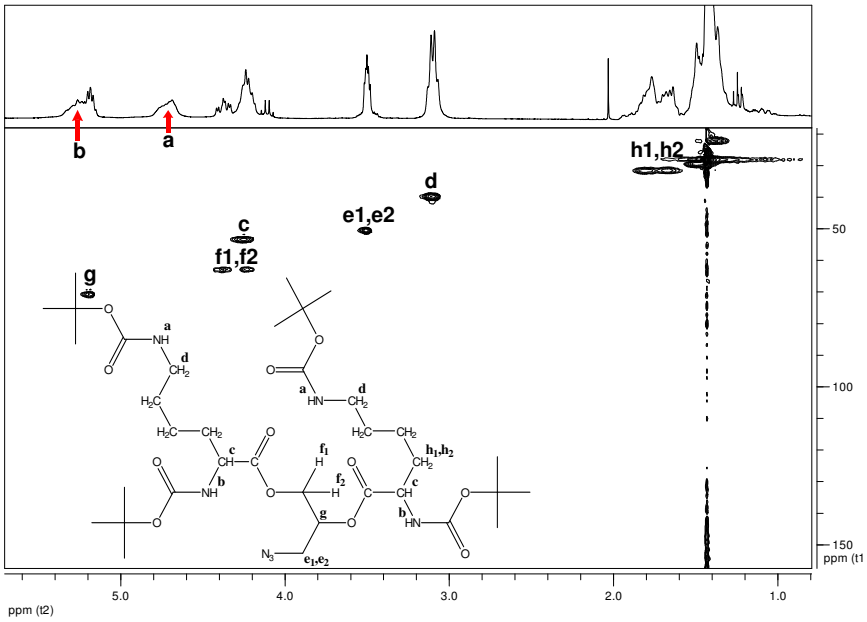

Fig. S1 ^{1}H and HSQC NMR spectra of **3**

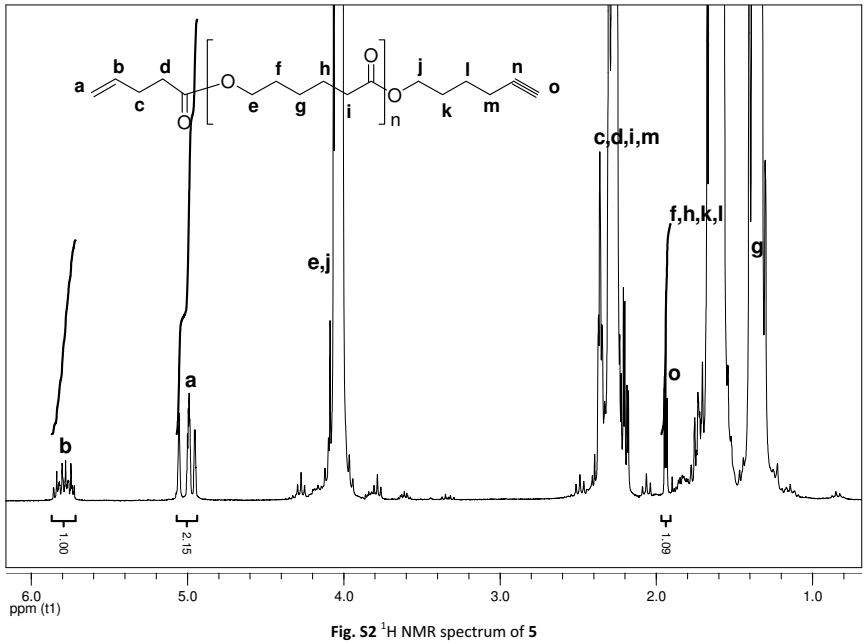

Fig. S2 ^{1}H NMR spectrum of **5**

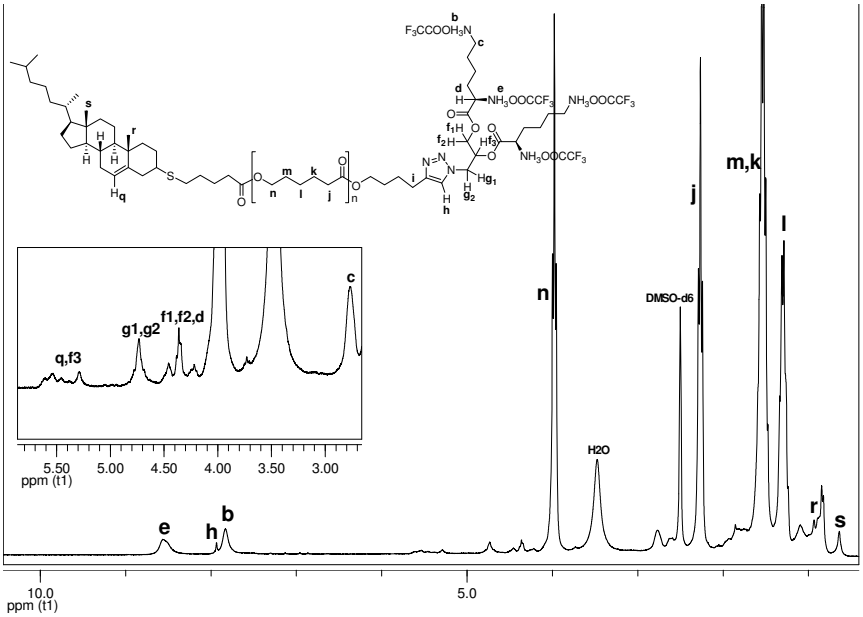

Fig. S3 ^{1}H NMR spectrum of **8**

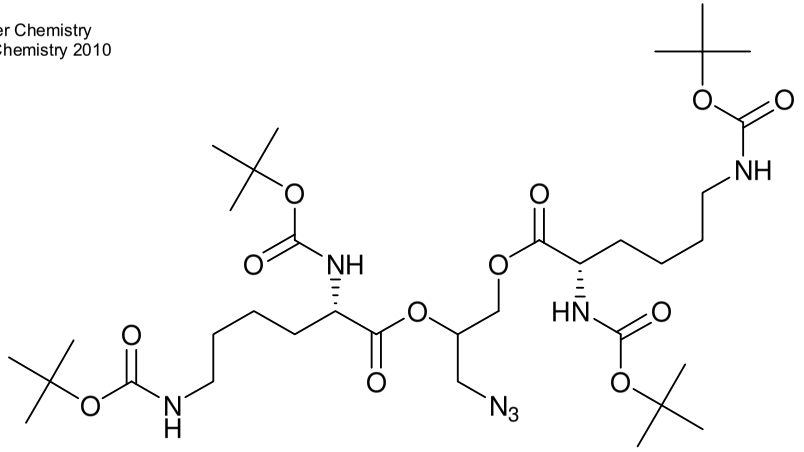

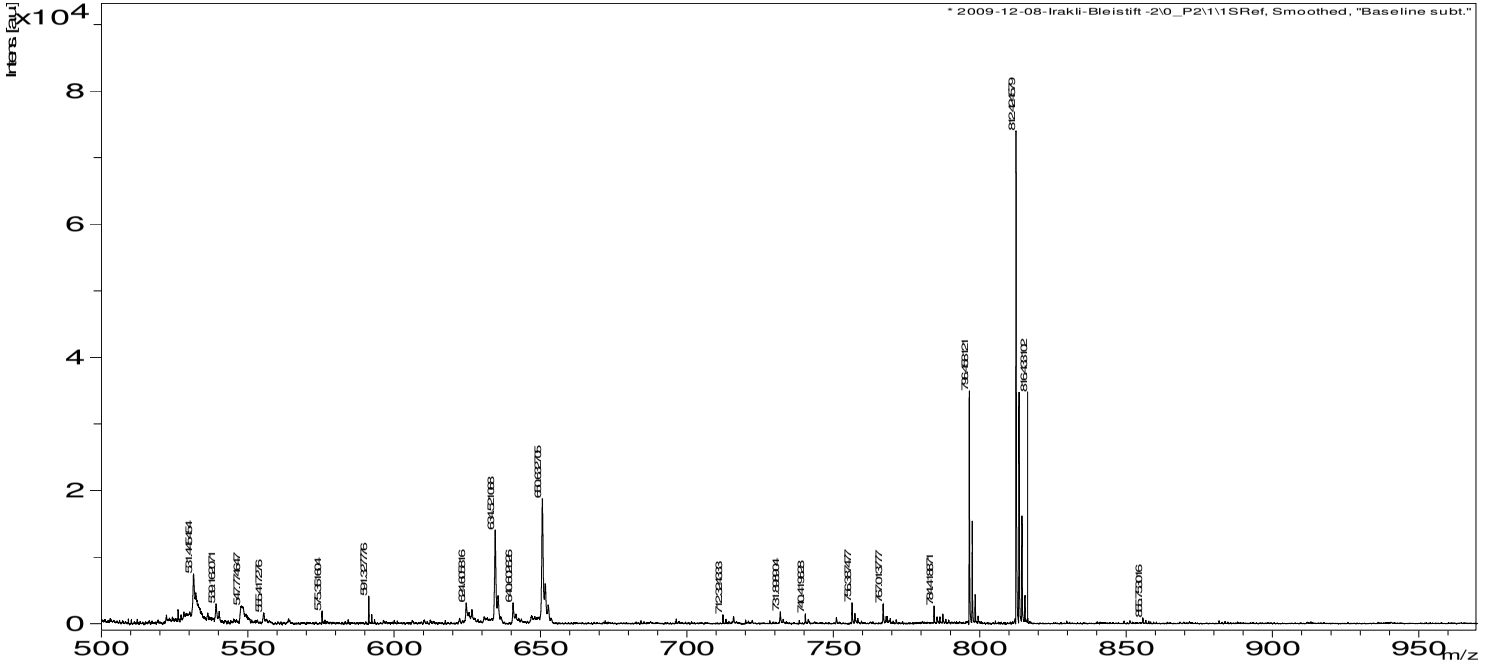

Fig. S4 MALDI-TOF of **3**

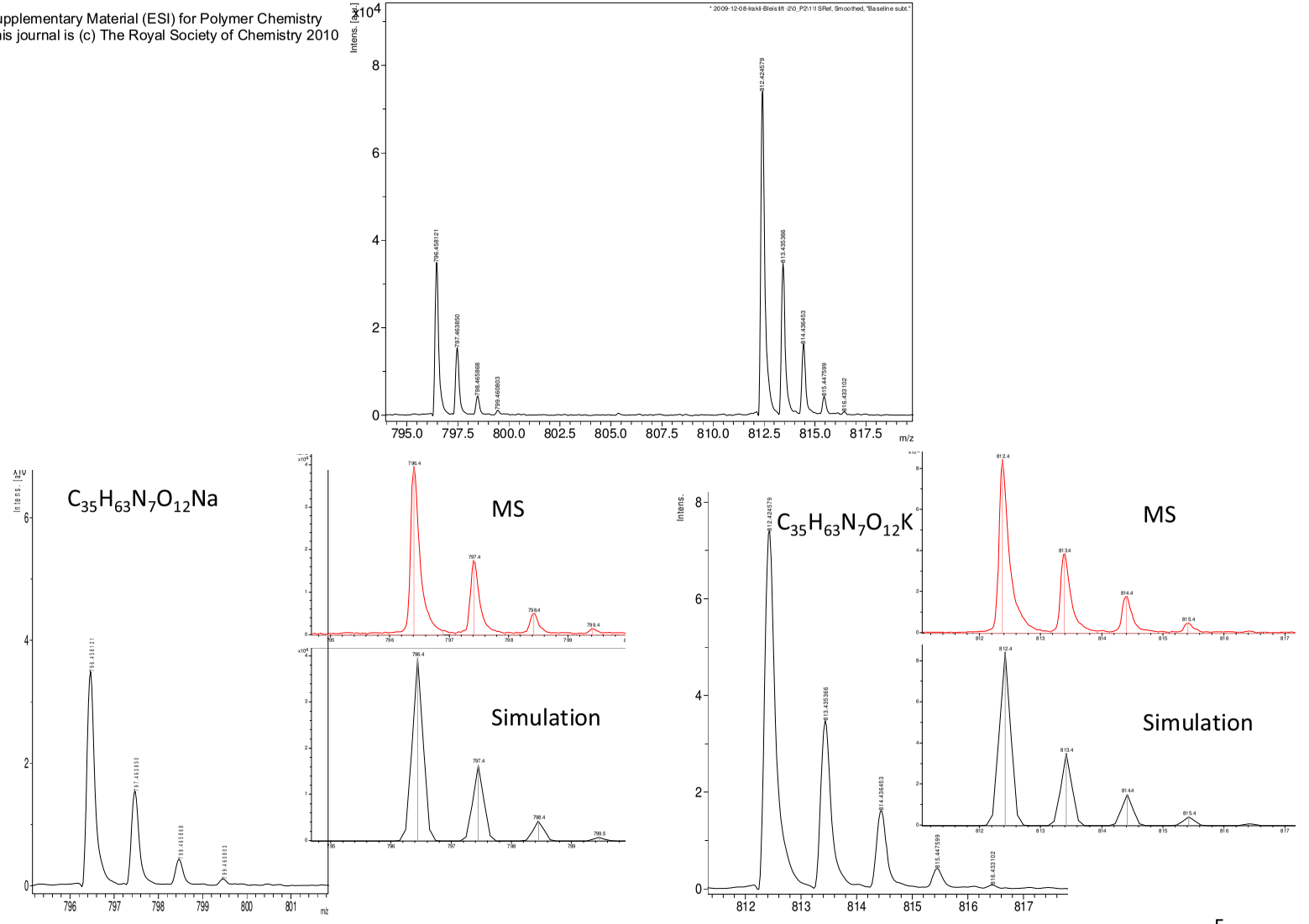

Fig. S5 Data of MALDI-TOF and isotopic pattern simulation of the compound **3**

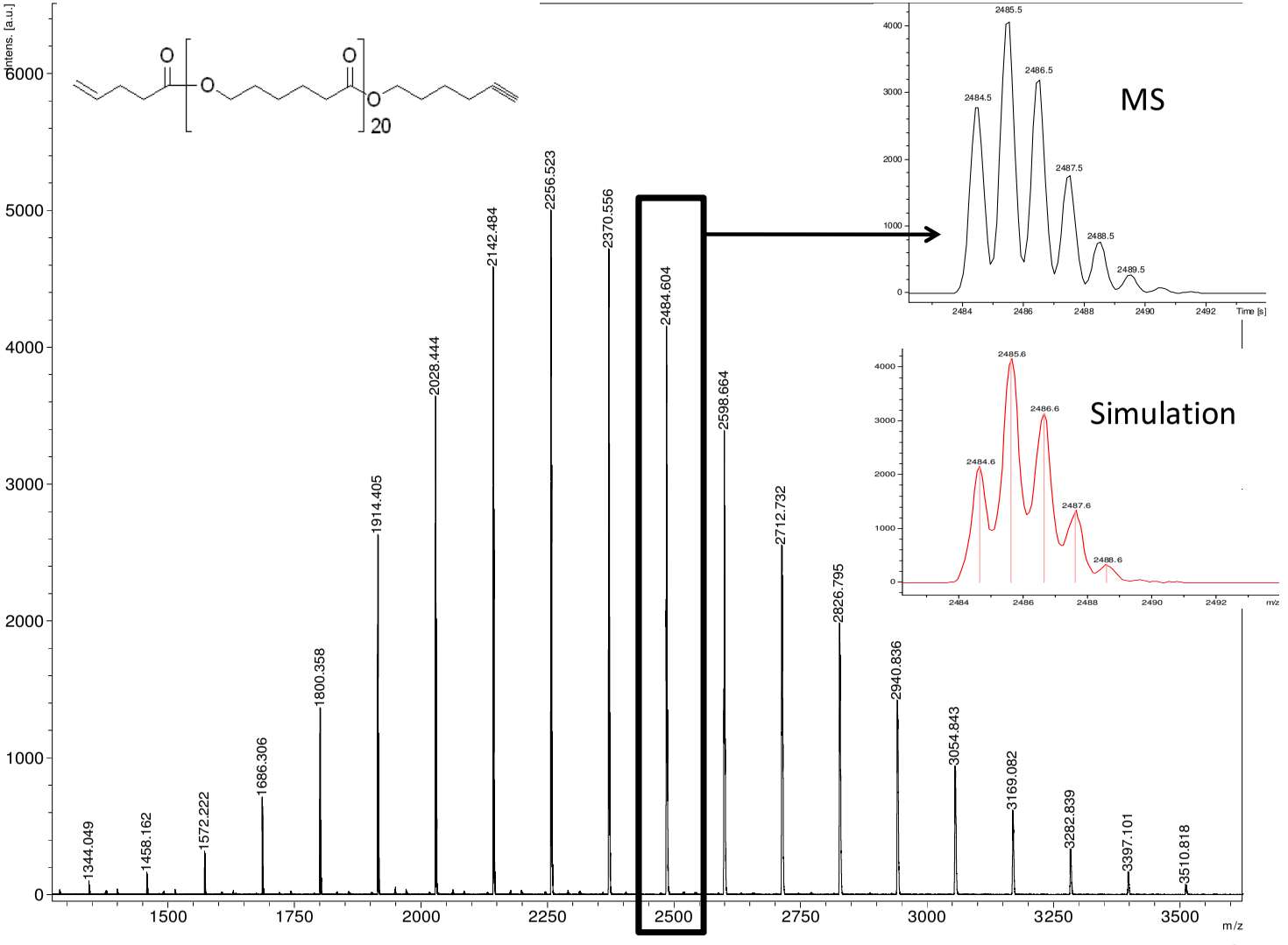

Fig. S6 MALDI-TOF of **5**

MS, 1st series
(found : 3889.96)

Simulation, 1st series
Simulated : 3889.3680
For n = 22
$C_{32}H_{52}O(C_6H_{10}O_2)_{n=22}C_{41}H_{72}O_{13}N_7Na$

MS, 2nd series
(found : 3902.8)

Simulation, 2nd series
Simulated : 3903.401
For n = 23 –minus 1x(Boc)
$C_{32}H_{52}O(C_6H_{10}O_2)_{n=23}C_{36}H_{64}O_{11}N_7Na$

MS, 3rd series
(found : 3917.3)

Simulation, 3rd series
Simulated : 3917.4173
For n = 24 –minus 2x(Boc)
$C_{32}H_{52}O(C_6H_{10}O_2)_{n=24}C_{31}H_{56}O_9N_7Na$

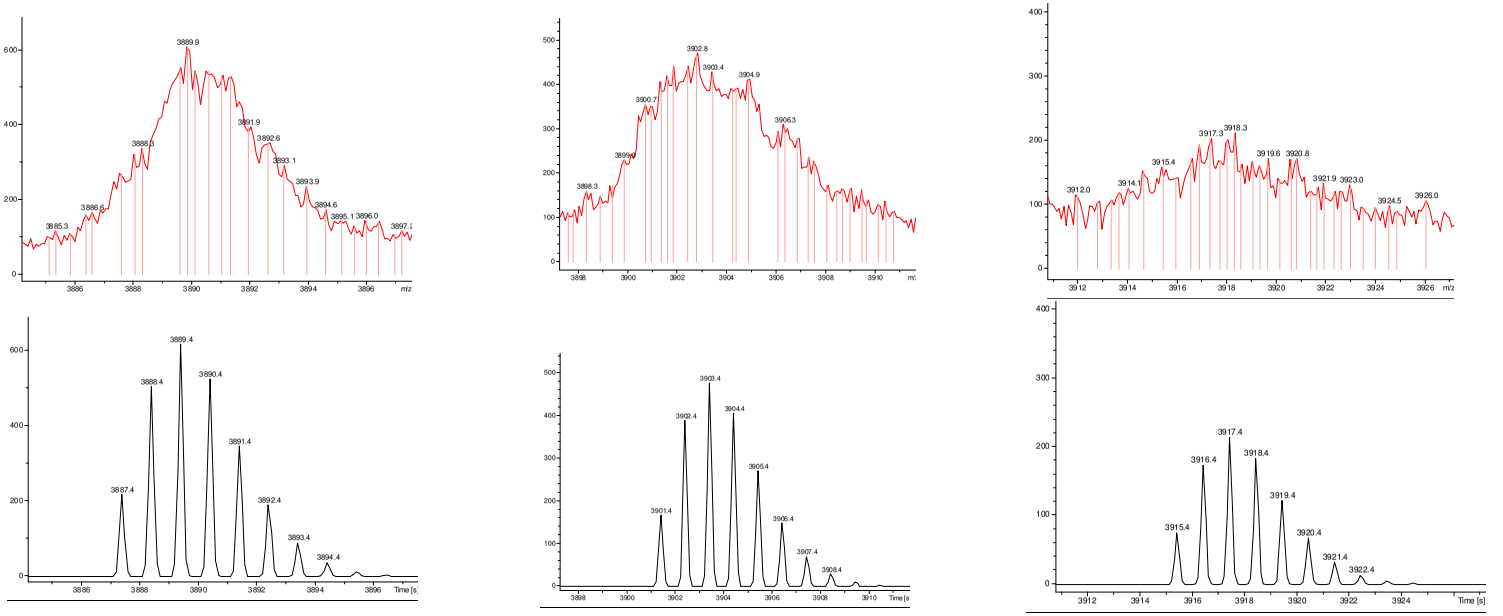

Fig. S7 Data of MALDI-TOF (top) and isotopic pattern simulation (bottom) of the compound **7**

MS, 1st series
(found : 3147.082)

Simulation, 1st series
Simulated : 3146.7
For n = 15
$C_{32}H_{53}OS(C_6H_{10}O_2)_{n=15}C_{29}H_{44}O_{13}N_7F_{12}Na$

MS, 1st series
(found : 3147.082)

Simulation, 1st series
Simulated : 3146.8
For n = 16 –minus 1x(TFA)
$C_{32}H_{53}OS(C_6H_{10}O_2)_{n=16}C_{27}H_{43}O_{11}N_7F_9Na$

MS, 1st series
(found : 3147.082)

Simulation, 1st series
Simulated : 3146.9
For n = 18 –minus 3x(TFA)
$C_{32}H_{53}OS(C_6H_{10}O_2)_{n=18}C_{23}H_{41}O_7N_7F_3Na$

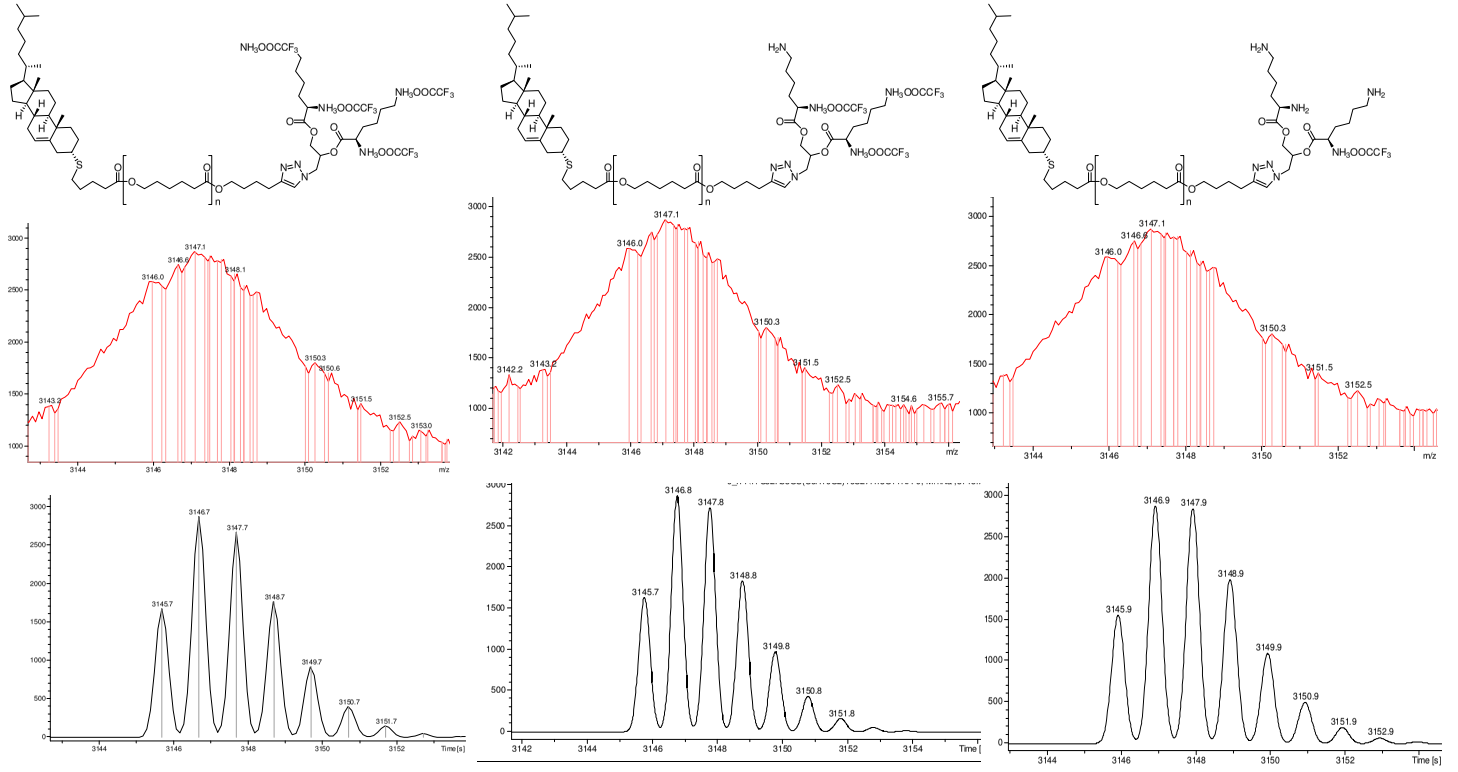

Fig. S8 Data of MALDI-TOF (top) and isotopic pattern simulation (bottom) of the compound **8**

MS, 2nd series
(found : 3132.426)

Simulation, 2nd series
Simulated : 3131.0
For n = 19 –minus 4x(TFA)

$C_{32}H_{53}OS(C_6H_{10}O_2)_{n=19}C_{21}H_{40}O_5N_7Li$

MS, 2nd series
(found : 3132.426)

Simulation, 2nd series
Simulated :3130.7
For n = 15

$C_{32}H_{53}OS(C_6H_{10}O_2)_{n=15}C_{29}H_{44}O_{13}N_7F_{12}Li$

MS, 2nd series
(found : 3132.426)

Simulation, 2nd series
Simulated : 3131.0
For n = 25

$(C_6H_{11}O_2)_{n=25}C_9H_{16}O_3N_3K$

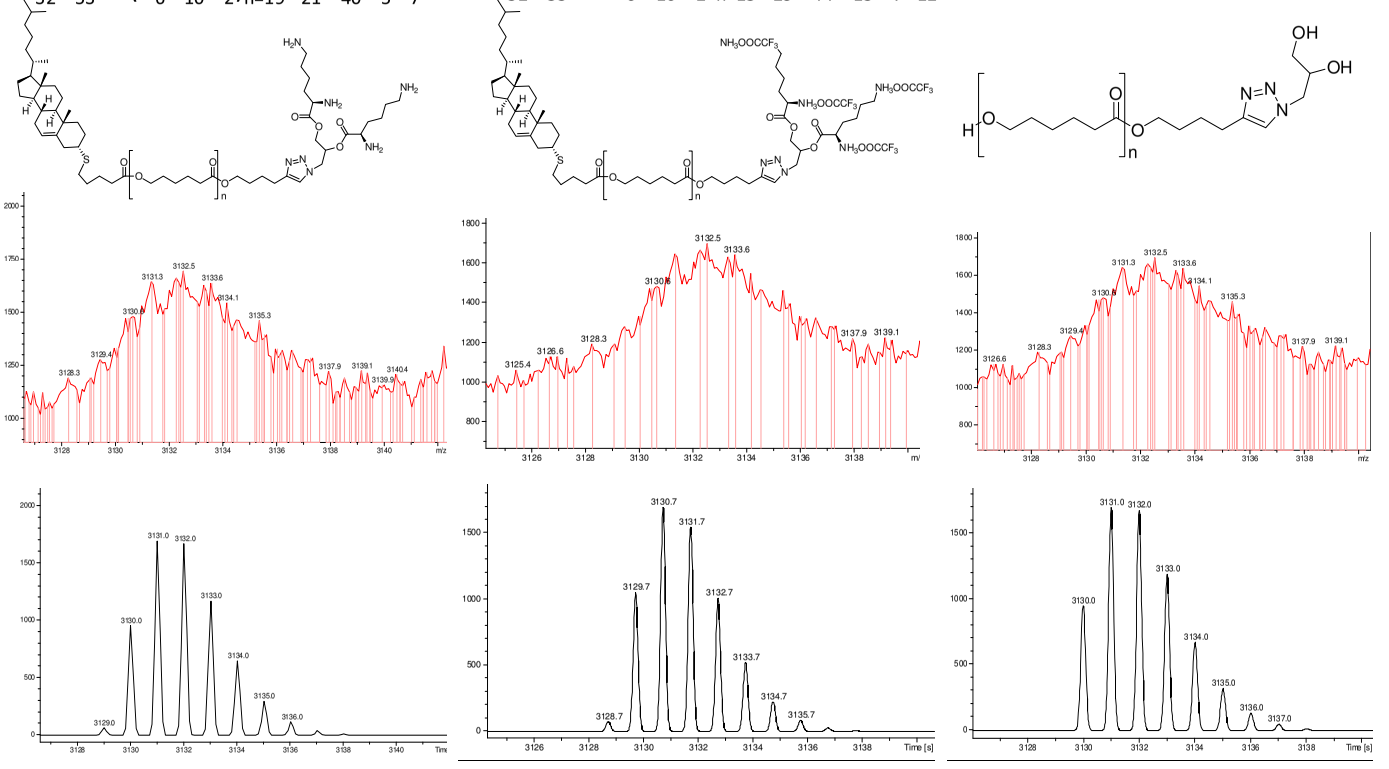

Fig. S9 Data of MALDI-TOF (top) and isotopic pattern simulation (bottom) of the compound **8**

MS, 3rd series
(found : 3118.572)

Simulation, 3rd series
Simulated :
For n = 21 –minus 2x(TFA)
$(C_6H_{11}O_2)_{n=21}C_{25}H_{42}F_6O_9N_7H$

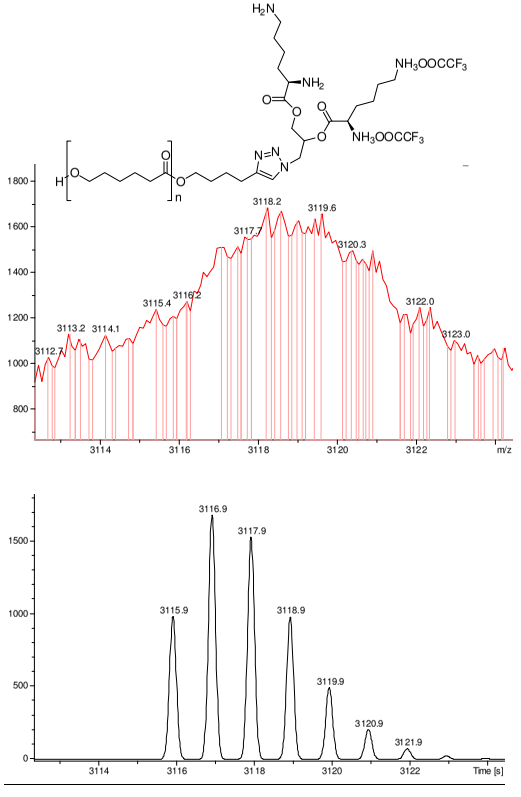

MS, 4th series
(found : 3102.107)

Simulation, 4th series
Simulated : 3102.9
For n = 21
$C_{32}H_{53}OS(C_6H_{10}O_2)_{n=21}C_9H_{16}N_3O_3Li$

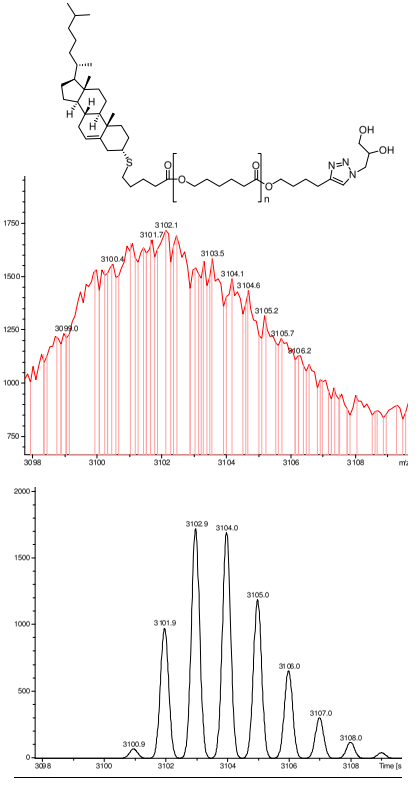

Fig. S10 Data of MALDI-TOF (top) and isotopic pattern simulation (bottom) of the compound **8**

MS, 5th series
(found : 3087.556)

Simulation, 5th series
Simulated : 3086.6
For n = 19 –minus 1x(TFA)-minus (Chol+Thiol)
$C_5H_7O(C_6H_{10}O_2)_{n=19}C_{27}H_{43}O_{11}N_7F_9Na$

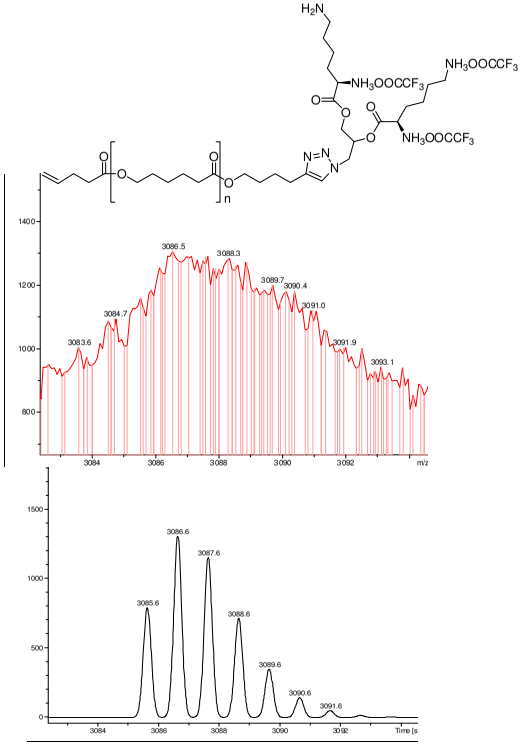

MS, 5th series
(found : 3087.556)

Simulation, 5th series
Simulated : 3086.6
For n = 15 –minus 1x(TFA)
$C_{32}H_{53}OS(C_6H_{10}O_2)_{n=15}C_{27}H_{42}O_{11}N_7F_9K_2$

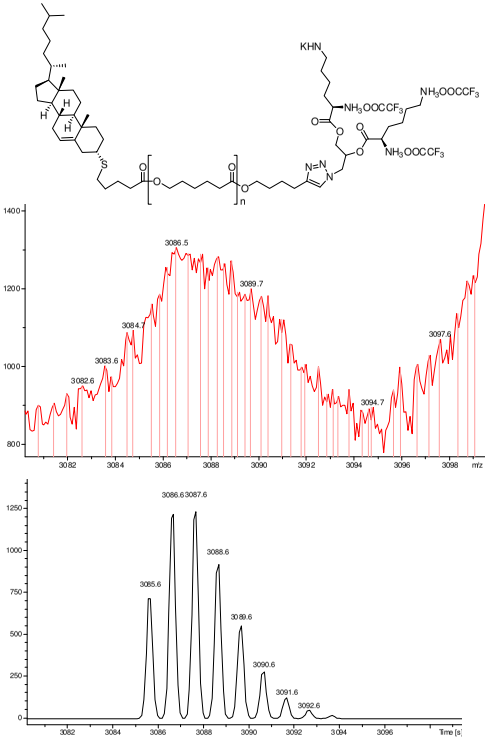

Fig. S11 Data of MALDI-TOF (top) and isotopic pattern simulation (bottom) of the compound **8**

MS, 7th series
(found : 3060.587)

Simulation, 7th series
Simulated : 3058.8
For n = 24
$C_5H_7O(C_6H_{10}O_2)_{n=24}C_9H_{16}N_3O_3Na$

MS, 8th series
(found : 3048.920)

Simulation, 8th series
Simulated : 3048.7
For n = 15 $(M-K)^+$
$C_{32}H_{53}OS(C_6H_{10}O_2)_{n=15}C_{27}H_{43}O_{11}N_7F_9K$

MS, 8th series
(found : 3048.920)

Simulation, 8th series
Simulated : 3048.0
For n = 22 –minus 4x(TFA)
$(C_6H_{11}O_2)_{n=22}C_{21}H_{39}O_5N_7Na_2$

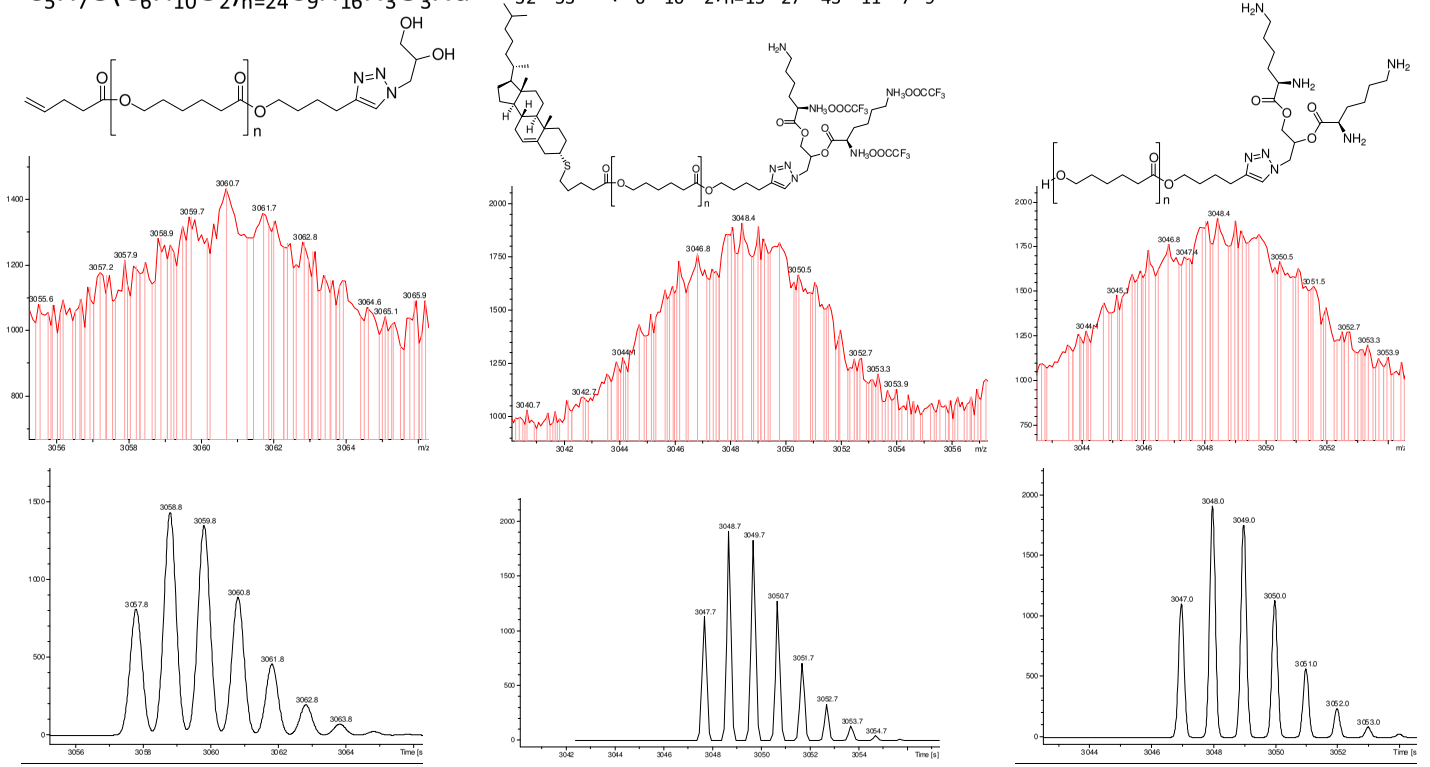

Fig. S12 Data of MALDI-TOF (top) and isotopic pattern simulation (bottom) of the compound **8**

Appendix IV

Javakhishvili, I.; Hvilsted, S. Miktoarm Core-crosslinked Star Copolymers with Biologically Active Moieties on Peripheries. *Polym. Chem*. 2010, *1*, 1650-1661 – Reproduced by permission of the Royal Society of Chemistry.

Miktoarm core-crosslinked star copolymers with biologically active moieties on peripheries

Irakli Javakhishvili and Søren Hvilsted*

Received 21st July 2010, Accepted 10th August 2010
DOI: 10.1039/c0py00226g

Miktoarm core-crosslinked star (CCS) copolymers featuring hydrophobic inner compartment based on poly(ε-caprolactone) (PCL), and hydrophilic multivalent exterior consisting of L-lysine dendritic wedges and estradiol or ferrocene moieties have been synthesized. Ring-opening polymerization (ROP) of ε-caprolactone (ε-CL) initiated by functional alcohols provides alkyne or azide end-capped linear PCL chains. Further derivatization of the hydroxyl chain ends of these hetero-telechelic macromolecules by methacrylic acid (MA), and subsequent Cu(I) mediated "click" coupling of terminal alkyne and azide groups with azide-functionalized dendritic wedge, 17α-ethynylestradiol and ethynylferrocene afford well-defined linear-dendritic and linear macromonomers (MMs), respectively. Atom transfer radical polymerization (ATRP) of the MMs together with a difunctional monomer 1,4-butanediol dimethacrylate (BDMA) results in miktoarm CCS copolymers. Elucidation of the structure and composition of the intermediate and final products demonstrates effectiveness, versatility, and high degree of control displayed by the proposed synthetic sequence.

Introduction

Unique globular shape, sophisticated macromolecular architecture providing core-shell microenvironment, and plethora of reactive functional groups of CCS polymers have bolstered their potential in myriads of applications ranging from polymer therapeutics and catalysis to membrane technology and lithography.[1,2] Synthesis of CCS polymers by ATRP involves exploitation of macroinitiators (MIs) and/or MMs in combination with difunctional cross-linkers.[1] Matyjaszewski and co-workers have prepared CCS polymer employing polystyrene (PS) MI and divinyl benzene (DVB) cross-linker.[3] The authors pointed out that the method suffers from the consequences of inevitable radical termination reactions in the radical polymerization which results in partially functionalized MIs. Employing similar approach, Matyjaszewski and co-workers have designed surface functionalized CCS polymers based on poly(*tert*-butyl acrylate) MIs. Epoxy, cyano, hydroxyl, and amino groups have been incorporated at the end of the MI *via* functional ATRP initiators.[4] While homoarm star polymers contain arms with similar molecular weight and same chemical composition, miktoarm stars are comprised of arms with diverse chemical compositions and/or molecular weights.[1] Miktoarm CCS copolymer with degradable core have been synthesized *via* "in-out" method: poly(methyl methacrylate) (PMMA) MI has been reacted with the cross-linker containing degradable disulfide moiety, and thus obtained CCS polymer has been exploited as MI in subsequent ATRP of n-butyl acrylate (BA).[5] Grafting the second monomer through the reactivation of the alkyl halide sites in the core of the star polymer features several obstacles such as star-star and intrastar couplings that broaden the molecular weight distribution (MWD), and low initiation efficiency of the star MI.[5] Star polymers with hydrolysable cores prepared *via* group transfer polymerization of MMA have also been reported.[6]

A characteristic trait of the star synthesis by cross-linking MI chains is star-star coupling reaction that takes place throughout the star formation process and broadens MWD.[7] Star-star reaction occurs between the star cores where the number of initiating sites equals to the number of arms per star. Therefore, reduction of the ratio of initiating sites to arms per star could diminish the star-star coupling providing better control and improved consistency.[7] In the quest of alleviating this intrinsic shortcoming, Matyjaszewski and co-workers have proposed preparation of CCS polymers by copolymerization of linear MM with cross-linker using low molecular weight ATRP initiator.[7] Under these circumstances the number of initiating sites and arms are independently controlled allowing limiting of star-star coupling reactions resulting in narrow MWD. Employing this strategy, miktoarm star copolymers incorporating PBA and poly(ethylene glycol) (PEG) MMs have been prepared.[8] Star congestion and obstruction of the initiating sites can be overpowered by addition of another portion of cross-linker and initiator. Thus, high yield and low polydispersity have been attained by stepwise addition of the cross-linker and initiator during cross-linking the mixture of the MMs.[8]

Miktoarm CCS copolymer bearing biocompatible PCL and PS arms have been developed.[9] PCL MI possessing bromoisobutyryl end group has been reacted with DVB giving CCS polymer with relatively broad MWD ($M_w/M_n > 2$). PS arms have then been grown from the star PCL MI by ATRP of styrene. Besides controlled radical polymerization methods such as ATRP, ROP has also been exercised for preparation of CCS PCL.[10] ROP of ε-CL affords MI for the ensuing cross-linking reaction *via* ROP of bislactone. This is a two-step one-pot

Technical University of Denmark, Department of Chemical and Biochemical Engineering, Danish Polymer Centre, Building 227, DK-2800 Kgs. Lyngby, Denmark. E-mail: sh@kt.dtu.dk; Tel: +45 4525 2965

approach which does not demand isolation and purification of the MI. However, adventitious water may produce α,ω-difunctional arms and facilitate star-star coupling leading to macrogelation.[10] Wiltshire and Qiao have designed a range of degradable CCS polymers featuring core-degradable, arm-degradable, partially arm-degradable, and fully degradable stars.[11] Dual initiator 2-hydroxyethyl 2-bromoisobutyrate has been used to prepare degradable PCL and nondegradable PS arms. Cross-linking of the mixture of PCL-Br and PMMA-Cl MIs provides partially degradable stars. Degradable core is formed by ROP of bislactone cross-linker, while DVB and ethylene glycol dimethacrylate (EGDMA) are employed in ATRP from the MI when nondegradable cores are desired.[11] Since tuning coronal composition of CCS polymers is the handle for manipulating the physical properties of the stars, ways for tailoring the corona have been suggested.[12] CCS polymers with degradable outer coronal layer, with initiating sites on the coronal surface, and with initiating groups in the core as well as on the peripheries have been prepared making use of the PCL building blocks amongst others.[12]

Hawker and co-workers have reported synthesis of CCS polymers with amine and hydroxyl surface functional groups employing functional initiators for nitroxide-mediated living free radical polymerization. The potential of star stabilized Pd nanoparticles in catalysis has also been demonstrated by exploiting them in hydrogenation and Heck reactions.[13] Linear-dendritic MIs, carrying Fréchet type or polyester dendrons, have been utilized for preparation of CCS with dendron-decorated peripheries.[14,15] Modification of the dendron functionalities results in dramatic changes in the morphologies produced by the star polymers.[15]

Potential application of star polymers in drug delivery stems from the inherent thermodynamic instability of classical amphiphilic copolymer micelles. The formation of classical micelles is thermodynamically favored only above critical micelle concentration (cmc). If the concentration of the copolymer drops below the cmc, the micelles tend to disassemble. Inasmuch as the delivery vehicle undergoes severe dilution upon injection into an animal or human, lysis of the micelles below the cmc impedes their application *in vivo*.[16] Dendrimers, star and CCS polymers, which may serve as unimolecular reservoirs, may be the remedy in circumventing the problems posed by micelle disintegration upon dilution.[16] Roovers and co-workers have prepared amphiphilic star polymer based on polyamidoamine dendritic core, which served as the macroinitiator for obtaining lipophilic PCL inner block, and hydrophilic PEG outer block. Thus, the arms of the star polymer are built by biocompatible and biodegradable blocks. The potential in encapsulation of hydrophobic anticancer drug etoposide has been demonstrated.[16] Besides high and controllable drug loading and release capabilities, biocompatibility, and the capacity to compartmentalize various drugs, the polymeric micelles offer a handle for passive targeting due to enhanced permeability and retention (EPR) effect in tumors.[17] By taking advantage of EPR effect highly selective delivery of the anticancer drugs can be attained.[17] Core-crosslinked micelles as unimolecular containers offer all the above mentioned benefits of classical micelles, and provide bonus in terms of enhanced stability in biological fluids.[17] Kissel and co-workers prepared core-crosslinked micelles by crosslinking di- and triblock copolymers PEG-*b*-PCL and PEG-*b*-PCL-*b*-PEG which incorporated a maleic acid residue at the end of PCL block.[17] These micelles have been successfully loaded with anticancer drug paclitaxel. Core-crosslinked micelles have displayed higher loading capacity than the classical ones.[17]

Alongside passive targeting, delivery of drugs involving a specific molecular recognition plays an important role.[18] Gadolinium based MRI contrast agent incorporating selective estrogen receptor modulator (SERM) which binds to the estrogen receptor (ER) with high affinity, and induces contrast enhancement in human breast cancer cells has been proposed.[18] 17β-Estradiol (E_2) is the most potent estrogen that enters freely the cell and binds to nuclear estrogen receptors. Modification of E_2 by introducing bulky substituents at the 17α position does not deteriorate its high affinity to ER.[18] Thus, coupling of 17α-ethynylestradiol with suitable chelate for gadolinium affords ER targeting contrast agent.[18] Since binding of E_2 to ER results in conformational change initiating the transcription of various genes commonly upregulated in cancerous cells, ER are overexpressed in 75–80% of all breast cancers.[19] ERs are located both intracellularly and on the cell membrane; antiestrogen compound tamoxifen competitively binds ER, and averts the recruitment of transcription cofactors.[19] Gold nanoparticles decorated with tamoxifen-PEG-SH derivative have been synthesized in the attempt to enhance potency and selective intracellular delivery. The study suggests that the membrane localized ER may assist selective particle uptake.[19]

Kostarelos and co-workers have reported tumor growth delay by sixth generation cationic poly-L-lysine dendrimer (G_6PLL).[20] This has been ascribed to the systemic antiangiogenic activity of G_6PLL. It has been shown that G_6PLL, which possesses 64 peripheral amino groups, has the ability to accumulate and remain at the tumor site as the result of strong electrostatic interactions between the positively charged PLL dendrimer surface and the negatively charged, heparin-rich walls of the tumor neovasculature.[20] The authors suggest that conjugation of these dendrimers with other therapeutic and diagnostic agents may provide a powerful tool in cancer therapy.[20]

In this paper, we describe the synthetic outline and structural characterization of PCL miktoarm CCS copolymers bearing multiple amine functional groups and targeting motifs on the periphery. The miktoarm CCS copolymers have been obtained through MM approach exploiting linear-dendritic (di-Boc-L-lysine)$_{G2}$-*b*-PCL-methacrylate and linear E_2-PCL-methacrylate or ferrocene-PCL-methacrylate. Synthesis of the MMs is the combination of ROP of ε-CL from a functional initiator, Mitsunobu coupling with MA, and Cu(I) catalyzed "click" reaction. Subsequent cross-linking of the mixtures of MMs with BDMA *via* ATRP affords miktoarm CCS copolymers. Unmasking of the amino groups of L-lysine dendritic wedge furnishes amphiphilic nanoparticles that may have potential in targeted drug delivery. Unlike classical micelles, our potential nanocarrier should exhibit robustness and versatility combining various exceedingly important features such as: positively charged hydrophilic surface, ER targeting vectors, covalently stabilized core, and hydrophobic and bioerodible interior. To the best our knowledge, this is a novel design based on elegant coupling of individual building blocks which may facilitate fine-tuning the composition and thus properties of these particular CCS copolymers.

Experimental

Materials and methods

ε-Caprolactone (ε-CL; Fluka, ≥99%) was dried over CaH_2, and distilled under reduced pressure. 1,4-butanediol dimethacrylate (BDMA; Aldrich, 95%) was passed through a short basic Al_2O_3 column. Tetrahydrofuran (THF; Sigma-Aldrich, 99.9%), *N*,*N*-dimethylformamide (DMF; Fluka, 99.8%), toluene (Sigma-Aldrich, 99.9%), and triethylamine (TEA; Sigma-Aldrich, 99%) were dried over CaH_2, and distilled under nitrogen flow. Diethyl ether (Sigma-Aldrich, 99.5%) was kept over molecular sieves. Tin octoate ($Sn(Oct)_2$; Sigma, ~95%) and 6-bromo-1-hexanol (Aldrich, 97%) were distilled under reduced pressure. Methanol (Sigma-Aldrich, 99.9%), heptane (Sigma-Aldrich, 99%), dichloromethane (DCM; Sigma-Aldrich, 99.8%), anisole (Aldrich, 99%), 5-hexyn-1-ol (Aldrich, 96%), L-lysine (Fluka, purum; crystallized; ≥98%), di-*tert*-butyl dicarbonate (Aldrich, 97%), *N*,*N*′-dicyclohexylcarbodiimide (DCC; Aldrich, 99%), 3-bromo-1,2-propanediol (Fluka, ≥96%), methacrylic acid (MA; Aldrich, 99%), diethyl azodicarboxylate (DEAD; Aldrich), triphenylphosphine (TPP; Fluka, ~97%), sodium azide (Aldrich, 99%), 17α-ethynylestradiol (Sigma, 98%), ethynylferrocene (Aldrich, 97%), CuI (Aldrich, 98%), CuBr (Aldrich, 98%), 1,1,4,7,10,10-hexamethyltriethylenetetramine (HMTETA; Aldrich, 97%), *N*,*N*,*N*′,*N*″,*N*″-pentamethyldiethylenetriamine (PMDETA; Aldrich, 99%), ethyl α-bromoisobutyrate (EB*i*B; Aldrich, 98%), and trifluoroacetic acid (TFA; Sigma-Aldrich, ≥98%) were used as received.

Characterization by NMR spectroscopy was conducted on a Bruker 300 MHz spectrometer using $CDCl_3$ or DMSO-d_6 as solvents (both from Aldrich). The coupling constants are given in Hz. Molecular weights and polydispersity indices were estimated by size exclusion chromatography (SEC) using the following instruments: (a) Viscotek 200 instrument using two PLgel mixed-D columns (Polymer Laboratories (PL)), assembled in series, and a refractive index (RI) detector. SEC samples were run in THF at room temperature (1 mL min^{-1}). (b) Viscotek GPCmax VE-2001 equipped with Viscotek TriSEC Model 302 triple detector array (RI detector, viscometer detector, and laser light scattering detector with the light wavelength of 670 nm, and measuring angles of 90° and 7°) and a Knauer K-2501 UV detector using two PLgel mixed-D columns (from PL). The samples were run in THF at 30 °C (1 mL min^{-1}). Molecular weights were calculated using PS standards from PL. Thermogravimetric analysis (TGA) was carried out on a TGA Q500 instrument from 20–600 °C with a heating rate of 20 °C min^{-1} under nitrogen flow. Transmission electron microscopy (TEM) images have been acquired using Tecnai T20 instrument operated at 200 kV. The samples for TEM were prepared by evaporating droplets of the dilute solutions of the CCS polymers in THF, filtered through 0.45 μm Teflon filters, on lacey carbon coated nickel grids.

Synthesis

All reactions were carried out under nitrogen atmosphere.

1 and **2** have been prepared according to the procedures described in ref. 21.

1: SEC_{PSS}: M_n = 4300 Da, M_w = 4700 Da, M_w/M_n = 1.09. Degree of polymerization (DP) has been estimated by ^1H NMR to be 21, M_n = 2560 Da.

δ_H (300 MHz; $CDCl_3$) 6.09 (1H, m, *H*CH=CCH$_3$), 5.55 (1H, m, *H*CH=CCH$_3$), 3.95–4.17 (44H, t, $J_{1,3}$ 6.7, (CH$_2$)$_4$C*H*$_2$OC(O) and C(O)OC*H*$_2$(CH$_2$)$_3$C≡CH), 2.28 (t, $J_{1,3}$ 7.4, OC(O)-C*H*$_2$(CH$_2$)$_4$), 2.21 (m, C*H*$_2$C≡CH) (2.16–2.42 corresponds to 44H), 1.89–2.00 (4H, m, CH$_2$C≡C*H*, C(C*H*$_3$)=CH$_2$), 1.50–1.89 (88H, m, OC(O)CH$_2$C*H*$_2$CH$_2$C*H*$_2$CH$_2$ and C(O)OCH$_2$C*H*$_2$C*H*$_2$CH$_2$C≡CH), 1.20–1.50 (42H, m, OC(O)CH$_2$CH$_2$C*H*$_2$CH$_2$CH$_2$).

3: Cu(I) catalyzed "click" coupling of **1** and **2** has been carried out as reported in ref. 21. SEC_{LS}: M_n = 3200 Da, M_w = 3300 Da, M_w/M_n = 1.02. M_n(^1H NMR) = 3340 Da.

δ_H (300 MHz; $CDCl_3$) 7.40–7.80 (1H, br s, Ar), 6.07 (1H, m, *H*CH=CCH$_3$), 5.53 (1H, m, *H*CH=CCH$_3$), 5.10–5.50 (br, CHN*H*Boc and OCH$_2$C*H*O), 3.93–5.00 (br m, CH$_2$N*H*Boc, OC*H*$_2$CHO, C*H*NHBoc, C*H*$_2$Ar, (CH$_2$)$_4$C*H*$_2$OC(O) and C(O)OC*H*$_2$(CH$_2$)$_3$Ar) (3.93–5.50 corresponds to 55H), 2.97–3.23 (4H, br, C*H*$_2$NHBoc), 2.60–2.86 (2H, br, C(O)O(CH$_2$)$_3$C*H*$_2$Ar), 2.29 (42H, t, $J_{1,3}$ 7.5, OC(O)C*H*$_2$(CH$_2$)$_4$), 1.92 (m, C(C*H*$_3$)=CH$_2$), 1.53–1.97 (m, CH$_2$C*H*$_2$CHNHBoc, OC(O)CH$_2$C*H*$_2$CH$_2$C*H*$_2$CH$_2$ and C(O)OCH$_2$C*H*$_2$C*H*$_2$CH$_2$Ar), 1.05–1.60 (m, BocNHCH$_2$C*H*$_2$C*H*$_2$CH$_2$CHNHBoc, C(C*H*$_3$)$_3$ and OC(O)CH$_2$CH$_2$C*H*$_2$CH$_2$CH$_2$) (1.05–1.97 corresponds to 181H).

4: ROP of ε-CL initiated by 6-bromo-1-hexanol has been conducted as in ref. 22. SEC_{PSS}: **4m**: M_n = 4300 Da, M_w = 4700 Da, M_w/M_n = 1.09; **4k**: M_n = 3800 Da, M_w = 4200 Da, M_w/M_n = 1.09; **4p**: M_n = 6000 Da, M_w = 6600 Da, M_w/M_n = 1.09. From ^1H NMR the DP and number average molecular weight: m = 29, M_n = 3490 Da; k = 22, M_n = 2690 Da; p = 41, M_n = 4860 Da.

δ_H (300 MHz; $CDCl_3$) 4.04 (58H, t, $J_{1,3}$ 6.6, (CH$_2$)$_4$C*H*$_2$OC(O) and C(O)OC*H*$_2$(CH$_2$)$_5$Br), 3.62 (2H, t, $J_{1,3}$ 6.4, (CH$_2$)$_4$C*H*$_2$OH), 3.39 (2H, t, $J_{1,3}$ 6.7, C*H*$_2$Br), 2.29 (58H, t, $J_{1,3}$ 7.4, OC(O)C*H*$_2$(CH$_2$)$_4$), 1.85 (2H, m, C*H*$_2$CH$_2$Br), 1.50–1.75 (118H, m, OC(O)CH$_2$C*H*$_2$CH$_2$C*H*$_2$CH$_2$ and CH$_2$C*H*$_2$(CH$_2$)$_4$Br), 1.25–1.50 (62H, m, OC(O)CH$_2$CH$_2$C*H*$_2$CH$_2$CH$_2$ and (CH$_2$)$_2$C*H*$_2$C*H*$_2$(CH$_2$)$_2$Br).

5: Mitsunobu coupling of **4** and methacrylic acid has been accomplished following the synthetic protocol in ref. 22. The esterified product has been precipitated twice from THF into cold MeOH to eliminate residue of TPP. SEC_{PSS}: M_n = 4600 Da, M_w = 5000 Da, M_w/M_n = 1.09.

δ_H (300 MHz; $CDCl_3$) 6.08 (1H, m, *H*CH=CCH$_3$), 5.54 (1H, m, *H*CH=CCH$_3$), 4.13 (2H, m, C*H*$_2$OC(O)C(CH$_3$)=CH$_2$), 4.05 (58H, t, $J_{1,3}$ 6.6, (CH$_2$)$_4$C*H*$_2$OC(O) and C(O)OC*H*$_2$(CH$_2$)$_5$Br), 3.40 (2H, t, $J_{1,3}$ 6.7, C*H*$_2$Br), 2.29 (58H, t, $J_{1,3}$ 7.5, OC(O)C*H*$_2$(CH$_2$)$_4$), 1.93 (3H, m, OC(O)C*H*$_3$C=CH$_2$), 1.85 (2H, m, C*H*$_2$CH$_2$Br), 1.50–1.78 (118H, m, OC(O)CH$_2$C*H*$_2$CH$_2$C*H*$_2$CH$_2$ and CH$_2$C*H*$_2$(CH$_2$)$_4$Br), 1.25–1.50 (62H, m, OC(O)CH$_2$CH$_2$C*H*$_2$CH$_2$CH$_2$ and (CH$_2$)$_2$C*H*$_2$C*H*$_2$(CH$_2$)$_2$Br).

6: **5** (2.54 g, 0.71 mmol), sodium azide (0.135 g, 2.07 mmol), and DMF (25 mL) were placed in a 50 mL round-bottom flask equipped with a magnetic stirring bar. The reaction was carried out at room temperature for 15 h. The product was precipitated into cold MeOH–H_2O (5 : 1) mixture, isolated by filtration, and dried in a vacuum oven at room temperature until constant weight. SEC_{PSS}: M_n = 4800 Da, M_w = 5200 Da, M_w/M_n = 1.1.

δ_H (300 MHz; $CDCl_3$) 6.08 (1H, m, *H*CH=CCH$_3$), 5.54 (1H, m, *H*CH=CCH$_3$), 4.13 (2H, m, C*H*$_2$OC(O)C(CH$_3$)=CH$_2$), 4.04 (58H, t, $J_{1,3}$ 6.6, (CH$_2$)$_4$C*H*$_2$OC(O) and C(O)OC*H*$_2$(CH$_2$)$_5$N$_3$), 3.27 (2H, t, $J_{1,3}$ 6.8, C*H*$_2$N$_3$), 2.29 (58H, t, $J_{1,3}$ 7.4,

$OC(O)CH_2(CH_2)_4$), 1.93 (3H, m, $OC(O)CH_3C{=}CH_2$), 1.50–1.78 (120H, m, $OC(O)CH_2CH_2CH_2CH_2CH_2$, $CH_2CH_2N_3$ and $CH_2CH_2(CH_2)_4N_3$), 1.22–1.50 (62H, m, $OC(O)CH_2CH_2CH_2CH_2CH_2$ and $(CH_2)_2CH_2CH_2(CH_2)_2N_3$).

7: A 50 mL two-neck flask was charged with **6** (0.80 g, 0.23 mmol), 17α-ethynylestradiol (0.20 g, 0.67 mmol), CuI (0.042 g, 0.22 mmol), and THF (7.5 mL). The reaction mixture was stirred at room temperate until the polymer dissolved completely. Then TEA (0.13 mL, 0.93 mmol) was introduced. The reaction was conducted at 35 °C for 24 h in the dark. Then, the macromonomer was precipitated into a large excess of cold MeOH. The product was isolated by filtration, and dried *in vacuo* at room temperature until constant weight. SEC_{PSS}: M_n = 5100 Da, M_w = 5600 Da, M_w/M_n = 1.1.

δ_H (300 MHz; $CDCl_3$) 7.41 (1H, s, Tr), 7.04 (1H, d, J_o 7.6, Ar), 6.55 (2H, br s, Ar), 6.08 (1H, s, $HCH{=}CCH_3$), 5.54 (1H, m, $HCH{=}CCH_3$), 5.35 (1H, br s, Ar–O*H*), 4.38 (2H, m, CH_2Tr), 4.14 (2H, t, $J_{1,3}$ 6.6, $CH_2OC(O)C(CH_3){=}CH_2$), 4.05 (58H, t, $J_{1,3}$ 6.7, $(CH_2)_4CH_2OC(O)$ and $C(O)OCH_2(CH_2)_5Tr$), 2.80 (2H, m, CH_2Ar), 2.30 (58H, t, $J_{1,3}$ 7.5, $OC(O)CH_2(CH_2)_4$), 1.93 (3H, m, $OC(O)CH_3C{=}CH_2$), 1.50–1.78 (m, $OC(O)CH_2CH_2CH_2CH_2CH_2$ and $CH_2CH_2CH_2CH_2CH_2CH_2Tr$), 1.22–1.50 (m, $OC(O)CH_2CH_2CH_2CH_2CH_2$ and $(CH_2)_2CH_2CH_2(CH_2)_2Tr$), 1.20–2.70 (signals from estradiol residue overlap with the resonances originating from the polymer backbone, and thus cannot be unambiguously assigned), 1.04 (3H, s, CH_3C).

8: The synthetic protocol is same as for the preparation of **7**. **6** (1.00 g, 0.28 mmol), ethynylferrocene (0.18 g, 0.86 mmol), CuI (0.055 g, 0.29 mmol), TEA (0.16 mL, 1.15 mmol) and THF (9.5 mL) were employed. SEC_{PSS}: M_n = 5200 Da, M_w = 5700 Da, M_w/M_n = 1.1.

δ_H (300 MHz; $CDCl_3$) 7.44 (1H, s, Tr), 6.08 (1H, s, $HCH{=}CCH_3$), 5.54 (1H, m, $HCH{=}CCH_3$), 4.71 (2H, m, Cp), 4.36 (2H, m, CH_2Tr), 4.28 (2H, m, Cp), 4.13 (2H, m, $CH_2OC(O)C(CH_3){=}CH_2$), 4.05 (58H, t, $J_{1,3}$ 6.6, $(CH_2)_4CH_2OC(O)$ and $C(O)OCH_2(CH_2)_5Tr$), 2.30 (58H, t, $J_{1,3}$ 7.5, $OC(O)CH_2(CH_2)_4$), 1.93 (3H, s, $OC(O)CH_3C{=}CH_2$), 1.50–1.78 (120H, m, $OC(O)CH_2CH_2CH_2CH_2CH_2$ and $CH_2CH_2CH_2CH_2CH_2CH_2Tr$), 1.22–1.50 (62H, m, $OC(O)CH_2CH_2CH_2CH_2CH_2$ and $(CH_2)_2CH_2CH_2(CH_2)_2Tr$).

Preparation of CCS polymers

General procedure. A dried Schlenk tube was charged with macromonomer, CuBr, toluene, and BDMA. Two freeze-pump-thaw cycles were performed. Then HMTETA was injected followed by two freeze-pump-thaw cycles. Finally, EB*i*B was added, and an additional freeze-pump-thaw cycle was performed. The reaction mixture was allowed to warm up to ambient temperature while stirring, and then the tube was immersed into a preheated oil bath at 50 °C. After various times the reaction mixture was cooled to room temperature, and exposed to air. The CCS polymer was precipitated into a large excess of MeOH–Et_2O (1 : 1) mixture at room temperature. The precipitate quickly sedimented, and the solvent mixture was removed by pipette. The product was isolated on filter paper, and washed with the fresh solvent mixture several times while applying vacuum with a water aspirator. It was then dried in a vacuum oven at room temperature until constant weight.

9: **6k** (0.20 g, 0.074 mmol), CuBr (0.023 g, 0.16 mmol), toluene (5 mL), BDMA (0.25 mL, 1.13 mmol), HMTETA (90 μL, 0.33 mmol), and EB*i*B (16 μL, 0.11 mmol) were employed. The reaction was carried out for 72 h. SEC_{LS}: $M_n = 1.13 \times 10^6$ Da, $M_w = 1.61 \times 10^6$ Da, M_w/M_n = 1.43.

10: **3** (0.25 g, 0.075 mmol), **6p** (0.51 g, 0.10 mmol), CuBr (0.059 g, 0.41 mmol), toluene (12 mL), BDMA (0.6 mL, 2.71 mmol), HMTETA (0.22 mL, 0.81 mmol), and EB*i*B (40 μL, 0.27 mmol) were employed. The reaction was carried out for 22.5 h. SEC_{LS}: $M_n = 1.30 \times 10^6$ Da, $M_w = 2.00 \times 10^6$ Da, M_w/M_n = 1.55.

11: A 50 mL two-neck flask was charged with **10** (0.2 g, 0.024 mmol of azide functional groups), ethynylferrocene (0.016 g, 0.076 mmol), CuI (0.015 g, 0.079 mmol), TEA (0.02 mL, 0.14 mmol) and THF (10.5 mL). The resulting slurry was stirred at 64 °C for 24 h. Then the product was precipitated into large excess of cold heptane. The solvent was decanted and the product was washed with heptane twice. It was then isolated on filter paper, and washed with the fresh solvent several times while applying vacuum with water aspirator. The product was dried in a vacuum oven at room temperature.

12: **3** (0.12 g, 0.036 mmol), **7** (0.25 g, 0.065 mmol), CuBr (0.034 g, 0.24 mmol), toluene (13.5 mL), BDMA (0.33 mL, 1.49 mmol), HMTETA (0.13 mL, 0.48 mmol), and EB*i*B (23 μL, 0.16 mmol) were employed. The reaction was carried out for 20.25 h. SEC_{LS}: $M_n = 2.06 \times 10^5$ Da, $M_w = 2.65 \times 10^5$ Da, M_w/M_n = 1.29.

13: **3** (0.12 g, 0.036 mmol), **8** (0.25 g, 0.067 mmol), CuBr (0.034 g, 0.24 mmol), toluene (13.5 mL), BDMA (0.35 mL, 1.58 mmol), HMTETA (0.13 mL, 0.48 mmol), and EB*i*B (23 μL, 0.16 mmol) were employed. The reaction was carried out for 16.5 h. SEC_{LS}: $M_n = 8.5 \times 10^4$ Da, $M_w = 1.16 \times 10^5$ Da, M_w/M_n = 1.37.

14: CCS polymer **12** (0.069 g) and DCM (3 mL) were placed in a 25 mL two-neck flask equipped with a magnetic stirring bar. The reaction mixture was stirred in the dark at room temperature until the polymer dissolved completely. The flask was immersed into an ice/water bath, and TFA (0.6 mL) was injected. The mixture was then stirred in the dark for 15 min on the ice/water bath, and for 2.5 h at room temperature. The product was recovered by precipitating into a large excess of cold heptane-Et_2O (2 : 1) and isolating on filter paper. The polymer was washed several times with the fresh solvent mixture, and dried in a vacuum oven at room temperature.

Results and discussions

The linear-dendritic macromonomer (di-Boc-L-lysine)$_{G2}$-*b*-PCL-methacrylate (MM **3**) has been prepared according to the synthetic cascade depicted in Scheme 1.

The synthetic procedures follow the algorithm which we have reported earlier.[21] To the best of our knowledge, the macromonomer thus obtained has not been documented before. This synthetic layout bears significant benefits of exhaustive characterization of the individual building blocks **1** and **2**. The Cu(I) catalyzed "click" coupling[23] affords MM **3** with narrow molecular weight distribution, which implies that the goal product is obtained without any considerable side reactions. The ^{1}H NMR spectroscopy confirms near to quantitative reaction (Fig. 1). The resonance signal originating from the methylene group next to the alkyne function (**i**) is shifted downfield, while the peak attributed to the acetylenic hydrogen disappears completely. The

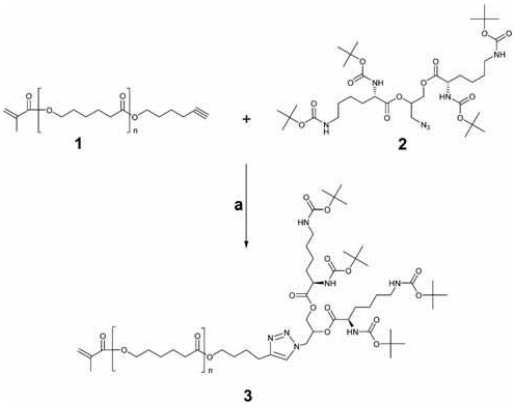

Scheme 1 Synthetic pathway for preparation of linear-dendritic macromonomer. *Reagents and conditions*: (a) CuI/NEt_3, 35 °C, THF.

resonances **o**, **p**, and **q** that correspond to the methacrylic acid residue verify the preservation of the vinyl double bond which is the prerequisite for effectual participation of the macromonomer in subsequent polymerization reactions. The resonance **h** has been ascribed to the triazole proton. The heteronuclear single quantum coherence (HSQC) NMR experiment has revealed that **h** is the combination of two resonance signals that may be attributed to two regioisomers resulting from the "click" reaction. Formation of two regioisomers is not uncommon when conducting the reaction in THF.[24] The number average molecular weight has been estimated by ^{1}H NMR to be 3340 Da.

Linear MMs N_3-PCL-methacrylate (MM **6**), E_2-PCL-methacrylate (MM **7**), and ferrocene-PCL-methacrylate (MM **8**) have been synthesized according to Scheme 2. Synthetic routes leading to azide functional PCL include nucleophilic substitution of bromo end group of Br-PCL-OH by sodium azide[25] and ROP of ε-CL using azide containing initiator.[26] Since the latter carries the risk of reducing the azide functions by TPP in subsequent Mitsunobu coupling of N_3-PCL-OH and MA,[25] we follow the path involving the conversion of bromo end groups to corresponding azides after the esterification reaction (Scheme 2).

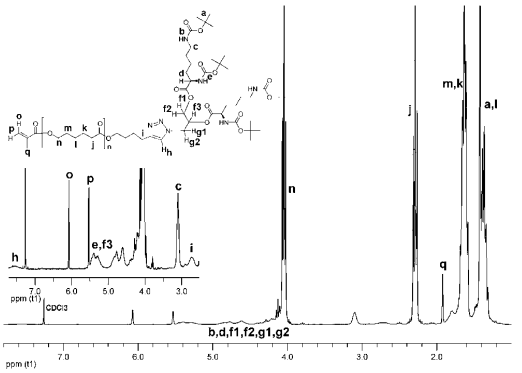

Fig. 1 ^{1}H NMR spectrum of MM **3**.

ROP of ε-CL initiated by diethylaluminium 2-bromoethoxide and diethylaluminium 12-bromo-1-dodecyloxide in toluene at 25 °C has been carried out with excellent control.[25] In a similar approach, we initially conducted the polymerization reaction in THF at 62 °C employing 2-bromoethanol and $Sn(Oct)_2$ as initiator and catalyst, respectively. However, poor control over the reaction, translated into relatively high polydispersity index (PDI) of 1.24 and unsymmetrical SEC trace, was observed. The reaction rate was higher than in case of earlier reactions when different initiators were used.[21,22] This may possibly be due to the inductive effects arising from the close proximity of Br and O in 2-bromoethanol. Indeed, when 6-bromo-1-hexanol was chosen as the initiator, the polymerization proceeded smoothly with SEC revealing monomodal, symmetrical trace and low PDI of 1.09. Br-PCL-OH with DP of 22, 29, and 41 has been obtained.

Esterification of the hydroxy chain end of **4** with MA was accomplished by Mitsunobu protocol as described earlier.[22] Near to quantitative functionalization was attained as judged from ^{1}H NMR data: resonance signal at 3.62 ppm corresponding to the methylene next to the hydroxy end group shifted completely at 4.13 ppm. After two-fold precipitation in MeOH, the product was free from residual TPP. This is important since TPP may lead to the reduction of azide groups in the reaction concomitant to the nucleophilic substitution of bromo chain ends by sodium azide. PDI remained same indicating preservation of the polyester backbone.

Conversion of bromo end groups into azide functions was first conducted as suggested by Teyssié and co-workers:[25] Br-PCL-methacrylate **5** was reacted with 5 equivalents of NaN_3 in DMF at 30 °C. The SEC chromatogram of the substituted product exhibited a small shoulder on the high molecular weight side. We reckoned that the appearance of the shoulder could be the result of the nucleophilic attack of the azide anion on the carbonyl

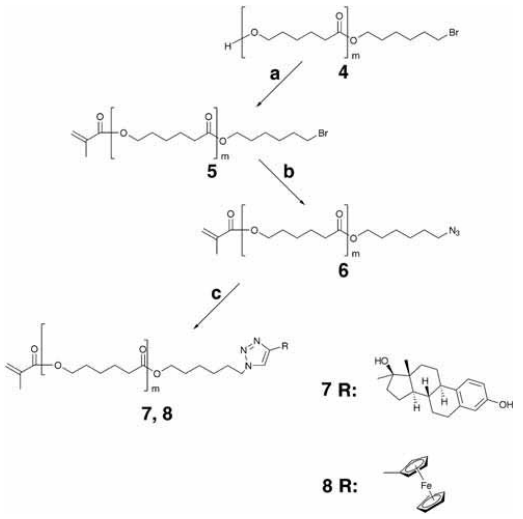

Scheme 2 Synthetic pathway for preparation of linear macromonomers. *Reagents and conditions*: (a) MA, DEAD, TPP, THF; (b) NaN_3, DMF; (c) 17α-ethynylestradiol or ethynylferrocene, CuI/NEt_3, 35 °C, THF.

carbons of the PCL backbone. Therefore, in the next trail 3 equivalents of NaN_3 were utilized at room temperature in DMF. The shoulder, though diminished in intensity, was still present (PDI = 1.1). The NMR experiments suggested that the extent of the reaction was near to quantitative, and no fathomable side products were identified. This gave birth to the speculation that the azide groups were reacting with the methacrylic units even at room temperature. To ascertain or eliminate such a conjecture, NaN_3 was reacted with Br-PCL-OH under identical conditions; the shoulder was no longer detected. Furthermore, MM **6** displayed a limited shelf-life at room temperature. After several days SEC trace with bimodal distribution was acquired. Triazolines, formed from 1,3-cycloaddition, were identified after careful investigation by ^{1}H, COSY, and HSQC NMR experiments. Despite earlier reports regarding relative stability of methacrylic monomers bearing pendant azide functions at room temperature, which was attributed to the steric hindrance,[27] our findings made it obvious that the uncatalyzed cycloaddition took place during the substitution reaction, though the share of this reaction was negligible, and then proceeded throughout the matrix of the isolated MM. This result is somewhat baffling if taken into consideration fairly low local concentration of the end functionalities in case of the MM with the molecular weight of almost 5 000 Da.

Cu(I) catalyzed azide-alkyne cycloaddition (CuAAC) between **6** and 17α-ethynylestradiol or ethynylferrocene[28] provides MM **7** and MM **8**, respectively (Scheme 2). To the best of our knowledge, participation of the azide end-capped PCL in CuAAC has been restricted to the synthesis of cyclic PCL.[26,29] Neither has 17α-ethynylestradiol enjoyed extensive application in CuAAC not to mention two fairly recent reports about the synthesis of E_2-peptoid[30a] and E_2-cyclodextrin[30b] conjugates. Hence, MM **7** represents a novel macromolecular architecture – hormone-synthetic polymer conjugate – built *via* CuAAC and employed in ATRP. **6** and 17α-ethynylestradiol or ethynylferrocene were reacted under similar conditions as **1** and **2**. However, 3 equivalents of the alkyne were taken to ensure complete conversion, and to avoid involvement of the methacrylic moieties in undesirable collateral reactions discussed above. Examination by SEC did not detect any chain scission or triazoline formation: PDI remained low (1.1), and the intensity of the shoulder did not increase. The ^{1}H NMR spectrum of MM **7** displays all the characteristic resonances (Fig. 2).

The peak at 3.27 ppm arising from the methylene group next to the azide function has disappeared completely, and the new peak at 4.38 ppm attributed to the methylene group next to the triazole ring has emerged. This implies that the coupling was near to quantitative. Furthermore, resonances at 6.08 ppm, 5.54 ppm, and 1.93 ppm correspond to the methacrylic acid residue, and confirm the maintenance of the double bond. The triazole proton resonates at 7.41 ppm, while the signals designated as **l**, **m**, **n**, **o**, and **p** are ascribed to the E_2 moiety. Investigation of MM **8** by SEC and NMR also rendered excellent results. While SEC trace convinced in the absence of chain scrambling and azide-methacrylate cycloaddition, the NMR experiment suggested almost complete functionalization (Fig. 3).

Still oblivious of the fact that methacrylic double bond could react with azide end group even at room temperature; we attempted to prepare the first type of CCS polymer comprised

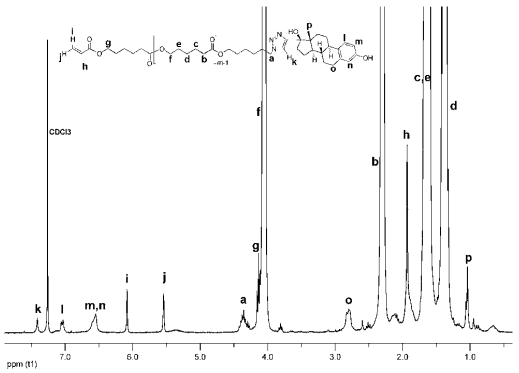

Fig. 2 ^{1}H NMR spectrum of MM **7**.

solely of the MM **6**. CCS polymers with peripheral alkyne functional groups have been reported earlier.[31] If successful, our approach would generate aggregates with azide functionalities on the surface. Thus, MM **6k** with the DP of 22 was cross-linked with BDMA *via* ATRP initiated by EB*i*B (Scheme 3).

PCL MMs have been scarcely employed in controlled radical polymerization techniques.[32] Therefore, it was necessary to adjust the reaction conditions in order to increase the MM conversion while maintaining narrow MWD. The MM conversion was roughly estimated from the peak intensities of RI detector signal on the SEC chromatogram. Initially the reaction was conducted in anisole, taking into consideration better solubility of copper(II) complex in polar solvents,[4] at 50 °C employing CuBr/PMDETA catalytic complex and low initiator to MM molar ratio $[MM\ \mathbf{6k}]_0 : [BDMA]_0 : [CuBr]_0 : [PMDETA]_0 : [EBiB]_0 = 1 : 3 : 0.15 : 0.15 : 0.1$. Only 3 equivalents of the cross-linker (BDMA) were employed to avoid premature gelation of the reaction mixture. Low MM conversion was achieved in a few hours, and it did not increase by extending the reaction time. This was ascribed to the rapid blocking of the initiating sites due to the core congestion, loss of the active alkyl bromide groups which has significant detrimental impact at such a low concentration of the initiating moieties, and catalyst deactivation since

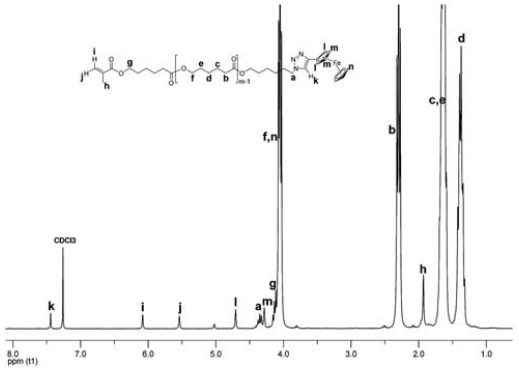

Fig. 3 ^{1}H NMR spectrum of MM **8**.

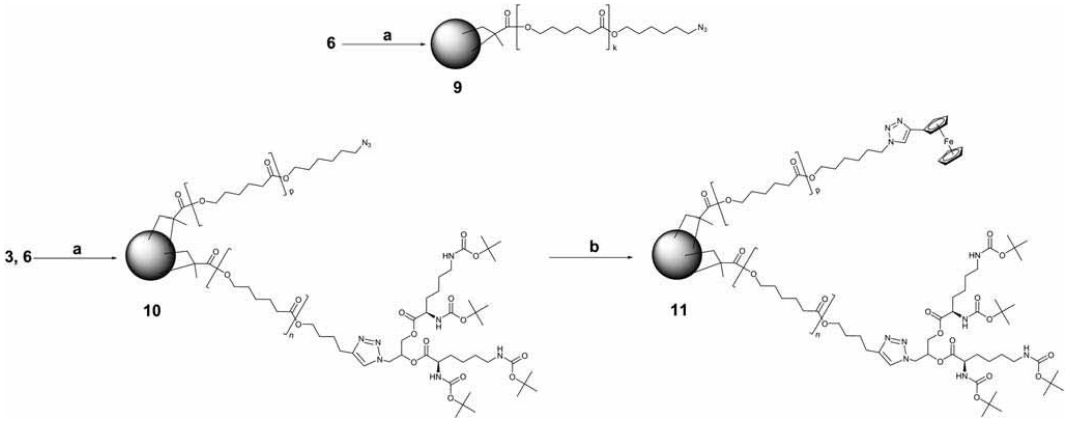

Scheme 3 Synthesis and derivatization of CCS polymers possessing peripheral azide functions. *Reagents and conditions*: (a) BDMA, CuBr/HMTETA, EB*i*B, 50 °C, toluene; (b) ethynylferrocene, CuI/NEt_3, 64 °C, THF.

characteristic color change to bright green was observed. Since long reaction times encourage star-star couplings resulting in high PDI, it was desirable to increase the MM incorporation at the early stage of the polymerization. We improved the reaction conditions by changing the reaction medium to toluene in order to enhance the solubility of PCL, replacing PMDETA with HMTETA to augment the stability of the catalytic complex, and using the following initial molar ratios: $[MM\ \mathbf{6k}]_0 : [BDMA]_0 : [CuBr]_0 : [HMTETA]_0 : [EBiB]_0 = 1 : 15 : 2.25 : 4.5 : 1.5$.

The large excess of the cross-linker, favoring gelation, was compensated by diluting the reaction mixture. Utilizing 1.5 equivalents of EB*i*B is in dissonance with the scheme proposed by Matyjaszewski suggesting decreasing the number of initiating groups to minimize the extent of star-star coupling.[7,8] Thus, we anticipated reaching reasonable MM conversion on the expense of the MWD: we simply tried to escape wasting of the MMs **3**, **6**, **7**, and **8**, because their synthesis involves multiple steps. The CCS polymer was analyzed by SEC and NMR spectroscopy. The molecular weight characteristics were determined using light scattering detector. While PDI was fairly narrow (1.43), weight average molecular weight M_w was estimated to be 1.61×10^6 Da. Such a large value for M_w has not been reported before.[3–5,7–12] We attribute the formation of such large CCS polymer to the star-star coupling throughout ATRP facilitated by relatively high concentration of the initiating sites, the cross-linker with soft aliphatic spacer,[33] and azide-methacrylate cycloaddition reaction perceived at the later stage of our experiments. The ^{1}H NMR spectroscopy data suggested the star formation, and preservation of the certain amount of peripheral azide functions (Fig. 4).

The resonances from the microgel core overlap with those from the PCL arms, and result in slight broadening at the baseline. The resonance signals arising from the unreacted double bonds are barely detected. The peak **a** corresponding to the methylene group next to the azide function of the arms has also been assigned.

The miktoarm CCS **10** was then prepared under similar reaction conditions: the mixture of the linear-dendritic MM **3** and the linear MM **6p** was cross-linked with BDMA. The structure of the CCS polymer was elucidated by NMR spectroscopy. The ^{1}H NMR experiment verified incorporation of both arms into the CCS (Fig. 5). Again, almost no unreacted methacrylic units were observed; resonances from the core were barely discernible. Signals from the methylene group next to the azide functionality (**c**), the methylene group adjacent to the Boc protected amine functions (**b**), and methyl groups of the Boc protection (**a**) have been identified together with the peaks characteristic to the PCL backbone.

SEC trace was not symmetrical (Fig. 6), however it suggested that precipitation afforded the product free from the unreacted MMs. PDI of 1.55 and M_w of 2.00×10^6 Da were obtained using the light scattering detector and THF as eluent.

However, upon standing a few days, the CCS **10** was only partially soluble in THF and other common organic solvents. This implies that certain type of cross-linking reaction persisted in the isolated product. At this point the analysis of MM **6** unveiled azide-methacrylate cycloaddition. This reaction, provoking the star-star coupling, is responsible for such a large M_w, broad MWD, and loss of a certain amount of azide end

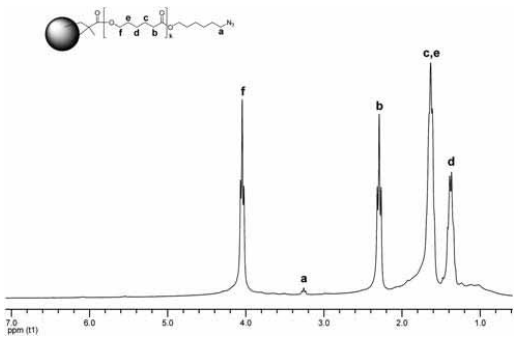

Fig. 4 ^{1}H NMR spectrum of CCS **9**.

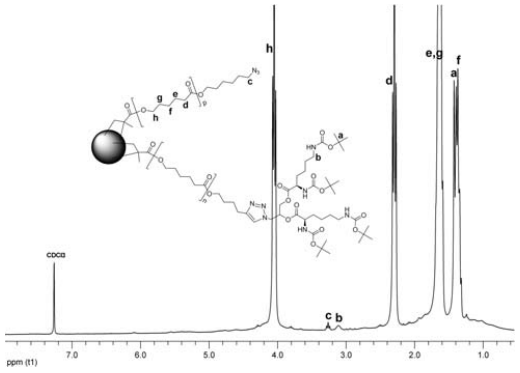

Fig. 5 ^{1}H NMR spectrum of CCS **10**.

groups. These results opted us for capping the MM **6** with the desirable moiety by CuAAC before employing it in ATRP with BDMA. Nevertheless, we decided to derivatize remaining accessible azide functions of CCS **10** with ethynylferrocene by conducting the CuAAC in a heterogeneous mixture (Scheme 3). Ferrocene would assume the role of stain in TEM investigations.

Three-fold excess of ethynylferrocene and CuI were used. The product was analyzed by NMR spectroscopy. The result, though inconclusive due to limited solubility of the CCS **11** in $CDCl_3$, suggested that available azide groups had reacted since the resonance **c** (Fig. 5) disappeared, and peaks related to ferrocene were detected. The heterogeneous mixture of the CCS **11** in THF was filtered twice through 0.45 μm Teflon filter to remove the agglomerates of large sizes, and the nanoparticles in the filtrate were visualized by TEM (Fig. 7). Clusters of the nanoparticles in the range of 10–20 nm were observed. Clustering may be ascribed to the lack of repulsive interactions amongst the coronas of CCS copolymers. Evidently, ferrocene did not impart significant contrast.

Being confronted by the destructive interference of azide-methacrylate cycloaddition with the cross-linking reaction, we utilized MMs **3**, **7** and **8** in preparation of miktoarm CCS copolymers as shown in Scheme 4. Initially, we adopted the reaction conditions used for the cross-linking of azide end capped MMs.

As a result, ATRP of the MM **3**, MM **7**, and BDMA produced insoluble gel. Dilution of the reaction mixture was the only adjustment necessary to attain the formation of the goal product CCS **12**. The molecular characteristics estimated by SEC (Fig. 8) include $M_w = 2.65 \times 10^5$ Da and PDI = 1.29 (both were determined using the light scattering detector). The SEC analysis revealed that the product did not contain unreacted MMs. Fairly narrow MWD suggests that the ATRP was under control, and that the contribution from the star-star coupling was reduced significantly.

The structure of the CCS **12** was examined by ^{1}H NMR spectroscopy (Fig. 9). The peaks corresponding to the PCL backbone overlap with the broad signals arising from the microgel core. This implies that the segmental mobility of the core has not been arrested completely. The resonances ascribed to the methyl group of the Boc protection (**a**), the methylene group neighboring the Boc protected amino group (**b**), and the triazole protons (**c**) of the MM **3** have been assigned. The MM **7** is represented by the signals attributed to the E_2 moiety (**d**, **e**, **f**, **g**), and the triazole proton (**h**). Protons from the unreacted methacrylic units of the core resonate at 5.56 ppm and 6.09 ppm. Since the intensities of the signals originating from the L-lysine and E_2 moieties are rather weak, the composition of the CCS **12** cannot be unambiguously estimated from the NMR data.

Therefore, TGA has been employed to gain insight about the ratio and the number of arms of the MMs. The overlay of TGA thermograms (Fig. 10) allows estimation of the weight fraction of the MM **3** as follows: the weight loss of 3.7% between 222 °C and 272 °C is attributed to the decomposition of the Boc protection groups, and corresponds to approximately 31% of the MM **3**. About 26% weight loss in the temperature range 424–516 °C is

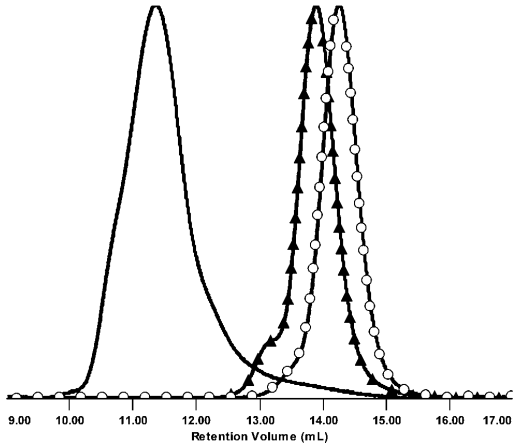

Fig. 6 Normalized SEC RI detector signals of MM **3** (○), MM **6p** (▲), and CCS **10**.

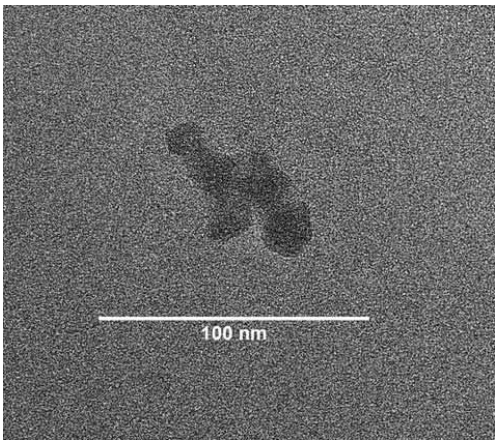

Fig. 7 TEM image of CCS **11** obtained after removal of the insoluble matter.

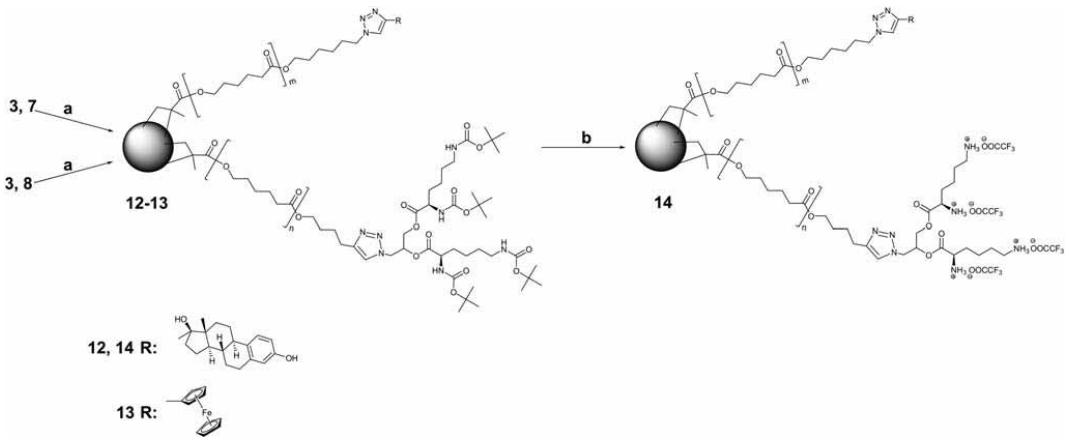

Scheme 4 Synthesis and deprotection of miktoarm CCS copolymers bearing surficial E_2 and ferrocene. *Reagents and conditions*: (a) BDMA, CuBr/HMTETA, EB*i*B, 50 °C, toluene; (b) TFA, CH_2Cl_2.

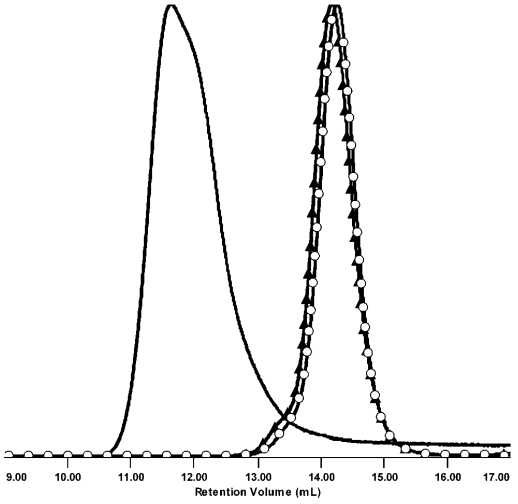

Fig. 8 Normalized SEC RI detector signals of MM **3** (○), MM **7** (▲), and CCS **12**.

ascribed to the decomposition of the core. Hence, the weight fraction of the MM **6** is roughly 43%. Obviously these results are crude estimates; nonetheless, they shed some light over the star composition. By making use of the following equation: $f = \frac{WF_{arms} \times M_{w,CCS}}{M_{w,arms}}$, where WF_{arms} is the weight fraction of the arms determined by TGA, and $M_{\mathrm{w,CCS}}$ and $M_{\mathrm{w,arms}}$ are the weight average molecular weights of the CCS copolymer and the arms, respectively, it can be calculated that the CCS **12** consists of on average 24 (di-Boc-L-lysine)$_{G2}$-*b*-PCL and 27 E_2-PCL arms. The molar ratio of the incorporated arms is [E_2-PCL]/[(di-Boc-L-lysine)$_{G2}$-*b*-PCL] = 1.2, whereas in the initial mixture [MM **7**]$_0$/[MM **3**]$_0$ = 1.8. This rift between the initial and final compositions may be explained by higher reactivity of the MM **3** as a consequence of its lower molecular weight.[11]

Deblocking of the amine functional groups of the L-lysine dendritic wedges was accomplished by treating the CCS **12** with TFA[21] as shown in Scheme 4. The product CCS **14** was analyzed with ^{1}H NMR spectroscopy using DMSO-d_6 as solvent (Fig. 11). The resonance **a** arising from the *tert*-butyl groups disappeared completely (**a** refers to Fig. 9), while the broad peaks $\mathbf{a_1}$ and $\mathbf{a_2}$ related to free amine functions were detected. Moreover, the peak **b** has shifted upfield, and is now overlapped with the peak **g** ascribed to the E_2 residue. Other resonances originating from the E_2 unit have been identified as well. The signals from the core are somewhat weaker, perhaps due to the limited solubility of the interior of the CCS **14** in as polar a solvent as DMSO-d_6.

After successful preparation of the CCS **12**, MM **3** and MM **8** were subjected to cross-linking with BDMA under similar conditions. Investigation of the product CCS **13** by ^{1}H NMR spectroscopy validated integration of both arms in the star copolymer (Fig. 12).

While the peaks **c** and **g** correspond to the triazole protons of MM **3** and MM **8** respectively, the signals **a** (*tert*-butyl) and **b** (CH_2NHBoc) from the MM **3** and **d** and **e** (both related to Cp) from the MM **8** can be identified as well. SEC analysis (Fig. 13) provided the following characteristics: $M_{\mathrm{w}} = 1.16 \times 10^5$ Da and PDI = 1.37 (both values were obtained using the light scattering detector).

The composition of the CCS **13** was assessed employing the TGA. Taking the same approach as in the case of CCS **12**, the following weight fractions have been estimated: 45% of the MM **3**, 41% of the MM **8**, and 14% of the core. Thus, the CCS **13** is comprised of 15 (di-Boc-L-lysine)$_{G2}$-*b*-PCL and 12 ferrocene-PCL arms. TEM revealed clusters of the CCS **13** without additional staining (Fig. 14). However, low contrast and star-star overlaps do not allow precise evaluation of the size of these nanoparticles.

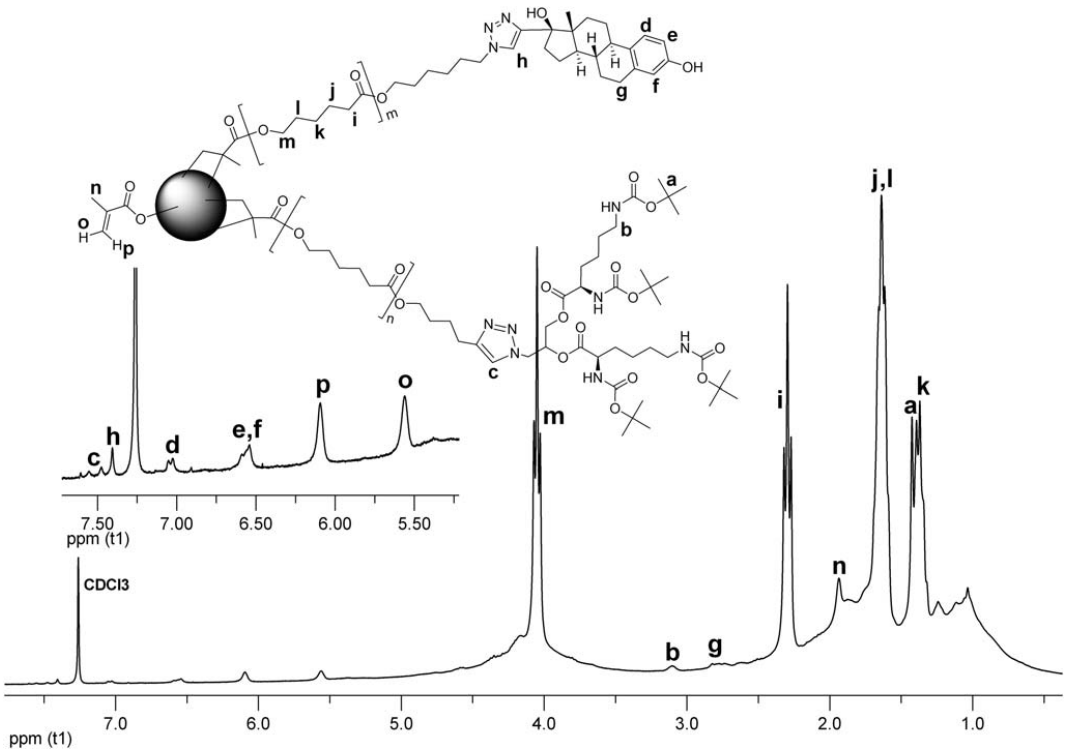

Fig. 9 ^{1}H NMR spectrum of CCS **12**.

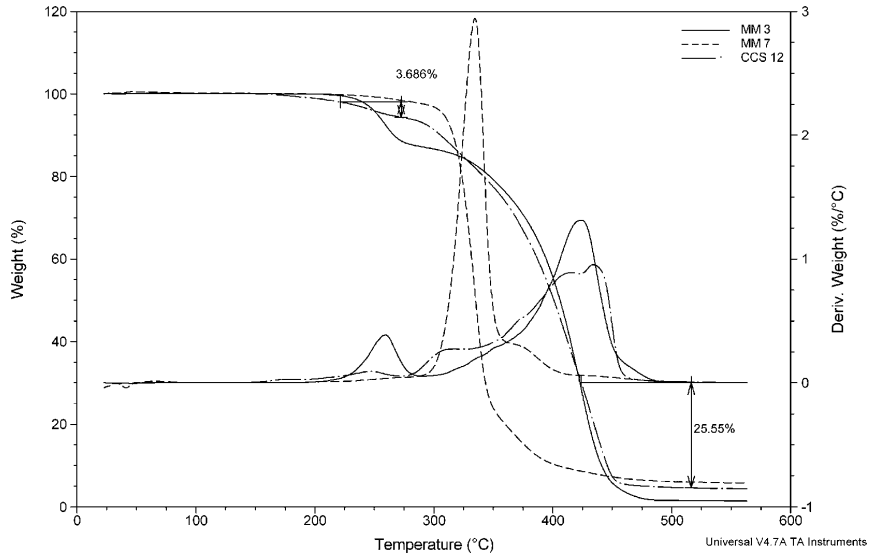

Fig. 10 TGA thermograms of MM **3**, MM **7**, and CCS **12**.

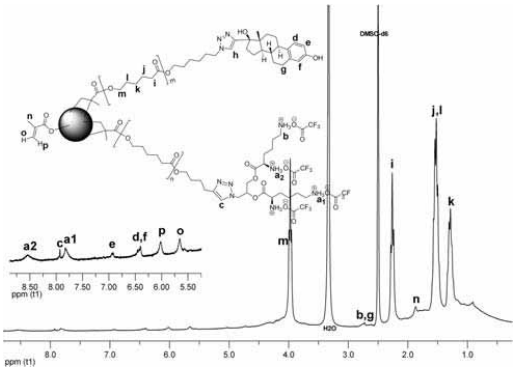

Fig. 11 ^{1}H NMR spectrum of CCS **14**.

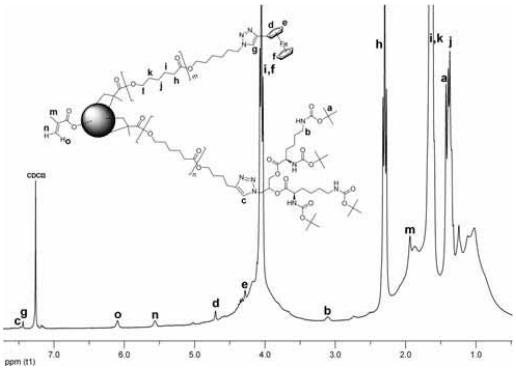

Fig. 12 ^{1}H NMR spectrum of CCS **13**.

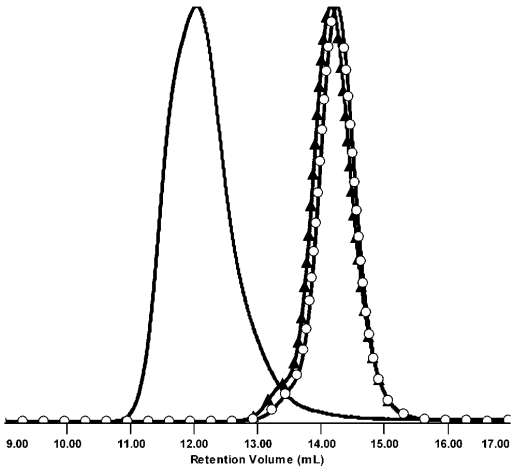

Fig. 13 Normalized SEC RI detector signals of MM **3** (○), MM **8** (▲), and CCS **13**.

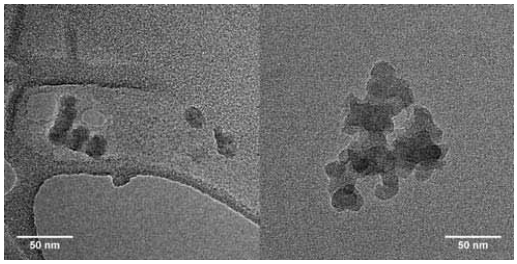

Fig. 14 TEM images of CCS **13**.

Conclusions

In conclusion, we have synthesized miktoarm CCS copolymers consisting of linear-dendritic and linear arms. The cornerstone for preparation of the MMs is ROP of ε-CL by a functional initiator and quantitative functionalization of the hydroxyl chain end with methacrylic unit providing PCL MMs with terminal alkyne and azide groups. These hetero-telechelic building blocks elaborated by SEC and NMR spectroscopy exhibit narrow MWD and high degree of functionality, and represent flexible and versatile structural elements. A Cu(I) catalyzed "click" reaction has been employed as a robust and effectual tool for derivatization of these end functionalities with L-lysine dendron – bis-(di-Boc-L-lysine)-3-azido-1,2-propandiol, and 17α-ethynylestradiol and ethynylferrocene to obtain linear-dendritic and linear MMs, respectively. Cross-linking of the mixture of the MMs with BDMA through ATRP allows synthesis of the miktoarm CCS copolymers with fairly low PDI. Removal of the Boc protection affords novel nanoscale aggregates with hydrophilic, charged surface, targeting motifs, and hydrophobic core that may serve as excellent candidates for targeted drug delivery.

Acknowledgements

The authors thank the Center for Electron Nanoscopy at Technical University of Denmark and Dr J. B. Wagner for acquiring the TEM images.

Notes and references

1 H. Gao and K. Matyjaszewski, *Prog. Polym. Sci.*, 2009, **34**, 317–350.
2 A. Blencowe, J. F. Tan, T. K. Goh and G. Qiao, *Polymer*, 2009, **50**, 5–32.
3 J. Xia, X. Zhang and K. Matyjaszewski, *Macromolecules*, 1999, **32**, 4482–4484.
4 X. Zhang, J. Xia and K. Matyjaszewski, *Macromolecules*, 2000, **33**, 2340–2345.
5 H. Gao, N. V. Tsarevsky and K. Matyjaszewski, *Macromolecules*, 2005, **38**, 5995–6004.
6 D. Kafouris, E. Themistou and C. S. Patrickios, *Chem. Mater.*, 2006, **18**, 85–93.
7 H. Gao, S. Ohno and K. Matyjaszewski, *J. Am. Chem. Soc.*, 2006, **128**, 15111–15113.
8 H. Gao and K. Matyjaszewski, *Macromolecules*, 2008, **41**, 4250–4257.
9 J. Du and Y. Chen, *Macromolecules*, 2004, **37**, 3588–3594.
10 J. T. Wiltshire and G. G. Qiao, *Macromolecules*, 2006, **39**, 4282–4285.
11 J. T. Wiltshire and G. G. Qiao, *Macromolecules*, 2006, **39**, 9018–9027.
12 J. T. Wiltshire and G. G. Qiao, *Macromolecules*, 2008, **41**, 623–631.
13 A. W. Bosman, R. Vestberg, A. Heumann, J. M. J. Fréchet and C. J. Hawker, *J. Am. Chem. Soc.*, 2003, **125**, 715–728.

14 L. A. Connal, R. Vestberg, C. J. Hawker and G. G. Qiao, *Macromolecules*, 2007, **40**, 7855–7863.
15 L. A. Connal, R. Vestberg, C. J. Hawker and G. G. Qiao, *Adv. Funct. Mater.*, 2008, **18**, 3706–3714.
16 F. Wang, T. K. Bronich, A. V. Kabanov, R. D. Rauh and J. Roovers, *Bioconjugate Chem.*, 2005, **16**, 397–405.
17 X. Shuai, T. Merdan, A. K. Schaper, F. Xi and T. Kissel, *Bioconjugate Chem.*, 2004, **15**, 441–448.
18 C. Gunanathan, A. Pais, E. Furman-Haran, D. Seger, E. Eyal, S. Mukhopadhyay, Y. Ben-David, G. Leitus, H. Cohen, A. Vilan, H. Degani and D. Milstein, *Bioconjugate Chem.*, 2007, **18**, 1361–1365.
19 E. C. Dreaden, S. C. Mwakwari, Q. H. Sodji, A. K. Oyelere and M. A. El-Sayed, *Bioconjugate Chem.*, 2009, **20**, 2247–2253.
20 K. T. Al-Jamal, W. T. Al-Jamal, S. Akerman, J. E. Podesta, A. Yilmazer, J. A. Turton, A. Bianco, N. Vargesson, C. Kanthou, A. T. Florence, G. M. Tozer and K. Kostarelos, *Proc. Natl. Acad. Sci. U. S. A.*, 2010, **107**, 3966–3971.
21 I. Javakhishvili, W. H. Binder, S. Tanner and S. Hvilsted, *Polym. Chem.*, 2010, **1**, 506–513.
22 I. Javakhishvili and S. Hvilsted, *Biomacromolecules*, 2009, **10**, 74–81.
23 (*a*) V. V. Rostovtsev, L. G. Green, V. V. Fokin and K. B. Sharpless, *Angew. Chem., Int. Ed.*, 2002, **41**, 2596–2599; (*b*) C. W. Tornøe, C. Christensen and M. Meldal, *J. Org. Chem.*, 2002, **67**, 3057–3064; (*c*) W. H. Binder and R. Sachsenhofer, *Macromol. Rapid Commun.*, 2008, **29**, 952–981.
24 B. C. Englert, S. Bakbak and U. H. F. Bunz, *Macromolecules*, 2005, **38**, 5868–5877.
25 Ph. Degée, Ph. Dubois, R. Jérôme and Ph. Teyssié, *Macromolecules*, 1992, **25**, 4242–4248.
26 J. N. Hoskins and S. M. Grayson, *Macromolecules*, 2009, **42**, 6406–6413.
27 (*a*) Y. Li, J. Yang and B. C. Benicewicz, *J. Polym. Sci., Part A: Polym. Chem.*, 2007, **45**, 4300–4308; (*b*) V. Ladmiral, T. M. Legge, Y. Zhao and S. Perrier, *Macromolecules*, 2008, **41**, 6728–6732; (*c*) G. Li, V. Zheng and R. Bai, *Macromol. Rapid Commun.*, 2009, **30**, 442–447.
28 J. P. Collman, N. K. Devaraj and C. E. D. Chidsey, *Langmuir*, 2004, **20**, 1051–1053.
29 Ph. Lecomte, R. Riva, C. Jérôme and R. Jérôme, *Macromol. Rapid Commun.*, 2008, **29**, 982–997.
30 (*a*) J. M. Holub, M. J. Garabedian and K. Kirshenbaum, *QSAR Comb. Sci.*, 2007, **26**, 1175–1180; (*b*) H.-Y. Kim, J. Sohn, G. T. Wijewickrama, P. Edirisinghe, T. Gherezghiher, M. Hemachandra, P.-Y. Lu, R. E. Chandrasena, M. E. Molloy, D. A. Tonetti and G. R. J. Thatcher, *Bioorg. Med. Chem.*, 2010, **18**, 809–821.
31 (*a*) J. T. Wiltshire and G. G. Qiao, *J. Polym. Sci., Part A: Polym. Chem.*, 2009, **47**, 1485–1498; (*b*) H. Durmaz, A. Dag, E. Erdogan, A. L. Demirel, G. Hizal and U. Tunca, *J. Polym. Sci., Part A: Polym. Chem.*, 2010, **48**, 99–108.
32 (*a*) C. J. Hawker, D. Mecerreyes, E. Elce, J. Dao, J. L. Hedrick, I. Barakat, Ph. Dubois, R. Jérôme and W. Volksen, *Macromol. Chem. Phys.*, 1997, **198**, 155–166; (*b*) L. Mespouille, Ph. Degée and Ph. Dubois, *Eur. Polym. J.*, 2005, **41**, 1187–1195.
33 K.-Y. Baek, M. Kamigaito and M. Sawamoto, *Macromolecules*, 2001, **34**, 215–221.

Danish Polymer Centre
Department of Chemical and
Biochemical Engineering
Technical University of Denmark
Søltofts Plads, Building 229
DK-2800 Kgs. Lyngby
Denmark

Phone: +45 4525 2800
Fax: +45 4525 4588
Web: www.kt.dtu.dk

ISBN : 978-87-92481-34-4